

FINAL REPORT

# **Evaluation of Elastomeric Bridge Bearings for Seismic Design**

**Project IA-H1, FY 99**

Report No. ITRC FR 99-4

Prepared by

Cale Ash  
Judie Schwartz  
Mark Aschheim  
Neil Hawkins  
Bill Gamble

Department of Civil and Environmental Engineering  
University of Illinois at Urbana-Champaign  
Champaign, Illinois

November 2002

**Illinois Transportation Research Center**  
Illinois Department of Transportation

# **ILLINOIS TRANSPORTATION RESEARCH CENTER**

This research project was sponsored by the State of Illinois, acting by and through its Department of Transportation, according to the terms of the Memorandum of Understanding established with the Illinois Transportation Research Center. The Illinois Transportation Research Center is a joint Public-Private-University cooperative transportation research unit underwritten by the Illinois Department of Transportation. The purpose of the Center is the conduct of research in all modes of transportation to provide the knowledge and technology base to improve the capacity to meet the present and future mobility needs of individuals, industry and commerce of the State of Illinois.

Research reports are published throughout the year as research projects are completed. The contents of these reports reflect the views of the authors who are responsible for the facts and the accuracy of the data presented herein. The contents do not necessarily reflect the official views or policies of the Illinois Transportation Research Center or the Illinois Department of Transportation. This report does not constitute a standard, specification, or regulation.

Neither the United States Government nor the State of Illinois endorses products or manufacturers. Trade or manufacturers' names appear in the reports solely because they are considered essential to the object of the reports.

## **Illinois Transportation Research Center Members**

**Bradley University  
DePaul University  
Eastern Illinois University  
Illinois Department of Transportation  
Illinois Institute of Technology  
Lewis University  
Northern Illinois University  
Northwestern University  
Southern Illinois University Carbondale  
Southern Illinois University Edwardsville  
University of Illinois at Chicago  
University of Illinois at Urbana-Champaign  
Western Illinois University**

Reports may be obtained by writing to the administrative offices of the Illinois Transportation Research Center at Southern Illinois University Edwardsville, Campus Box 1803, Edwardsville, IL 62026 [telephone (618) 650-2972], or you may contact the Engineer of Physical Research, Illinois Department of Transportation, at (217) 782-6732.

<b>1. Report No.</b> ITRC FR 99-4	<b>2. Government Accession No.</b>	<b>3. Recipient's Catalog No.</b>	
<b>4. Title and Subtitle</b> Evaluation of Elastomeric Bridge Bearings for Seismic Design		<b>5. Report Date</b> November 2002	<b>6. Performing Organization Code</b>
<b>7. Author(s)</b> Cale Ash, Judie Schwartz, Mark Aschheim, Neil Hawkins, and Bill Gamble		<b>8. Performing Organization Report No.</b>	
<b>9. Performing Organization Name and Address</b> Department of Civil and Environmental Engineering University of Illinois at Urbana-Champaign 205 N. Mathews Ave. Urbana, IL 61801		<b>10. Work Unit No. (TRAIS)</b>	
<b>11. Sponsoring Agency Name and Address</b> Illinois Transportation Research Center Southern Illinois University Edwardsville Engineering Building, Room 3026 Edwardsville, IL 62026-1803		<b>11. Contract or Grant No.</b>  IA-H1, FY 99	
<b>15. Supplementary Notes</b>		<b>13. Type of Report and Period Covered</b> Final Report December 1999 through February 2002	
<b>16. Abstract</b>  Elastomeric bridge bearings have been used by various states in the mid-america region to accommodate thermal movement of bridge decks for over thirty years. Their potential role for mitigating damage in the infrequent but high consequence earthquakes that characterize the central United States is explored in this project. The potential protective role of conventional elastomeric bearings is critically influenced by material properties such as shear modulus, known to be temperature dependent. The degree of influence at low temperatures is determined through experimental studies. Slip characteristics of in-service aged and contaminated Teflon interfaces are determined. Full-scale bearings taken from existing bridges in addition to new bearings form the basis of these tests. Materials tests performed on the elastomer characterize the properties of aged bearings. The influence of these physical properties on possible bridge damage caused by earthquake ground shaking is assessed through computational simulations. A retrofit bearing with improved details for seismic isolation is designed and tested.  An apparatus for testing the bearings was developed to simulate actual loading conditions. The apparatus provides a temperature-controlled chamber to allow for low temperature testing. Test protocols are developed to address the influence of testing parameters such a low temperature exposure and compressive stress. The prototype retrofit bearing design was also tested in this setup. The seismic response of a representative bridge is assessed by computational simulations conducted using the nonlinear analysis software DRAIN-2DX.		<b>14. Sponsoring Agency Code</b>	
<b>17. Key Words</b>  Elastomeric bearings, low temperature stiffness, Seismic response, Illinois bridges	<b>18. Distribution Statement</b>  No restrictions. This document is available to the public through the National Technical Information Service (NTIS), Springfield, Virginia 22161		
<b>19. Security Classification (of this report)</b>  Unclassified	<b>20. Security Classification (of this page)</b>  Unclassified	<b>21. No. of Pages</b>  228	<b>22. Price</b>



# Evaluation of Elastomeric Bearings for Seismic Design

Cale Ash, Judie Schwartz, Mark Aschheim, Neil Hawkins, and Bill Gamble  
University of Illinois Urbana-Champaign



## Executive Summary

This report presents the results of a research program sponsored by the Illinois Transportation Research Center in concert with the Illinois Department of Transportation, conducted at the University of Illinois. The performance of elastomeric bridge bearings at low temperatures was examined experimentally and implications on the seismic response of Illinois bridges were determined by nonlinear dynamic analysis of a representative bridge. The testing made use of a specially-designed apparatus that allowed reversed cyclic lateral testing of full size elastomeric bridge bearings while simultaneously subjected the bearings to a simulated dead load, all in a temperature-controlled environment.

Several used and one new full-sized elastomeric bearings were tested to determine the influence of various parameters, including low temperature, on bearing behavior. Of greatest interest for seismic response are the elastomer shear modulus and Teflon coefficient of friction (for Type II bearings). ASTM materials tests were performed on specimens obtained from the bearings after completion of the bearing tests.

A review of the literature indicates that elastomeric materials stiffen at various rates and to different levels when exposed to low temperatures, and that the rate of stiffening and degree of stiffening depend strongly on the chemical compounds used in formulating the elastomer. While other researchers have reported low temperature stiffnesses that were an order of magnitude greater than room temperature stiffness, the used Illinois bearings had increases in stiffness of only approximately 30%. When exposed for as long as 3 days to temperatures as low as  $-25^{\circ}\text{C}$  ( $-13^{\circ}\text{F}$ ). The new bearing, however, had increases of stiffness of over 600% when exposed to similar low temperatures. This is likely to be due to a compound difference as the used bearings are formulated with natural rubber and the new bearing formulated with neoprene, a significant finding since all bearings were manufactured to comply with the same procurement specification.

While coefficients of friction for sliding between the TFE and stainless steel materials of a Type II bearing are assumed to be approximately 0.07 or 0.08 in design guidelines, the possibly contaminated surfaces of the used bearing displayed coefficients of friction as high as 0.27 when subjected to relatively rapid lateral cycles that may be representative of earthquake loading. The new Type II bearing, having an uncontaminated sliding surface that was free from wear had a coefficient of friction of 0.23 when subjected to relatively rapid lateral cycles, still relatively high compared with typical design values for thermal movements.

Representative values obtained from the tests were used in nonlinear dynamic analyses of a representative bridge supported on Type I and Type II bearings. A maximum considered earthquake event at a location at the southern tip of Illinois was used as a basis for establishing the ground motions used in the analyses. Multiple configurations of fixed and expansion bearings are analyzed with both room and low temperature values of elastomer shear modulus and Teflon coefficient of friction. The effect of low-temperature stiffening on overall bridge response is assessed and reported and recommendations for use in design can be inferred from this discussion.

Based on the results from previous dynamic analyses, a prototype retrofit bearing design was constructed and tested. The prototype bearing displays stick-slip behavior in

order to provide resistance to service loads while allowing slip for higher loads, thereby protecting the substructure from excessive force demands. Analyses indicate that such bearings have the ability to change the locations where large deformations develop and can protect vulnerable piers from damage. However, further development is needed to balance the slip force level and the required slip displacements, considering the range of possible bearing types that can be used at each support location.

## Abstract

Elastomeric bridge bearings have been used by various states in the Mid-America region to accommodate thermal movement of bridge decks for over 30 years. Their potential role for mitigating damage in the infrequent but high consequence earthquakes that characterize the central United States is explored in this project. The potential protective role of conventional elastomeric bearings is critically influenced by material properties such as shear modulus, known to be temperature dependent. The degree of at low temperatures is determined through experimental studies. Slip characteristics of in-service aged and contaminated Teflon interfaces are determined. Full-scale bearings taken from existing bridges in addition to new bearings form the basis of these tests. Materials tests performed on the elastomer characterize the properties of aged bearings. The influence of these physical properties on possible bridge damage caused by earthquake ground shaking is assessed through computational simulations. A retrofit bearing with improved details for seismic isolation is designed and tested.

An apparatus for testing the bearings was developed to simulate actual loading conditions. The apparatus provides a temperature-controlled chamber to allow for low temperature testing. Test protocols are developed to address the influence of testing parameters such as low temperature exposure and compressive stress. The prototype retrofit bearing design was also tested in this setup. The seismic response of a representative bridge is assessed by computational simulations conducted using the nonlinear analysis software DRAIN-2DX.



## **Acknowledgements**

This work was conducted for the Illinois Department of Transportation (IDOT) through a contract between the University of Illinois and the Illinois Transportation Research Center (ITRC). The work was conducted in close collaboration with a Technical Review Panel, consisting of IDOT staff members Dr. Manoucher Karshenas, Mr. Tom Domagalski, Mr. Ben Garde, and Mr. Byron Nesbitt. Mr. Salah Khayyat of the IDOT Office of Bridges and Structures also was helpful. The assistance and council of these individuals is greatly appreciated. The management of the project by Dr. Steve Hanna of ITRC is also greatly appreciated. The assistance of Mr. Mark Whitlock of Structural Rubber Products, Springfield, IL, with obtaining a new Type II bearing is appreciated.



## Table of Contents

1	Introduction .....	1
	1.1 Scope of Work .....	2
	1.2 Illinois Bearing Types .....	3
	1.3 Common Bearing Configurations .....	4
2	Literature Review .....	7
	2.1 Research by IDOT on Elastomeric Bearings .....	7
	2.2 Research on Elastomer Stiffness .....	9
	2.3 Research on TFE Coefficient of Friction .....	14
	2.4 Conclusions .....	15
3	Experimental Test Procedures and Apparatus .....	26
	3.1 Description of Test Apparatus .....	26
	3.2 Studies for Development of Test Protocol .....	29
	3.2.1 Effect of Compressive Stress .....	30
	3.2.2 Effect of Low Temperature Exposure .....	31
	3.2.3 Effect of Dwelling Vertical Load .....	32
	3.2.4 Effect of Initial Beam Slope .....	33
	3.2.5 Effect of Cyclic Frequency .....	34
	3.2.6 Summary of Test Protocol Development .....	34
	3.3 Bearing Test Procedure .....	35
	3.4 Material Tests .....	36
4	Bearing Description and Reporting Format .....	47
	4.1 Bearing Identification Convention .....	47
	4.2 Description of Used Bearings .....	49
	4.3 Description of New Bearings .....	49
5	Bearing Test Results and Analysis .....	53
	5.1 Characteristic Behavior and Data Reduction .....	53
	5.1.1 Elastomer Shear Stiffness .....	53
	5.1.2 Coefficient of Friction .....	54
	5.2 Summary Data .....	55
	5.2.1 Effect of Temperature on Shear Modulus .....	56
	5.2.2 Effect of Temperature on Coefficient of Friction .....	56
	5.3 Summary of Used Bearing Behavior and Properties .....	58
6	Elastomer Test Results .....	64
	6.1 Durometer Hardness .....	64
	6.2 Tensile Strength, Elongation and Compression Set .....	65
	6.3 Peel Strength .....	65
	6.4 Summary .....	66

7	Retrofit Bearing Details .....	69
	7.1 Design Objectives .....	69
	7.2 Proposed Solution and Design .....	70
	7.3 Test Results & Conclusions .....	71
8	Modeling .....	76
	8.1 Representative Bridge Description .....	77
	8.2 Bridge Modeling .....	78
	9.3 Site Seismicity and Ground Motions .....	79
	8.4 Results .....	80
	8.4.1 Scenario 1 – Typical configuration .....	81
	8.4.2 Scenario 2 – Retrofit bearing .....	81
	8.4.3 Scenario 3 – All elastomeric bearings .....	82
	8.4.4 Scenario 4 – All fixed .....	82
	8.5 Conclusions .....	82
9	Summary and Conclusions .....	91
	9.1 Research Summary .....	91
	9.2 Conclusions .....	92
	Appendix Introduction .....	95
	Appendix A – Test Results for 2A1 & 2A2 .....	96
	Appendix B – Test Results for 2B1 & 2B2 .....	113
	Appendix C – Test Results for 2C1 & 2C2 .....	130
	Appendix D – Test Results for 1D1 & 1D2 .....	147
	Appendix E – Test Results for 1S2 .....	167
	Appendix F – DRAIN-2DX Input Files .....	178
	Appendix G – Units Conversions .....	206
	References .....	207

## List of Tables

2.1	Coefficient of friction for TFE sliding against TFE and stainless steel.....	17
2.2	Characterization of hardness and chemical composition.....	17
4.1	Bearing information and report reference summary .....	50
4.2	Used bearing dimension and condition summary .....	50
5.1	Mean shear moduli for used bearings .....	59
5.2	Mean TFE coefficient of friction for used bearings .....	59
6.1	ASTM tests and requirements.....	67
6.2	Durometer hardness summary .....	67
6.3	Tensile strength, elongation, and compression set test summary .....	67
6.4	Peel test summary .....	68
8.1	Bearing configurations.....	78



## List of Figures

1.1	Illinois standard bearing types .....	5
1.2	Typical bridge configuration .....	6
2.1	Coefficient of friction vs. compressive stress for unfilled Teflon at 0 and 7000 cycles .....	18
2.2	Coefficient of friction vs. vertical pressure for unfilled and filled Teflon at 7000 cycles .....	18
2.3	Horizontal rubber strain vs. compressive stress for laminated elastomeric bearing..	19
2.4	Coefficient of friction vs. vertical pressure for laminated elastomeric – TFE sliding bearing .....	19
2.5	Typical time-dependent low-temperature behavior of elastomer .....	20
2.6	Stiffness of full-size bearings at -25°C .....	20
2.7	Effect of temperature on crystallization rate of two neoprene compounds .....	21
2.8	Experimental data for thermal stiffening of neoprene .....	21
2.9	Six successive freeze/thaw cycles with test pieces subjected to +/- 25°C .....	22
2.10	Increase in stiffness with exposure time with and without offset shear .....	22
2.11	Force displacement behavior of low temperature shear test .....	23
2.12	Effect of changed temperature on measured stiffness .....	24
2.13	Comparison of the measured stiffness of CR55 elastomer compound as a function of time with different test frequencies .....	24
2.14	Variation of maximum sliding coefficient of friction with velocity .....	25
3.1	Laboratory testing setup .....	38
3.2	Type II bearings installed in test setup .....	39
3.3	Stainless steel sliding surface mounted to glulam beam .....	39
3.4	Type I bearing installed in test setup .....	40
3.5	Horizontal actuator mounted to glulam beam.....	40
3.6	Insulated chamber and liquid nitrogen tank .....	41
3.7	Used Type II bearing with embedded thermocouple .....	41
3.8 – 3.26	Various bearing load-displacement plots .....	42-45
3.27	Typical schedule for test protocol .....	45
3.28	Protocol temperature history and test times .....	46
4.1	Initial conditions of used Type II bearings .....	51
4.2	Evidence of contaminants on TFE surface of used Type II bearing .....	51
4.3	New Type I bearing .....	52
4.4	New Type II bearing .....	52
5.1	Typical load-displacement hysteresis loops for Type II bearings .....	60
5.2	Shear modulus definition .....	61
5.3	$C_f$ definition .....	61
5.4	Normalized shear modulus for all bearings – protocol 1 .....	62
5.5	Normalized shear modulus for used bearings only .....	62
5.6	Used bearing $C_f$ summary .....	63
5.7	New bearing $C_f$ summary .....	63
7.1	Retrofit bearing elevation .....	73
7.2	Retrofit bearing installed in test setup .....	74
7.3	Fracture of shear stud welds after warm temperature cyclic test .....	74

7.4	Warm temperature retrofit bearing test result .....	75
7.5	Retrofit bearing test after 72 hours at -25°C .....	75
8.1	Spectral acceleration scaling .....	84
8.2	Unscaled ground motion record .....	84
8.3	Spectral displacement scaling .....	85
8.4	Scaled ground motion record .....	85
8.5	Scenario 1a peak relative displacement .....	86
8.6	Scenario 1b peak relative displacement .....	86
8.7	Scenario 2a peak relative displacement .....	87
8.8	Scenario 2b peak relative displacement .....	87
8.9	Scenario 3a peak relative displacement .....	88
8.10	Scenario 3b peak relative displacement .....	88
8.11	Scenario 4 peak relative displacement .....	89
8.12	Damage assessment table .....	90

## Chapter 1 – Introduction

Elastomeric bridge bearings have been used in the state of Illinois to accommodate the thermal movement of bridge decks for over 30 years. These bearings have become widely used and have replaced many of the steel rocker bearings that had been previously used. This is in part due to the perceived superior performance and reliability of elastomeric bearings compared to the corrosion-prone steel bearings. More recently, the seismic hazard posed by the New Madrid seismic zone has been recognized and concerns about the seismic performance of existing bridges in Illinois have surfaced. The potential role of conventional elastomeric bearings for mitigating damage in the infrequent but high consequence earthquakes that characterize the seismicity of the central US was explored in this project<sup>1</sup>. The protective role of conventional elastomeric bearings may be critically influenced by the degree to which they stiffen with age and exposure to cold winter temperatures. This project investigated the phenomenon of low-temperature stiffening and the influence of age on the lateral behavior of standard Illinois elastomeric bearings through experimental and analytical studies. The slip characteristics of the in-service aged and contaminated polytetrafluoroethylene (TFE or Teflon®) sliding surfaces used in Type II and Type III bearings were also examined. A prototype bearing design characterized by stick-slip behavior was developed and tested with the intent of possible use in the retrofitting of existing fixed bearings. By quantifying the physical properties of bearings analytically, the potential benefits of these bearings in reducing the damage caused by a potential earthquake could be studied by nonlinear

---

<sup>1</sup>The conventional elastomeric bearings studied in this project differ from seismic isolation bearings, which are typically larger, and may be formulated with high-damping rubber or contain a lead energy-dissipating core.

dynamic analyses. The experimental tests on full-size bearings, material tests on samples cut from the bearings, and analytical results are described in the following chapters.

### *1.1 Scope of Work*

The Illinois Department of Transportation (IDOT) provided bearings obtained from existing bridges for use in this project. The bearings were subjected to reversed cyclic lateral loading at varied rates, at different levels of shear strain, at different temperatures and under nominally constant vertical stress. These tests were conducted in the Newmark Structural Engineering Laboratory located at the University of Illinois Urbana-Champaign. A retrofit bearing designed to have stick-slip behavior was constructed and tested. The test data were used in numerical simulations of the seismic response of a representative bridge with multiple bearing configurations. Recommendations for analysis and design are made based on the experimental and computational results.

New Type I and both new and older Type II bearings were tested as described in Section 1.2. Testing variables for the full size bearings included temperature, vertical compressive stress, and lateral loading rates and strains. Test parameters were established to represent a likely range of in-service conditions. However, lateral shear strains in excess of design values and temperatures characteristic of extreme wintertime lows were used during testing. Based on the resulting test data, elastomer shear moduli were determined for all bearings and coefficient of friction values were determined for the TFE surfaces of all Type II bearings. In addition to tests on the full-size bearings, standard ASTM materials tests were conducted on representative bearing samples from

the aged bearings to assess any consequences of aging. The ASTM materials tests included D2240 (Durometer Hardness), D412 (Rubber Properties in Tension), D573 (Rubber – Deterioration in Air Oven), D395B (Rubber Property – Compression Set), and D429B (Adhesion to Steel Peel Strength).

Computer modeling simulations were performed to evaluate the influence of elastomer properties on the dynamic response of a representative bridge and to evaluate the potential improvement in response that may be obtained by replacing fixed bearings with suitable retrofit bearings. Based on this information, recommendations for design, rehabilitation, and analysis are made and can be found in the later chapters of this report.

### *1.2 Illinois Bearing Types*

The IDOT Bureau of Bridges and Structures Bridge Manual (IDOT, 1994) includes specifications for three types of steel-reinforced elastomeric bearings (Figure 1.1). The Type I bearing consists of a steel-reinforced elastomeric pad bonded to a steel mounting plate. The Type II bearing is essentially a Type I bearing with a TFE sliding surface attached to a steel plate bonded to the top of the elastomeric pad. This bearing type is designed to provide additional translational movement capacity, beyond that provided by deformation of the elastomer alone. The Type III bearing is designed to accommodate bridge deck expansion and contraction which exceed the limitations of the Type II bearing. The Type III bearing is essentially a Type II bearing modified to include a central steel shear-restrictor pin. The shear-restrictor pin is designed to be strong enough to force slip to occur on the TFE surface once the strain in the elastomer reaches

a limiting value (IDOT, 1994). Bearing Types I and II are the most commonly used and it was these types that were tested in this research investigation.

### *1.3 Common Bearing Configurations*

Elastomeric bearings are often used to support the expansion ends of bridge superstructures. They may be installed during initial construction operations or during rehabilitation operations such as deck replacement. A representative bridge with elastomeric expansion bearings is shown in Figure 1.2. This bridge is an idealization of Structure Number 016-2023, a four-span bridge carrying Darmstadt Road over I-88 in Cook County, Illinois. Typically, bridges such as this one have a fixed bearing at the central pier (Pier 3) and elastomeric bearings at the other piers and abutments. Where the bridge deck expansion (measured from the fixed pier) would result in strains exceeding 50% in the elastomer, a Type II bearing must be used, as is the case with Abutments 1 and 5. Because the strains in the elastomer are expected to be less than 50% at Piers 2 and 4, Type I bearings are used at these locations. This representative bridge is referred to frequently in this report and is the basis for the computer modeling simulations described in Chapter 8.

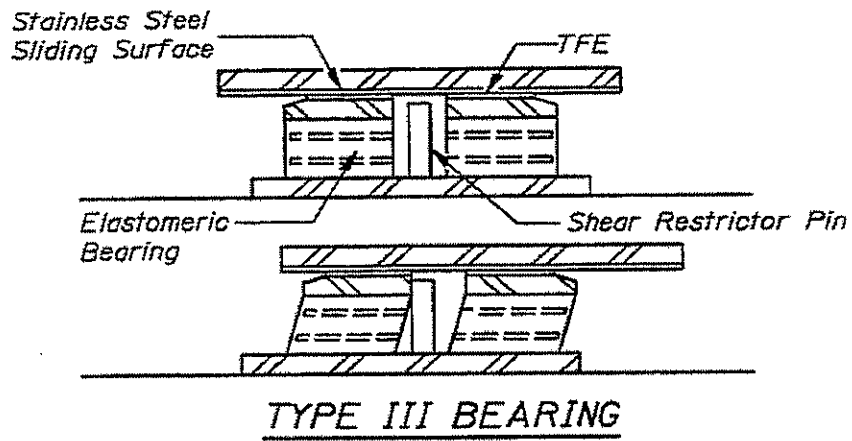
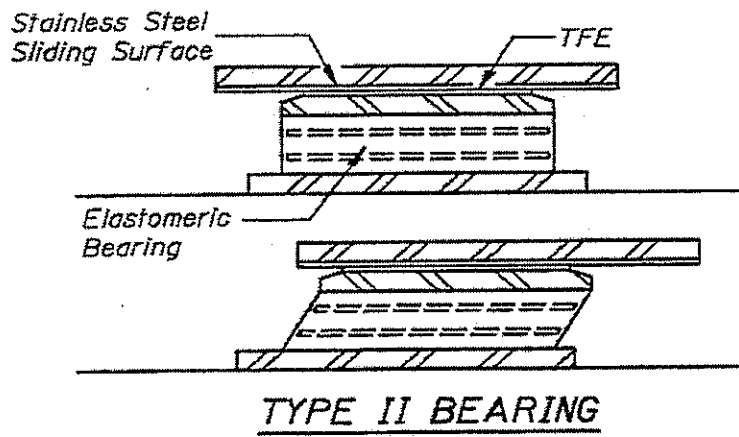
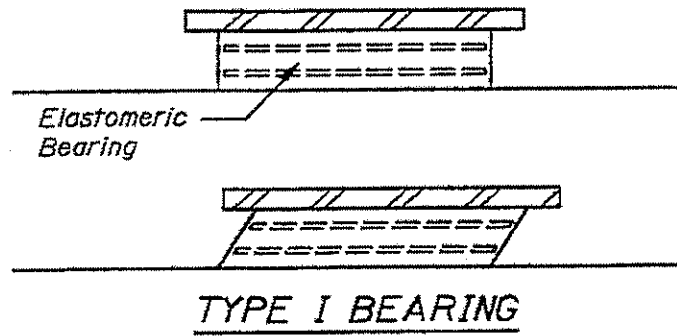
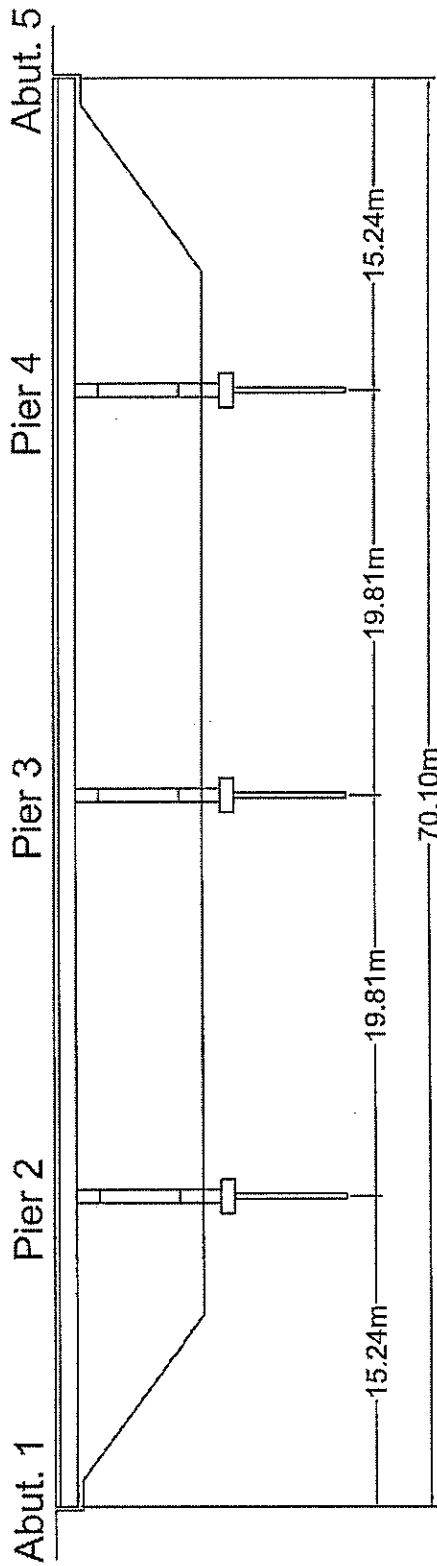
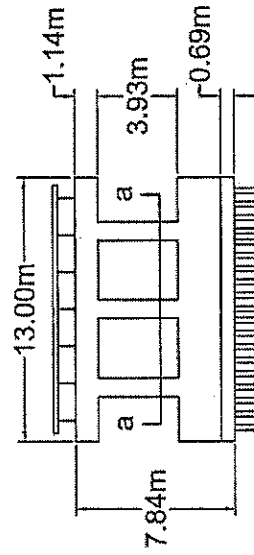


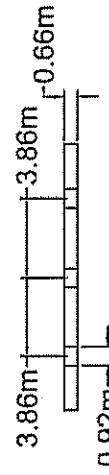
Figure 1.1 Illinois standard bearing types



Bridge Elevation



Pier Elevation



Pier Section a-a

Figure 1.2 Typical bridge configuration  
(Elastomeric bearings at Abuts. 1 & 5 and Piers 2 & 4)

## **Chapter 2 – Literature Review**

Although the conventional elastomeric bearings used in Illinois bridges were not selected with the intent of providing resistance to seismic actions, their presence will influence seismic response. As such, it is important to understand key physical properties such as elastomer shear modulus and TFE coefficient of friction. Wide variations in elastomer stiffness have been reported in the literature, and a variety of information, sometimes conflicting, has been reported regarding the low temperature stiffening behavior of various elastomeric compounds. Many factors including age, chemical compound, and thermal and strain histories may affect the properties of the elastomer. This chapter reviews the literature on the stiffness of elastomers and elastomeric bearings as affected by temperature and loading as well as the slip characteristics of polytetrafluoroethylene (TFE).

### *2.1 Research by IDOT on Elastomeric Bearings*

A program of study was undertaken by the Illinois Department of Transportation (IDOT) in the 1970's to investigate the properties of elastomeric bearings and TFE sliding surfaces. The intent was to replace the currently used bearing types, steel rocker bearings and graphite impregnated bronze bearings, with an improved design featuring better performance and increased service life. The elastomeric bearings were subjected to in-service field tests in an existing bridge along with laboratory tests. The coefficient of friction of the TFE and the performance characteristics of the elastomeric pads were studied in a series of tests performed by Jacobsen (1977). The results of these tests were used to develop a design method and specifications for use in bearing procurement.

From the coefficient of friction tests, it was determined that as compressive load on a TFE sample increases, the coefficient of friction ( $C_f$ ) decreases (Figure 2.1). The result is a TFE surface which is dimpled to reduce the effective contact area, thereby increasing the contact stress and reducing the coefficient of friction and the force required to initiate sliding. Tests were also performed to determine the most suitable TFE material to specify for Type II bearings. Figure 2.2 shows that after 7000 testing cycles filled TFE displayed higher  $C_f$  values than did unfilled TFE. Unfilled TFE showed little reduction in  $C_f$  with increased cycling as indicated on Figure 2.1. Consequently, Illinois adopted unfilled TFE in its bearing specification. Unlike some states, Illinois does not use a lubricant on the TFE surfaces because of concern that the lubricant would become contaminated over time. Figure 2.3 shows the elastomer shear strain necessary to induce slip on an unfilled TFE sheet when attached to a laminated bearing pad of varying hardness. This gives an indication of the elastomer hardness to specify in order to limit shear strains to an acceptable level during service conditions.

Tests were also conducted to determine an appropriate mating surface. Table 2.1 shows little difference in  $C_f$  between TFE and stainless steel as a mating surface. The results of these tests were compared with the performance of self-lubricating bronze bearings, which were commonly used on concrete bridges. TFE was shown to have comparable behavior to the bronze bearings at the loading speed used in the tests. However, it was recognized that at the slower expected rate of loading characteristic of thermally induced displacements the bronze bearing would have a higher resistance than the TFE.

The potential for contaminants to affect  $C_f$  and to impact design was identified. Jacobsen (1977) reports  $C_f$  values increasing from 0.08 to as high as 0.29 for an unfilled TFE sheet contaminated with sand particles. A change of this magnitude would increase the forces transmitted to the substructure, possibly to a damaging level.

From the results of these tests, the three currently used types of elastomeric expansion bearings were developed. A prototype Type II bearing was subjected to translational loading resulting in the coefficient of friction data shown in Figure 2.4.

The final standard design includes a laminated bearing pad of specified durometer elastomer with a steel mounting plate vulcanized to it, now referred to as Type I. Two of the standard designs, the current Types II and III, include bonding of a TFE sheet to the top steel plate to serve as a sliding surface, as discussed earlier in this report.

## *2.2 Research on Elastomer Stiffness*

Seismic loading can be expected to impose relatively rapid, varied, and unpredictable cyclic strain histories on the elastomer. Standardized strain histories are usually imposed in research to provide a uniform basis for evaluation and comparison. The present investigation examines the stiffness of the elastomer in steady state conditions at varied low temperatures, using several vertical compressive stresses and lateral strain histories.

Low temperature stiffening can have important effects on elastomeric bearing and bridge performance during an earthquake event (Wissawapaisal and Aschheim, 1999). Past research has indicated that elastomeric compounds will crystallize and stiffen at low temperatures to different degrees and at varied rates (Murray and Detenber, 1961). In

their 1961 report, Murray and Detenber describe two transitions. The first order transition, crystallization, is reported to be a time- and temperature-dependent process in which the microstructure of the elastomer undergoes realignment into a stiffer form. Crystallization may cause increases in shear modulus of an order of magnitude (Bruzzone and Sorta, 1978). The time-dependent nature of stiffening is shown in Figure 2.5, which shows typical results of normalized stiffness (with respect to room temperature stiffness) for a constant low temperature. Crystallization may be measured by monitoring the change in durometer hardness (Shore A) and any change in volume (Murray and Detenber, 1961). The durometer test measures the resistance of the elastomer to indentation by a standard needle-like probe. Results of durometer tests on bearing samples are operator-dependent and may be difficult to duplicate, even in room-temperature circumstances. The durometer testing of cool bearings at room temperature introduces variability in the results due to surface warming once the sample is removed from the cold chamber (Roeder et al., 1989). Table 2.2 shows that the durometer hardness of elastomer samples depends on the chemical composition of the elastomer. These compounds, in turn, crystallize at different rates and to different degrees as shown in Figure 2.6. Based on these results, durometer hardness is a poor indicator of bearing stiffness and performance at low temperatures. Yura, et al. (2001) recognized this and have proposed alternate stiffness tests for bearing certification and quality control.

There is disagreement in the literature regarding the temperature at which various elastomer compounds crystallize most rapidly. Yura, et al. (2001) and Long (1974) indicate that polychloroprene (neoprene) crystallizes most rapidly at  $-10^{\circ}\text{C}^2$  and natural

---

<sup>2</sup> See Appendix G for temperature conversions

rubber crystallizes fastest at  $-25^{\circ}\text{C}$ . Murray and Detenber (1961) also report that neoprene crystallizes fastest at around  $-10^{\circ}\text{C}$  as shown in Figure 2.7. Other authors report a range of temperatures between  $5^{\circ}\text{C}$  and  $-40^{\circ}\text{C}$  for the most rapid crystallization of neoprene (Wood and Bekkedahl, 1946). Roeder et al. (1989) report the maximum rate of crystallization of natural rubber to be between  $-30^{\circ}\text{C}$  and  $-35^{\circ}\text{C}$ . These authors also report that as the temperature decreases, there may be a delay in onset of rapid crystallization, but, once this time has passed, the crystallization rate and rate of stiffening will increase and then stabilize (Roeder et al., 1989).

The glass transition occurs when the elastomer sample becomes glass-like and brittle and may fracture when bent or strained. The glass transition temperature for neoprene is around  $-35^{\circ}\text{C}$  as indicated by the sharp rise in elastic modulus displayed in Figure 2.8. Natural rubber also undergoes a glass transition, but at a much colder temperature of  $-65^{\circ}\text{C}$ . These reported glass transition temperatures are too low to be of practical interest in the state of Illinois. However, the increased rate of crystallization (near  $-10^{\circ}\text{C}$  for neoprene and  $-25^{\circ}\text{C}$  for natural rubber) is relevant, as these temperatures are reached in many portions of the state during the coldest times of winter.

The range in the reported temperatures of fastest crystallization may be a result of the chemical compounds used in the elastomer formulation. Rates of crystallization vary with temperature and the specific formulation (compound) of the elastomer as Figure 2.6 has illustrated. The percent volume of neoprene, the type of plasticizer, and concentration of low-temperature plasticizer may also affect crystallization rate (Murray and Detenber, 1961). Research also indicates that compounds that crystallize faster also exhibit greater stiffening due to crystallization (Roeder et al., 1987).

Some research (Yura et al., 2001) suggests that the low temperature crystallization stiffness may depend only on the current temperature of the bearing and the length of time that the bearing has been subjected to temperatures sufficient to cause crystallization. In particular, natural rubber is less susceptible to low temperature stiffening than other compounds (Roeder et al., 1989; Eyre and Stevenson, 1991; Yakut, 2000). Crystallization is a completely reversible process. Reversal apparently occurs at a particular temperature and, depending on the researcher, may occur at 15°C (Leitner, 1955) or 10 to 15°C above the temperature of most rapid crystallization (Roeder et al., 1989).

Stiffness of an elastomer as it warms from low temperatures cannot be predicted according to its stiffness during cooling. Rather, the stiffness depends upon how long the elastomer has been crystallized in addition to the rate of warming (Roeder et al., 1989). Previous crystallization may accelerate crystallization in future cooling cycles. Eyre and Stevenson (1991) conducted tests to study the effects of simulated seasonal change. Test pieces cut from full-size bearings were cycled between “summer” and “winter” temperatures and tested. The results, shown in Figure 2.9, indicated that the crystallization rate increased initially with each seasonal temperature cycle, but after the initial cycles, the increase in stiffness with low temperature stabilized for subsequent seasonal cycles.

Any offset shear strain applied to the bearing from installation in a testing device or a bridge may increase the crystallization above that observed when the bearing is in a neutral position (Eyre and Stevenson, 1991; Yakut, 2000). This trend is shown in Figure 2.10. Those specimens with offset shear exhibited a higher stiffness than those without.

Slow shearing or strain application does not retard crystallization and will result in a higher measured shear modulus than a test in which the loads or strains are applied more quickly. However, frequent movements can generate enough heat to destroy crystals (Long, 1974), an important consideration during cyclic testing. This effect is shown in Figure 2.11 with stiffness decreasing with increasing number of cycles. Applications of small strains disturb crystallization less than larger amplitudes of strain (Yakut, 2000; Eyre and Stevenson, 1991). Figure 2.12 indicates that moderate temperature fluctuations do not affect the overall stiffening trend (Roeder, et al., 1989). In addition, the interval between elastomer tests does not seem to affect the stiffness of the test specimen, as shown in Figure 2.13 (Roeder, et al., 1989).

Determining the low-temperature stiffness for a particular bearing based on small elastomer samples can be complicated. Much of the previous research has tested pieces cut from new bearings or new rubber samples. There is some evidence that the low-temperature stiffness and crystallization are affected by the size of the sample tested. The stiffness of an elastomer is affected by the rate at which load or strain is applied (Roeder, et al., 1987). Faster tests seem to yield a higher shear modulus (Yura, et al., 2001). With decreasing temperature, the rate of loading has a more significant effect on crystallization (Yakut, 2000).

Dynamic tests in compression and shear indicate that the low temperature axial and shear stiffnesses may be correlated. It was also determined that cyclic shear can inhibit crystallization while cyclic compression does not (Yakut, 2000). Therefore, compressive loads may be applied to the bearing immediately before cyclic testing without any anticipated effects.

The effect of age on elastomer crystallization has not been clearly established. Elastomers subjected to accelerated aging tests show an increase in room temperature stiffness with age, but the artificial aging process may produce unrealistic results (Yura, et al., 2001).

### *2.3 Research on TFE Coefficient of Friction*

The coefficient of friction of the TFE surface is an important factor in the overall behavior of the bearing. If the coefficient of friction is high, large displacements will cause large forces and strains to develop in the elastomer, possibly causing damage to the bearing. In addition, these forces will be transmitted to the substructure, possibly causing damage to components of the substructure. The coefficient of friction of TFE increases with the number of slip cycles and decreases with increasing pressure applied to the sliding surface, as shown in the aforementioned Figures 2.1 and 2.2 (Jacobsen, 1977; Campbell and Kong, 1989). Other researchers (Mokha, et al., 1988), using new TFE samples, show an increase in  $C_f$  with increasing sliding velocity. As shown in Figure 2.14,  $C_f$  values increase with velocity and then are approximately constant for sliding velocities in excess of 4 to 8 in/sec. Dimpled TFE surfaces are used to increase the normal stress on the contact surface, because the coefficient of friction is lower for increasing contact pressure.

Of particular relevance to this study is the increase in the coefficient of friction as temperature decreases. Constantinou, et al. (1999) find that the TFE coefficient of friction increases with reductions in temperature and find that the coefficient of friction decreases as the size of the TFE surface increases. It should be noted that slipping causes

the TFE sliding surface to warm due to friction (Mokha, et al., 1988), and thus dynamic laboratory tests at a given low temperature, while realistic in some respects, may not reflect the actual surface temperature of the TFE when slip occurs.

#### *2.4 Conclusions*

Many factors have been found to influence the low temperature stiffening of elastomers and the coefficient of friction of the TFE surface. These trends, sometimes contradictory, are summarized as follows:

- Durometer hardness is not an accurate measure of elastomer shear modulus
- Research indicates that elastomers can stiffen considerably at low temperatures, with some researchers reporting increases of many times the room temperature stiffness
- Different investigators have reached different conclusions regarding the temperature at which elastomeric compounds crystallize most rapidly
- Reported TFE  $C_f$  values vary considerably in the research

Much of the past research has been on small samples of virgin elastomer. Very complex interactions between chemical microstructure and current and previous strain histories affect the measured properties. Past research has not resolved ambiguities related to thermal stiffening and crystallization. The performance of older bearings in service may also be affected by age and prior thermal and strain cycling, and these effects may vary with the elastomer compound, in ways that may not be entirely clear based on past research.

Most TFE samples that were tested were also new at the time of testing. Only the IDOT research (Jacobsen, 1977) tested complete bearings with an attached TFE sheet. The effect of low temperature on the TFE coefficient of friction was not investigated at all in this early research.

Vertical Pressure (psi)	$C_f$	$C_f$
	TFE vs. TFE	TFE vs. Stainless Steel
200	.13	.14
400	.12	.12
600	.10	.11
800	.10	.10
1000	.09	.09
1200	.08	.08
1400	.08	.07

**Table 2.1** Coefficient of friction for TFE sliding against TFE and stainless steel  
(Jacobsen, 1977)

Compound	Hardness IRHD	Sulphur Content pphr	Carbon Black pphr
A	54	1.52	34
B	54	3.37	20
C	49	1.81	20
D	59	1.55	40
E	71	3.75	50
F	60	3.80	80
G	69	4.18	90
H	48	3.02	19
J	69	2.50	74

**Table 2.2** Characterization of hardness and chemical composition (Eyre and Stevenson,  
1991)

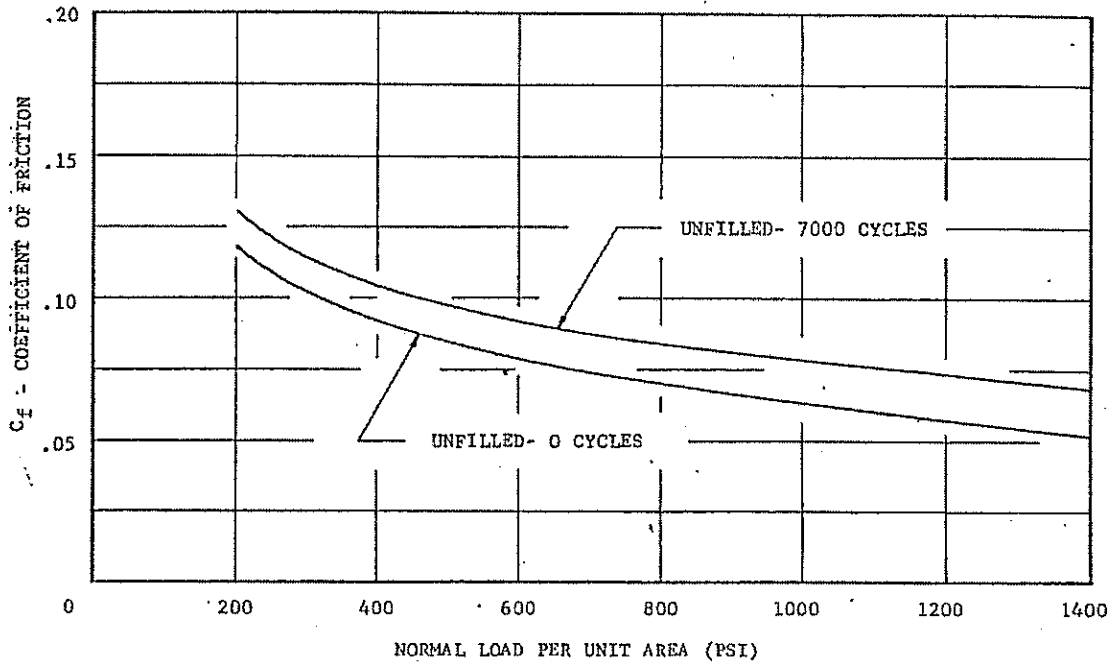


Figure 2.1 Coefficient of friction vs. compressive stress for unfilled Teflon at 0 and 7000 cycles (Jacobsen, 1977)

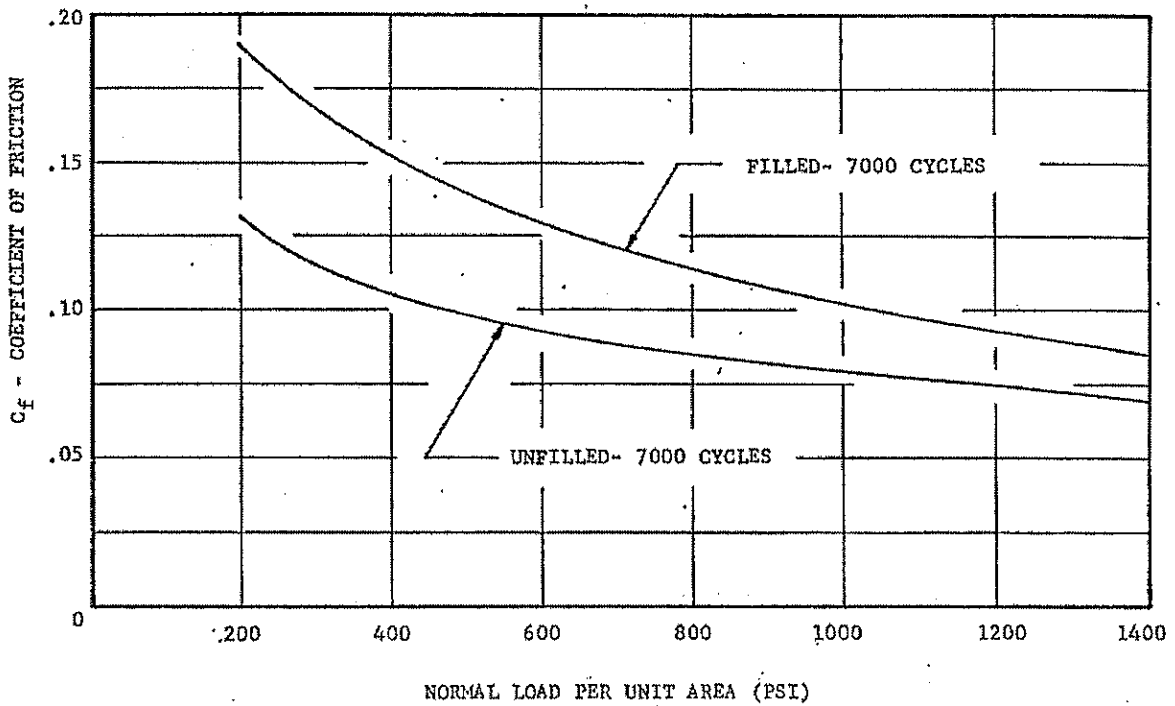


Figure 2.2 Coefficient of friction vs. vertical pressure for unfilled and filled Teflon at 7000 cycles (Jacobsen, 1977)

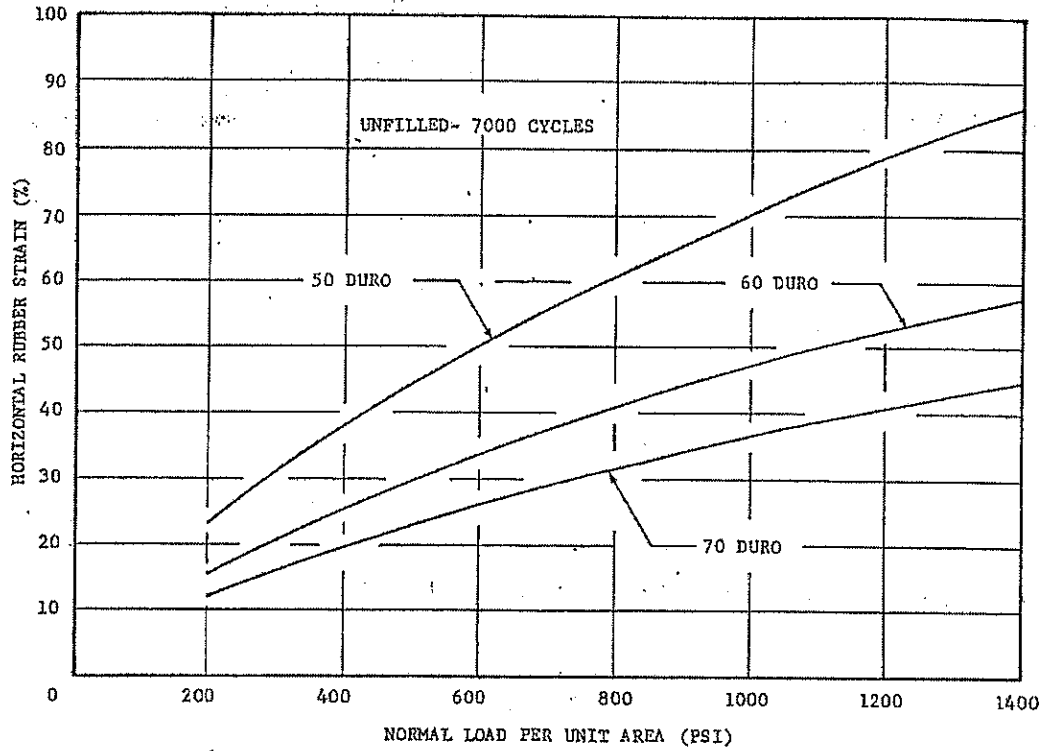


Figure 2.3 Theoretical horizontal rubber strain vs. compressive stress for laminated elastomeric - TFE bearing (Jacobsen, 1977)

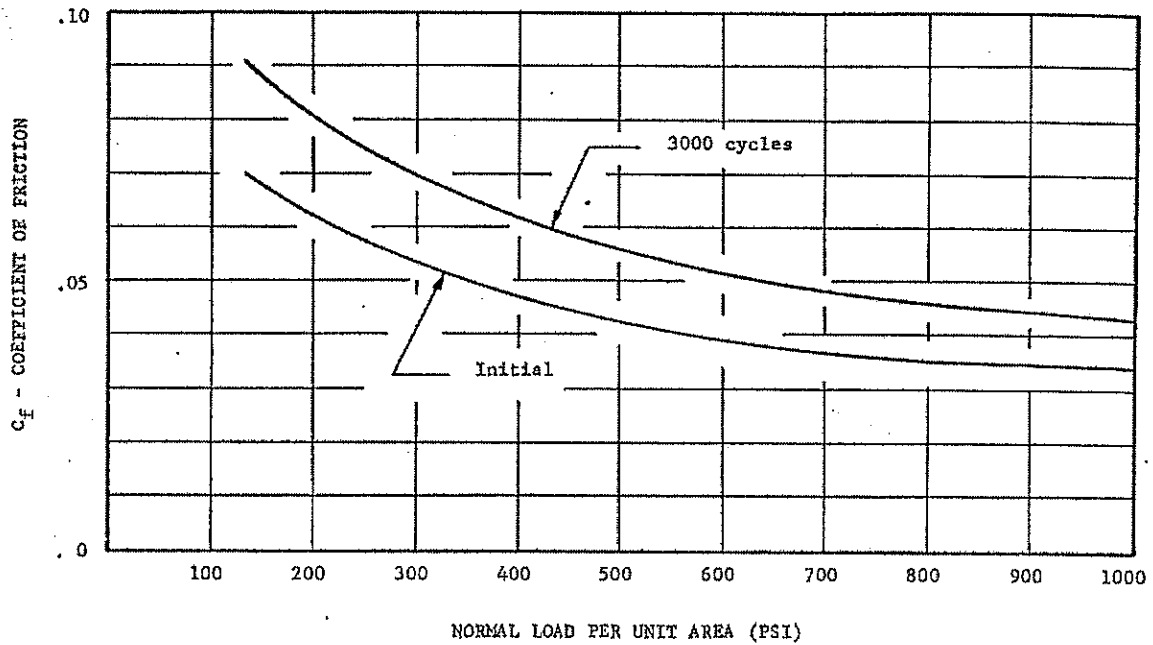


Figure 2.4 Coefficient of friction vs. vertical pressure for laminated elastomeric - TFE sliding bearing (Jacobsen, 1977)

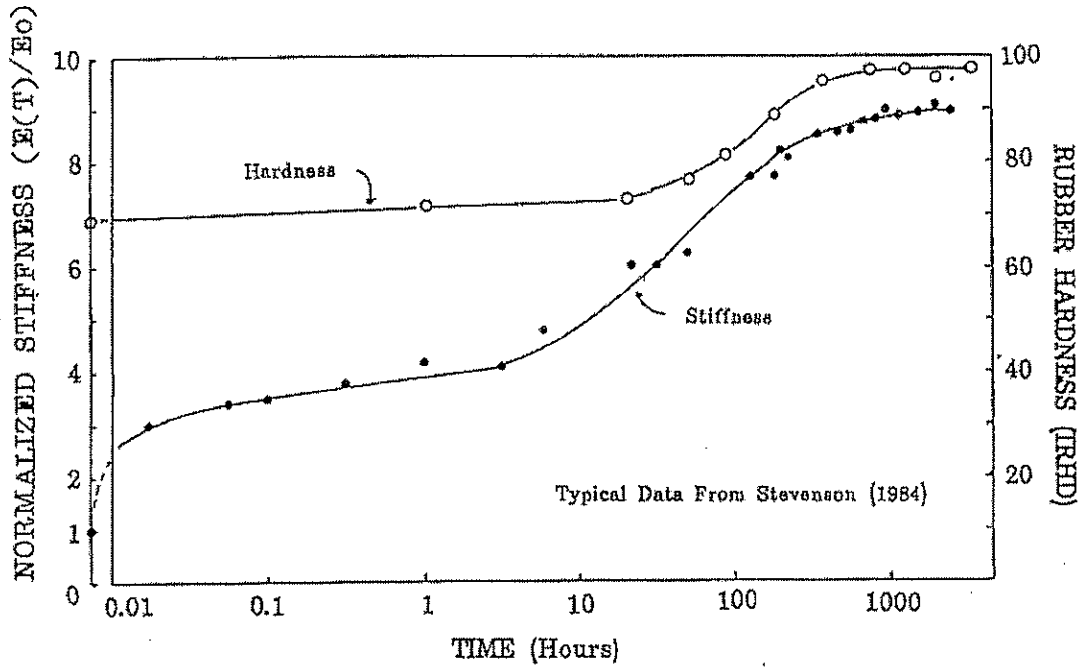


Figure 2.5 Typical time-dependent low-temperature behavior of elastomer (Roeder, et al., 1987)

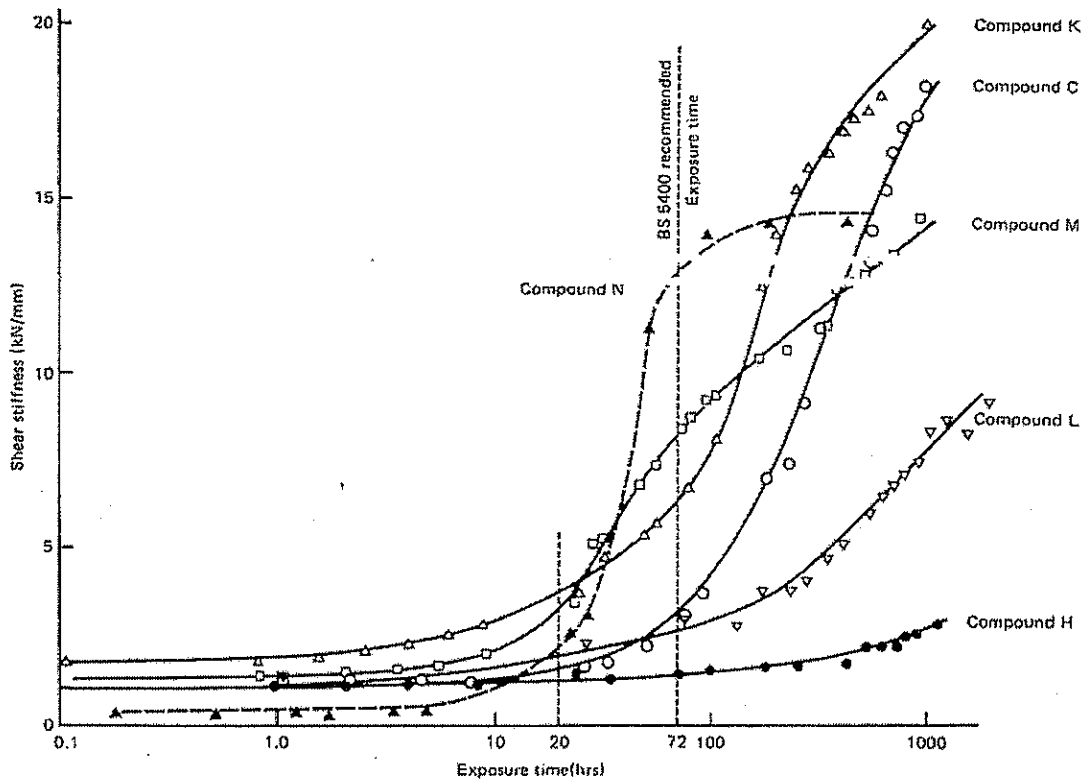


Figure 2.6 Stiffness of full-size bearings at  $-25^{\circ}\text{C}$  (Eyre and Stevenson, 1991)

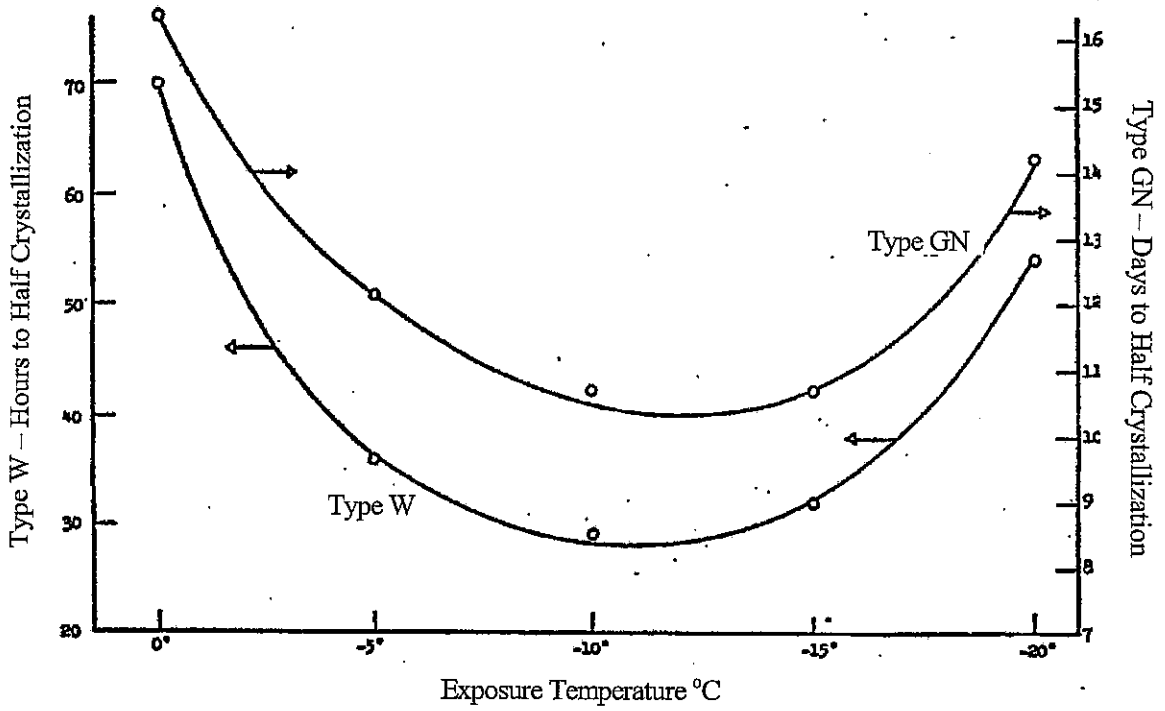


Figure 2.7 Effect of temperature on crystallization rate of two neoprene compounds (Murray and Detenber, 1961)

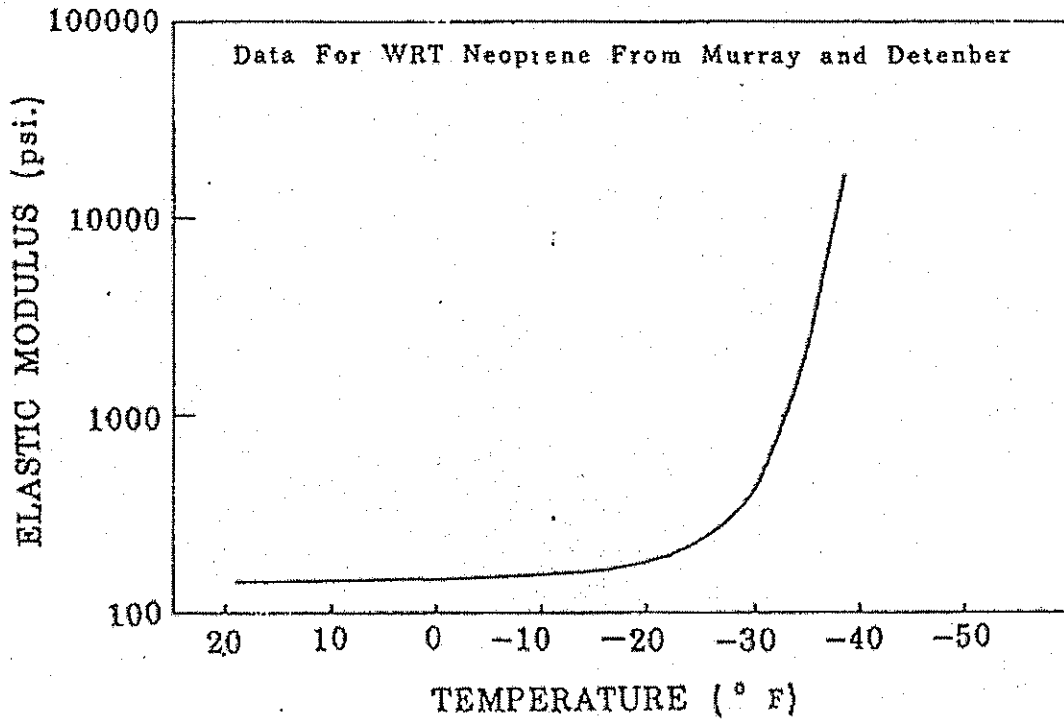


Figure 2.8 Experimental data for thermal stiffening of neoprene (Roeder, et al., 1987)

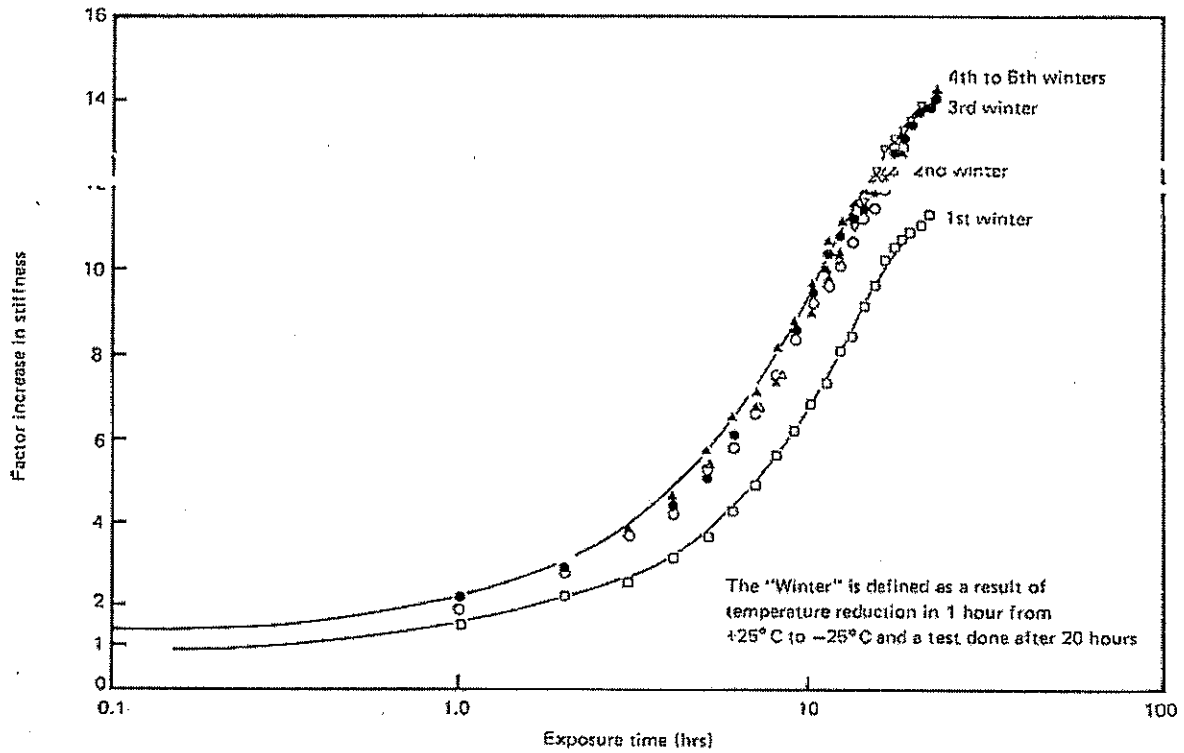


Figure 2.9 Six successive freeze/thaw cycles with test pieces subjected to  $\pm 25^{\circ}\text{C}$  (Eyre and Stevenson, 1991)

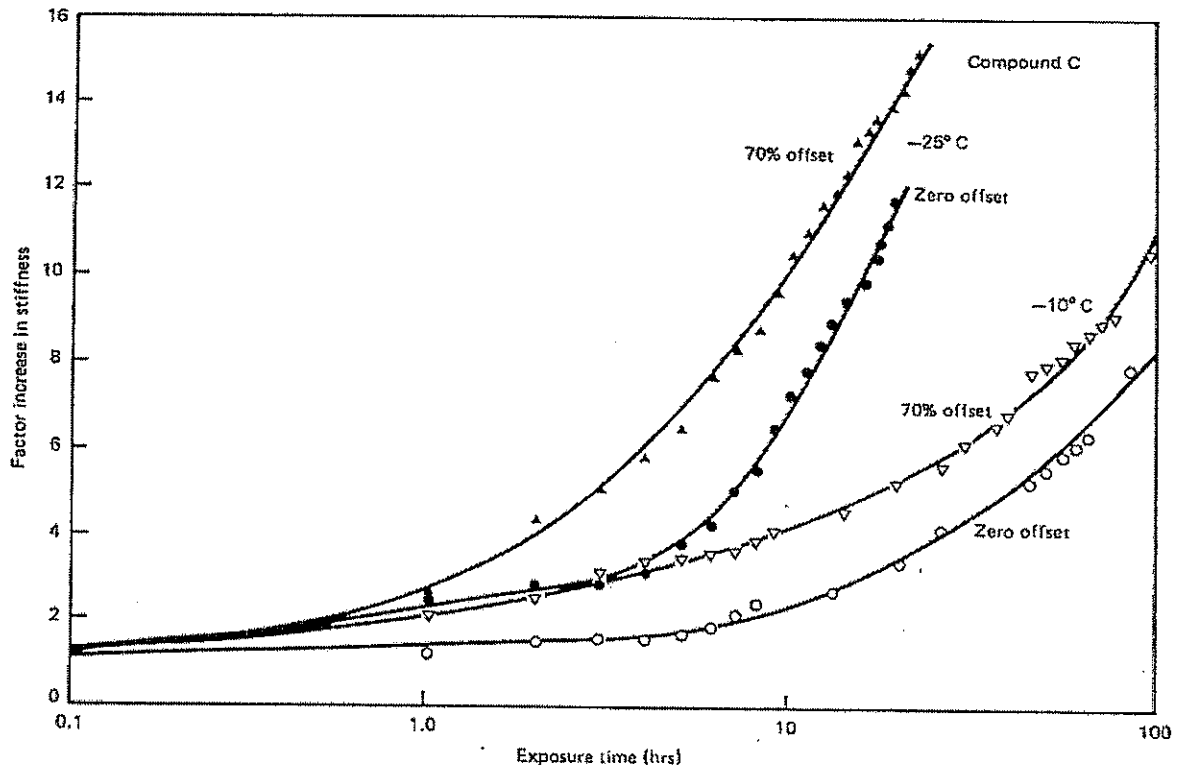
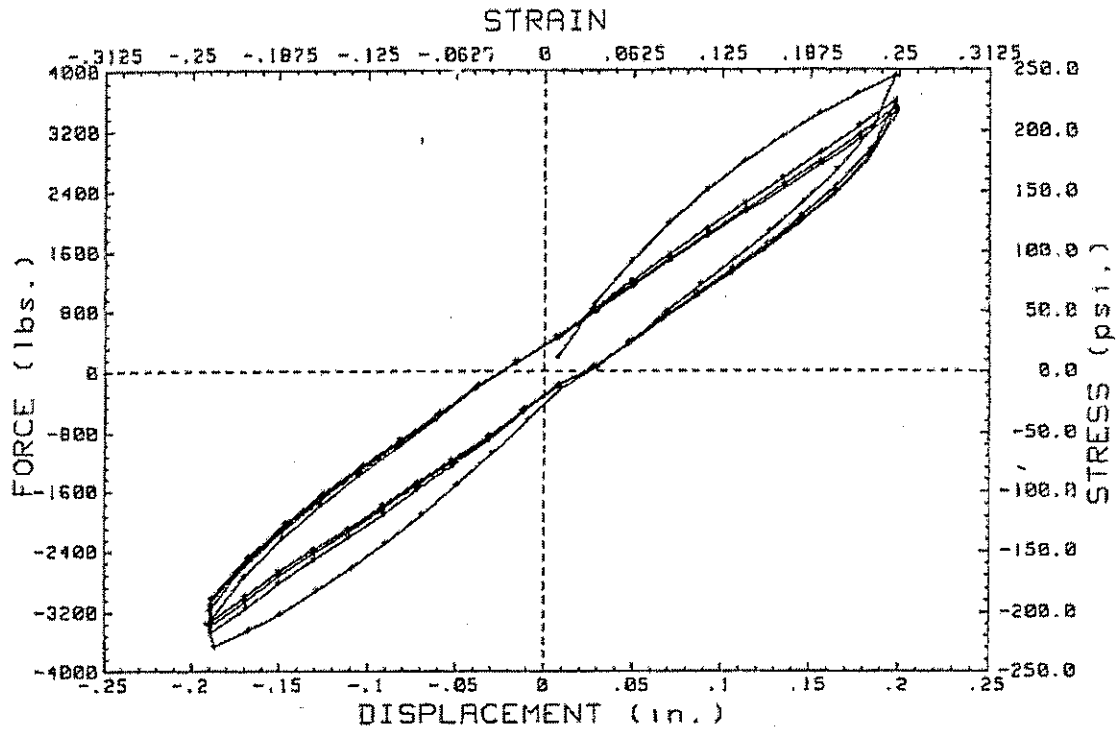
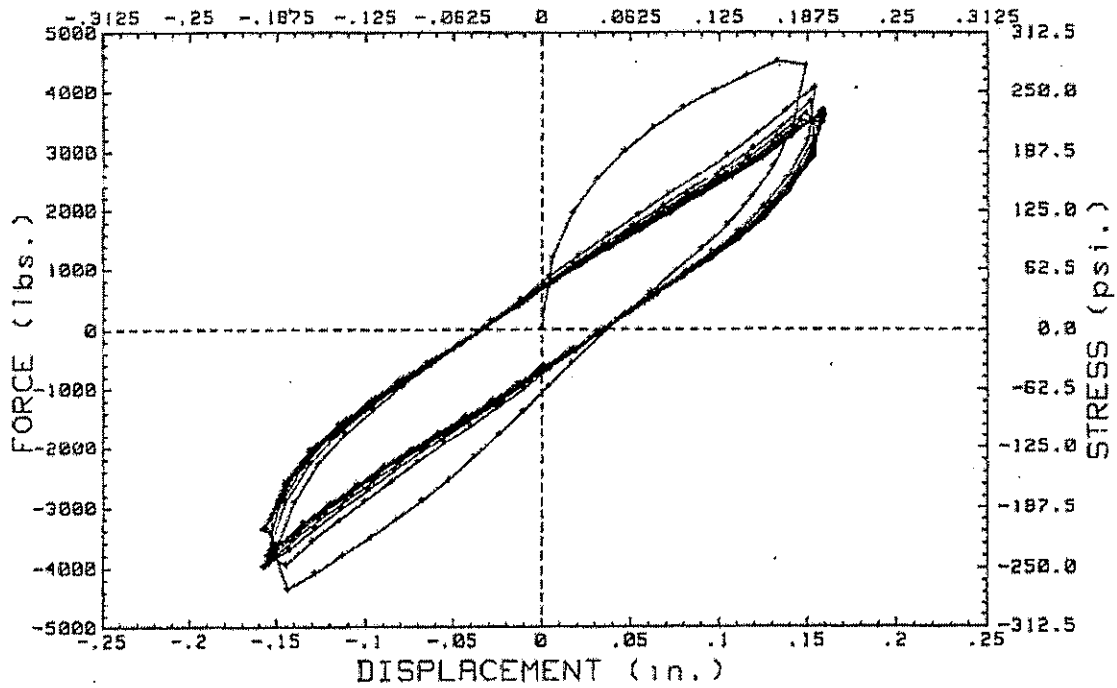


Figure 2.10 Increase in stiffness with exposure time with and without offset shear (Eyre and Stevenson, 1991)



a) at -10 Degrees C



b) at -30 Degrees C

Figure 2.11 Force displacement behavior of low temperature elastomer shear test (Roeder, et al., 1989)

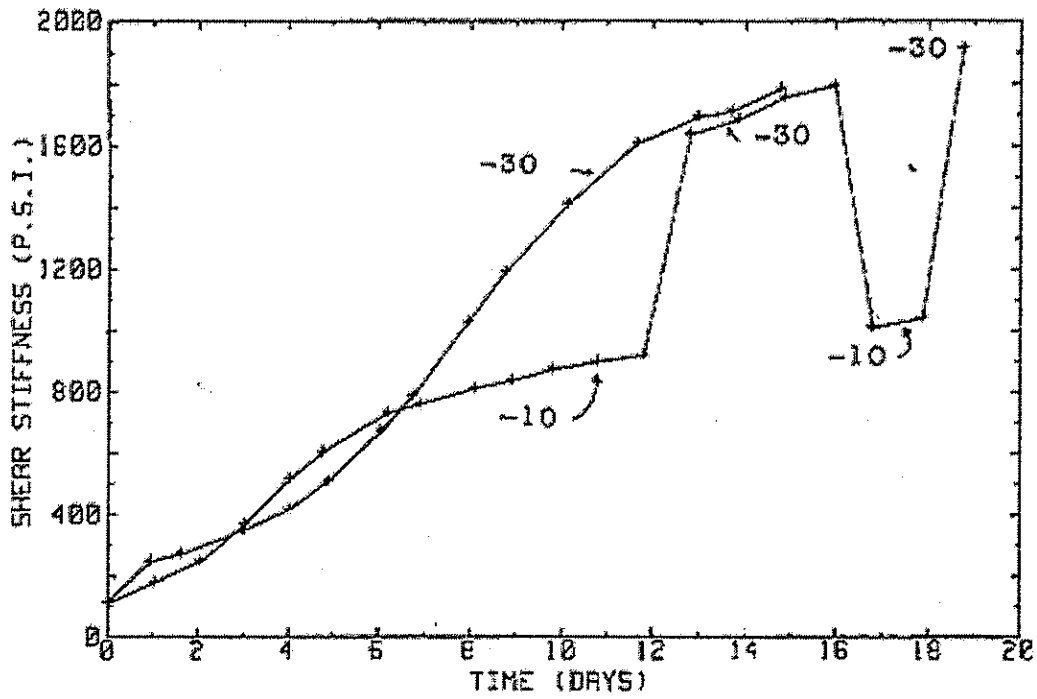


Figure 2.12 Effect of changed temperature on measured stiffness (Roeder, et al., 1989)  
 \*Temperatures are in °C

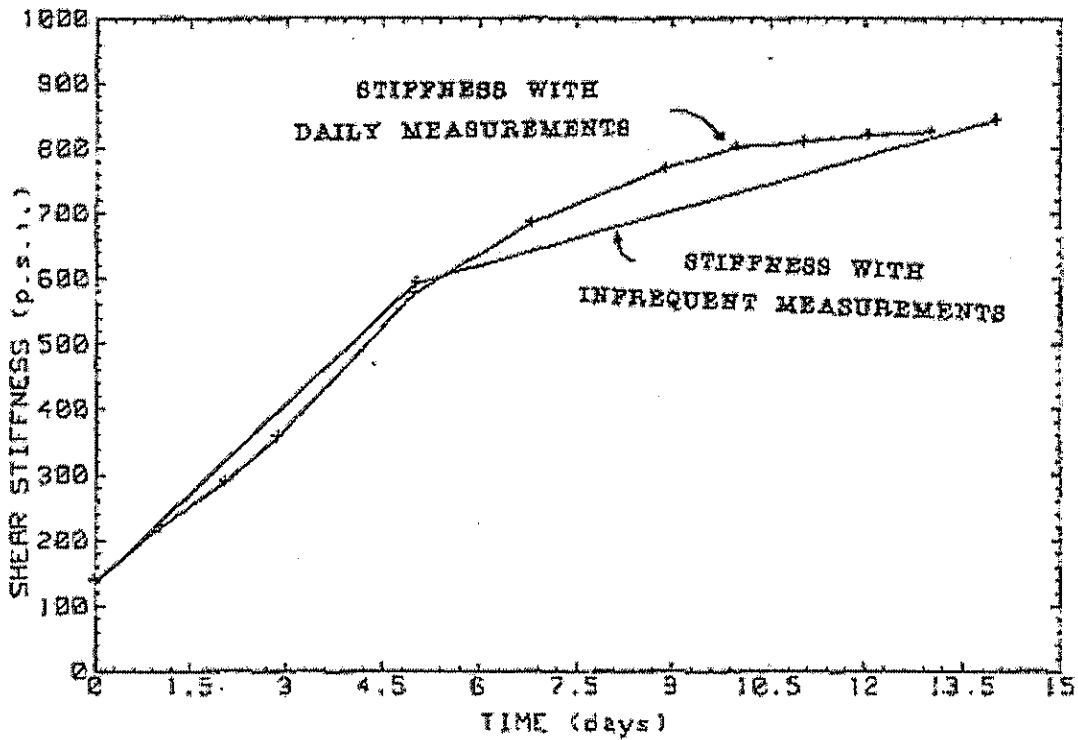
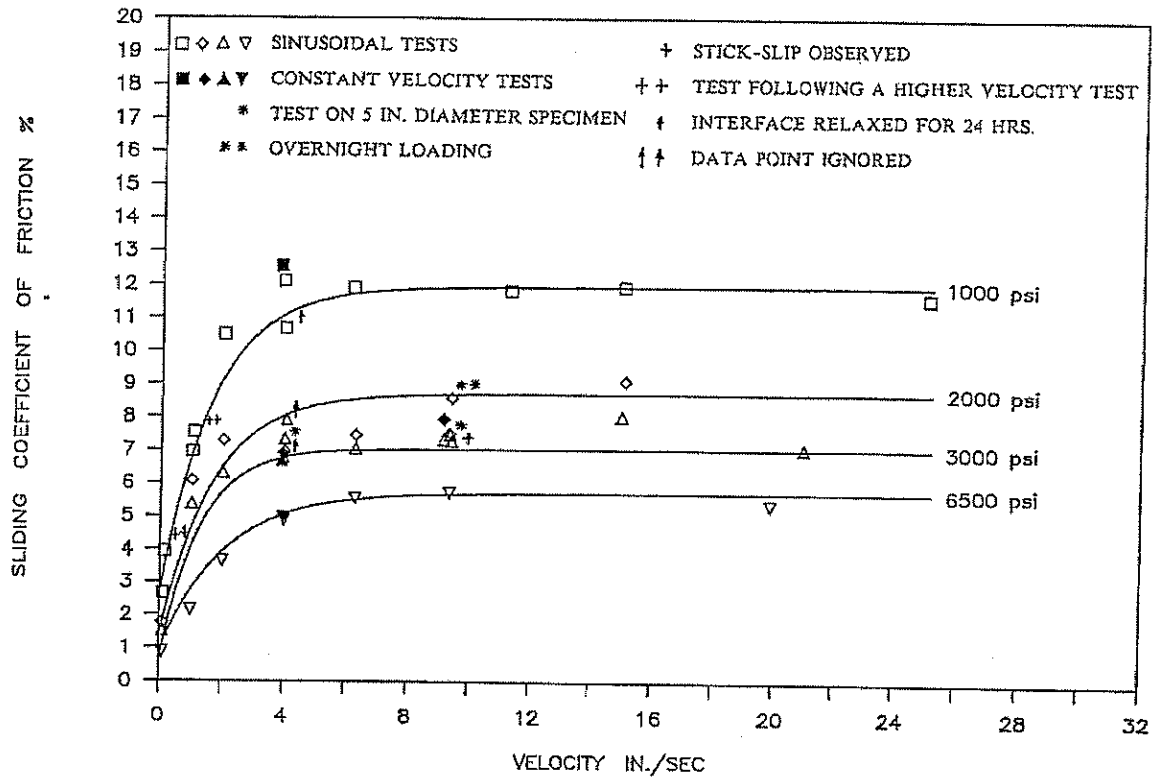


Figure 2.13 Comparison of the measured stiffness of CR55 elastomer compound as a function of time with different test frequencies (Roeder, et al., 1989)



**Figure 2.14** Variation of maximum sliding coefficient of friction with velocity of unfilled Teflon (Mokha et al., 1988)



## **Chapter 3 – Experimental Test Procedures and Apparatus**

The literature review of Chapter 2 identified several circumstances in which the measured stiffness of elastomeric materials was affected by prior testing and described findings regarding the temperature at which the rate of stiffening is highest. Because a seismic event may occur after any temperature history characteristic of Illinois, it was necessary to establish a program of testing that was both relevant and simple enough to characterize the main influences on the low temperature stiffening behavior. As much detail as possible was desired, but the potential for prior testing to influence and interfere with the results had to be contended with. Thus, a number of separate tests were done to establish a test protocol and to ascertain that prior testing according to the test protocol was not producing appreciably different results. The test protocol was developed with the aim that it be simple enough that it could be used as a standard test protocol for the evaluation of low temperature stiffening behavior in future studies.

### *3.1 Description of Test Apparatus*

The test apparatus was designed and constructed to allow control over vertical loads and the application of cyclic lateral loads in a temperature-controlled environment. An elevation view of the test apparatus is shown in Figure 3.1. The test apparatus consists of three fundamental parts: the bearing mount, the loading system, and the controlled thermal chamber.

The bearing mount simulates the structural and thermal characteristics of a bridge pier and receives the load applied to the bearing by the vertical jacks and horizontal actuator. It consists of a 200-mm (8-in.) tall reinforced concrete pedestal cast against the

laboratory strong floor with eight threaded rods protruding up around the perimeter, serving as anchor bolts. Multiple steel shim plates were fabricated, with holes matching the pattern of the threaded rods, to allow for testing bearings of various heights. Type II bearings were fastened to the uppermost shim plate as shown in Figure 3.2. Figure 3.3 shows the stainless steel mating surface for testing Type II bearings and determining TFE coefficient of friction. A removable reinforced concrete pad was fabricated to provide a concrete bearing surface for the testing of Type I bearings as shown in Figure 3.4. Type I bearings were fastened to the glulam loading beam, similarly to a bridge application. Each bearing was mounted and tested transverse to the long axis of the bearing, simulating longitudinal movement of the bridge deck.

The loading system consists of one hydraulic actuator and two hydraulic jacks fitted with servo-controlled valves. Hydraulic pressure was supplied via an electric motor-driven 76 liter per minute (20 GPM) pump. The two 156 kN (35 kip) capacity servo-controlled two-way hydraulic jacks were located beneath the test floor and were used to apply vertical load to the bearing through two 19 mm ( $\frac{3}{4}$  in.) diameter wire ropes. Externally mounted LVDT's provided displacement control over these jacks. The vertical load bears on a 254 x 152 x 12.7 mm (10 x 6 x  $\frac{1}{2}$  in.) steel tube section which, in turn, bears on a 510 x 130 mm (20 x 5  $\frac{1}{8}$  in.) glulam beam. Both the steel tube and glulam beam are loaded in weak-axis bending. The actuator force is applied through the glulam beam, which extends beyond the thermal chamber. A glulam beam was selected because of its low thermal conductivity. The 110-kN (25-kip) capacity servo-hydraulic actuator (shown in Figure 3.5), with  $\pm 75$  mm (3 in.) displacement capacity, applied the reversed cyclic lateral loading. The actuator is mounted to a stiff steel support block.

Both the actuator support block and the 200-mm (8-in.) concrete pedestal are securely fastened to the laboratory strong floor with post-tensioned 38-mm (1½ in.) diameter DYWIDAG anchor bars at multiple locations.

The insulated chamber shown in Figure 3.6 was constructed around the concrete pedestal to allow for low-temperature testing. This chamber consists of two 50-mm (2-in.) layers of polyisocyanurate foam board bonded to provide thermal insulation for the walls and top ceiling. A specially fabricated rubber bellows visible near the penetration of the glulam beam in Figure 3.5 was used to seal this large opening. A double layer clear acrylic window which is visible in Figure 3.6 was installed in one wall of the chamber to allow observation of the bearing during testing.

Data recording was handled by an Apple Macintosh Power PC running LabView version 5.1. A sampling rate of 10 msec was used to measure the output from each of six channels. These channels recorded the positions and loads of the two vertical actuators as well as the position and load of the horizontal actuator.

Bearing temperature was monitored using a Micristar Model 828D heat-processing controller with two separate thermocouples. One thermocouple was installed within the core of each bearing specimen (Figure 3.7), approximately at the center of the bearing. This temperature is used to characterize the temperature of the bearing. The other thermocouple was used to monitor the temperature of the insulated chamber and control the release of the coolant.

The cooling system consisted of a tank of liquid nitrogen fed into the testing chamber through a cryogenic hose and controlled by an ASCO Model 8264G9 solenoid.

valve. A second Apple Macintosh Power PC running LabView was used to record the temperature history of both thermocouples.

### *3.2 Studies for Development of Test Protocol*

One main objective of the research was to establish the likely stiffness of elastomeric bearings as affected by age and temperature in field applications. Because past research (Chapter 2) has identified that many factors can affect the low temperature stiffness of the bearings, comparative studies were done to establish a suitable test protocol that would detail the low temperature stiffening behavior without having the results be appreciably affected by the act of prior testing. The data obtained should be relevant and representative of the properties that can be expected in field conditions. What follows is a discussion of the variables initially believed to have some influence on the behavior of either the elastomer or the polytetraflouroethylene (TFE) sliding surface. In addition, the effect of the configuration of the test setup is explored both for completeness of this discussion and to ensure that the testing procedures themselves do not introduce systematic errors.

The test protocol provides specific instructions for conducting a multitude of cyclic tests at various temperatures, times, vertical compressive stresses, and horizontal cyclic amplitudes and frequencies. A Type II bearing from Structure Number 016-2023 was used to run a number of comparative tests for development of the test protocol. The tests examined the effect of (1) compressive stress, (2) temperature, (3) dwelling of vertical load, (4) initial beam slope, and (5) cyclic frequency. Because other investigators have reported that damage to elastomeric bearings begins at elastomer shear strains of

70%, the test sequences for protocol development and for the majority of tests were limited to 50% shear strain or less, so that the results would reflect the variation of test parameters and not the occurrence or accumulation of damage to the bearings. Higher amplitude tests that may have induced damage in the bearings were conducted only after the time and temperature effects were studied.

### *3.2.1 Effect of Compressive Stress*

The lateral load-displacement response of a bearing was examined at room temperature conditions for different levels of compressive stress. Design dead load stresses are around 3.45MPa (500 psi), as measured on the nominal cross-sectional area of the elastomer. Figure 3.8 shows the lateral load displacement response under a 3.45-MPa (500-psi) vertical compressive stress. Figure 3.9 shows results for a lower vertical compressive stress of 1.73 MPa (250 psi) for comparison. All other test parameters were kept nominally identical, with five cycles of sinusoidal displacement being applied at a frequency of 2 Hz and amplitude of 22-mm (7/8-in). As indicated by the flattened top and bottom portions of Figure 3.9, the lower vertical stress resulted in slip on the TFE sliding surface. No slip was apparent at 3.45 MPa (500 psi). If no slip occurs, the  $\pm$  22-mm (7/8-in) lateral displacement will induce a nominal shear strain of 50% in the elastomer of this bearing. The presence of slip allows the coefficient of friction to be determined. The shear modulus of the elastomer,  $G$ , can be determined from the slope of the load-displacement curve for each test result. In Figures 3.8 and 3.9,  $G$  is approximately 1.25 MPa (180 psi) for 1.73 MPa (250 psi) compressive stress and 1.04 MPa (150 psi) for 3.45 MPa (500 psi) compressive stress, a reduction of approximately

17 percent with increasing compressive stress. Because compressive stress has a small effect on the shear modulus at room temperature, most bearing tests were done at 3.45MPa (500 psi) compressive stress to represent the shear modulus of an elastomer under nominal dead load conditions. A limited number of tests were performed at 1.73MPa (250 psi) to determine the coefficient of friction,  $C_f$ , of the TFE sliding surface.

### *3.2.2 Effect of Low Temperature Exposure*

Figures 3.10 through 3.13 present load-displacement plots that show the effect temperature has on elastomer lateral stiffness and the TFE coefficient of friction. Figures 3.10 and 3.12 are results for room temperature tests. Figures 3.11 and 3.13 show results for tests conducted at  $-18^{\circ}\text{C}$  ( $0^{\circ}\text{F}$ ) after cooling for approximately 24 hours. Each test was performed twice to establish repeatability. The figures illustrate that low temperatures do alter the load-displacement response of the bearing as indicated by the 30% higher initial slope for the cold plots than the warm plots. Furthermore, for the cold bearings, slip on the TFE sliding surface occurs at a higher horizontal load and at a lower value of shear strain. Accounting for the small differences in compressive load, the apparent coefficient of friction increases by about 10% with a reduction in temperature of about  $40^{\circ}\text{C}$  ( $72^{\circ}\text{F}$ ). The test protocol will examine the effects of time and temperatures on shear modulus and apparent coefficient of friction. Because past research has indicated temperatures of fastest crystallization of  $-10^{\circ}\text{C}$  ( $14^{\circ}\text{F}$ ) for neoprene and  $-25^{\circ}\text{C}$  ( $-13^{\circ}\text{F}$ ) for natural rubber, and because these temperatures may realistically occur in Illinois, these temperatures are used to anchor the test protocol.

### *3.2.3 Effect of Dwelling Vertical Load*

Prior research (Chapter 2) indicates that the initial shear offset of a bearing can increase the rate of stiffening of elastomers at low temperatures. Initial offsets, due to thermal movements of the bridge deck, for example, can be expected to produce shear stress in the elastomer. In the preceding tests, the bearing was subjected to a given temperature history, with the compressive load being applied just minutes before application of the reversed lateral displacement cycles. Because compressive stress also induces shear in the elastomer, the presence of continuous dead load in service possibly may increase the rate of low temperature stiffening of the bearings. The influence of sustained compressive stress on lateral response is illustrated in Figures 3.14 through 3.21. Figures 3.14, 3.16, 3.18, and 3.20 are cases at room temperature and low temperature in which the compressive load was applied just minutes before the reversed cyclic lateral loads were applied. Figures 3.15, 3.17, 3.19, and 3.21 represent the bearings under the same nominal testing conditions as Figures 3.14, 3.16, 3.18, and 3.20, respectively, but with the vertical load maintained for 2 hours prior to the reversed cyclic loading. The test results indicate that dwelling the vertical load has little effect on the shear stiffness of the room temperature specimens and only a minor effect on the coefficient of friction of these same specimens. The cold temperature specimens (Figures 3.16, 3.17, 3.20, and 3.21) show a slight increase in shear stiffness and a slight increase in the coefficient of friction over the 2-hour period compared to the corresponding room temperature tests. Thus, there is little observed increase in shear stiffness due to the dwelling of vertical compressive stress and it is concluded that dwelling of vertical load plays only a secondary role to duration of low temperature exposure. Therefore, it was

not considered necessary to maintain vertical stress for a significant length of time prior to lateral load application.

#### *3.2.4 Effect of Initial Beam Slope*

Due to the manner in which vertical loads are applied to the bearing in the test setup, care was taken to ensure that the glulam beam remained in a level horizontal orientation prior to each cyclic test. Figures 3.22 and 3.23 investigate the effect of a deviation of the loading beam from horizontal. Each test was conducted with an initial beam slope of approximately plus or minus  $0.5^\circ$  from the horizontal, with all other parameters remaining unchanged. Figure 3.22 displays the results from a test with the free end of the beam higher than the actuator end of the beam. Figure 3.23 displays the results when the free end of the beam was lower than the actuator end of the beam. The initial beam slope is seen to cause some differences in the load-displacement plots. These differences appear as an overall bias or shift of the horizontal load, either positive or negative, in the lateral load-displacement plots. Therefore, it was necessary to maintain a level beam slope by carefully monitoring both the vertical displacement transducers and a carpenter's bubble level placed on the exposed end of the beam. Both the vertical displacement transducers and the bubble level were monitored during the protocol development tests. Because the bearings were taken from existing bridges, non-uniform loading in the field and manufacturing tolerances may have produced asymmetries in the bearings that become apparent in the lateral load tests. It was not possible to establish the "natural" alignment of the girders and bearings in their service conditions based on physical observations. This deviation may explain the differences in the apparent coefficient of friction evident in Figures 3.22 and 3.23.

### *3.2.5 Effect of Cyclic Frequency*

The effect of loading at cyclic frequencies of 0.5, 1, and 2 Hz with a constant sinusoidal amplitude of  $\pm 22$  mm (7/8 in.) is shown in Figures 3.24, 3.25, and 3.26 respectively. The elastomer shear stiffness and apparent coefficient of friction varied by less than 5% as the frequencies varied from 0.5 to 2 Hz. Of greater significance, the lower frequency tests resulted in smoother load-displacement plots and display less “spiking” on displacement reversal. This trend may reflect the dynamic characteristic of the test setup, including the rotation (and rotational inertia) of the loading beam under rapid load reversals. Therefore, because the transition from “smooth” results was encountered at 1 Hz, this frequency was used for horizontal cyclic displacements under 25 mm (1 in.). Where higher displacements are required (e.g. to achieve desired displacements in thicker elastomeric bearings, or to test Type II bearings at higher cyclic amplitudes), a slower cyclic frequency was needed to achieve stable results. However, no tests were performed at a frequency lower than 0.5 Hz.

### *3.2.6 Summary of Test Protocol Development*

Based on the preceding discussion, the most significant parameters for testing are low temperature exposure for elastomer shear modulus determination and vertical compressive stress for TFE coefficient of friction determination. Based on the preceding tests, a test protocol (described in Figure 3.27) was developed. Most of the tests are to be conducted at 3.45 MPa (500 psi) vertical stress and displacements corresponding to 50% shear strain (assuming no slip) to reflect normal service conditions and to enable comparison between bearing specimens. Two distinct low temperature histories were used, as shown in Figure 3.28, emphasizing exposure to  $-10^{\circ}\text{C}$  and  $-25^{\circ}\text{C}$  while allowing

the effects of duration at low temperatures to be identified. Bearing 1 and Bearing 2 designate two distinct bearings obtained from a single bridge. In the absence of contradictory information, it may be assumed that these bearings are nominally identical in manufacture and original properties. Based on the literature review, frequent testing has little effect on the stiffness measurements. Therefore, periodic tests were performed during the cooling period at intervals of 6 hours. For practicality, these times were 8am, 2pm and 8pm. The 12-hour period from 8pm to 8am was used for cooling to the low temperatures required by the test protocol (Figure 3.28). This figure also indicates the times at which the three daily tests were performed.

The protocol includes tests in which reduced vertical bearing stresses and/or increased horizontal cyclic amplitudes are used, so that slip is induced in order to evaluate the apparent coefficient of friction for all Type II bearings. All tests are described in tabular form as part of the Appendices.

### *3.3 Bearing Test Procedure*

Two bearings from each bridge were tested in the experimental test setup. Bearing 1 was tested according to Protocol 1 and Bearing 2 was tested according Protocol 2 as described in Section 3.2.6. After completion of the test protocol, the ASTM materials tests were performed as needed on portions of the used bearings only. The tests on samples of elastomer cut from the tested bearings were done to assess the effects of aging and the effects of strains potentially large enough to induce damage to the elastomer.

The bearings were received with varied amounts of contaminants on the TFE surfaces as described in Chapter 4. These contaminants were not removed prior to testing. The Type I bearings were bolted to the glulam beam with the rubber surface resting on the concrete pad, used to represent the thermal and functional characteristics of a concrete bridge seat. Type II bearings were bolted to the shim plates with a polished stainless steel plate attached to the glulam beam providing the mating surface. This configuration allowed for the determination of the TFE coefficient of friction at various temperatures and vertical compressive loads. The stainless steel plate affixed to the loading beam was cleaned prior to the installation of each Type II bearing.

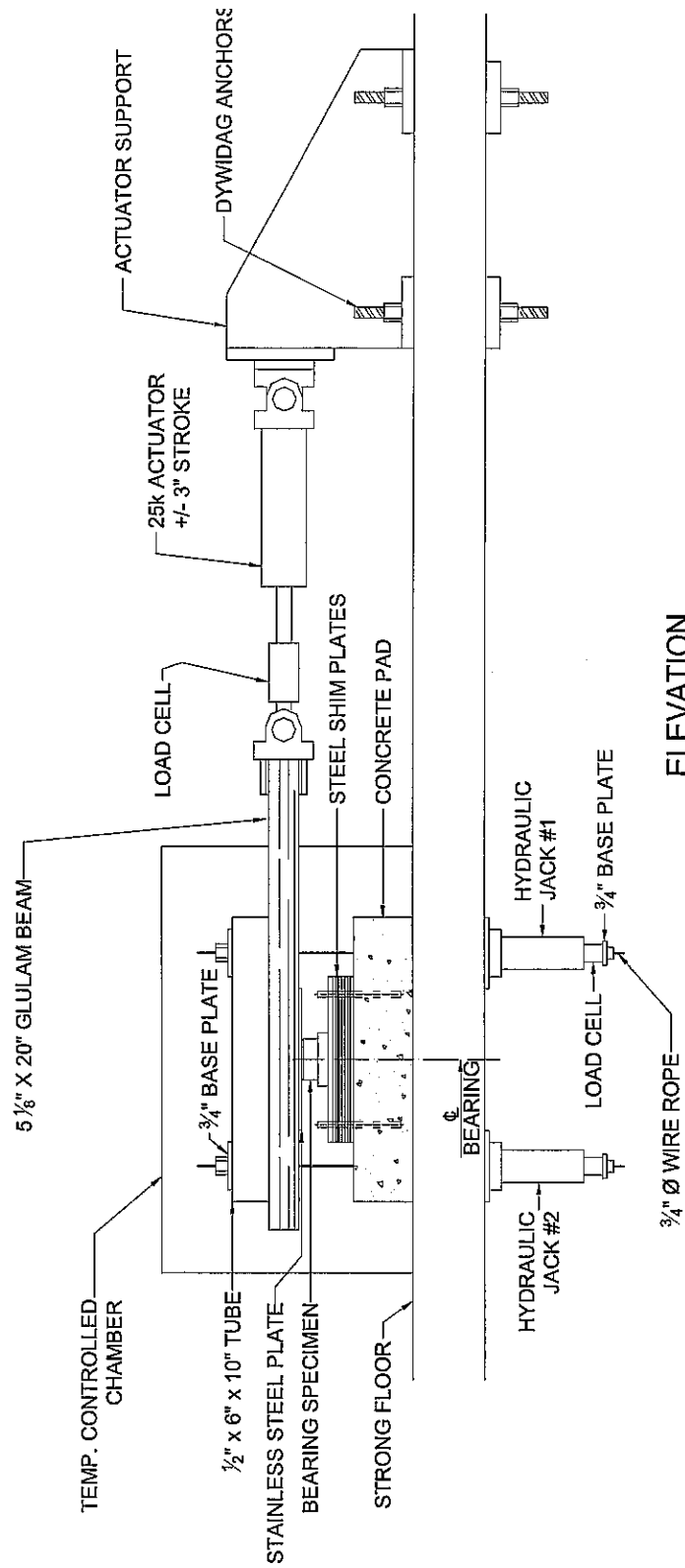
Each cyclic test was performed in a similar fashion. Prior to cyclic loading, the bearing was slowly loaded to the desired vertical compressive stress over a period of several minutes using the two vertical hydraulic jacks. The displacements from the vertical LVDT's were monitored so as to keep the glulam beam in a level orientation. After the desired load was obtained, the displacements in the vertical jacks were locked in order to establish a stable configuration for cyclic testing. Cyclic loads were then applied using a sinusoidal displacement-controlled profile via the horizontal actuator. Testing variables for each test were recorded and are reported in the Appendices. The vertical load was slowly removed after each test and was not maintained during the cooling process.

### *3.4 Material Tests*

In addition to testing the bearings in cyclic shear, an array of standard ASTM tests were performed on samples of the elastomer taken from the bearings after completion of

the reversed cyclic tests. These tests include ASTM D2240, D412, D573, D395 Method B, and D429B. The IDOT Bureau of Materials and Physical Research carried out many of these tests. The results of these tests and their relevance to experimentally determined properties are discussed in Chapter 6.

# LABORATORY TESTING EQUIPMENT



SETUP SHOWN IS FOR TYPE II BEARING  
 MODIFICATIONS FOR TYPE I BEARING DESCRIBED IN TEXT

**Figure 3.1 Laboratory Testing Setup**  
 (Conversion: 1 in = 25.4 mm)

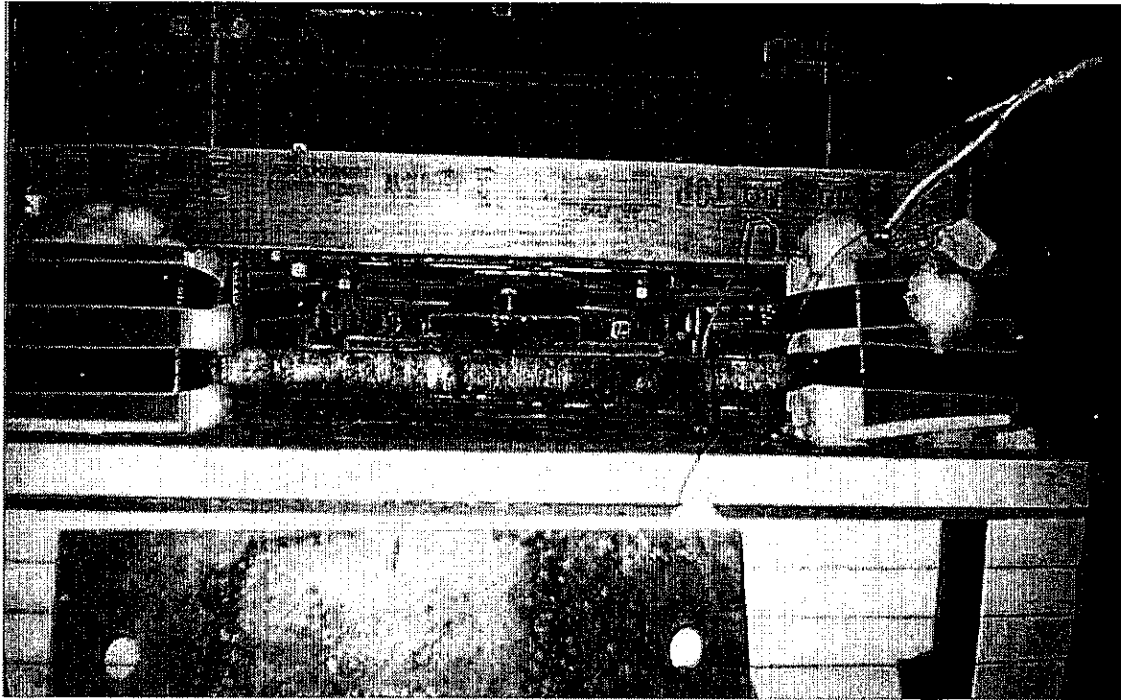


**Figure 3.2** Photo showing Type II bearing installed in test setup, note stainless steel plate for sliding on TFE surface

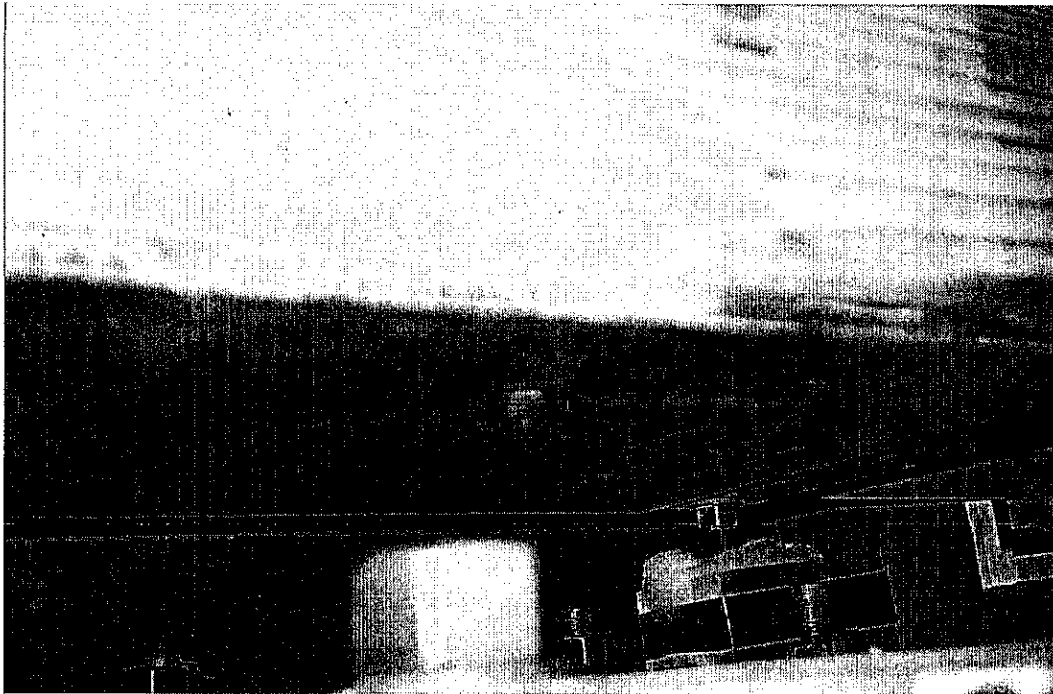


**Figure 3.3** Stainless steel sliding surface mounted to glulam beam

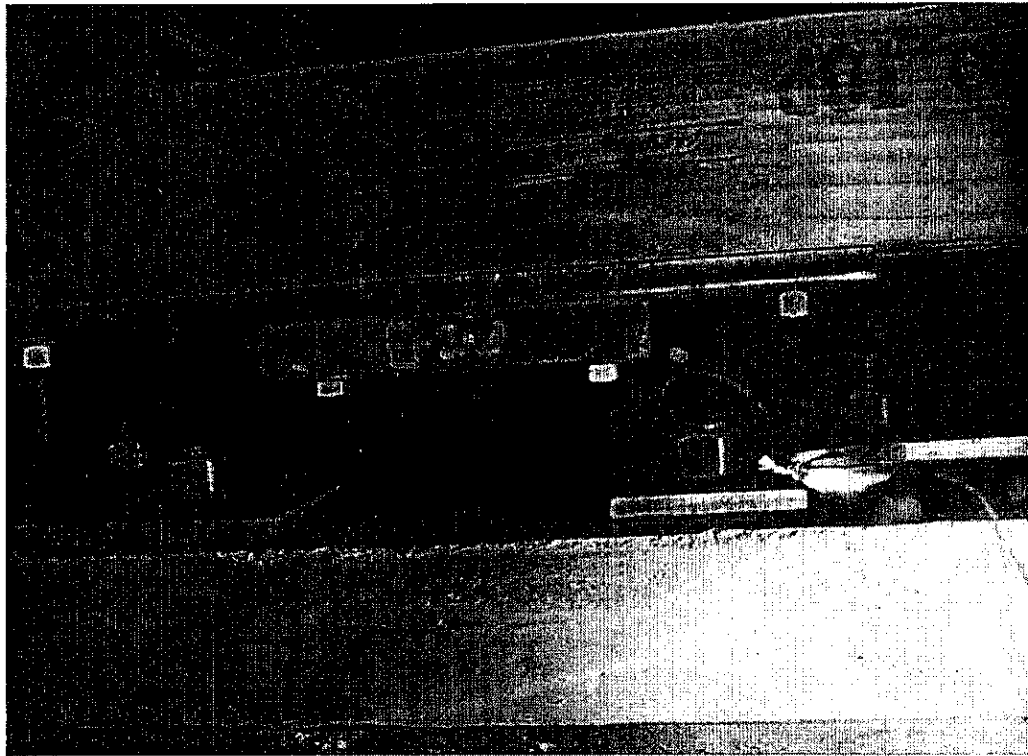


**Figure 3.4** Photo showing Type I bearing installed in test setup, note concrete bearing surface

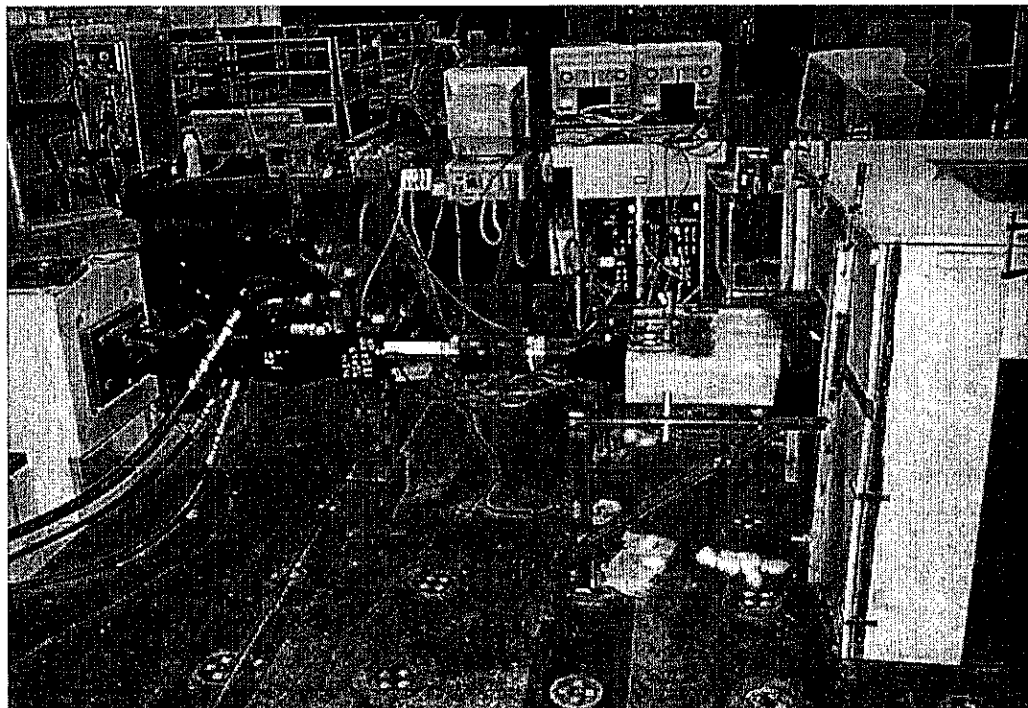


**Figure 3.5** Photo of horizontal actuator mounted to glulam beam extending from cold chamber

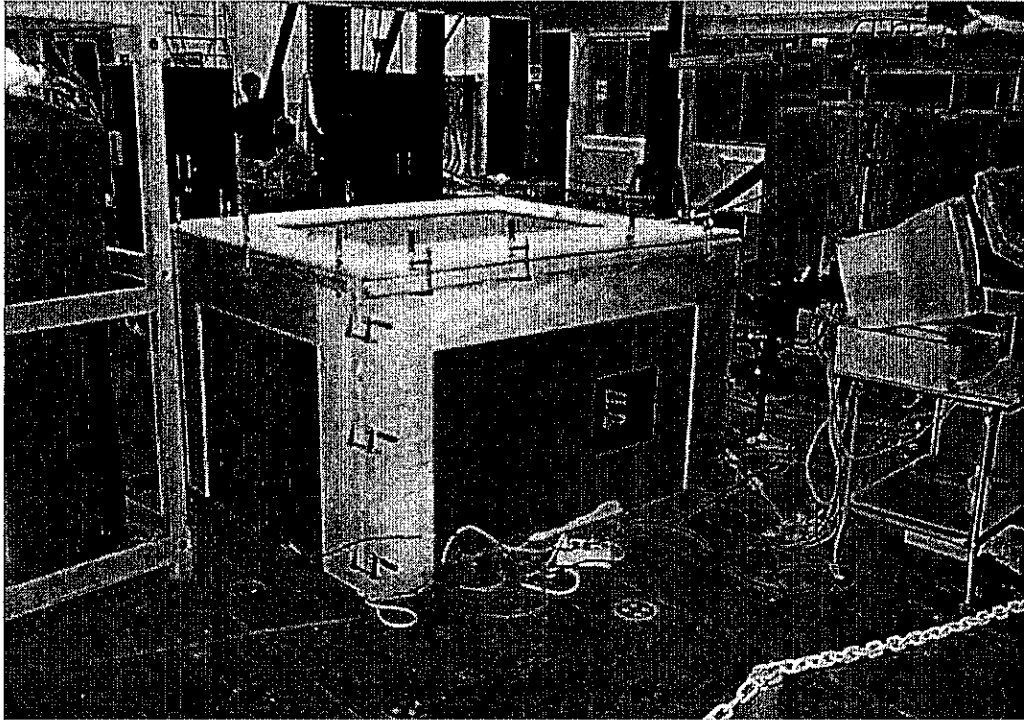


**Figure 3.6** Photo of insulated chamber and liquid nitrogen tank used for cooling system

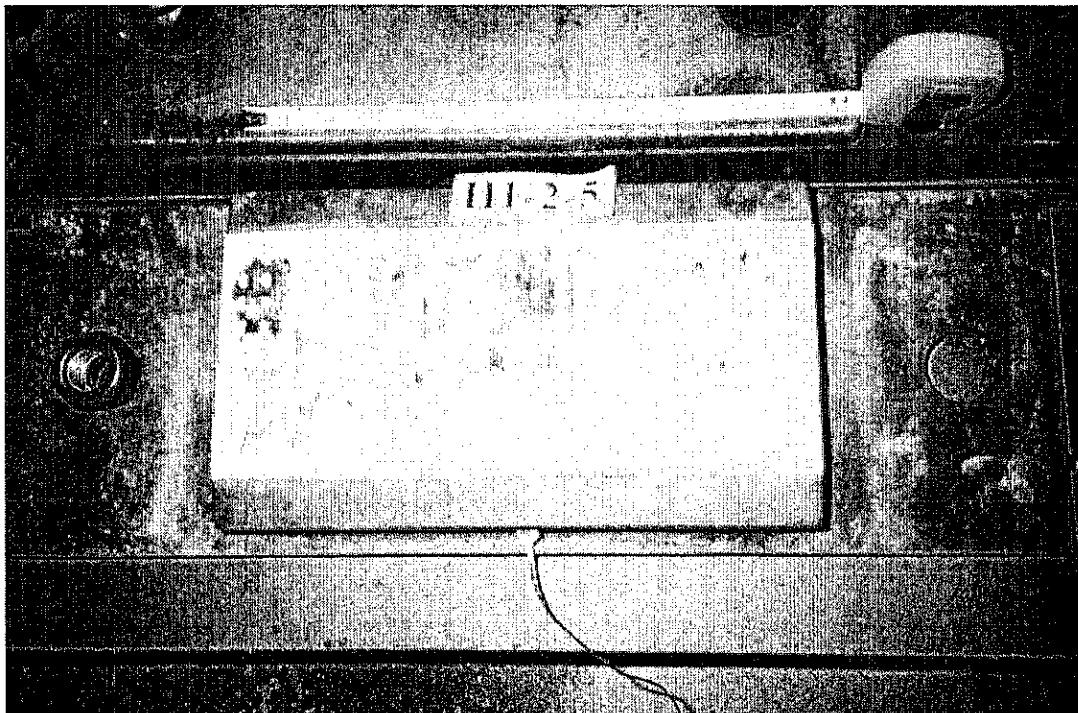


**Figure 3.7** Used Type II bearing with embedded thermocouple

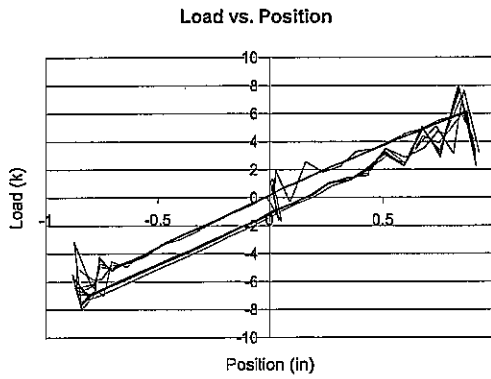


**Figure 3.8**  
2 Hz, 7/8", 500 psi, 21°C<sup>3</sup>

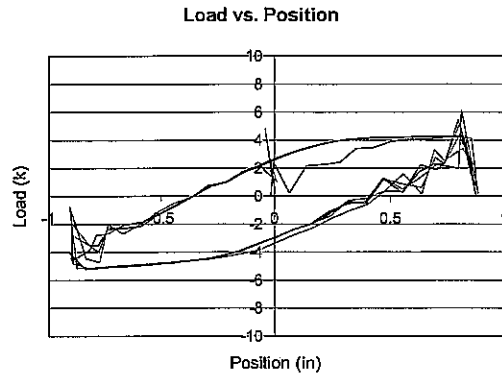


**Figure 3.9**  
2 Hz, 7/8", 250 psi, 21°C

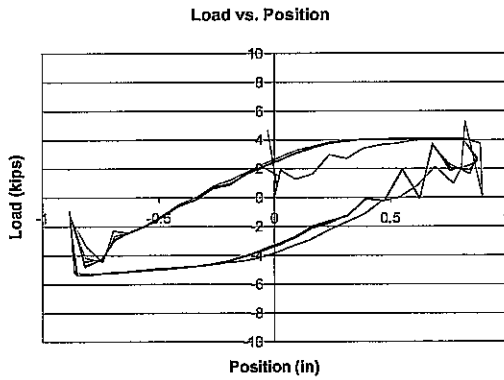


**Figure 3.10**  
2 Hz, 7/8", 255 psi, 20.8°C

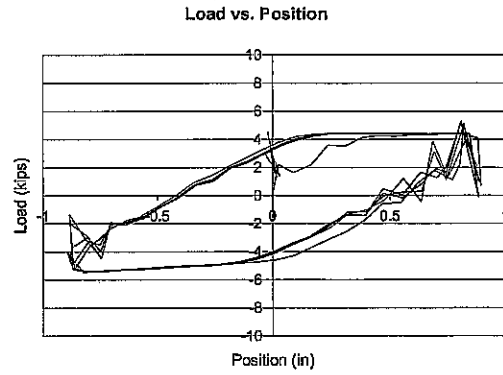


**Figure 3.11**  
2 Hz, 7/8", 247 psi, -18.4°C

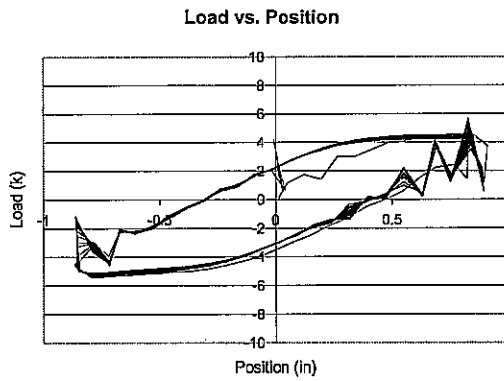


**Figure 3.12**  
2 Hz, 7/8", 257 psi, 25.9°C

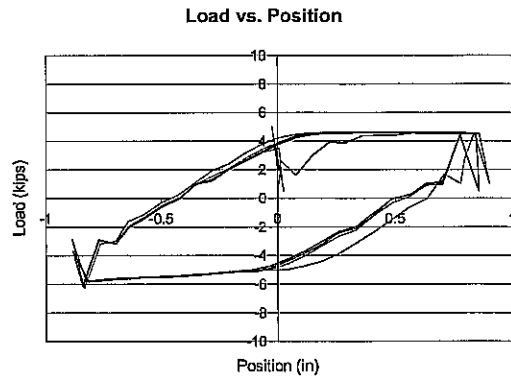


**Figure 3.13**  
2 Hz, 7/8", 249 psi, -18.3°C

<sup>3</sup> Captions in Figures 3.8 to 3.26 are as follows: Cyclic frequency, lateral displacement amplitude, nominal compressive stress, temperature, miscellaneous information.

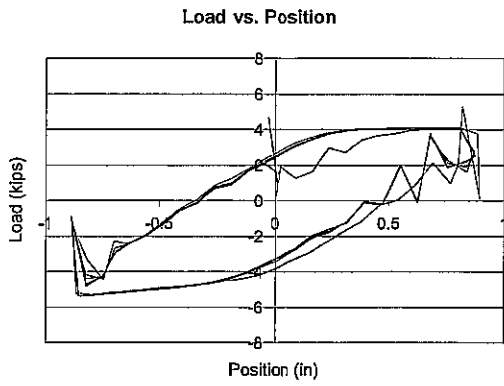


**Figure 3.14**  
2 Hz, 7/8", 255 psi, 20°C

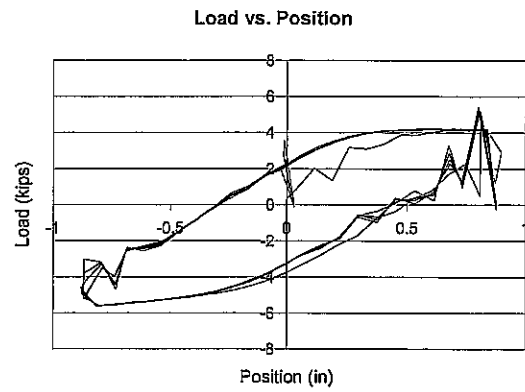


**Figure 3.15**  
2 Hz, 7/8", 248 psi, 20°C, 2 hrs. later

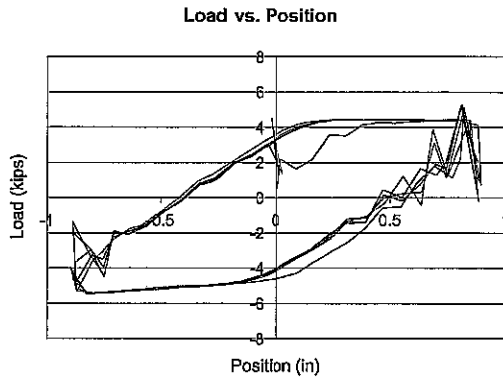


**Figure 3.16**  
2 Hz, 7/8", 247 psi, -18°C

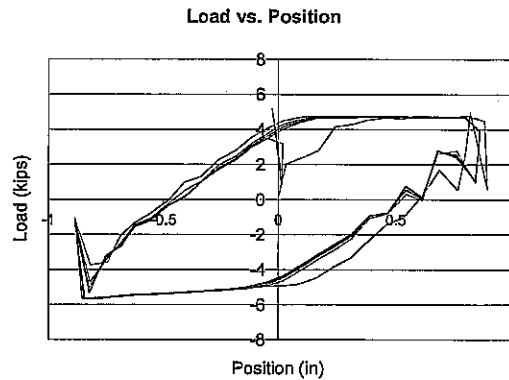


**Figure 3.17**  
2 Hz, 7/8", 255 psi, -18°C, 2 hrs. later

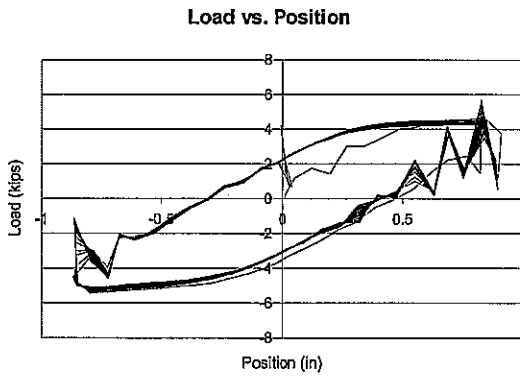


**Figure 3.18**  
2 Hz, 7/8", 257 psi, 20°C

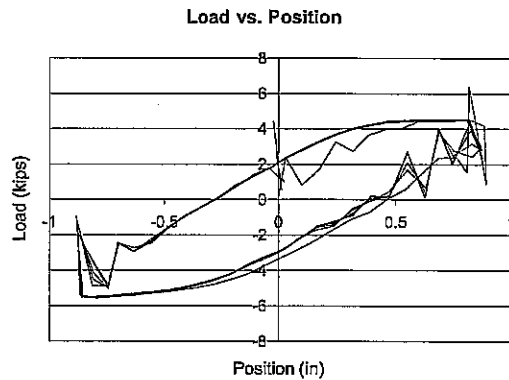


**Figure 3.19**  
2 Hz, 7/8", 250 psi, 20°C, 2 hrs. later

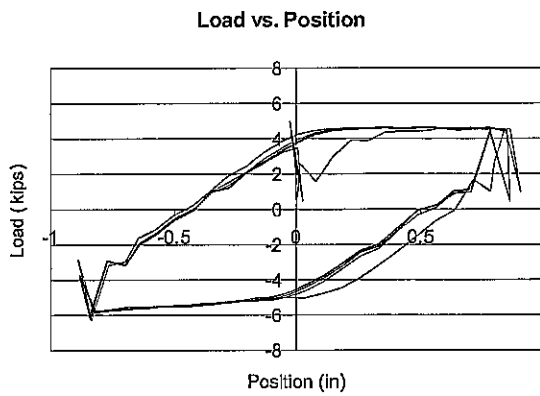


**Figure 3.20**  
2 Hz, 7/8", 249 psi, -18°C

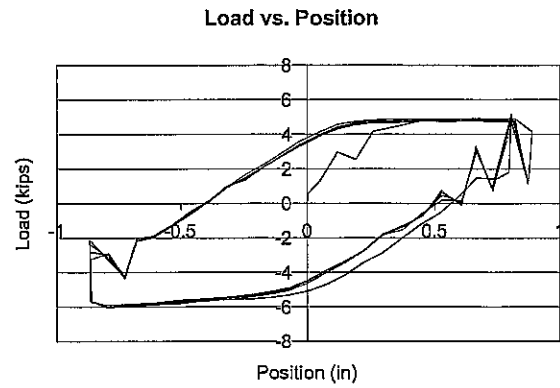


**Figure 3.21**  
2 Hz, 7/8", 247 psi, -18°C, 2 hrs. later

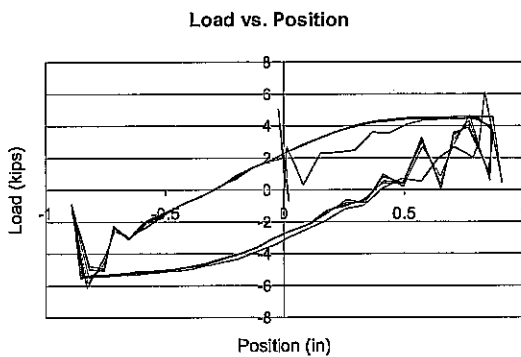


**Figure 3.22**  
2 Hz, 7/8", 246 psi, 21°C, negative slope

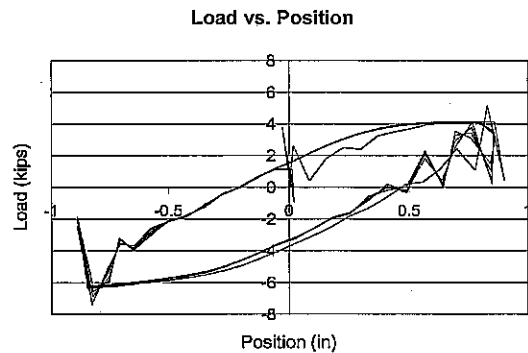


**Figure 3.23**  
2 Hz, 7/8", 263 psi, 21°C, positive slope

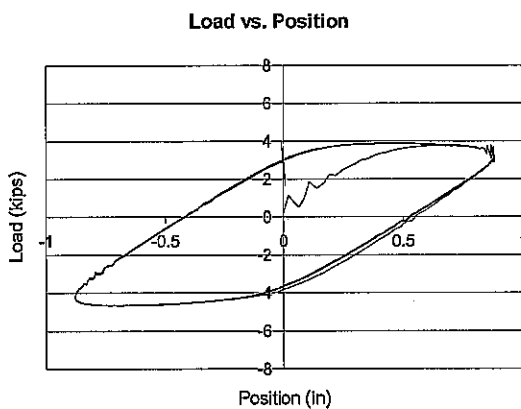


**Figure 3.24**  
0.5 Hz, 7/8", 249 psi, 21°C

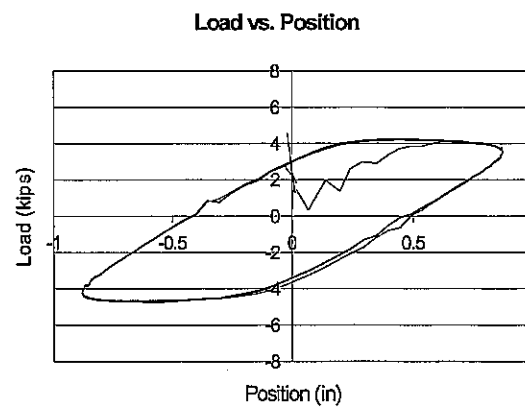


**Figure 3.25**  
1 Hz, 7/8", 250 psi, 21°C

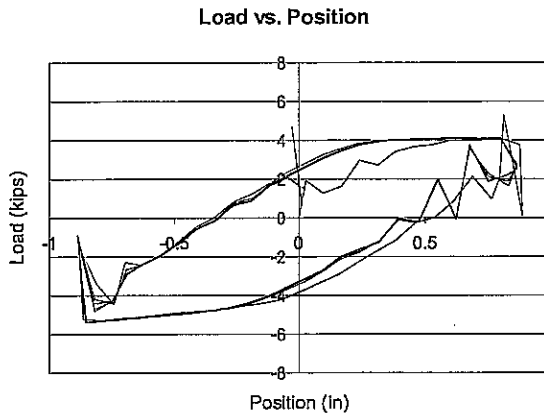


**Figure 3.26**  
2 Hz, 7/8", 255 psi, 21°C

Sunday afternoon: Insert Bearing 1 into test apparatus and prepare for 8pm test.

Sunday 8pm: Run tests on Bearing 1 at 250, 500, and 750 psi, 50% shear strain. Start cooling with set point at  $-15^{\circ}\text{C}$  or lower to reach  $-10^{\circ}\text{C}$  inside bearing by Monday 8am.

Monday, 8am, 2pm, and 8pm: Run tests at 500 psi and 50% shear strain. Bearing temperature should be held at  $-10^{\circ}\text{C}$ .

Tuesday 8am, 2pm, and 8pm: Run test at 500 psi and 50% shear strain. Bearing temperature should be held at  $-10^{\circ}\text{C}$ .

Wednesday 8am: Run test at 500 psi and 50% shear strain. Begin cooling to  $-25^{\circ}\text{C}$ . Adjust set point so that bearing will reach  $-25^{\circ}\text{C}$  by 6pm.

Wednesday 2pm and 6pm: Run test at 500 psi and 50% shear strain. Bearing temperature should be held at  $-25^{\circ}\text{C}$ .

Thursday 8am and 1pm: Run test at 500 psi and 50% shear strain. Bearing temperature should be held at  $-25^{\circ}\text{C}$ .

Thursday 6pm: Run tests at 250 psi (50% shear strain), 500 psi (100% and 200% (0.5 Hz) shear strain), and 750 psi (100% and 200% (0.5 Hz) shear strain). Remove Bearing 1 from test apparatus. Warm stainless steel plate with heat gun for 10 minutes (or as necessary) to remove any frost accumulation resulting from condensation. Once no condensation forms, dry stainless steel plate and clean with rubbing alcohol. Insert warm Bearing 2 with thermocouple inserted. Begin cooling to  $-25^{\circ}\text{C}$ , using set point low enough to reach  $-25^{\circ}\text{C}$  by Friday 8am.

Friday 8am, 2pm, 8pm: Run test at 500 psi and 50% shear strain. Bearing temperature should be held at  $-25^{\circ}\text{C}$ .

Saturday 8am: Run test at 250, 500, and 750 psi, 50% shear strain. Following tests, turn off nitrogen system and open thermal chamber. Position fan to dry any condensation off plates by Sunday afternoon. Repeat process for Bearing 1 and 2 of another set.

**Figure 3.27** Typical Schedule for Test Protocol  
(All tests are 5 cycles and 1 Hz unless noted)

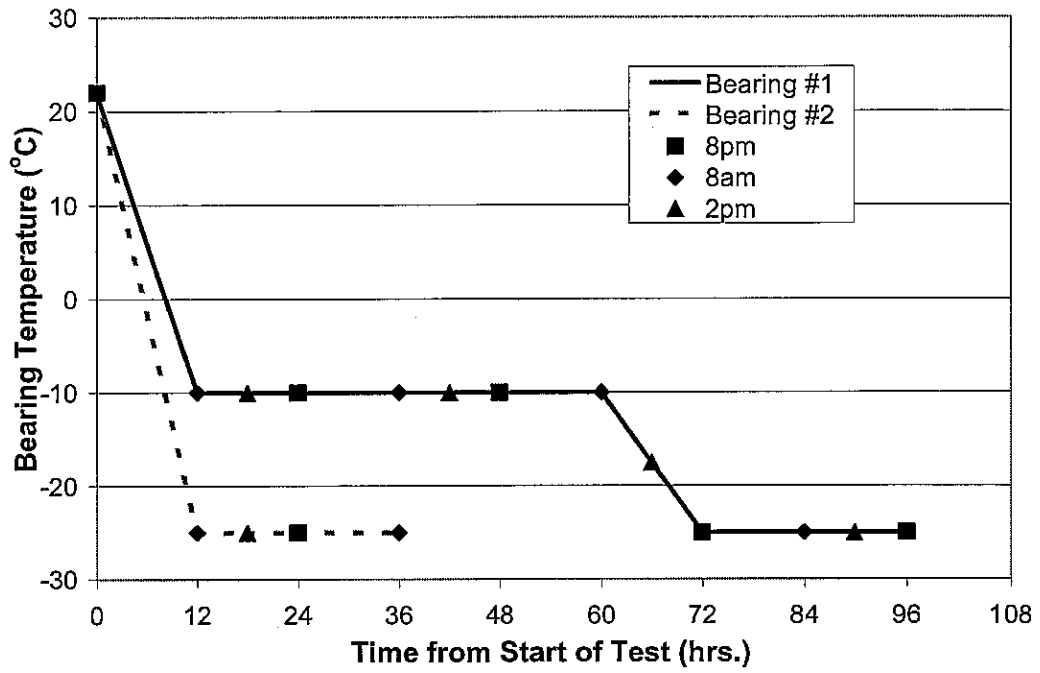


Figure 3.28 – Protocol Temperature History and Test Times

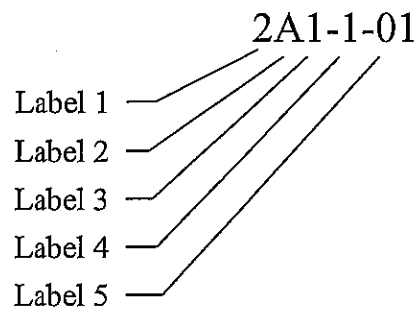
## Chapter 4 – Bearing Description and Reporting Format

Physical descriptions of the bearings, along with a description of the identification scheme used to identify the bearings throughout this report are provided in the following sections.

### *4.1 Bearing Identification Convention*

Bearings tested in this research program came from a number of locations. They include new Type I bearings and both new and used Type II bearings. The term “used” indicates that the bearings were removed from service in existing bridges during rehabilitation operations. A summary of bridge structure number/source, bearing type, bearing size, assumed elastomeric compound (based on results from flame test), and approximate years in service is included as Table 4.1. This table also correlates these physical descriptors with the identification numbers used throughout the report. An initial reference system was used which contained information about the bridge location and a bearing number within each set from a particular location. However, in order to provide the most information in the bearing reference, an alternate numbering system was established. This information is labeled “Report Reference” and its format is described on the next page.

A typical report reference is:



Where:

**Label 1** indicates bearing type

- 1 = Type I bearing
- 2 = Type II bearing

**Label 2** indicates bearing source

- A = Structure #016-2023
- B = Structure #010-0012
- C = Structure #010-0013
- D = New Type I bearing
- S = New Type II bearing from Structural Rubber Products

**Label 3** indicates a sequential bearing number from a particular source

**Label 4** indicates test protocol used during testing

- 1 = Protocol "1"
- 2 = Protocol "2"

**Label 5** indicates sequential test number for a particular bearing

#### *4.2 Description of Used Bearings*

Bearings were obtained from four bridges undergoing rehabilitation in Illinois. Their structure number/source is summarized in Table 4.1. The bearings, being 8 to 10 years old, exhibited signs of wear. Typically, the TFE surfaces were worn unevenly and showed visible signs of contamination, however, the dimples were still clearly visible, indicating the extent of such wear. Figures 4.1 and 4.2 show the initial conditions of the used Type II bearings. The steel plate to which the TFE had been bonded in some cases had corroded, breaking the bond to the TFE surface. Bulging of the elastomer material was evident in some cases, as was corrosion of the steel mounting plates. A record of initial dimensions and conditions was established and this information is presented in Table 4.2.

#### *4.3 Description of New Bearings*

In addition to the used bearing population, several new bearings were also tested using the same test protocol. The new bearings consisted of two Type I bearings and one Type II bearing. Photos of these bearings are shown in Figures 4.3 and 4.4. The Type I bearings came from a bridge construction site south of Lexington, IL on Rt. 66. These bearings had been installed on the bridge but were removed because of an unrelated problem during construction that resulted in the bearings requiring replacement. The bearings had never been subjected to traffic loading, although they had been outdoors for some period of time. The new Type II bearing was supplied by Structural Rubber Products, located in Springfield, IL.

**Table 4.1 Bearing Information and Report Reference Summary**

Bearing Number	Report Reference	Bridge Location/Source	Structure #	Bearing Type	Flame Test*	IDOT Bearing Reference	Approx. Years in Service
H1-2-1	2A1-1	Hillside, IL	016-2023	II	Yes - N.R.	7-b	8
H1-2-2	2A2-2	Hillside, IL	016-2023	II	Yes - N.R.	7-b	8
R1-2-1	2B1-1	Rantoul, IL	010-0012	II	Yes - N.R.	7-b	10
R1-2-2	2B2-2	Rantoul, IL	010-0012	II	Yes - N.R.	7-b	10
R2-2-1	2C1-1	Rantoul, IL	010-0013	II	Yes - N.R.	7-b	10
R2-2-2	2C2-2	Rantoul, IL	010-0013	II	Yes - N.R.	7-b	10
E1-1	1D1-1	New Bearing/IDOT	N/A	I	Yes - N.R.	9-c	New
E1-2	1D2-1	New Bearing/IDOT	N/A	I	Yes - N.R.	9-c	New
N2	2S1-1	Structural Rubber Prod.	N/A	II	No - Neo	7-b	New

\* If material supports combustion (Yes) it is assumed to be natural rubber (N.R.) if not (No) it is assumed to be neoprene (Neo)

**Table 4.2 Used Bearing Dimension and Initial Condition Summary**

	2A1-1	2A2-2	2B1-1	2B2-2	2C1-1	2C2-2
Base Plate Length	23"	22 15/16"	22 11/16"	22 9/16"	22 9/16"	22 9/16"
Base Plate Width	8 1/32"	8 1/16"	8 1/16"	8 1/8"	8 3/32"	8 1/16"
Base Plate Height	1 5/16"	1 5/16"	1 5/16"	1 5/16"	1 9/32"	1 5/16"
Elastomer Length	12 3/32"	12 1/16"	12 1/4"	12 3/8"	12 3/16"	12 5/32"
Elastomer Width	7 1/8"	7 1/16"	7 1/16"	7 5/32"	7 9/32"	7 1/4"
Elastomer Height	1 25/32"	1 3/4"	1 3/4"	1 3/4"	1 3/4"	1 13/16"
PTFE Length	12 1/32"	12 1/16"	12 1/32"	12 1/4"	12 1/16"	12 1/16"
PTFE Width	5 1/16"	5 1/32"	5 1/16"	5 1/4"	5 3/16"	5 7/32"

**Initial Condition Comments:**

**2A1-1** Some corrosion of base plate. Fairly even wear toward center of TFE. Wear is primarily in short-direction of bearing. Elastomer in good condition, some bulging on two sides.

**2A2-2** Uneven wear on TFE, wear primarily in long direction of bearings. Elastomer is square in cross-section, but bulging on four sides.

**2B1-1** TFE has irregular very worn, shiny spots. Some corrosion of steel TFE mounting plate. Elastomer in good condition but not rectangular in section, no bulging.

**2B2-2** Chunk of TFE missing and irregular wear pattern. No bulging of elastomer. Some corrosion of mounting plate. Mostly rectangular in section.

**2C1-1** Least corroded mounting plate. More evenly worn TFE. More elastomer bulging than 2C2-2. Looks the best of all Rantoul, IL bearings. Not level across the top but mostly rectangular in cross-section.

**2C2-2** Bearing has been shimmed. Least bulged. TFE is peeling badly, extensive corrosion of all exposed steel plates. All four edges of TFE are worn. Symmetric cross-section.

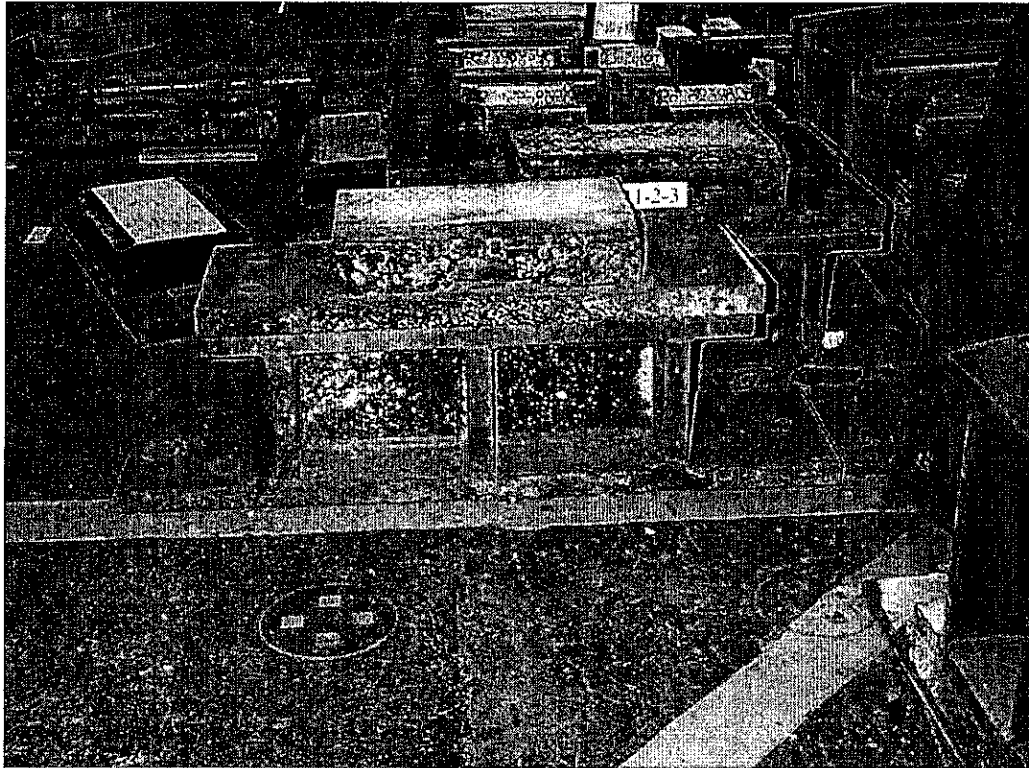


**Figure 4.1** Initial conditions of used Type II bearings. Note corrosion of steel mounting plates and evidence of contaminants on TFE surface.

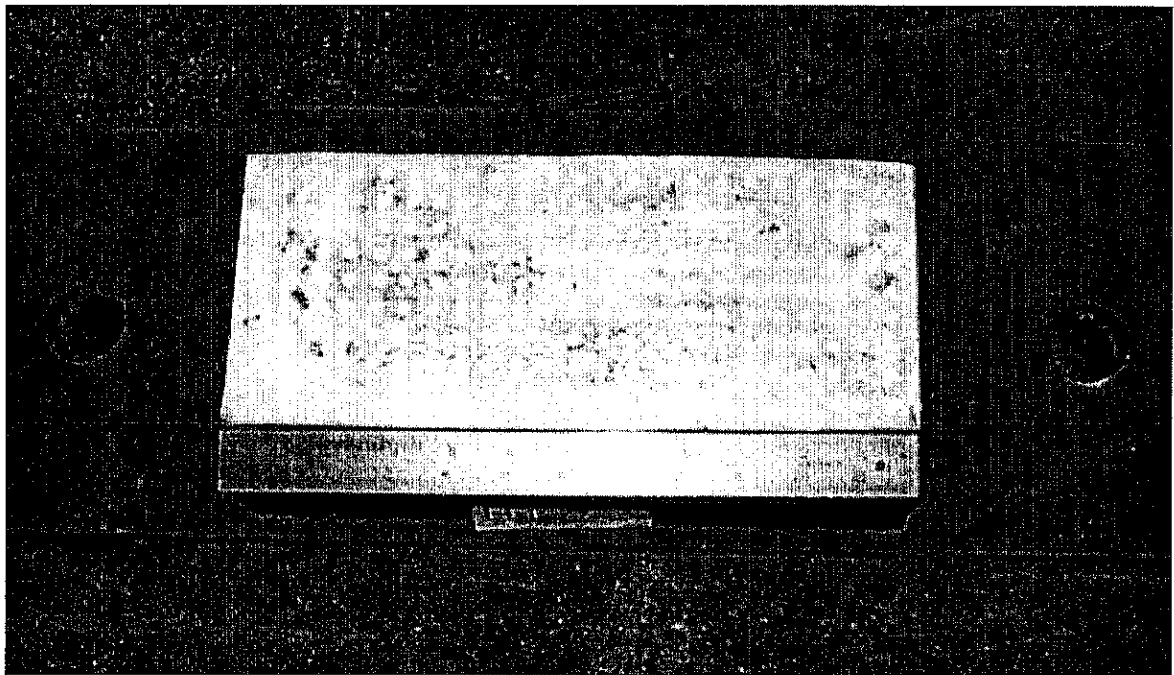


**Figure 4.2** Evidence of contaminants on TFE surface of used Type II bearing

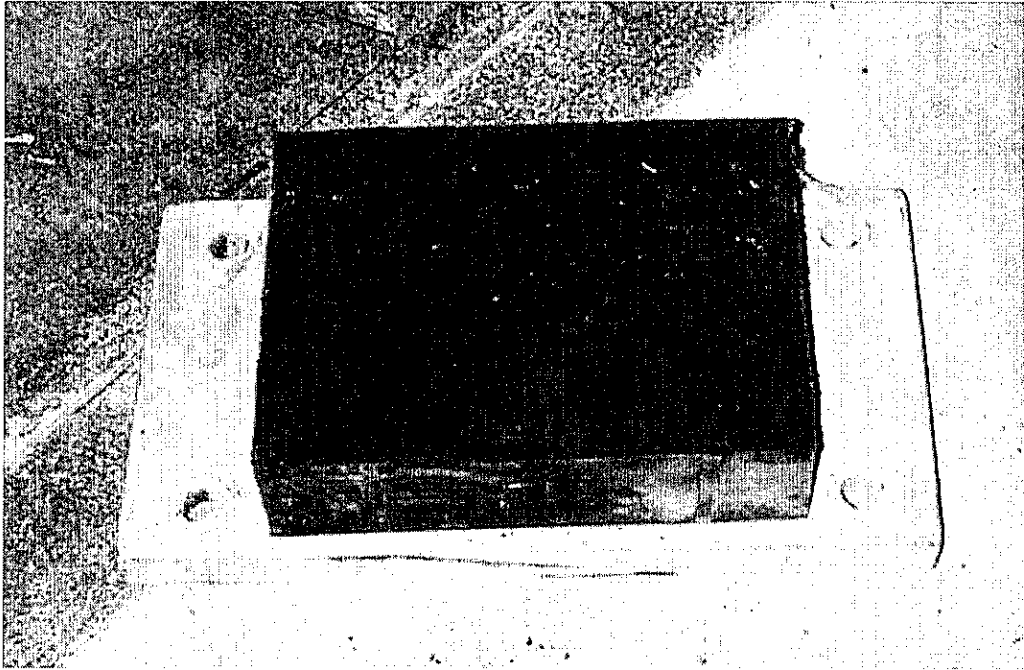


**Figure 4.3** New Type I bearing

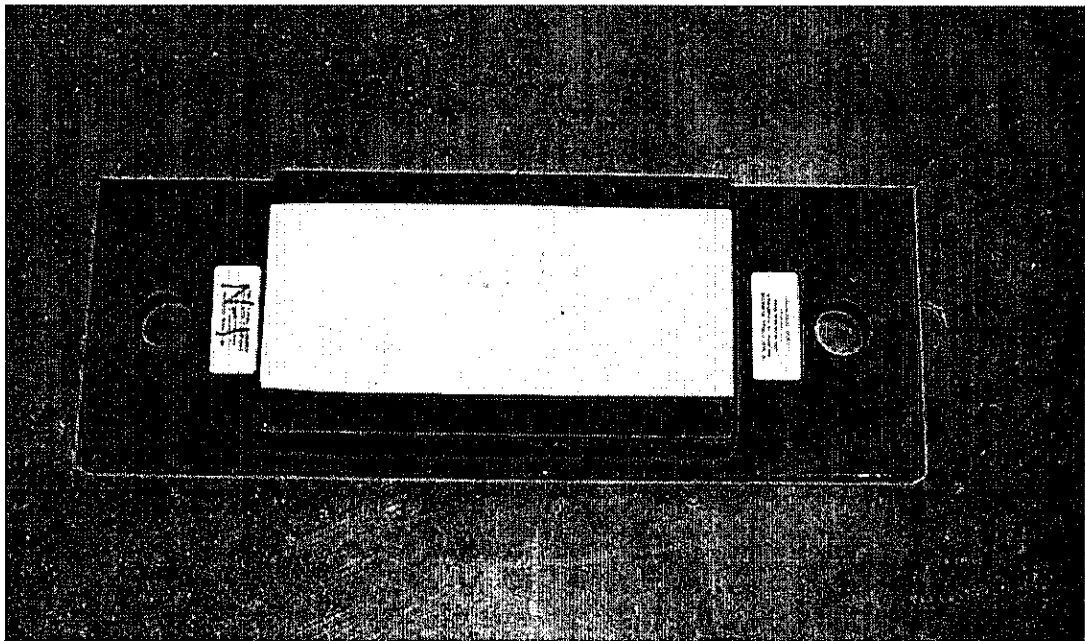


**Figure 4.4** New Type II bearing

## Chapter 5 – Bearing Test Results and Analysis

This chapter describes overall trends and observations gleaned from the test data. Individual test results are provided for all specimens in the appendices of this report.

### *5.1 Characteristic Behavior and Data Reduction*

This section describes a typical test result and its interpretation. Data recorded during the tests were horizontal actuator load and displacement, vertical load and position of each jack, test chamber temperature and internal bearing temperature. Various combinations of these results are plotted for each test in the Appendices. Figure 5.1 shows the hysteretic behavior observed in a typical test. The actuator load is plotted versus the lateral position of the actuator. Often, the first cycle showed a slightly higher stiffness than did subsequent cycles, which displayed very consistent behavior. Figure 5.1a shows a result in which no slip occurred at the TFE-stainless steel interface. Figure 5.1b shows a result where slip did occur at this interface. From these plots, both the shear modulus and apparent TFE coefficient of friction can be calculated. The methods used to calculate these quantities are discussed in the following.

#### *5.1.1 Elastomer Shear Stiffness*

Figure 5.2 graphically presents the manner in which the shear modulus is obtained. The shear modulus, denoted by  $G$ , is calculated as:

$$G = \frac{V}{\Delta} \times \frac{h}{A}$$

where:

$V/\Delta$  = Slope of tangent line A-B

$h$  = Nominal height of elastomer only (excluding reinforcing plates)

$A$  = Plan area of elastomer

The shear modulus was calculated for all tests of all bearings. A graphical interpretation of the quantity  $V/\Delta$  is shown in Figure 5.2. This slope is taken between values nearest  $\pm 25\%$  shear strain, for both directions of the load-displacement plot, and for each cycle of loading and used to calculate the shear modulus for each test. This value of shear strain was selected to accommodate cases where slip occurred. Most tests were conducted for five cycles; therefore 10 values of shear modulus were collected from each test. An average was computed for the data excluding the data obtained for the first quarter cycle and the last quarter cycle, because these cycles did not span over the complete range ( $-25$  to  $+25\%$  shear) used for the calculations. The average values are reported in the summary figures to be discussed herein.

### *5.1.2 Coefficient of Friction*

Because of the difficulty of identifying exactly when slip initiates, the coefficient of friction is defined here as the maximum horizontal load if slip occurs divided by the vertical compressive load applied at the start of the test. This apparent slip coefficient is denoted by  $C_f$  and is calculated as:

$$C_f = \frac{V_{max}}{P}$$

where:

$V_{max}$  = Maximum actuator load during slipping

$P$  = Vertical load applied at start of test

Not all tests of each Type II bearing specimen resulted in slip at the TFE sliding interface. Slip was inferred to have occurred if a flattened portion at the top and/or bottom of the load-displacement plot is apparent, as illustrated in Figure 5.3. The apparent slip coefficient is calculated for both top and bottom portions of the load-displacement plot, similarly to shear modulus. Bearings with higher shear stiffness develop higher lateral loads at a given displacement and they are more prone to overcome friction and slip at the TFE – stainless steel surface. In addition, tests were performed at both lower vertical compressive stress and at higher shear displacements to ensure that slip was initiated in each Type II bearing. Coefficient of friction data was also obtained at both warm and cold temperatures for all bearings. This was done to establish  $C_f$  values for comparison with those values used in design. What is reported throughout this report is an average of the  $C_f$  values, taken from both the “pushing” and “pulling” portions of the load-displacement plots.

## *5.2 Summary Data*

This section summarizes significant trends in the data. Load-displacement plots for each test are provided in the Appendices along with a chart for identifying test

parameter values. The main effects of test variables are described in the following sections. The data files are available on the CD release of this report.

### *5.2.1 Effect of Temperature on Shear Modulus*

As described in previous research studies, shear stiffness increases with reductions in temperature. This observation held true for each bearing tested in this research study. The literature indicates a large range of potential stiffness increases, associated with various elastomer compounds. The used bearings tested in this research program exhibited an increase in stiffness at low temperatures of less than 40%, not by over five hundred percent as found in the studies described in Chapter 2 (e.g. Figure 2.5). The new Type II bearing, however, displayed a cold temperature stiffness which was seven times the room temperature stiffness ( $G_{20}$ ), as shown in Figure 5.4. However, Figure 5.5 shows the limited amount of stiffening observed amongst the used bearings. This difference in stiffening is likely the result of the difference in compounds between the new Type II bearing (neoprene) and the other bearings (natural rubber). An important consideration is that all bearings are assumed to have met the same procurement specification for durometer hardness yet the low temperature performance can vary widely.

### *5.2.2 Effect of Temperature on Coefficient of Friction*

All Type II bearing specimens were tested so as to obtain both shear moduli and apparent TFE coefficient of friction, because both properties are needed for seismic performance evaluations. In terms of general behavior at a given value of normal stress,

a bearing with a relatively stiff elastomer will engage the TFE sliding surface at a lower lateral displacement. Conversely, a bearing with less stiff elastomer will require more lateral displacement to initiate slip. In order to measure the TFE coefficient of friction for each Type II test specimen it was necessary to produce slip at the sliding interface. This was achieved through either increased cyclic amplitude or decreased normal stress. The following trends were observed for the cases where slip initiated.

Decreasing temperatures resulted in increased values of  $C_f$ , as illustrated in Figures 5.6 and 5.7, suggesting that the TFE coefficient of friction is temperature dependent. However, the coefficient of friction did not appear to change with the amount of time held at a given low temperature, suggesting that this property is not time dependent. The values obtained from testing are shown in Figure 5.6 for the used Type II bearings and in Figure 5.7 for the new Type II bearing. These values are typically in the range of 0.17 to 0.25 for cold temperatures ( $-22^{\circ}\text{C}$ ) and between 0.13 and 0.19 for warm temperatures ( $21^{\circ}\text{C}$ ).

One important observation is that all experimentally determined  $C_f$  values are significantly higher than 0.08 as specified in the AASHTO bridge design specifications. The experimentally obtained  $C_f$  values for the used bearings are higher by factors of two and three as shown in Figure 5.6. Even the new Type II bearing displayed significantly increased values of  $C_f$  as shown in Figure 5.7. This finding is an important consideration for use in design and analysis.

### 5.3 Summary of Used Bearing Behavior and Properties

The properties obtained from results of the reversed cyclic tests of the used bearings are summarized in this section. The results for shear moduli are reported for used bearings tested with an applied vertical compressive stress of 3.45 MPa (500 psi) at three specific temperature ranges: 20°C (20 to 22), -10°C (-8 to -12), and -25°C (-23 to -27). All tests of used bearings that induced slip at the sliding interface were used for obtaining  $C_f$  statistical data; results are reported for two temperature ranges, 20°C (20 to 22) and -25°C (-20 to -27). This broader range is justified due to the general stability of  $C_f$  at low temperatures.

As discussed in Section 5.2 above, low temperature is the most important parameter influencing elastomer behavior. Research presented in Chapter 2 suggests that the temperatures of -10°C and -25°C may be the temperatures at which neoprene and natural rubber crystallize most rapidly. The low temperature history and the duration of exposure to low temperatures appear to be of secondary importance. Therefore, only temperature is used in this summary of results, given in Table 5.1. The 6% increase in  $G$  from as the temperature decreases from 20°C to -10°C is a relatively minor change. The mean shear modulus at -25°C is approximately 30% larger than the mean value at 20°C.

Since sliding at the TFE interface can significantly affect the overall behavior of Type II bearings, the  $C_f$  of the TFE interface is a critical parameter. Table 5.2 indicates that the mean value of the coefficient of friction increased only 5% as the temperature decreased from 20°C to -25°C. The mean results presented in the following tables are used in the simulated seismic response studies reported in Chapter 8.

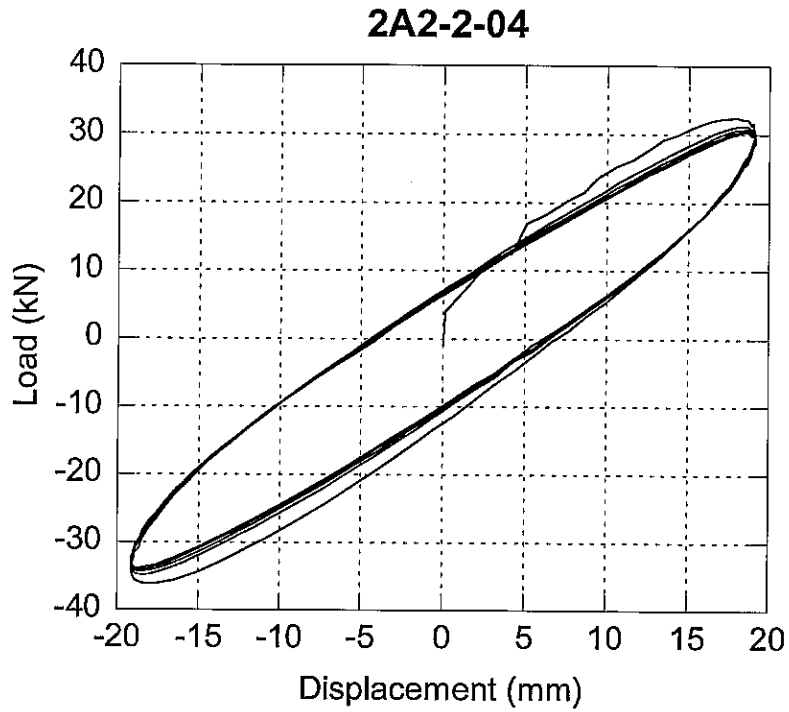
**Table 5.1** Mean shear moduli for used bearings at nominal 3.45 MPa (500 psi) compressive stress.

Property	n	$\mu$	$\sigma$	COV
G (20°C)	4	0.990 MPa	0.110 MPa	0.111
G (-10°C)	15	1.049 MPa	0.106 MPa	0.101
G (-25°C)	20	1.266 MPa	0.100 MPa	0.0792

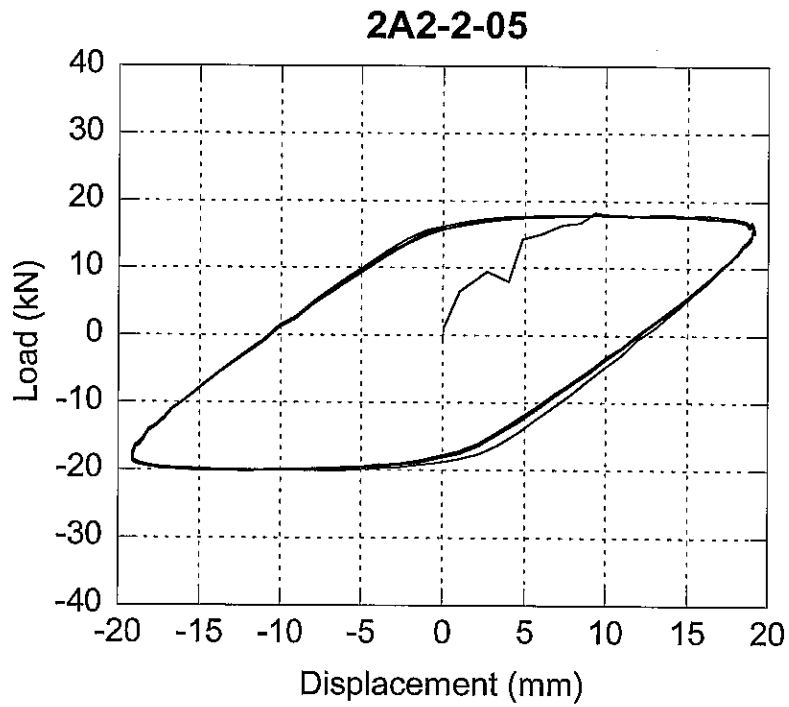
**Table 5.2** Mean coefficient of friction for the TFE interface of used bearings at nominal 3.45 MPa (500 psi) compressive stress.

Property	n	$\mu$	$\sigma$	COV
C <sub>f</sub> (20°C)	12	0.164	0.0188	0.115
C <sub>f</sub> (-25°C)	18	0.218	0.0219	0.1

In Tables 5.1 and 5.2, n = Number of tests in which the property was measured,  $\mu$  = Average of n values,  $\sigma$  = Standard deviation of n values, and COV = Coefficient of variation =  $\sigma/\mu$ .



a) No slip



b) With slip

Figure 5.1 Typical load-displacement hysteresis loops for Type II bearings

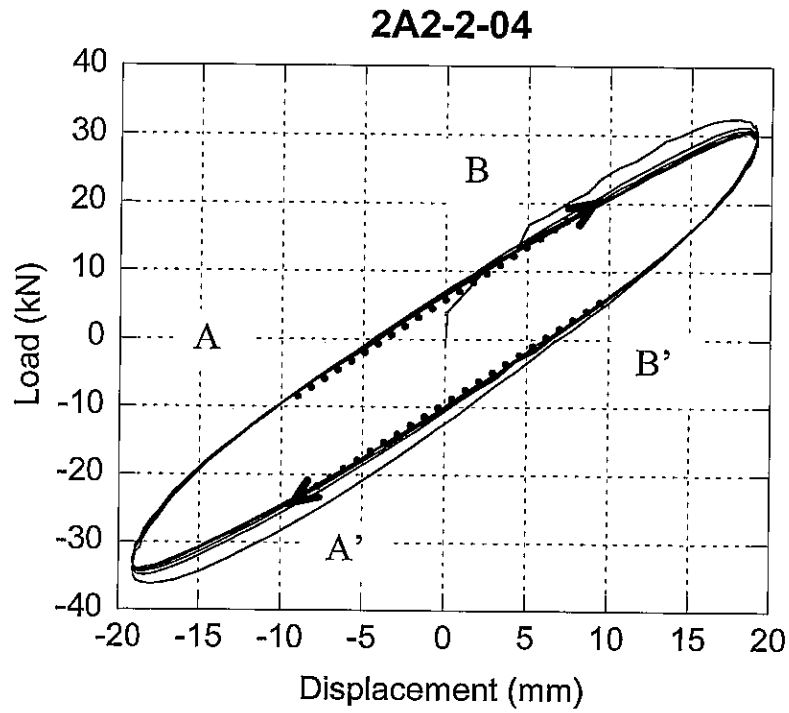


Figure 5.2 Shear modulus definition ( $\pm 25\%$  shear strain)

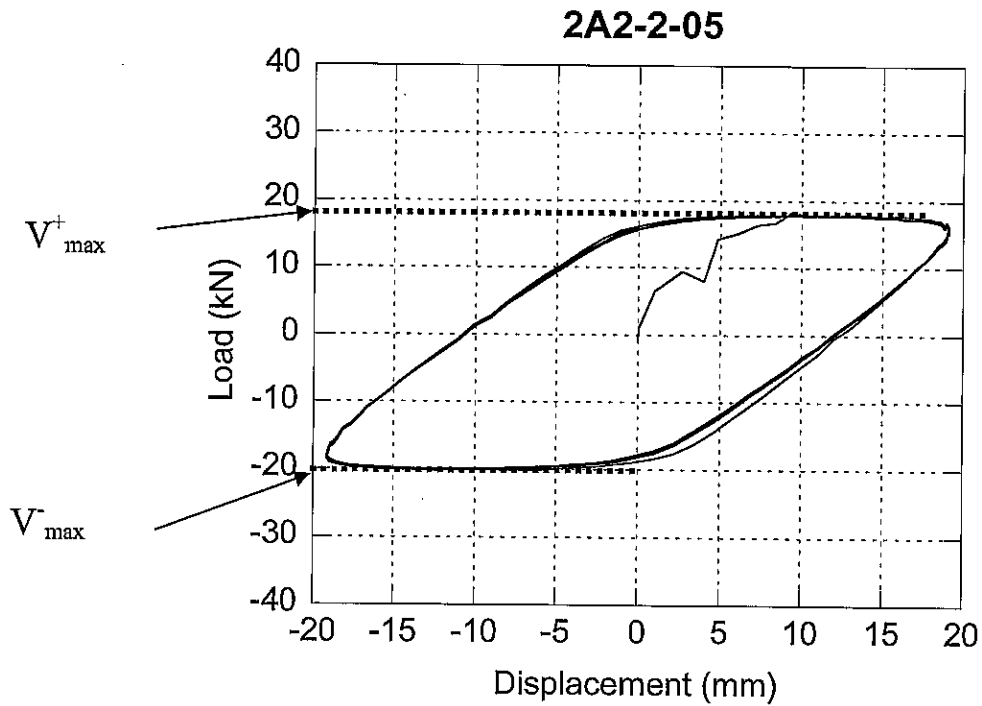
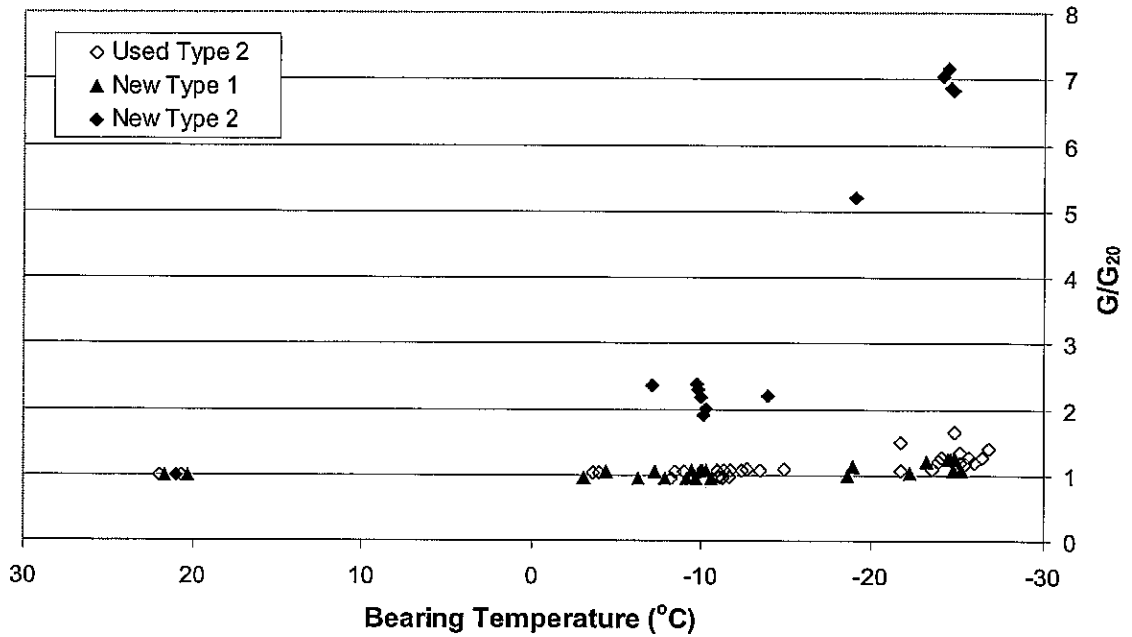


Figure 5.3  $C_f$  definition

**Normalized Shear Modulus - All Bearings Protocol 1  
(3.45 MPa Compressive Stress)**



**Figure 5.4** Normalized shear modulus for all bearings, Protocol 1

**Normalized Shear Modulus - Used Bearings  
(3.45 MPa Compressive Stress)**

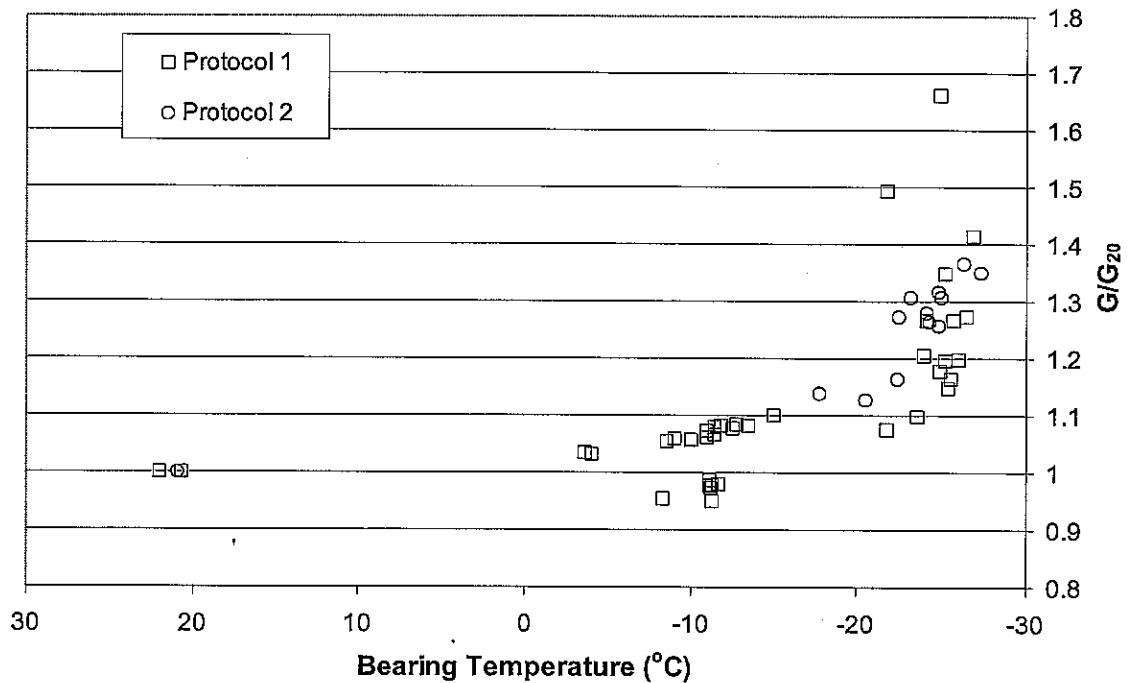


**Figure 5.5** Normalized shear modulus for used bearings only

**Used Bearing  $C_f$  Summary  
(3.45 MPa Compressive Stress)**

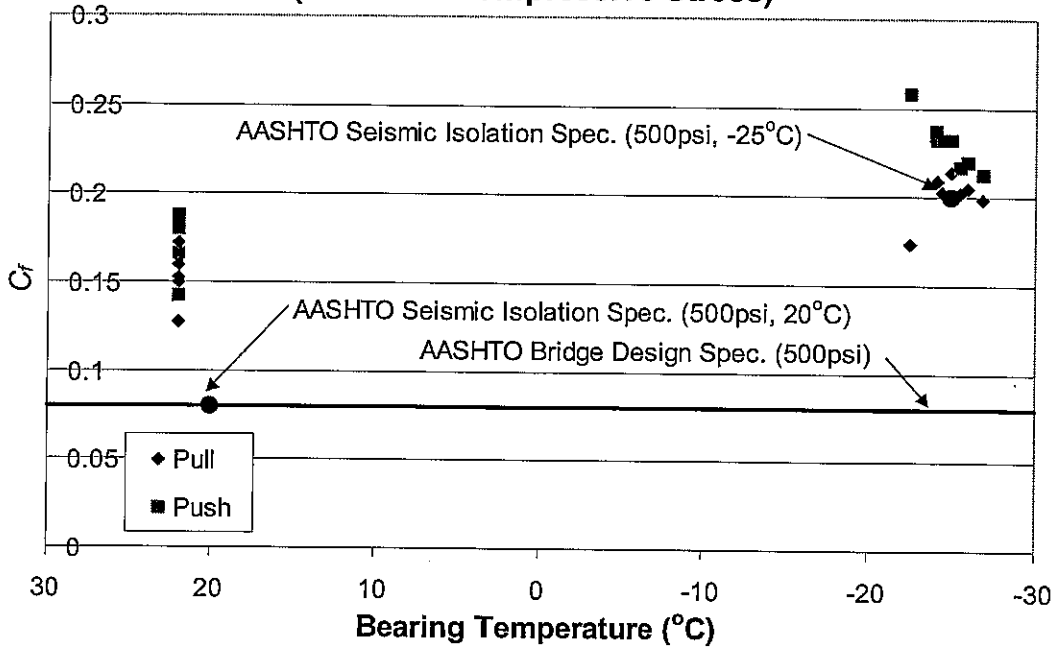


**Figure 5.6** Used bearing  $C_f$  summary

**New Bearing  $C_f$  Summary  
(3.45 MPa Compressive Stress)**

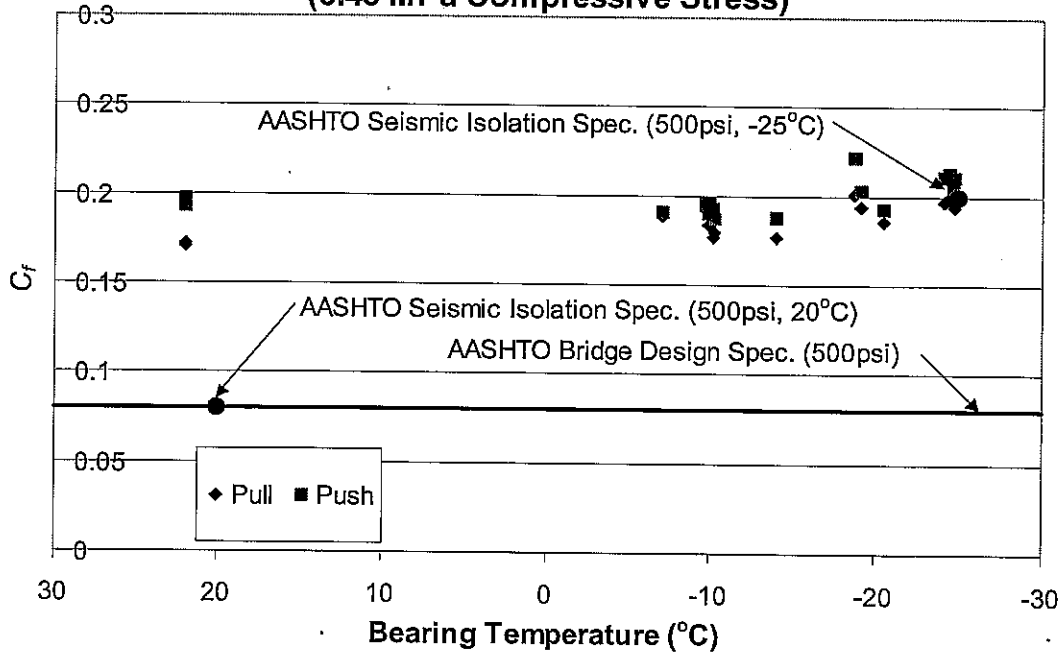
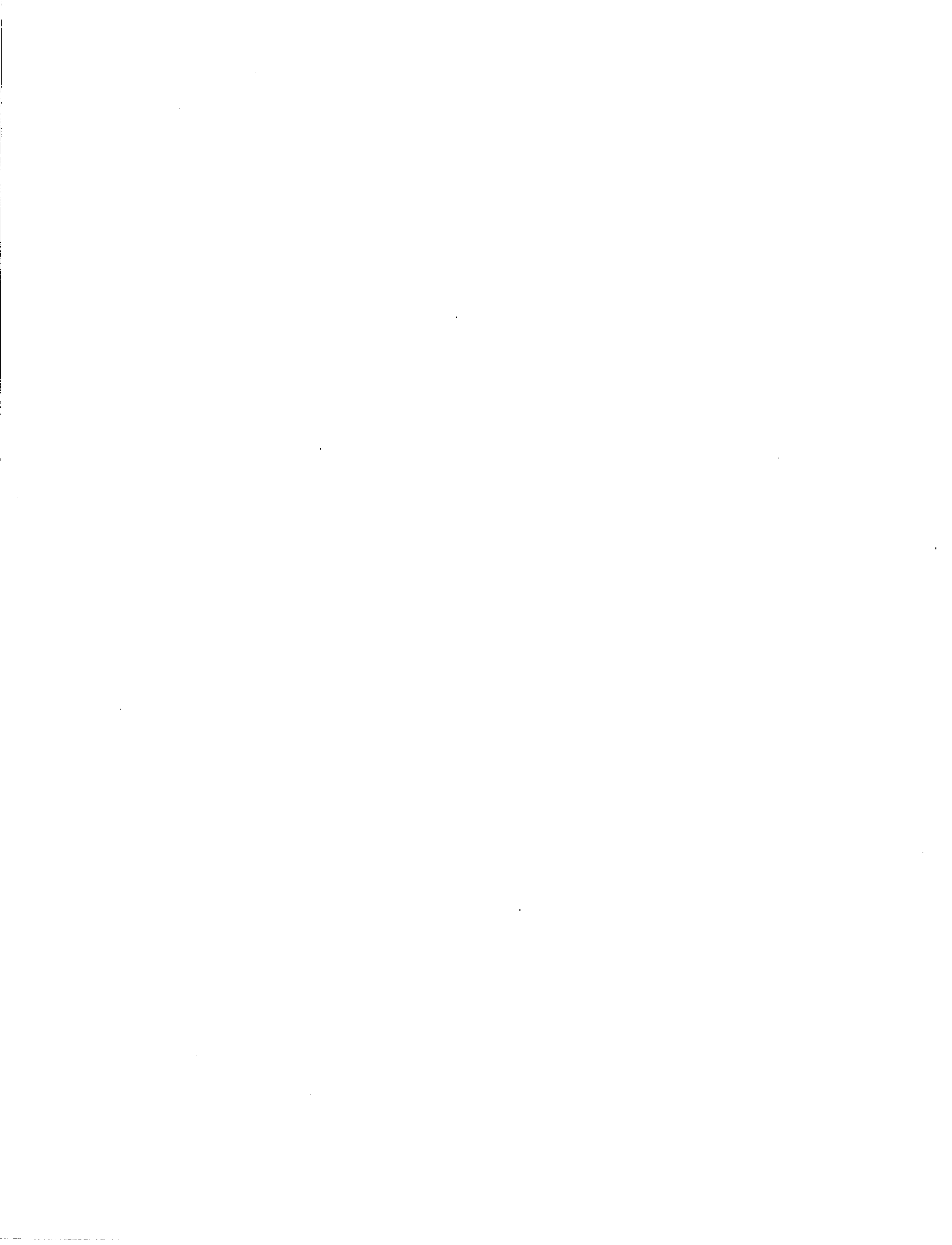


**Figure 5.7** New bearing  $C_f$  summary



## Chapter 6 – Elastomer Test Results

Materials tests were conducted on portions of the bearings after completion of the full scale reversed cyclic loading tests. The materials tests were performed on specimens taken from the used bearings 2A1, 2A2, 2B1, 2B2, 2C1, and 2C2 at the IDOT materials testing facility in Springfield. The specimens were subjected to a battery of standard ASTM tests for both regular (ASTM D 2240) and heat-aged (ASTM D 573) durometer hardnesses, tensile strength (ASTM D412), compression set (ASTM D395), and peel strength (ASTM D 429 B). Results were compared to the values specified in AASHTO M 251-92 *Standard Specification for Plain and Laminated Elastomeric Bridge Bearings* as adopted by the IDOT Bridge Manual and as shown in Table 6.1. The tests and results are described in detail in the following sections.

### *6.1 Durometer Hardness (regular and heat-aged)*

ASTM D 2240 provides procedures for durometer hardness testing. As specified by AASHTO, the Shore A hardness must fall between 50 and 60. ASTM D 573 provides instructions for heat aging of elastomer. After the heat aging process, the maximum allowable increase in Shore A hardness is 10 points for natural rubber and 15 points for neoprene. Table 6.2 summarizes the results of these two durometer tests. Based on the AASHTO requirements given in Table 6.1, all samples from the used bearings pass this test.

### *6.2 Tensile Strength, Elongation, and Compression Set*

Samples of elastomer obtained from the used bearings were subjected to the ASTM tests D 412 (rubber properties in tension) and D 395 (compression set). Table 6.3 summarizes the results of these tests. These tests were performed on control samples, obtained from the used bearings in their as-is condition and on heat-aged (ASTM D 573) samples. Results, reported in Table 6.3, indicate that all elastomer samples satisfy the AASHTO requirements for minimum tensile strength and minimum ultimate elongation. Compression set results are also shown in Table 6.3 and all samples satisfy the respective AASHTO requirements.

### *6.3 Peel Strength*

ASTM D 429 B provides procedures for elastomer-steel bond strength testing. Peel tests were conducted on samples from each of the used bearings mentioned above. Table 6.4 summarizes the results of this test. Unlike the previous tests, there is a wide range of values obtained from this test. Some of the bearing specimens literally fell apart once cut open. AASHTO specifies minimum peel strength of 6.9 N/mm. Based on this specification, two of these used bearings failed this test in their condition after many years of service followed by the reversed cyclic load tests. These bearings are 2B1 and 2C2, which were obtained from nearby bridges in Rantoul, IL. Because these bearings may have been installed at the same time, they may have come from the same manufacturer.

#### *6.4 Summary*

Based on the preceding discussion, the ASTM tests indicate that the used bearings generally continue to satisfy the specifications used for procuring new bearings.

Assuming that these bearings originally satisfied these specifications when new, eight to ten years of aging and use are seen to have caused insubstantial changes to the elastomer properties. The only exceptions were the two bearings which failed the peel test. These failures may have been influenced by the high shear strains applied during the laboratory testing of the bearing, prior to the materials evaluation tests, and may not be representative of field strain histories.

**Table 6.1** ASTM Tests and Requirements

Material Property	ASTM Standard	Test Requirements	Natural Rubber			Polychloroprene			Units
			50 Duro	60 Duro	70 Duro	50 Duro	60 Duro	70 Duro	
Physical properties	D 2240	Hardness	50 ± 5	60 ± 5	70 ± 5	50 ± 5	60 ± 5	70 ± 5	Shore points
	D 412	Min tensile strength	15.5	15.5	15.5	15.5	15.5	15.5	MPa
		Min ultimate elongation	(2250)	(2250)	(2250)	(2250)	(2250)	(2250)	psi
Heat resistance	D 573 at specified temp.	Specified temp. of the test	450	400	300	400	350	300	%
		Aging time	70	70	70	100	100	100	°C
		Max change in durometer hardness	(158)	(158)	(158)	(212)	(212)	(212)	°F
		Max change in tensile strength	168	168	168	70	70	70	Hours
		Max change in ultimate elongation	+ 10	+ 10	+ 10	+ 15	+ 15	+ 15	Shore points
Compression set	D 395	Specified temp. of test	- 25	- 25	- 25	- 15	- 15	- 15	%
		Max permissible (after 22 hrs.)	- 25	- 25	- 25	- 40	- 40	- 40	%
Tear resistance	D 624	Specified temp. of test	70	70	70	100	100	100	°C
		Max permissible (after 22 hrs.)	(158)	(158)	(158)	(212)	(212)	(212)	°F
Brittleness	D 2137	Min kN/m (Die C)	25	25	25	35	35	35	percent
		Low temp. brittleness at $-40^{\circ}\text{C}$ ( $-40^{\circ}\text{F}$ )	31.5	31.5	31.5	31.5	31.5	31.5	kN/m
Ozone Resistance	D 1149	Duration of test	(180)	(180)	(180)	(180)	(180)	(180)	lb/in.
		Tested at 20-percent strain $37.7 \pm 1^{\circ}\text{C}$ ( $100 \pm 2^{\circ}\text{F}$ ) mounting procedure	Pass	Pass	Pass	Pass	Pass	Pass	
		Partial pressure of ozone during test	25	25	25	100	100	100	MPa
		D 518, procedure A	48	48	48	100	100	100	Hours
			No	No	No	No	No	No	
			Cracks	Cracks	Cracks	Cracks	Cracks	Cracks	

**Table 6.2** Durometer Hardness Test Summary

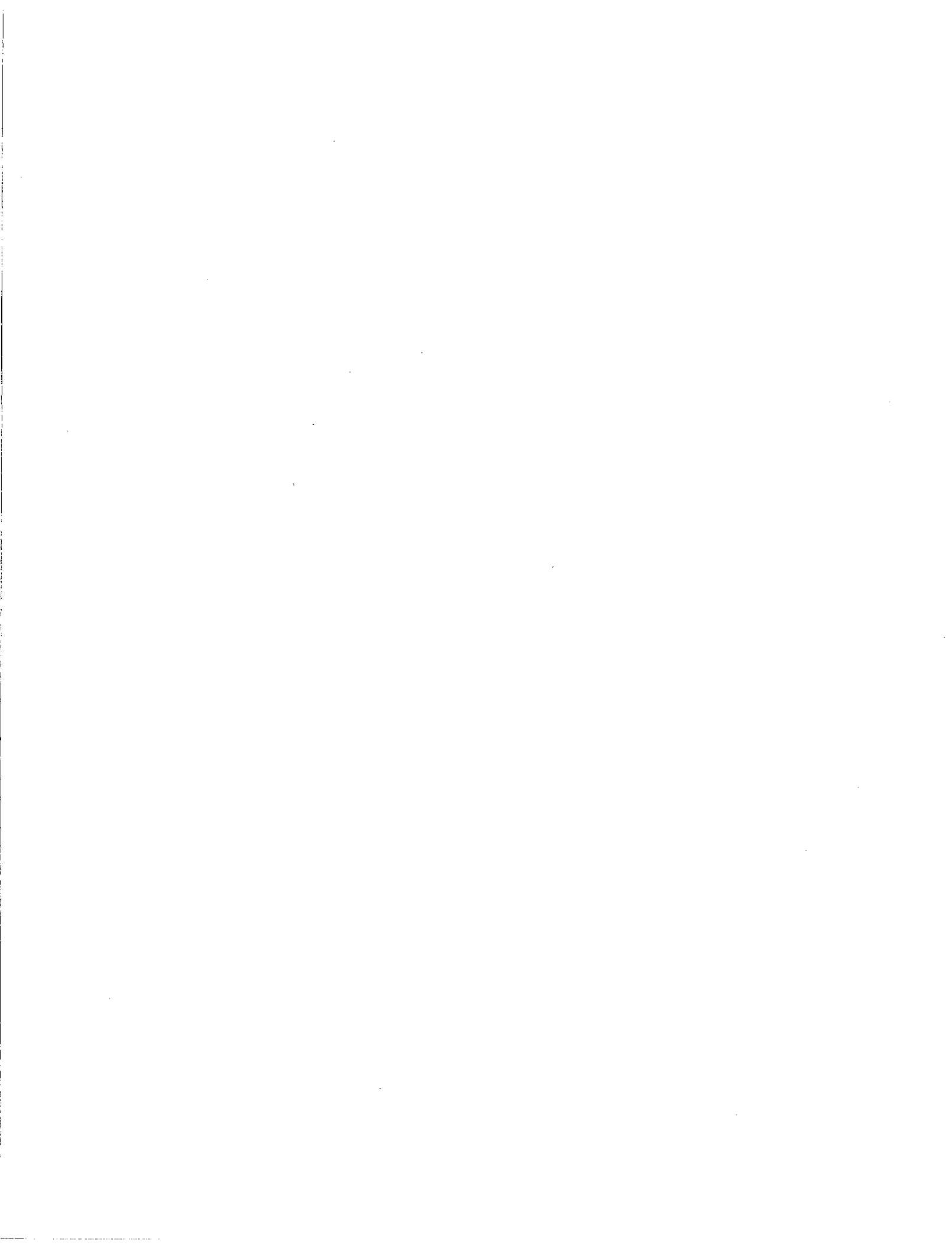
Specimen	Control Durometer	Heat Aged Durometer
2A1	53	56
2A2	55	56
2B1	54	55
2B2	55	56
2C1	60	63
2C2	56	58

**Table 6.3** Tensile Strength, Elongation and Compression Set Test Summary

Specimen	Control			Heat Aged	
	Tensile Strength (MPa)	Elongation (%)	Compression Set (%)	Tensile Strength (MPa)	Elongation (%)
2A1	25.51	470	9	26.04	480
2A2	26.06	470	14	25.00	480
2B1	25.79	460	11	28.28	450
2B2	27.74	520	13	26.67	480
2C1	24.82	440	13	24.33	390
2C2	22.31	420	15	26.85	350

**Table 6.4 Peel Test Summary**

Specimen	Shim	Strength (N/mm)	Adhesion (%)
2A1	Top	18.7	98
	1	24.3	100
	2	19.3	98
	3	20	95
	Sole	25	100
2A2	Top	16.1	100
	1	10.5	95
	2	11.7	93
	3	12.2	95
	Sole	24.3	92
2B1	Top	24	95
	1	Damaged	
	2	0.7	0
	3	1.4	0
	Sole	32	95
2B2	Top	19	80
	1	17	100
	2	24	98
	3	17	99
	Sole	16	80
2C1	Top	11	10
	1	14	80
	2	14	90
	3	16	90
	Sole	23	100
2C2	Top	19	99
	1	0.5	0
	2	No test	
	3	Peel off completely	
	Sole	20	90



## Chapter 7 – Retrofit Bearing Details

One objective of this research project was to develop a suitable retrofit bearing design to be used to replace fixed bearings that are typically located at the central pier. Some of the considerations for such a design and the physical test results are included in this section.

### *7.1 Design Objectives*

In existing bridges, fixed bearings often are used to transfer forces associated with wind and traffic to the ground via a pier. This pier often is one of the central piers of a continuous, multi-span bridge. Seismic excitations can develop substantial forces at existing fixed bearings, possibly sufficient to induce damage to the piers, to cause failure of the fixed bearing pintels that provide translational fixity to the bearing, or to dislodge the bearing from its anchor bolts, thereby losing whatever translational resistance was available. Any of these would cause damage and possibly collapse of the bridge. Developing high forces in the piers is problematic because these piers typically lack the ductile details now provided in new seismic-resistant construction. The lack of ductile details can lead to brittle shear or lap-splice failures of the piers. The objective of the retrofit bearing is to provide the fixity needed for service loads while allowing slip or deformation during a seismic event to protect the substructure from damage.

The retrofit bearing must be simple, durable, reliable, inexpensive, and easy to install and inspect. Because Illinois seismicity is characterized by infrequent large ground motions, the aim of the retrofit is to protect the existing bridge inventory from catastrophic damage, recognizing that with time these bridges will be gradually replaced

with more resilient construction. Thus, the strategy employed is to accept damage to bearings and damage associated with pounding at the abutments, recognizing that those bridges sustaining this type of damage can be repaired after the event. The retrofit detail should allow service level fixity to be restored after the event and may even provide limited functionality until these repairs are complete.

### *7.2 Proposed Solution and Design*

A prototype design was developed in consultation with IDOT personnel and others. As shown in Figures 7.1 through 7.3, the design employs field-weldable shear studs (such as those manufactured by the Nelson Stud Welding Company) in order to provide service level fixity for lateral loads, while carrying gravity loads in bearing on a Type II elastomeric bearing. This prototype bearing allows girder rotation under live load through the use of 1.5 mm (0.0625”) oversized holes in the top plate. The shear studs are designed to yield (and their welds may fracture) during strong seismic loads, thereby allowing slip to occur at the TFE – stainless steel interface. The slip surfaces must be large enough to prevent the girders from losing seat support, or suitable retention measures must be considered. The required slip distances determined in the dynamic analyses are reported in Chapter 8.

For any particular bridge application, the strength of the retrofit bearing should be less than the ultimate strength of the pier. The strength of this bearing may be selected so as to limit the force transmitted to the substructure to a predetermined “safe” level. The prototype retrofit bearing was designed such that the ultimate strength would be below the capacity of the testing apparatus. The distance from the point of load application to

the weld was selected so as to force yielding to occur at the base of each stainless steel shear stud. Each stud was analyzed as a cantilever beam with a fixed base and a pin-type loading condition at the free end. Based on these assumptions and using a 50.8 mm (2") length for the cantilever, 6 – 19 mm (0.75") diameter shear studs should achieve their fully plastic moment at about 50 kN (11 kips) of total horizontal load. This value is determined using the listed yield strength of 345 MPa (50 ksi) for 316 stainless steel. Any material over-strength will result in an increase in the load required for failure. The ratio of clear distance to shear stud diameter was selected so as to avoid a shear controlled failure mechanism.

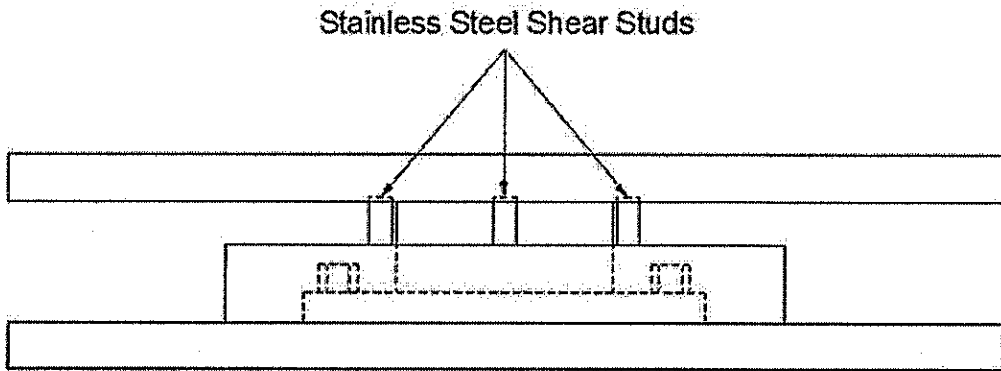
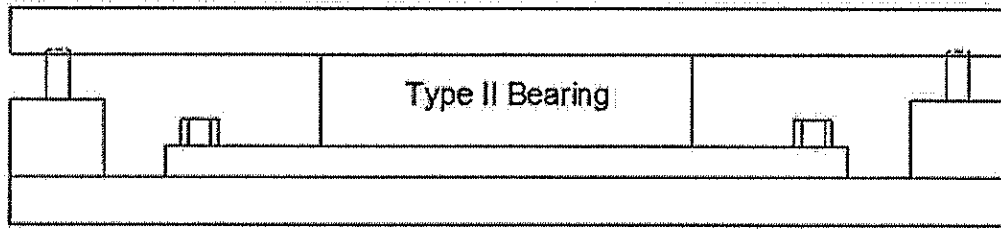
### *7.3 Test Results & Conclusions*

Two tests were conducted on the retrofit bearing. Both tests were conducted on the same unit, illustrating the reusability of the prototype design. Only the shear studs needed replacement between tests. The lateral load-displacement plots from these tests are shown in Figures 7.4 and 7.5. Figure 7.4 shows the results from the warm temperature test. A plot of the same Type II bearing at the same temperature is superimposed to illustrate the manner in which the behavior of the retrofit bearing approaches that of the elastomeric bearing. This test was run at a low cyclic frequency in order to observe the behavior of the shear studs and their welds. Both Figure 7.4 and 7.5 show the high initial stiffness of the shear studs, followed by a softening and then progressive fracture of the stud welds. Each fracture is evidenced by the sudden drop in the load measured in the actuator load cell. This test fractured all 6 welds within the first half-cycle of loading and the behavior is then controlled by the Type II bearing. The

calculated strength of 50 kN (11 kips) is considerably lower than the measured strength of about 100 kN (22 kips). This difference in strengths is likely due to a higher strength of the stainless steel material than published and strain hardening of the material.

After the warm temperature test, new studs were rewelded in the retrofit bearing in the same configuration as before and the unit was reinstalled in the test setup. The cold temperature test was run at a higher cyclic frequency to both approximate the likely loading speed of an earthquake and to determine if the stud welds might fail at a lower load after being subjected to  $-25^{\circ}\text{C}$  for 72 hours prior to testing. As shown by Figure 7.5, the cold temperature did little to affect the overall strength of the retrofit bearing. However, the cold temperature specimen sustained more displacement reversals before the shear stud welds failed, allowing the behavior to approach that of the Type II bearing which is also plotted in Figure 7.5.

In both tests, the retrofit bearing did provide service level strengths in excess of the calculated values. If the strength is too high, forces large enough to damage the substructure piers could result. The stud welds failed in both the slow warm test and the fast cold test, allowing the bearing to slip and thereby protecting the substructure from excessive force demands. Cold temperatures are usually implicated in weld fracture, so it is not clear why the second specimen evinced greater cyclic displacement ductility. Additional tests may be useful to fully develop this prototype design into a final retrofit bearing design that can be used reliably for the range of configurations found throughout Illinois.



## Retrofit Bearing Design

Figure 7.1 Retrofit bearing elevation

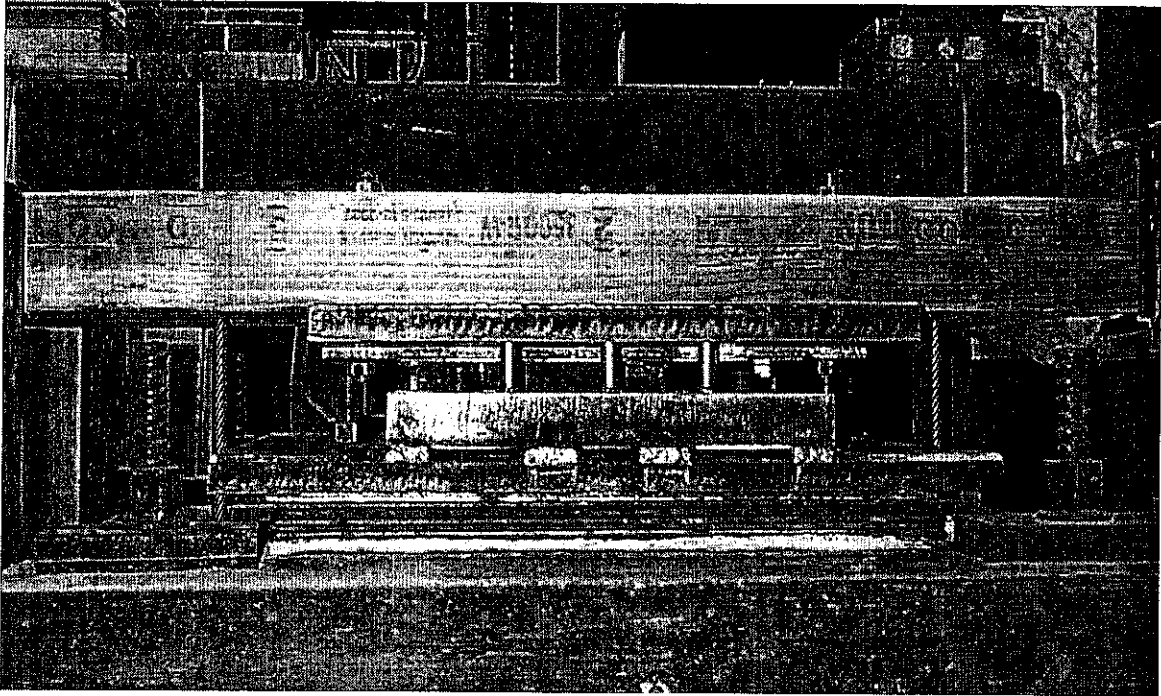


**Figure 7.2** Retrofit bearing installed in test setup. Note provision of Type II bearing to support vertical loads and allow slip on TFE surface.

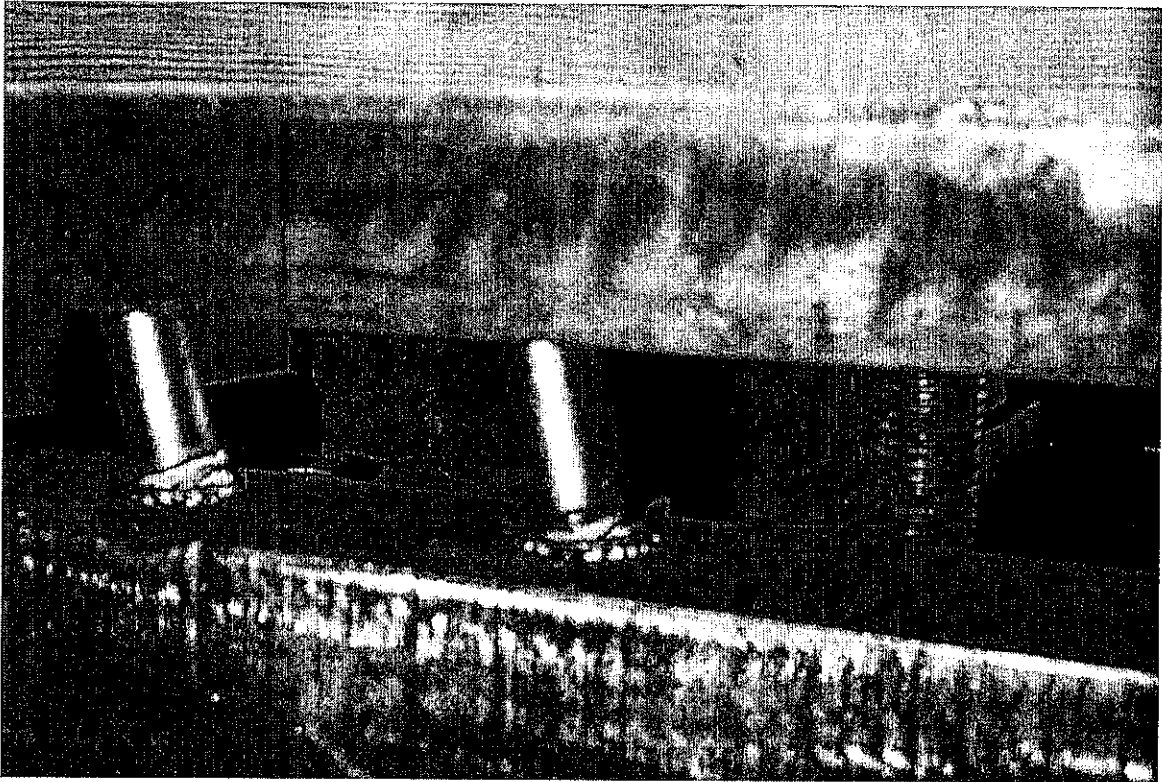


**Figure 7.3** Fracture of shear stud welds after warm temperature cyclic test

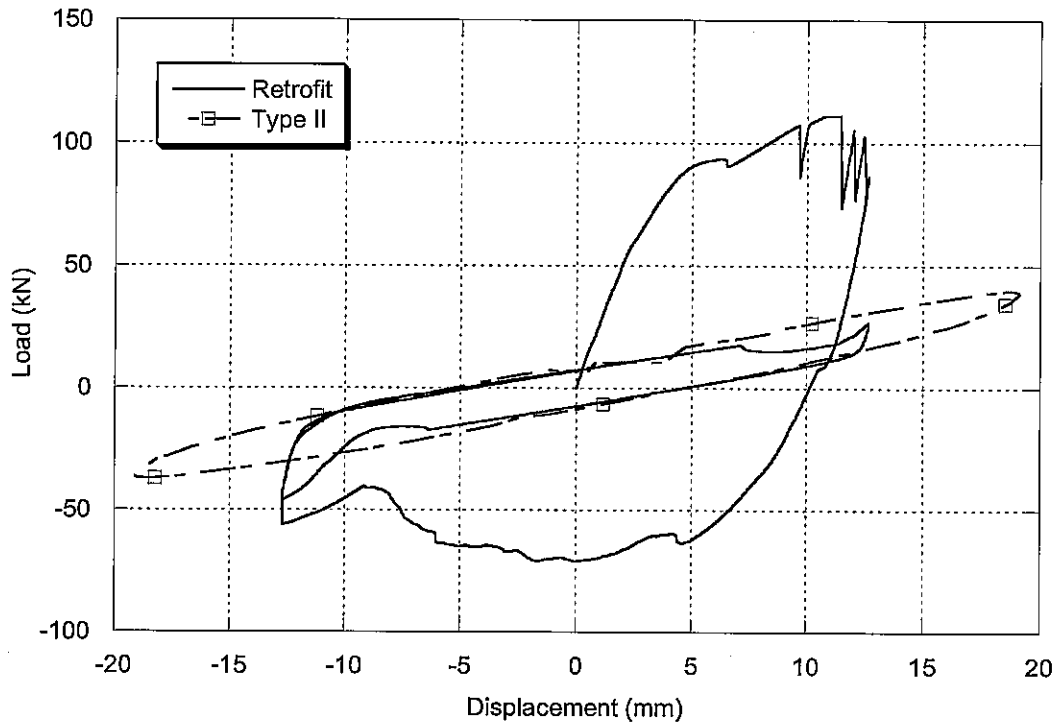


**Figure 7.4** Warm temperature retrofit bearing test result with superimposed result from Type II bearing at same temperature

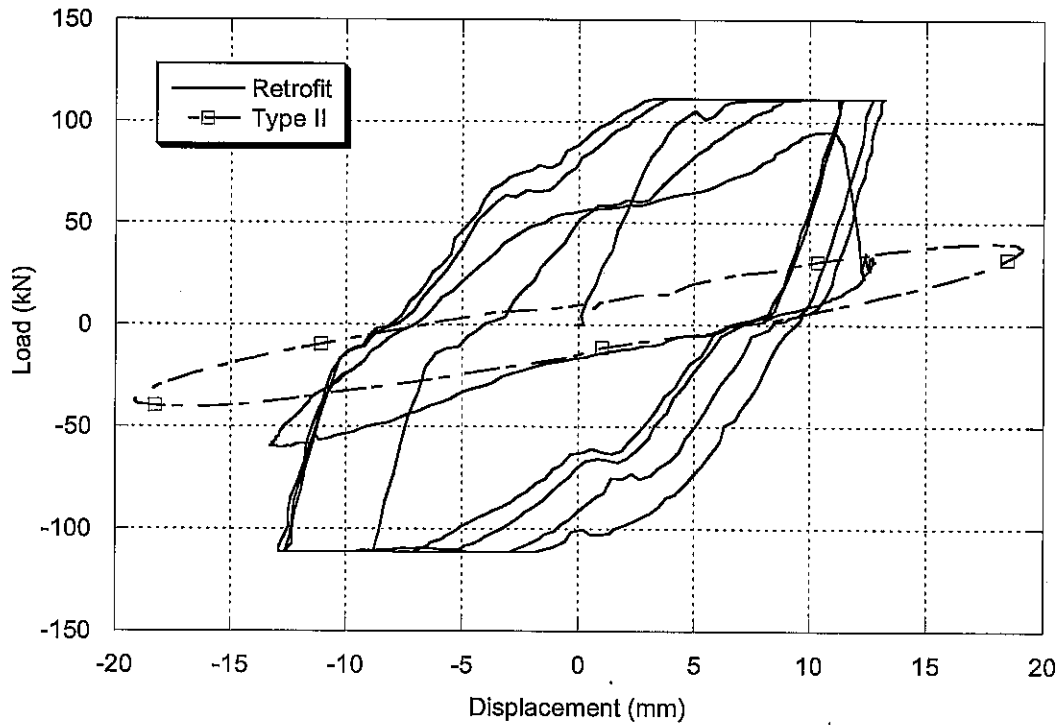


**Figure 7.5** Retrofit bearing test after 72 hours at  $-25^{\circ}\text{C}$  with superimposed result from Type II bearing at same temperature



## Chapter 8 – Modeling

This chapter describes analytical results that address the effectiveness of both conventional elastomeric bearings and the prototype retrofit bearing at mitigating seismic damage to bridge piers. The results are obtained by nonlinear dynamic analysis of a representative bridge employing various configurations of fixed and elastomeric bearings, subject to a ground motion representing the maximum considered earthquake for a location in the southern tip of Illinois. Previous experience and studies (e.g., Zhong 2001) indicates that highway bridge piers may be damaged under strong earthquake ground motions. The types of damage that may occur to the pier include shear failures of the reinforced concrete columns and/or bent caps, failures of lap splices in the columns, and failure of the bearings or loss of girder seat support. Elastomeric bearings may serve to isolate the response of the superstructure and reduce the forces and deformations imposed on the substructure. The flexibility of the bearing causes a period lengthening, which typically reduces elastic response force demands while requiring that larger displacements be accommodated. In addition, damping and hysteretic energy dissipation in the elastomer can further reduce the force and displacement demands experienced by the substructure.

To assess the potential role of traditional elastomeric bearings, the dynamic response of a representative bridge was determined for various bearing configurations and modeling assumptions. The stiffness and slip characteristics of the bearings as a function of temperature were based on the recommendations of Section 5.3. This chapter describes the representative bridge (Figure 1.2), the mathematical model of the bridge,

and computed results obtained for different bearing configurations and different temperatures.

### *8.1 Representative Bridge Description*

The bridge shown in Figure 1.2 was chosen to represent a typical highway overcrossing. It consists of four spans, the longest of which is 19.81 m (65 ft). The total length is 70.1 m (230 ft). The substructure consists of two abutments and three reinforced concrete bents. Each bent consists of three columns having a rectangular cross section of 66 cm x 92 cm (26 in x 36 in). The columns have a clear height of 3.93 m (12.9 ft). The concrete bridge deck is 12.2 m (40 ft) wide, 15 cm (7 in) thick, and acts compositely with 7 equally spaced W33x130 steel girders. The bridge is symmetric about the central pier and has no skew.

Multiple configurations of fixed and elastomeric bearings were analyzed. Table 8.1 summarizes these scenarios. Scenarios 1a and 1b represent typical existing configurations, with a fixed bearing at the central pier and Type I and II elastomeric bearings at other locations. Scenarios 2a and 2b replace the central fixed bearing with an idealized stick-slip retrofit bearing. The yield strength of the bearing was assumed to be 481.5 kN to resist service level wind and braking loads amounting to 68.8 kN per bearing. For simplicity the bearing was modeled as having no post-yield stiffness. Scenarios 3a and 3b consider the extreme case of having elastomeric bearings at all supports. Although this configuration may not provide sufficient stiffness for service lateral loads, it represents the case of complete isolation of the bridge deck, for comparison with the other scenarios. Scenario 4 represents fixed bearings at all supports

of the bridge in Figure 1.2. This scenario can be considered to represent a simple model in which bearing flexibility is neglected or a real case where the steel rocker bearings provide complete fixity for transverse movement. The elastomeric bearings in these scenarios are modeled with the temperature-dependent material properties given in Section 5.3. The fixed bearings were assumed to be completely fixed; that is, the possibility of pintel failure or disengagement of the pintel due to vertical accelerations was not considered in the models.

**Table 8.1** Bearing configurations

Scenario	Description	Support				
		Abut. 1	Pier 2	Pier 3	Pier 4	Abut. 5
1a	Typical configuration (20°C)	Type II	Type I	Fixed	Type I	Type II
1b	Typical configuration (-25°C)	Type II	Type I	Fixed	Type I	Type II
2a	Retrofit bearing (20°C)	Type II	Type I	Retrofit	Type I	Type II
2b	Retrofit bearing (-25°C)	Type II	Type I	Retrofit	Type I	Type II
3a	All elastomeric bearings (20°C)	Type II	Type I	Type I	Type I	Type II
3b	All elastomeric bearings (-25°C)	Type II	Type I	Type I	Type I	Type II
4	All fixed	Fixed	Fixed	Fixed	Fixed	Fixed

## 8.2 Bridge Modeling

The transverse response of the bridge was modeled using DRAIN-2DX (Prakash et al., 1993). A two-dimensional analysis (considering the length of the bridge and the transverse response) was considered adequate due to the symmetry of the bridge and lack of skew. The nonlinear static (pushover) analysis conducted by Zhong (2001) was used to characterize the load-deformation response of each pier. The piers were considered fixed at their bases. This simple approximation provides an upper bound estimate of the deformation demands in the bridge substructure. The pier response was modeled using a bilinear inelastic element. This element was coupled to elements representing the

bearings. The elastomeric bearing pad was modeled using a bilinear inelastic element. A slider was attached in series with the elastomeric pad for simulating the Type II bearing; no slider was needed for the Type I bearings. This model follows those developed by Wissawapaisal (2001). The deck stiffness is modeled using the ATC-32 (1996) assumption of 75% of the gross moment of inertia. Input files are provided in Appendix F.

### *8.3 Site Seismicity and Ground Motions*

The bridge was assumed to be located in Cairo, Illinois, because this location is near the New Madrid seismic zone. A site class D (NEHRP, 2002) condition was chosen to represent the soil conditions. Figure 8.1 shows the NEHRP spectrum obtained for this site (using zip code for Cairo, IL) using the USGS utility (USGS, 2002), representing the maximum considered earthquake (MCE) at the 2% probability of exceedance in 50 years level (2500 year return period).

The Lolleo record from the Central Chile Earthquake of March 3, 1985 was selected for analysis since its elastic spectral shape approximately matches the NEHRP spectrum for this site. Figure 8.2 plots the unscaled record as a function of time. As shown in Figure 8.1, the amplitude of the ground motion was scaled uniformly by a factor of 3.1 to better match the design spectrum in the period range from 1.3 to 1.5 seconds. This period range represents the upper and lower bounds of the first mode period for the elastomeric bearing supported bridge models given by Scenarios 1, 2, and 3. The period of the all fixed case, Scenario 4, is about 0.3 seconds, also shown in Figure

8.1. Figure 8.3 shows the spectral displacements for the scaled record and for the MCE hazard in this same period range. Figure 8.4 shows the scaled ground motion.

#### *8.4 Results*

This section describes the results obtain from the DRAIN-2DX analyses. Significant results are summarized below and in Figures 8.5 through 8.11. These figures plot the peak relative displacement computed for each designated component in the nonlinear dynamic analyses; these peaks do not necessarily all occur at the same time. Results are presented for Abutment 1, Pier 2, and Pier 3. The results for Pier 4 and Abutment 5 are identical to the results for Pier 2 and Abutment 1 due to the overall symmetry of the bridge.

This bridge was chosen to represent one constructed in the 1960's, and therefore lacks the ductile reinforcement details of bridges designed using modern seismic codes. For the purposes of assessing damage in these analyses, a table from Zhong (2001) which classifies damage as a function of column drift levels for older, non-ductile Illinois bridge bents will be relied upon, given in Figure 8.12. Drifts exceeding 1.2% (~50 mm for this bridge) can be expected to result in "moderate" damage and drifts exceeding 2% (~80 mm for this bridge) can be expected to result in "major" damage to the bridge substructure. Damage may arise from different types of failures, including flexural lap-splice failures or shear failures. The following describes the effect of the bearing scenarios described in Table 8.1.

#### *8.4.1 Scenario 1 – Typical configuration*

Figures 8.5 and 8.6 show the peak relative displacements for Scenarios 1a and 1b, respectively. For Scenario 1a, Pier 2 just exceeds 80mm drift (86.8 mm) while Pier 3 far exceeds this limit (256 mm). In Scenario 1b, colder temperatures cause the deformation of the elastomer to decrease, while increasing both the drift of the piers and the slip on the TFE sliding surface of the Type II bearings. In this scenario both Pier 2 (145 mm) and Pier 3 (282 mm) would sustain “major” damage. The low-temperature stiffening of the elastomeric bearing causes the drift to increase from Scenario 1a to Scenario 1b. Transverse slip on the TFE surfaces of the Type II bearings of approximately 250 mm is significant and may be sufficient to cause loss of seat support for the girders.

#### *8.4.2 Scenario 2 – Retrofit bearing*

Figures 8.7 and 8.8 show the peak relative displacements for Scenarios 2a and 2b, respectively. As shown by the reduced displacement of Pier 3 in both figures, the retrofit bearing offers protection in the maximum considered earthquake event. However, the lack of fixity at the retrofit bearing causes a general increase in the transverse displacements of the bridge deck. This results in an increased drift of Piers 2 and 4 which would sustain “major” damage in an earthquake of this intensity. Slip on the TFE surfaces approaching 400 mm may result in loss of seat support for the girders unless additional restraint is provided. In this scenario, the effect of low temperature on computed demands is relatively modest.

#### *8.4.3 Scenario 3 – All elastomeric bearings*

Figures 8.9 and 8.10 show the peak relative displacements for Scenarios 3a and 3b, respectively. Relative to Scenario 1, the demands at Pier 3 are reduced while those at Pier 2 are increased. All piers in both cases would experience major damage from this earthquake event. The effect of low-temperature stiffening is evident by the increase in pier relative displacement from Scenario 3a to Scenario 3b. These increases are 30% to 40% over the warm temperature case.

#### *8.4.4 Scenario 4 – All fixed*

Figure 8.11 shows the peak relative displacement for Scenario 4. The exclusion of the flexible bearing elements results in major damage to both Pier 2 (90 mm) and Pier 3 (155 mm). However, these demands are reduced relative to other cases due to the rigidity provided by the fixed bearings at all supports and the high transverse stiffness of the deck. Therefore, neglecting the flexibility of the bearings (by assuming fixity) can lead to underestimation of the displacement demands of the substructure bents.

### *8.5 Conclusions*

This chapter described the bridge configurations, ground motions, and bridge model. The temperature dependent properties of the elastomeric bearings were based on recommendation presented in Section 5.3. Low temperatures were shown to increase the drift for Type I bearing bents and were shown to reduce the displacement required to induce slip for the Type II bearings. The beneficial effects of the retrofit bearing were explored in Scenario 2. The use of this bearing at the central pier (Pier 3) reduced the

columns drift levels, to the point that only minor damage is expected. However, the increased displacements due to slip resulted in increased drifts on the adjacent Type I bearing supported piers. While the large displacements may be a concern for bridges located nearest the New Madrid Seismic Zone, responses with the stick-slip retrofit bearing may be acceptable for more frequent earthquakes and at locations further from the epicenter of a maximum considered earthquake. Provision of Type II bearings at the adjacent piers in conjunction with the stick-slip retrofit bearing at the central pier may be necessary at sites subjected to more intense shaking. Additional analyses would indicate the general viability of these retrofit solutions across the state of Illinois. Detailed investigations are appropriate where any specific bridge is of concern.

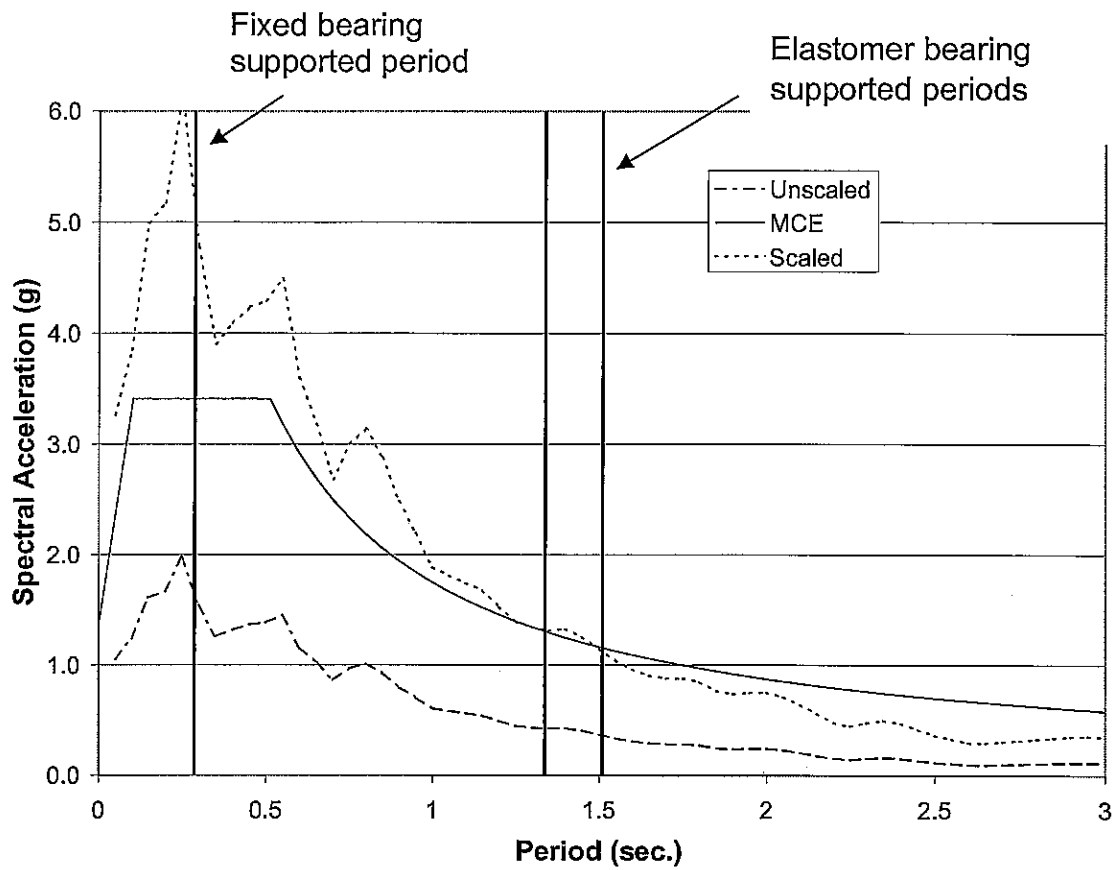


Figure 8.1 Spectral Acceleration Scaling

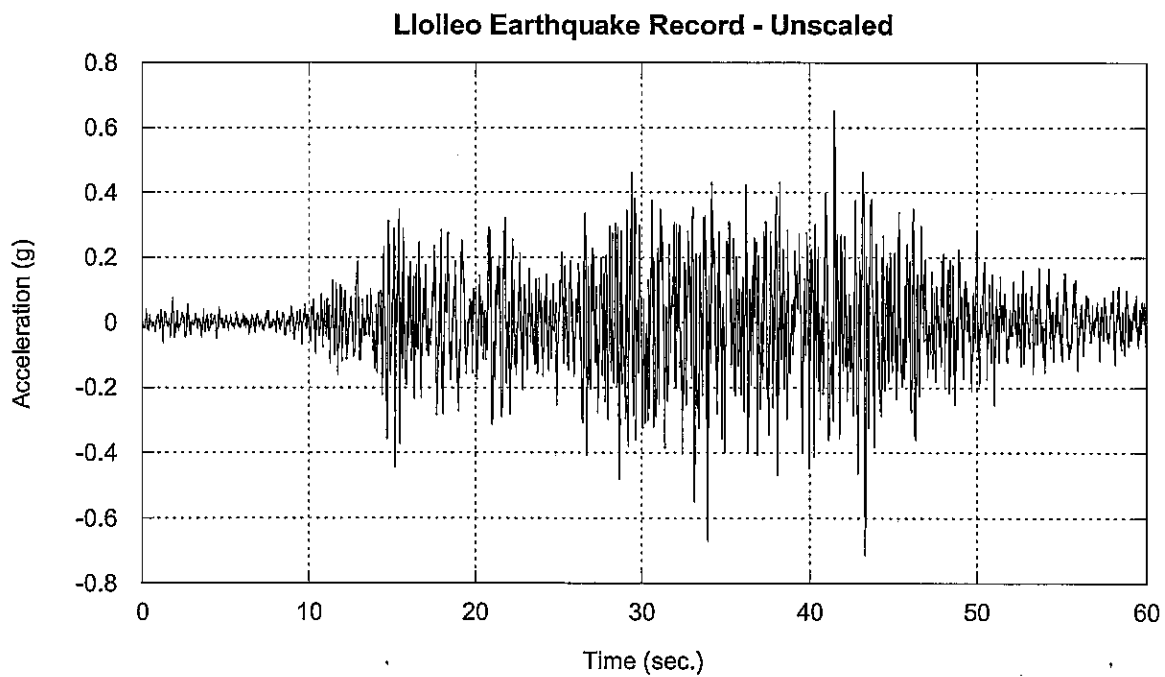


Figure 8.2 Unscaled Ground Motion Record

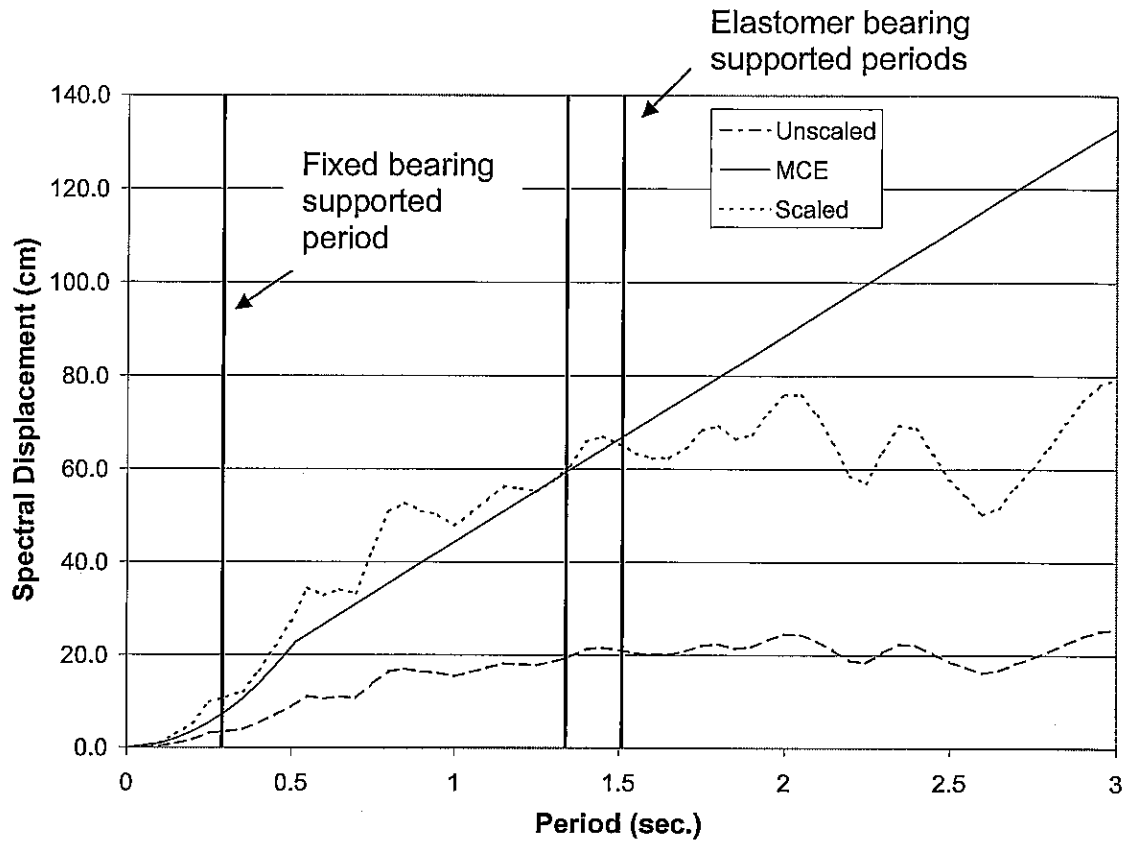


Figure 8.3 Spectral Displacement Scaling

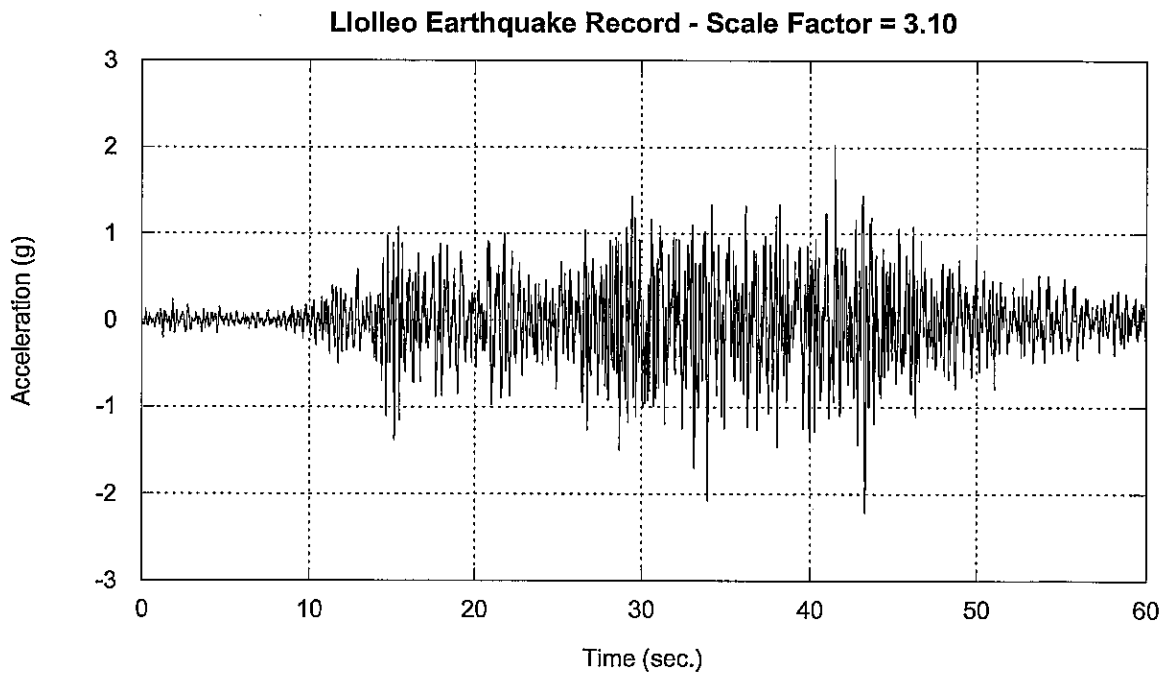


Figure 8.4 Scaled Ground Motion Record

### Scenario 1a

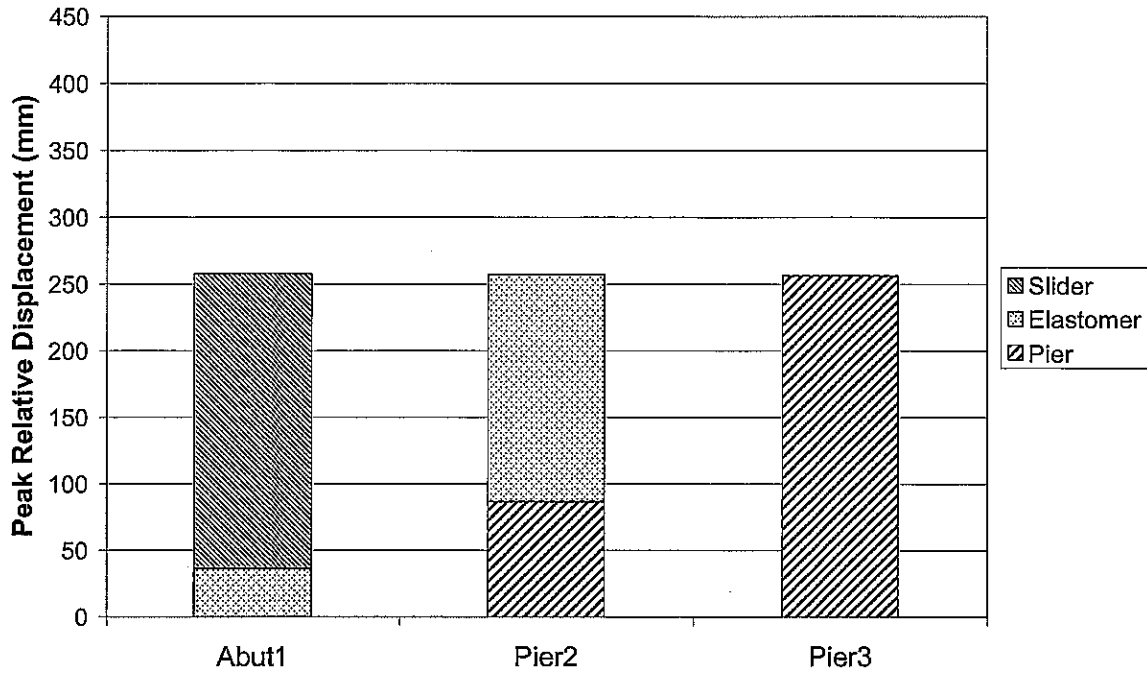


Figure 8.5 Scenario 1a Peak Relative Displacements

### Scenario 1b

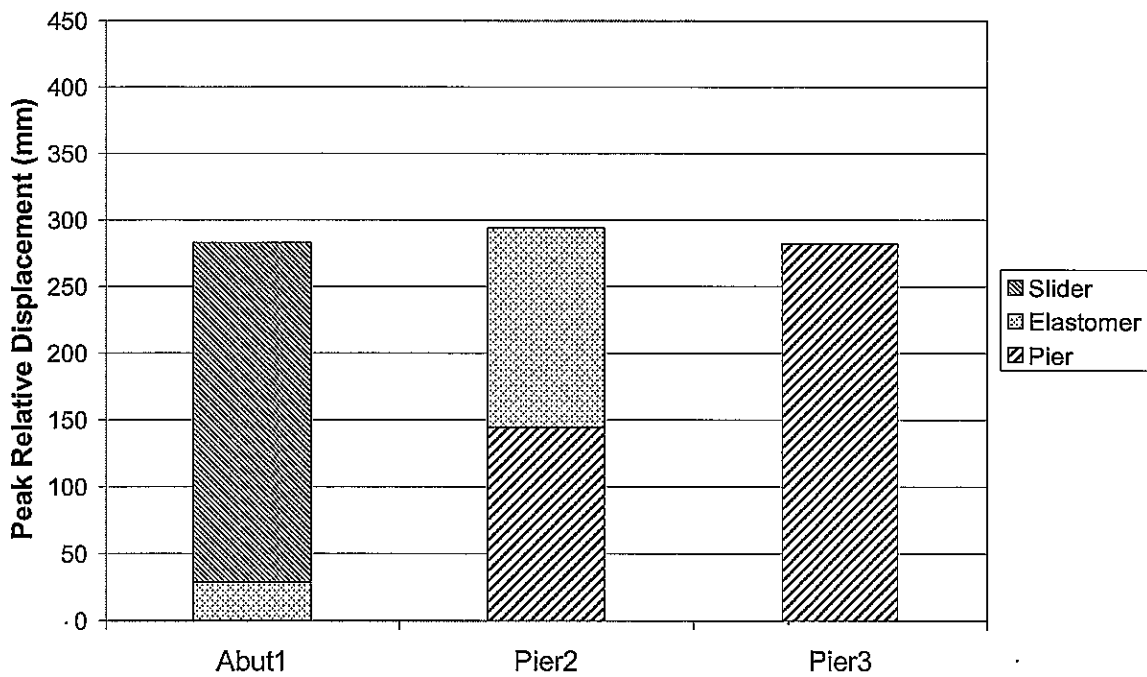


Figure 8.6 Scenario 1b Peak Relative Displacements

### Scenario 2a

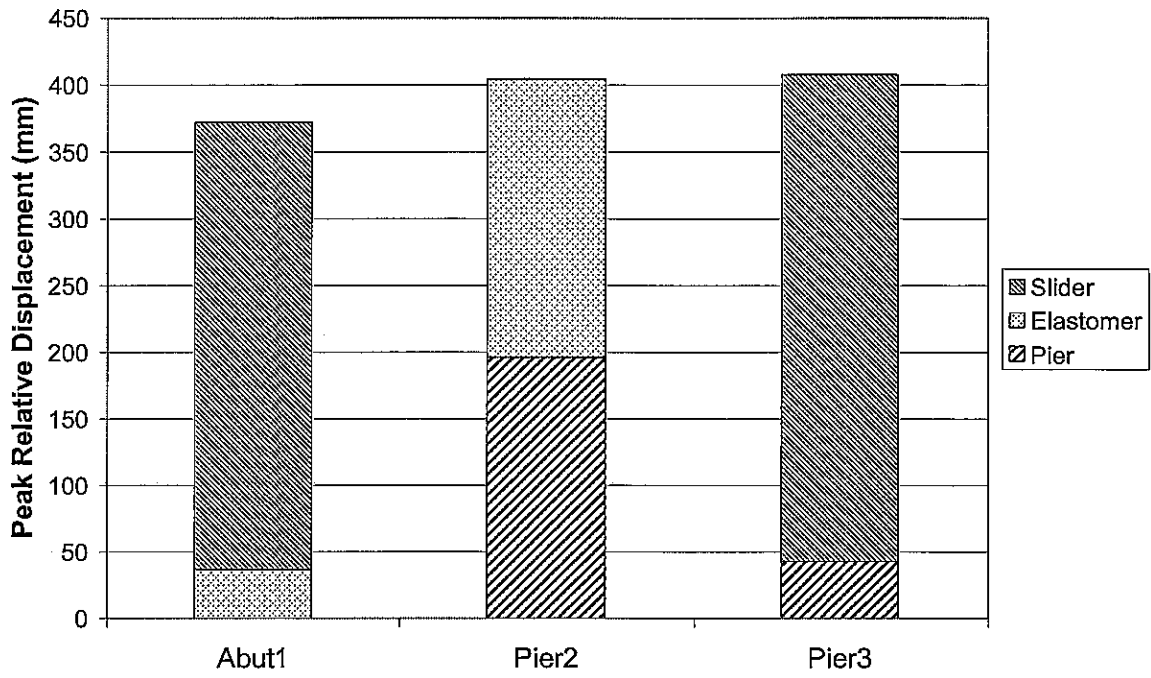


Figure 8.7 Scenario 2a Peak Relative Displacements

### Scenario 2b

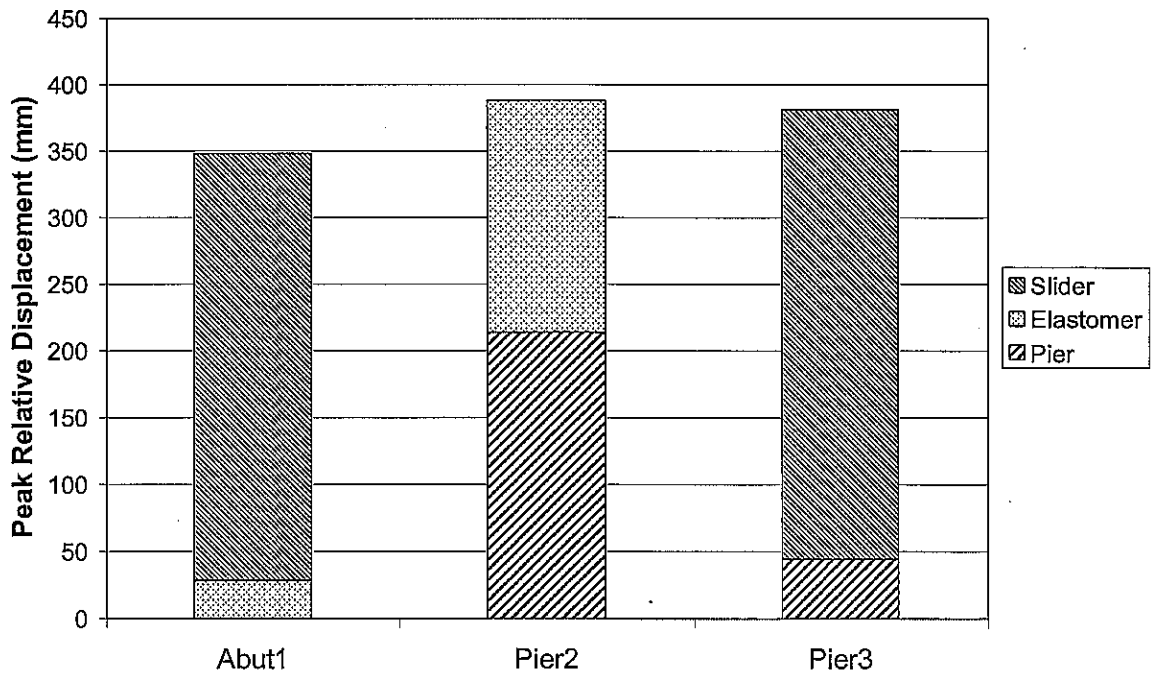


Figure 8.8 Scenario 2b Peak Relative Displacements

### Scenario 3a

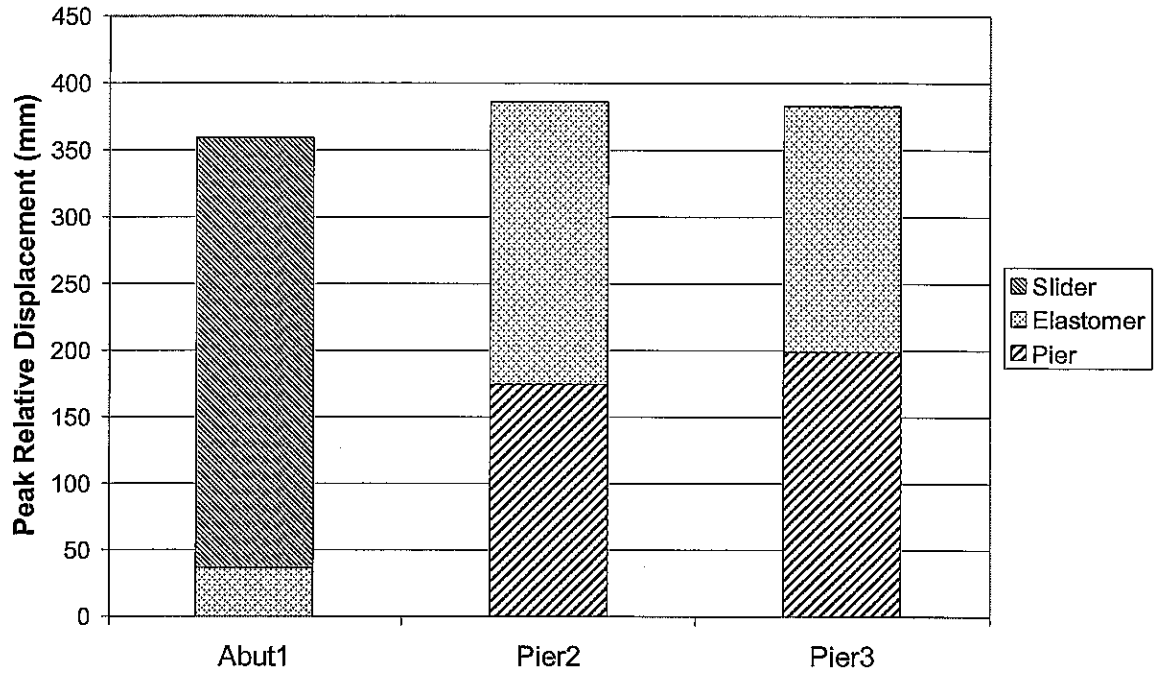


Figure 8.9 Scenario 3a Peak Relative Displacements

### Scenario 3b

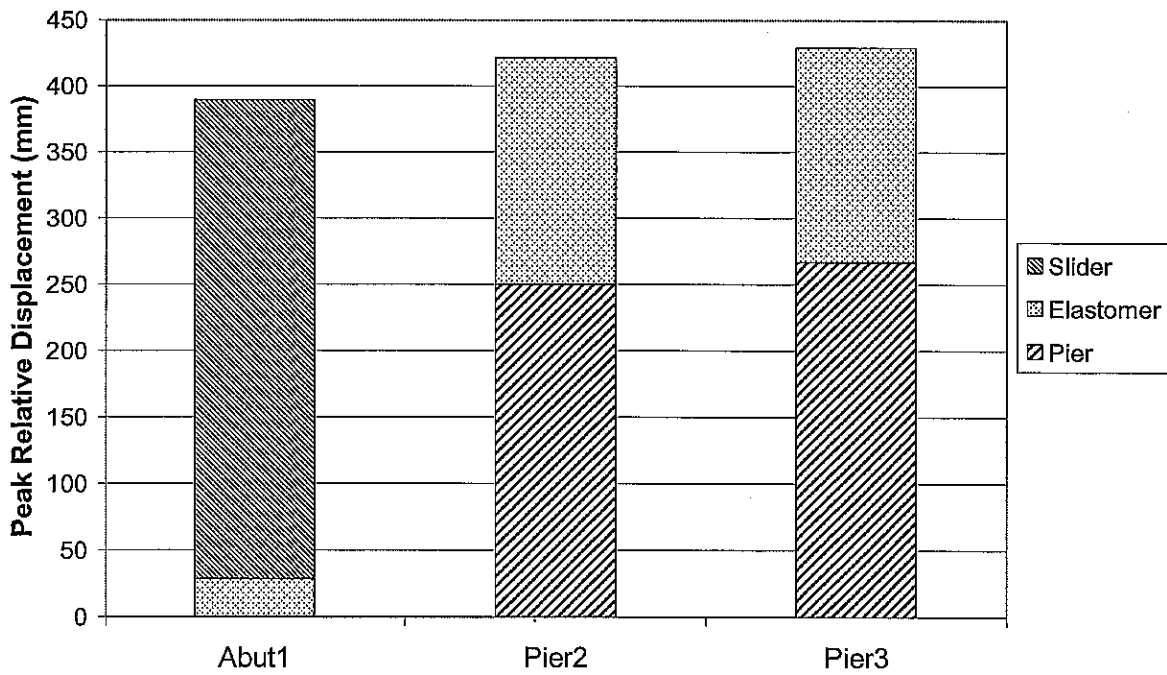
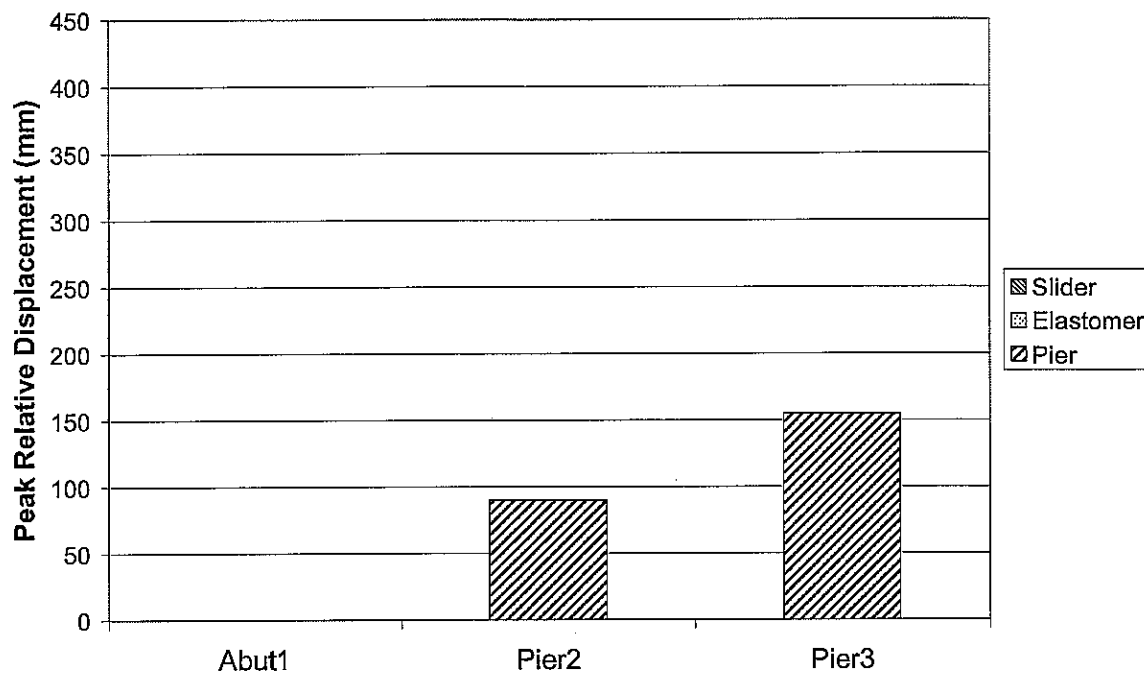


Figure 8.10 Scenario 3b Peak Relative Displacements

### Scenario 4



**Figure 8.11** Scenario 4 Peak Relative Displacements

Table 4.1 Damage Assessment Threshold for Illinois Multi-Column Bridge Piers

Level	Damage Classification	Element Damage Description	Pier Damage Description	element C/D ratio		Drift Ratio structural	Movement (inch)			Repair Description	
				flexural (brittle) $M_y/M_{y,elem}$	shear (brittle) $V/V_{elem}$		structural (inch)	non-structural (inch)	ground structural (inch)		ground non-structural (inch)
I	NO	Barely visible cracking		1.5	1.5	< 0.3%					No repair
II	MINOR	Horizontal flexural cracking; Onset of longitudinal crack at column ends.	individual column yield or lap-splice-debonding starts.			> 0.3%					Possible repair
III	MODERATE	Onset of Shear cracks; Open horizontal flexural cracks in column; of horizontal flexural crack; Lengthened longitudinal cracks at column ends; Onset of spalling in plastic hinge zones of column; Rocker bolt cracking.	columns yield at bottom; individual column top lap-splice debond starts; beam or pile yield with plastic curvature ratio less than one; moderate shear inefficiency; rocker bearing failure or overturn; moderate pier drift;	1.25	1.2	> 1.2%					some repair
IV	MAJOR	Wide shear crack; Wide horizontal flexural cracks; Fork-shaped longitudinal cracks formed; Extensive concrete spalling.	columns yield and degrade at bottom top; or mechanism forms; column shear failure; pile overloaded, pile shear failure; excessive pier drift, or deck drops off bearings.	1.0	1.0	> 2%					Repair
V	LOCAL FAILURE COLLAPSE	Visible permanent deformation; Buckling/rupture of reinforcement	plastic hinges experience significant rotation, or column collapse by shear, columns totally lose load resistance capacity; deck drops off piers; foundation failure due to liquefaction, landslide etc (not investigated in this study)	< 1.0	< 1.0	> 3%					Replacement

failure mode 'flexural brittle' - lap splice bond failure

For 'non-degrading flexural ductile' failure mode,  $M_{dev}/M_y$  (i.e., curvature ductility ratio  $\mu_{\phi}$ ) allowable up to 3 or 4 before concrete section shear capacity decreases. the 'non-degrading' mode is achievable in a beam with small steel ratio or a well-confined column.

maximum allowed section curvature ductility ratio is based on maximum deflection ductility ratio that does not cause concrete shear capacity to decrease.

Figure 8.12 Damage Assessment Table (Zhong, 2001)



## Chapter 9 – Summary and Conclusions

### *9.1 Research Summary*

This research investigation determined physical properties of conventional elastomeric bridge bearings. The test specimens consisted of six used (8 to 10 years old) Type II bearings obtained from three different bridges, two new Type I bearings, and one new Type II bearing. A special testing apparatus was designed, constructed, and used to conduct a series of reversed cyclic tests of the test specimens. Tests were conducted inside a temperature-controlled chamber at temperatures ranging from approximately 20°C to -25°C and the results of these tests were analyzed and reported. The experimentally-determined properties were used in a series of nonlinear dynamic analyses characterizing the implications of these material properties on the seismic response of a representative bridge to a maximum considered event in southern Illinois. The effects of temperature changes were assessed for multiple bearing configurations for the representative bridge. Computed results depended on whether the flexibility and slip of the bearings were modeled or not. A relative improvement in performance obtainable with a stick-slip retrofit bearing was identified in the nonlinear dynamic analyses. This retrofit bearing, intended to replace the fixed bearing on a multi-span continuous bridge, was constructed as a prototype and tested in the test apparatus at both room and cold temperatures (-25°C) and the results were reported.

## 9.2 Conclusions

By means of experimental tests and ensuing calculations, the following was observed:

- Effect of low temperature on elastomer shear modulus

Unlike results obtained in other published research (Murray and Detenber, 1961; Bruzzone and Sorta, 1978; Roeder, et al., 1987; Roeder, et al., 1989; Eyre and Stevenson, 1991), large increases in stiffness with low temperatures were not observed for the used natural rubber bearings. Increases of approximately 30% in the elastomer shear modulus were observed as the temperature decreased from 20°C to -25°C. The modulus did not increase appreciably with time held at low temperatures, for the applied exposure durations. However, the new neoprene Type II bearing had an increase of 600% in the shear modulus as the temperature dropped from 20°C to -25°C, illustrating the dependence of low temperature stiffening on elastomer compound, and perhaps on age.

- Observed TFE sliding surface coefficient of friction,  $C_f$

The TFE sliding surfaces of the used Type II bearings exhibited wear, discoloration, and possible contamination after being in service for 8-10 years. These bearings exhibited higher coefficient of friction values than those reported in the literature and those used in design manuals. Mean values of the apparent coefficient of friction were approximately 0.17 at 20°C and approximately 0.22 at -25°C. These values are much higher than the value of 0.07 listed in the IDOT materials specifications. This higher coefficient of friction will result in larger

lateral forces transmitted across the sliding interface and into the substructure piers.

To assess the role of the conventional bearings on the response of a typical bridge subjected to a strong earthquake, experimentally obtained properties were used in nonlinear dynamic analyses of a representative bridge model. The model was subjected to a ground motion representing the intensity of a motion having a 2% probability of exceedance in 50 years at the southern tip of Illinois on Site Class D soils. The nonlinear dynamic analyses considered several bearing configurations and temperatures. The results of this phase are:

- The importance of explicitly modeling the bearings

Neglecting the flexibility of the elastomeric bearings can result in misleading results during dynamic analyses. As shown in Chapter 8, these results are non-conservative and may lead to an underestimation of the ductility demands experienced by components of the bridge.

- Brittle substructure behavior may result for typical bearing configurations

The fixed bearing in a multi-span continuous bridge receives much of the lateral force during earthquake ground shaking. The force and deformation demands may cause brittle lap-splice and column shear failures in the columns of the bridge substructure.

- The use of the stick-slip retrofit bearing is promising

The provision of the retrofit bearing at the fixed pier succeeded in reducing the force and deformation demands below the damage threshold. However, mitigation of the damage at other piers requires additional interventions such as provision of Type II bearings in place of Type I bearings and suitable restraint measures to prevent loss of girder seat support.

## **Appendix Introduction**

Appendices A through E present results for each bearing tested. As such, they share a common format. The order of presentation for the results is:

1. Testing parameter summary
2. Shear modulus summary and normalized shear modulus summary

Followed by a:

3. Raw Load vs. Displacement plot for each test
4. Normalized Load/Area vs. Displacement/Height plot for each test
5. Vertical Load vs. Displacement plot for each test

Appendix F contains DRAIN-2DX input files for the nonlinear dynamic analyses.

Appendix G contains various units conversions.



**APPENDIX A**

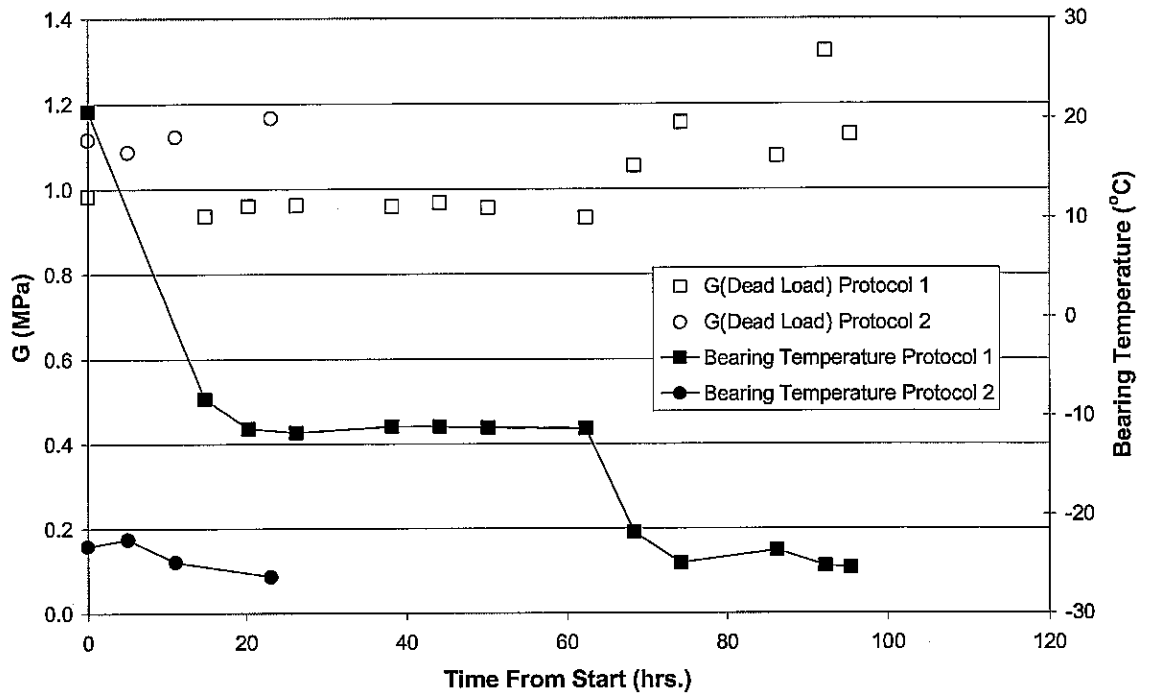
**Test Results for 2A1 & 2A2**



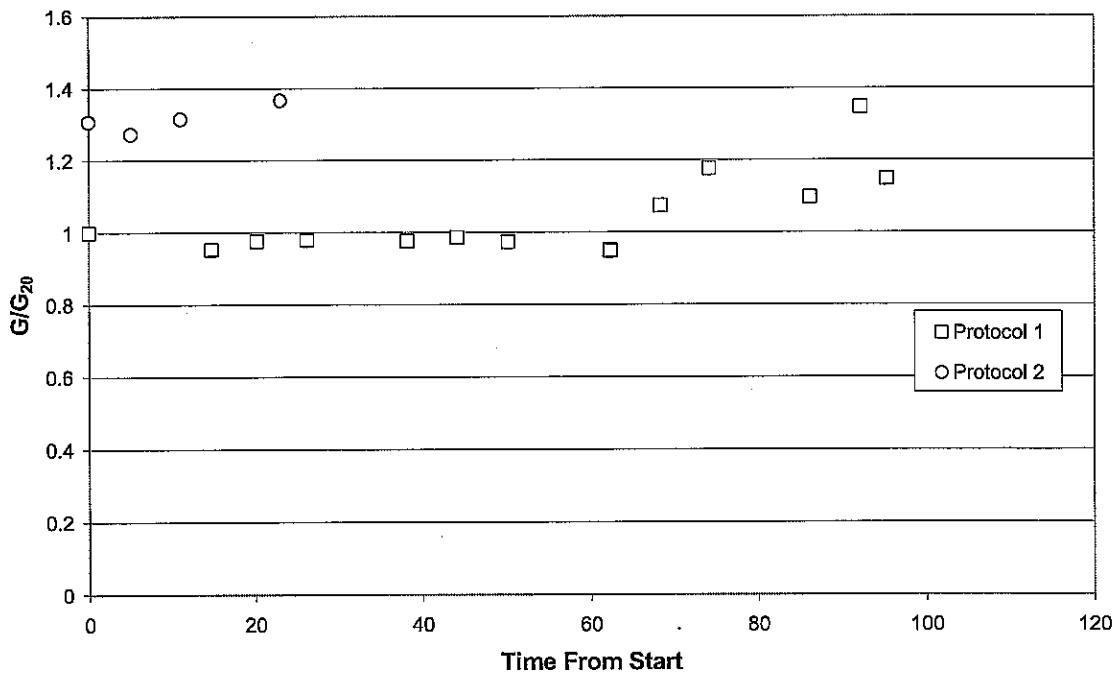
**Appendix A – Test Results for 2A1 & 2A2**

Report Reference	Date & Time	Time From Start, hrs.	Brg. Temp. °C	Vert. Load		Amp.		Freq. hz
				psi	MPa	in	mm	
2A1-1-01	6/24/01 18:00	0.00	20.7	500	3.447	0.75	19.05	1
2A1-1-02	6/25/01 8:51	14.85	-8.3	500	3.447	0.75	19.05	1
2A1-1-03	6/25/01 14:16	20.27	-11.3	500	3.447	0.75	19.05	1
2A1-1-04	6/25/01 20:18	26.30	-11.7	500	3.447	0.75	19.05	1
2A1-1-05	6/26/01 8:13	38.22	-11.1	500	3.447	0.75	19.05	1
2A1-1-06	6/26/01 14:09	44.15	-11.1	500	3.447	0.75	19.05	1
2A1-1-07	6/26/01 20:13	50.22	-11.2	500	3.447	0.75	19.05	1
2A1-1-08	6/27/01 8:21	62.35	-11.3	500	3.447	0.75	19.05	1
2A1-1-09	6/27/01 14:21	68.35	-21.8	500	3.447	0.75	19.05	1
2A1-1-10	6/27/01 20:13	74.22	-24.9	500	3.447	0.75	19.05	1
2A1-1-11	6/28/01 8:16	86.27	-23.6	500	3.447	0.75	19.05	1
2A1-1-12	6/28/01 14:18	92.30	-25.2	500	3.447	0.75	19.05	1
2A1-1-13	6/28/01 17:24	95.40	-25.4	500	3.447	0.75	19.05	1
2A1-1-14	6/28/01 17:29	95.48	-24.8	250	1.724	0.75	19.05	1
2A1-1-15	6/28/01 17:36	95.60	-24.6	500	3.447	1.5	38.1	1
2A1-1-16	6/28/01 18:18	96.30	-24.4	500	3.447	3	76.2	0.5
2A1-1-17	6/28/01 18:39	96.65	-24.4	750	5.171	1.5	38.1	1
2A1-1-18	6/28/01 18:52	96.87	-24.4	750	5.171	3	76.2	0.5
2A2-2-01	7/24/01 9:00	0.00	-23.2	500	3.447	0.75	19.05	1
2A2-2-02	7/24/01 14:06	5.10	-22.5	500	3.447	0.75	19.05	1
2A2-2-03	7/24/01 20:09	11.15	-24.8	500	3.447	0.75	19.05	1
2A2-2-04	7/25/01 8:09	23.15	-26.3	500	3.447	0.75	19.05	1
2A2-2-05	7/25/01 8:40	23.67	-24.3	250	1.724	0.75	19.05	1
2A2-2-06	7/25/01 9:04	24.07	-21.7	750	5.171	0.75	19.05	1
2A2-2-07	7/27/01		20.9	750	5.171	0.75	19.05	1
2A2-2-08	7/27/01		20.9	500	3.447	0.75	19.05	1
2A2-2-09	7/27/01		20.9	250	1.724	0.75	19.05	1

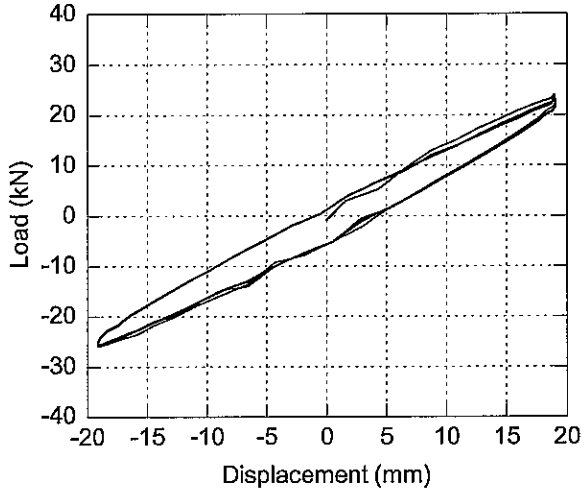
### Shear Modulus Summary - 2A1-1 & 2A2-2



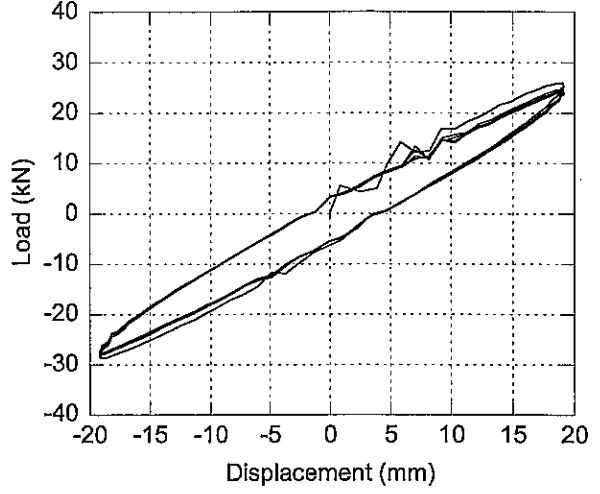
### Normalized Shear Modulus - 2A1-1 & 2A2-2



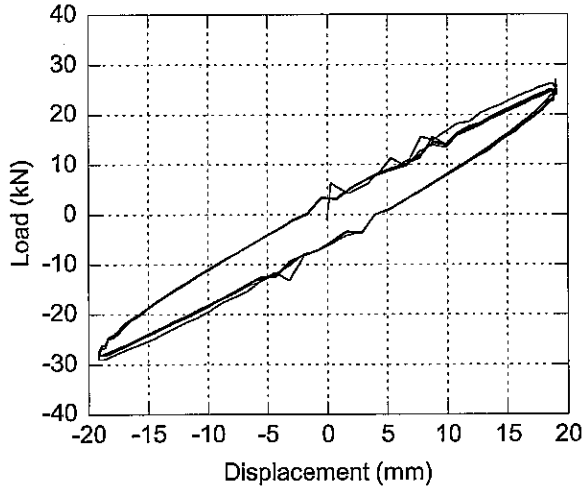
**2A1-1-01**



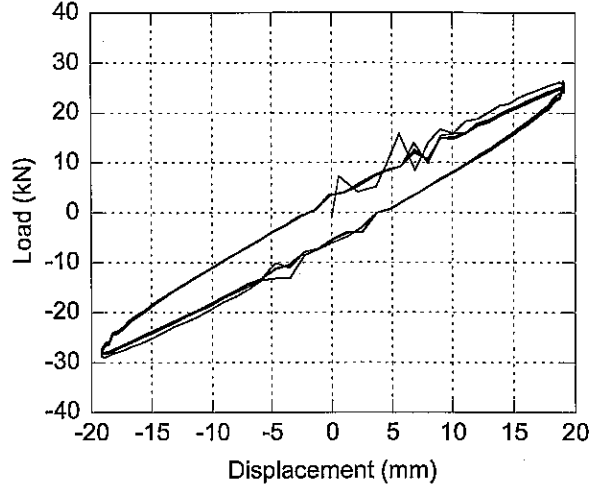
**2A1-1-02**



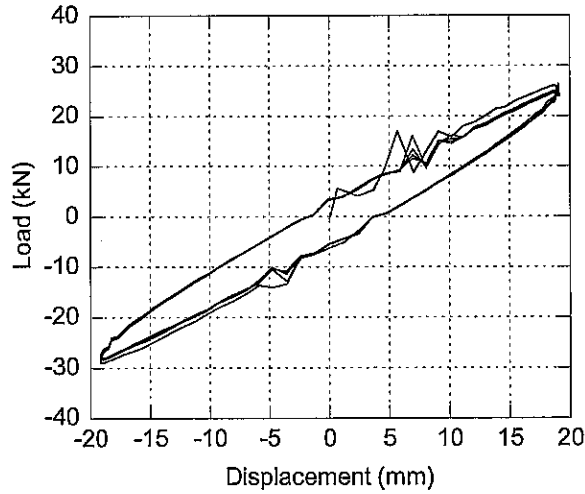
**2A1-1-03**



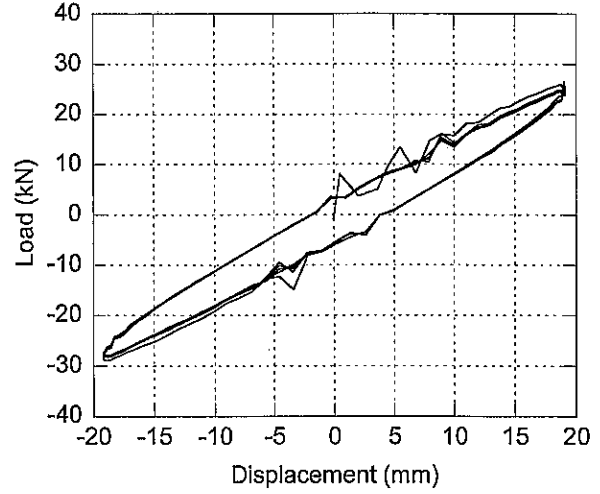
**2A1-1-04**



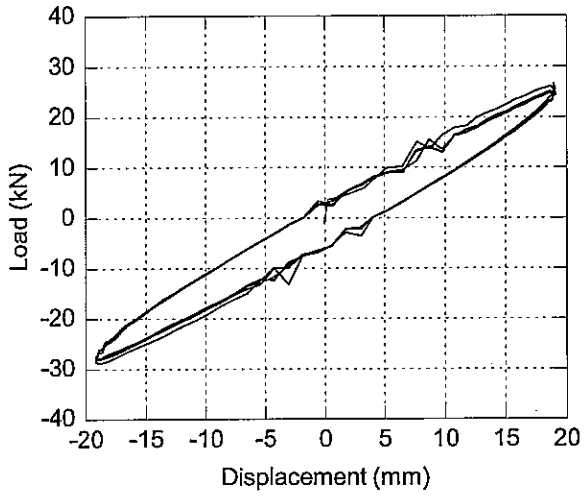
**2A1-1-05**



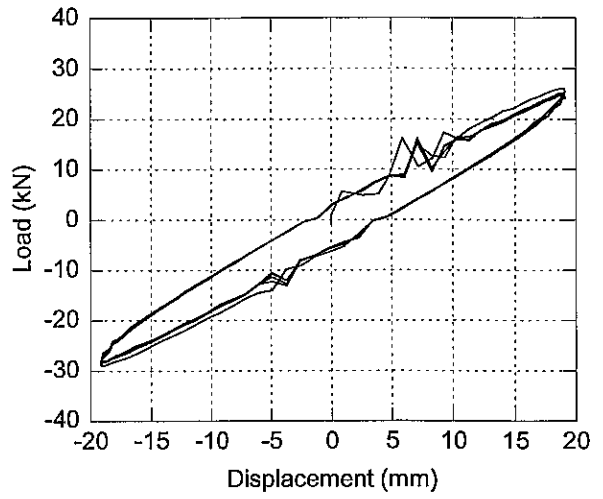
**2A1-1-06**



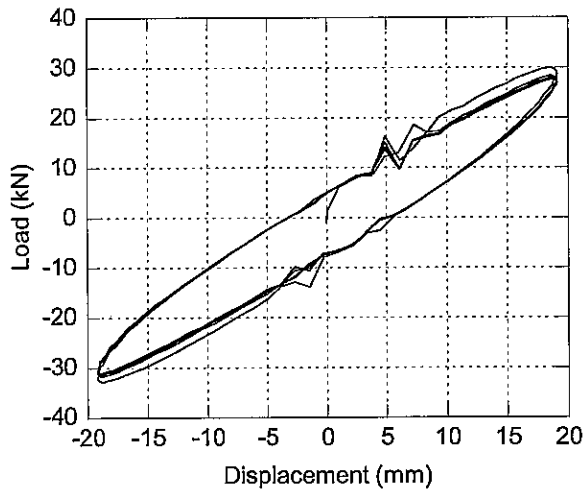
**2A1-1-07**



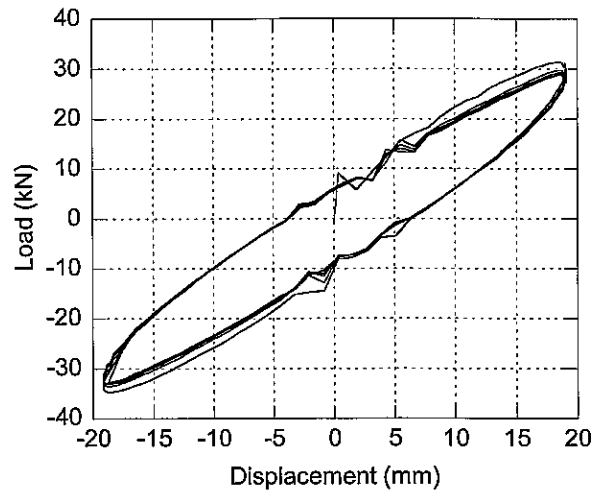
**2A1-1-08**



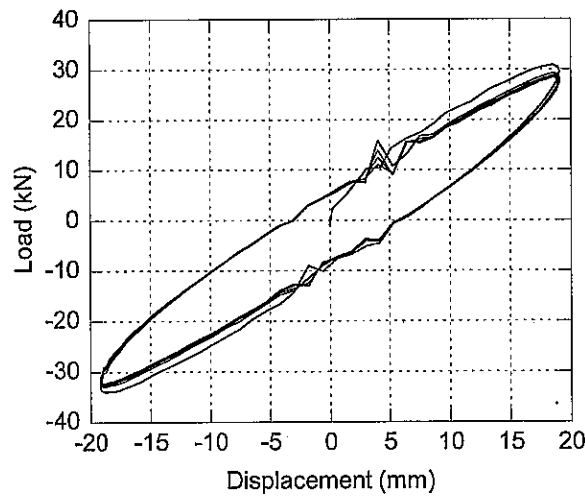
**2A1-1-09**



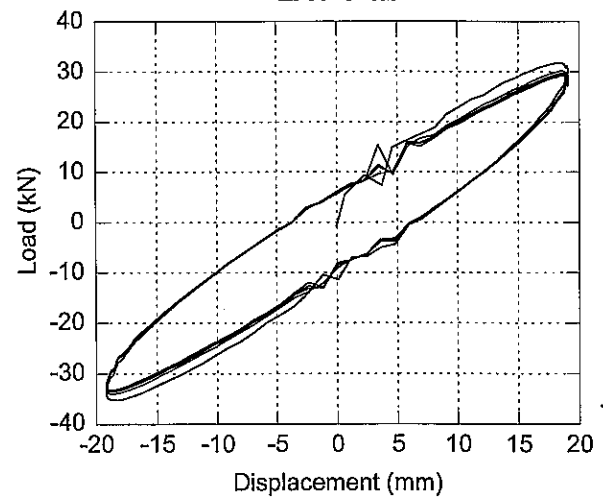
**2A1-1-10**



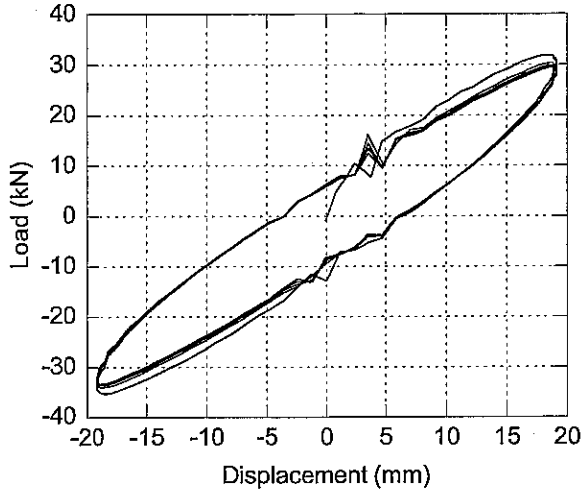
**2A1-1-11**



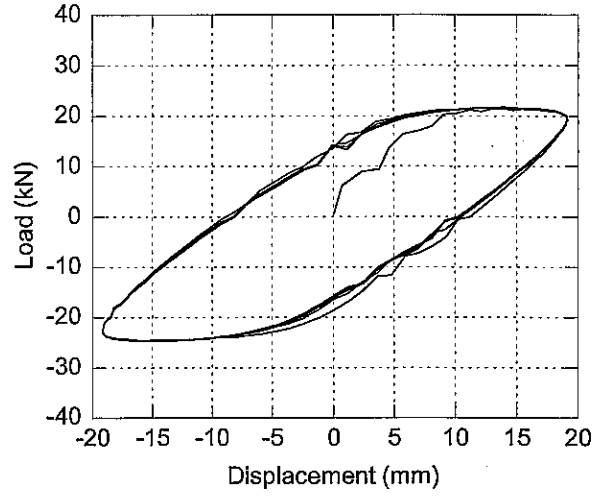
**2A1-1-12**



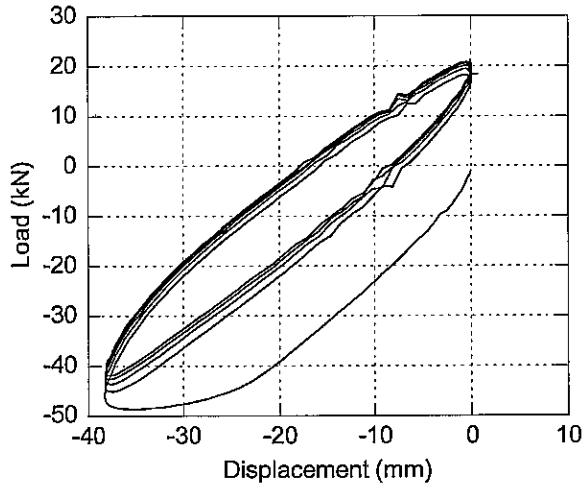
2A1-1-13



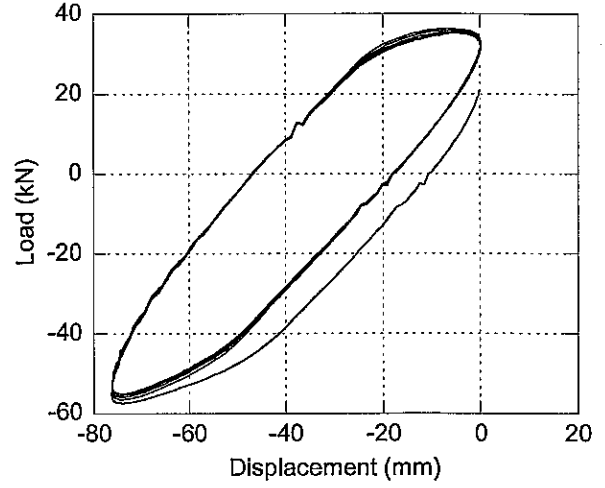
2A1-1-14



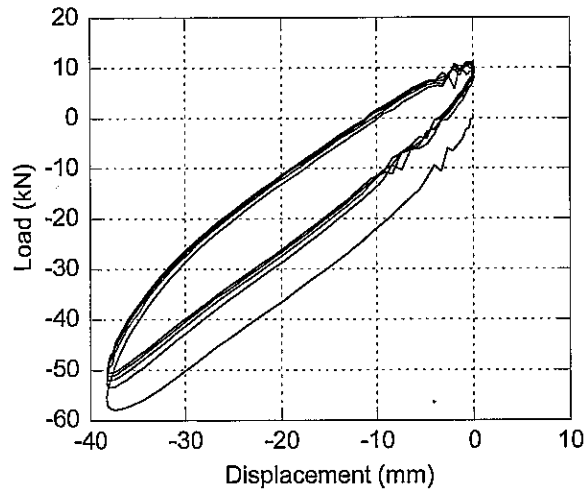
2A1-1-15



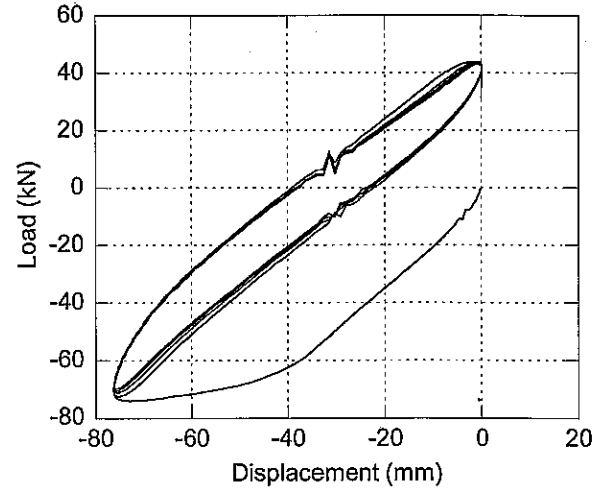
2A1-1-16



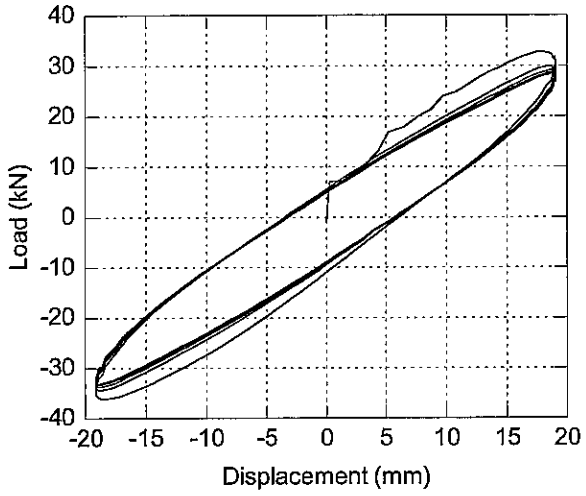
2A1-1-17



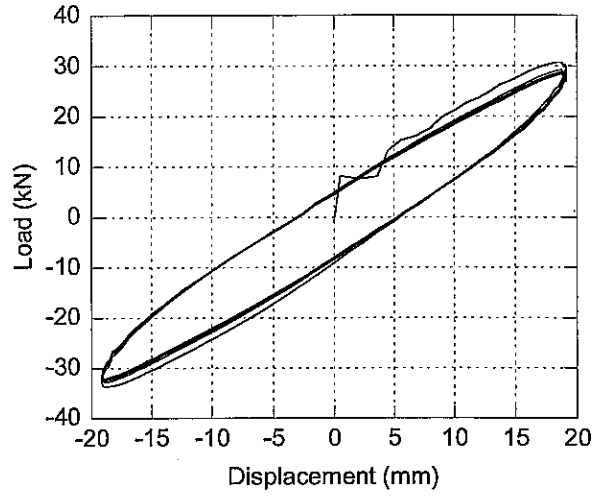
2A1-1-18



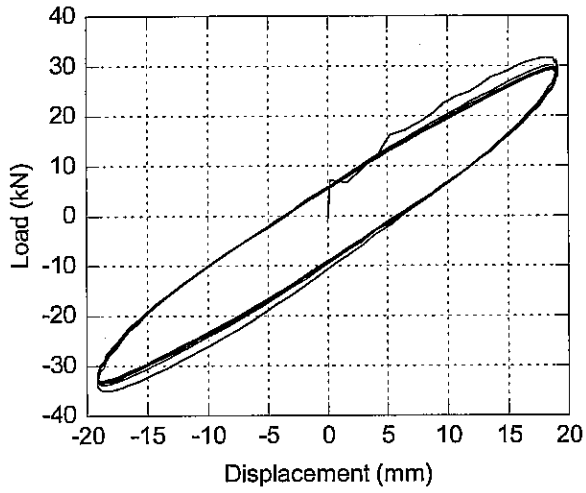
**2A2-2-01**



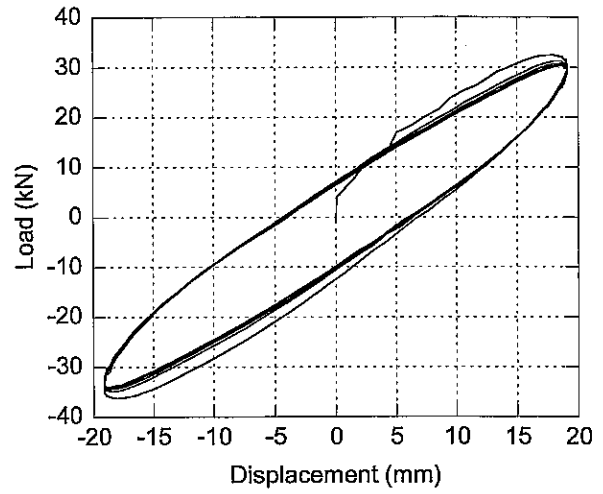
**2A2-2-02**



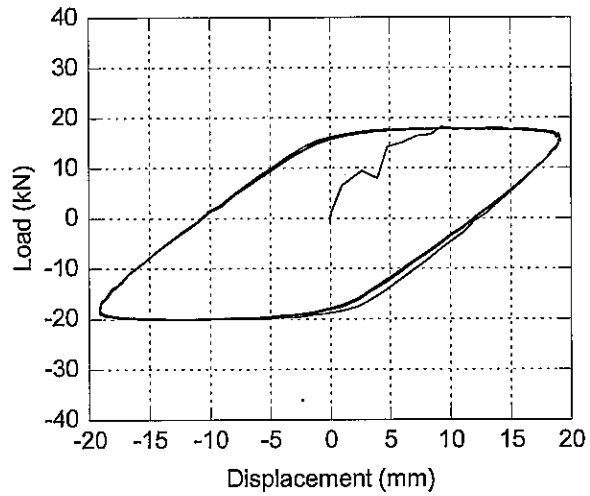
**2A2-2-03**



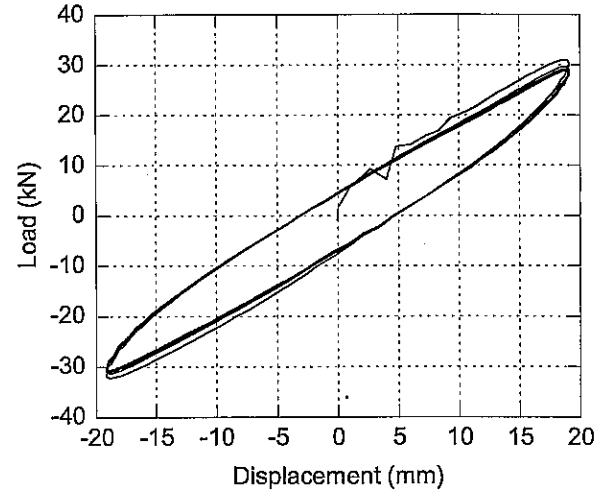
**2A2-2-04**



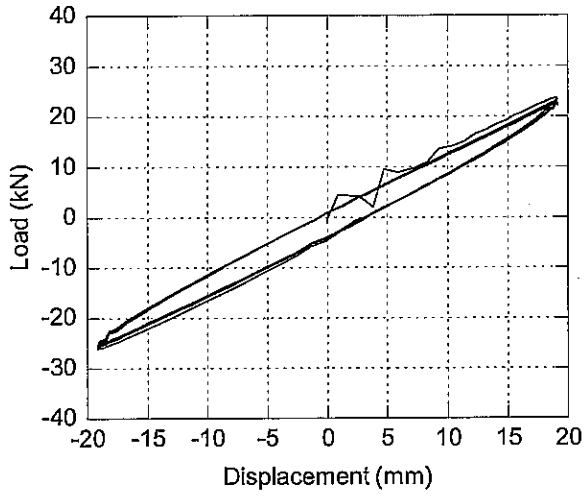
**2A2-2-05**



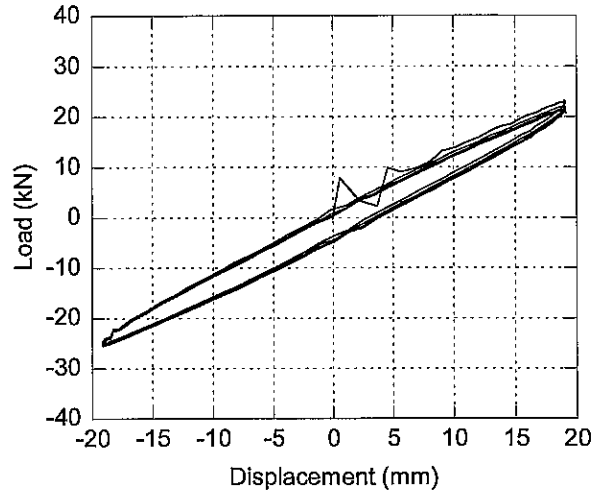
**2A2-2-06**



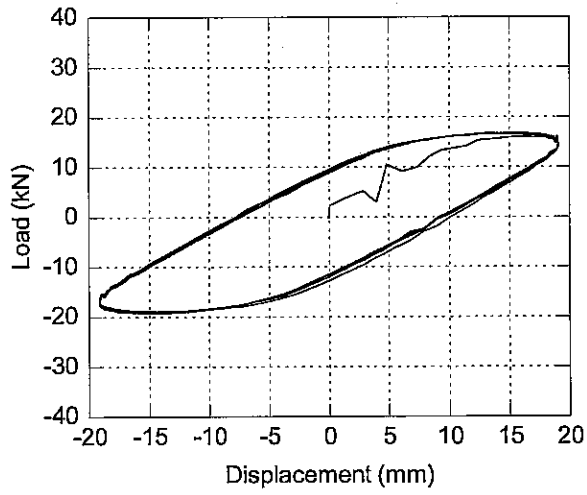
2A2-2-07



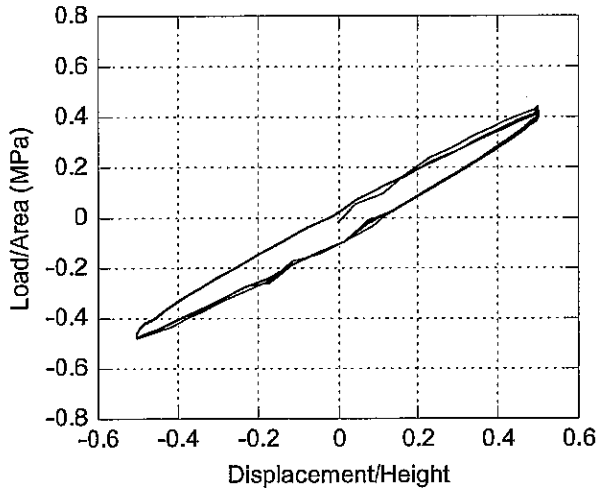
2A2-2-08



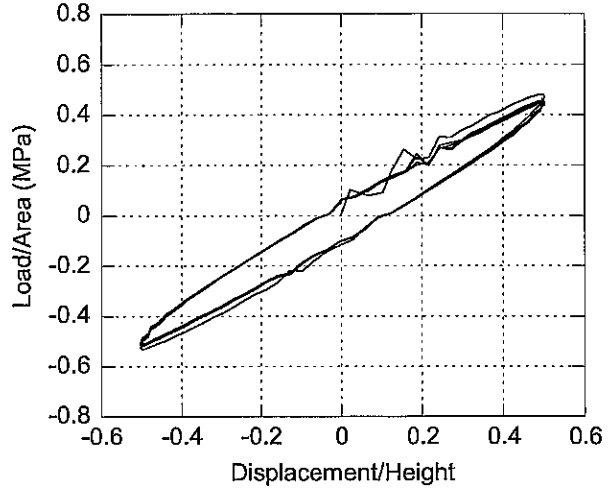
2A2-2-09



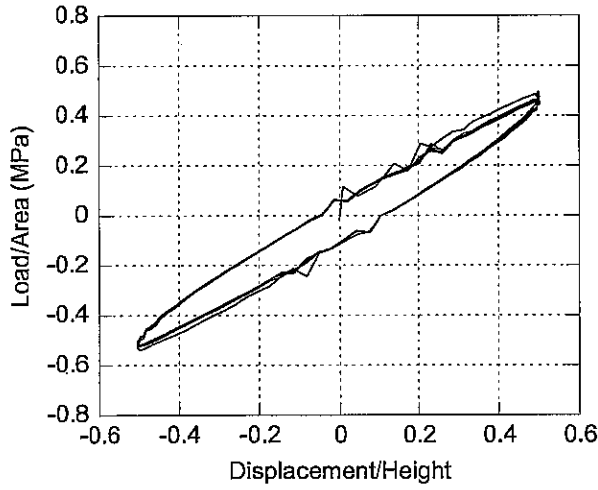
2A1-1-01



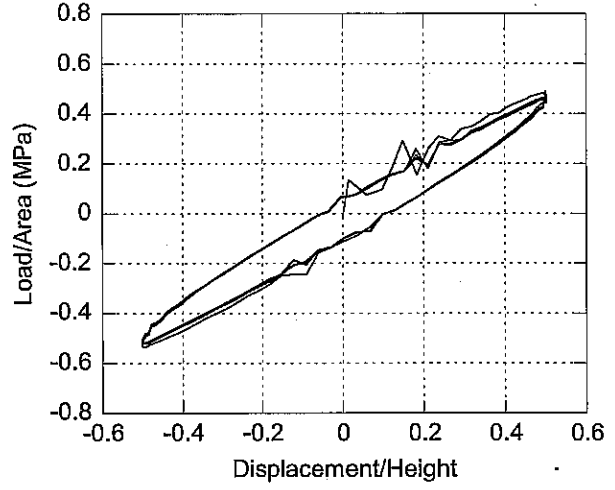
2A1-1-02



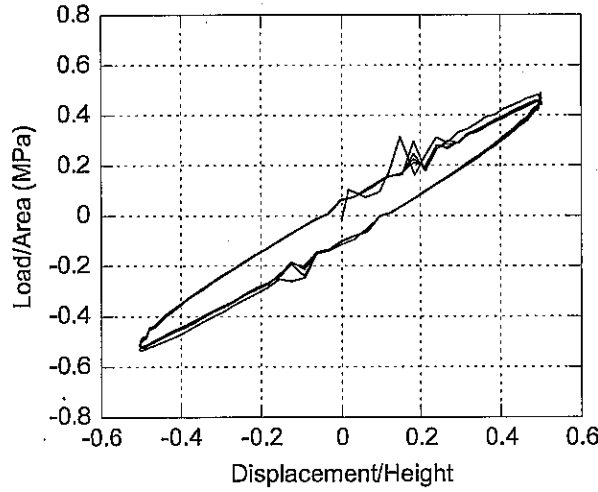
2A1-1-03



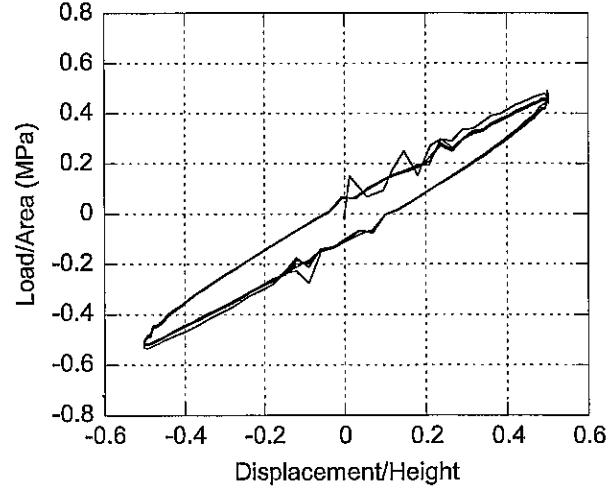
2A1-1-04



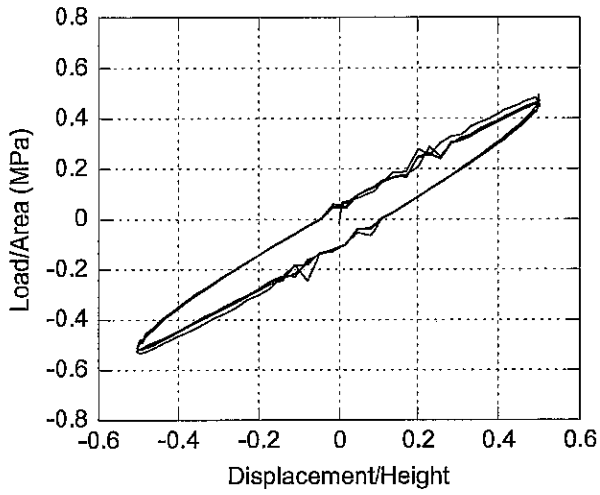
2A1-1-05



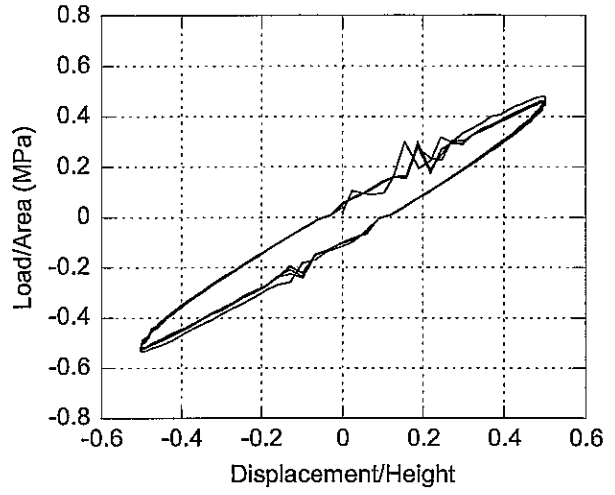
2A1-1-06



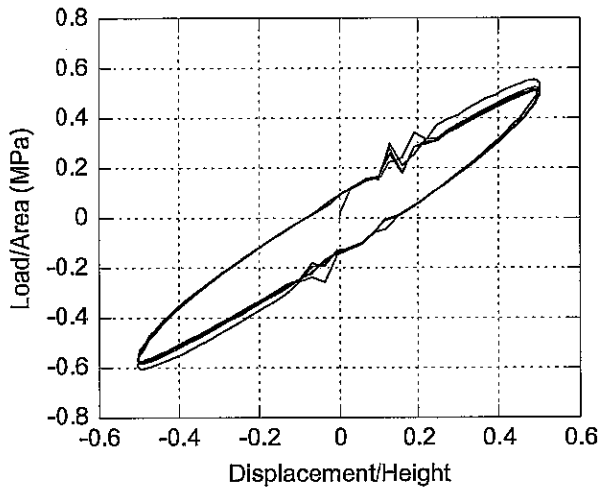
2A1-1-07



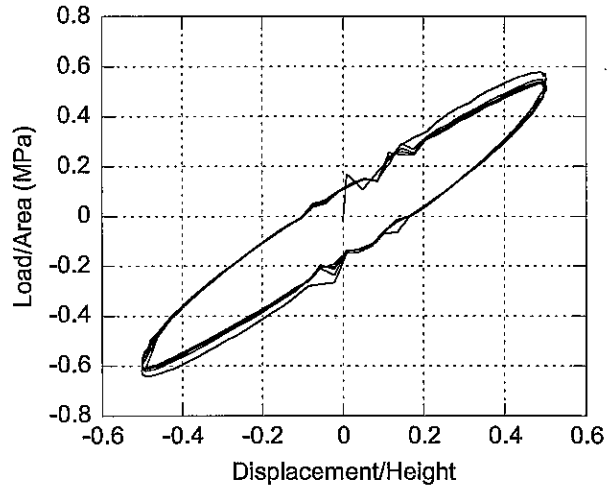
2A1-1-08



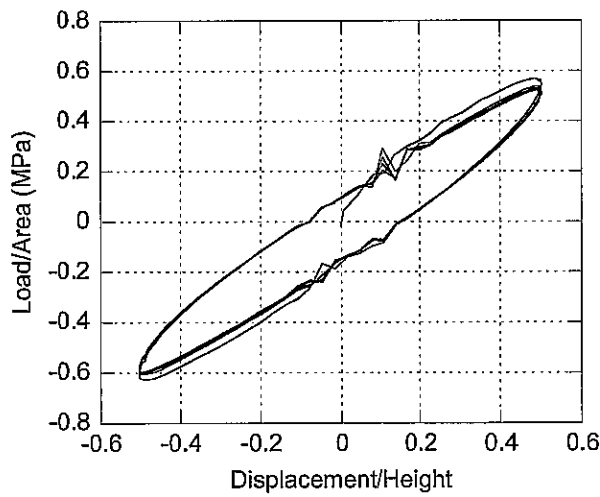
2A1-1-09



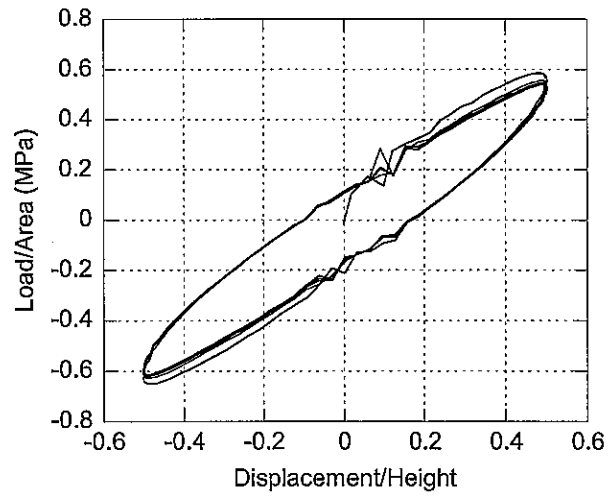
2A1-1-10



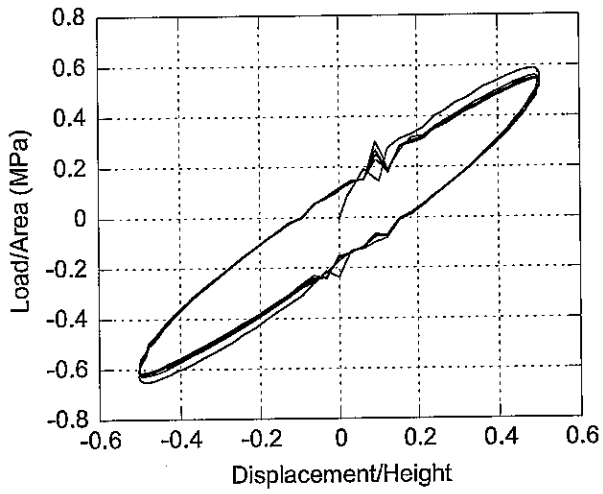
2A1-1-11



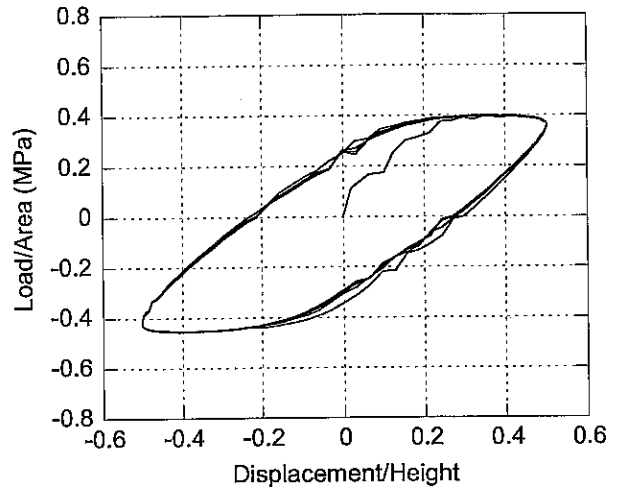
2A1-1-12



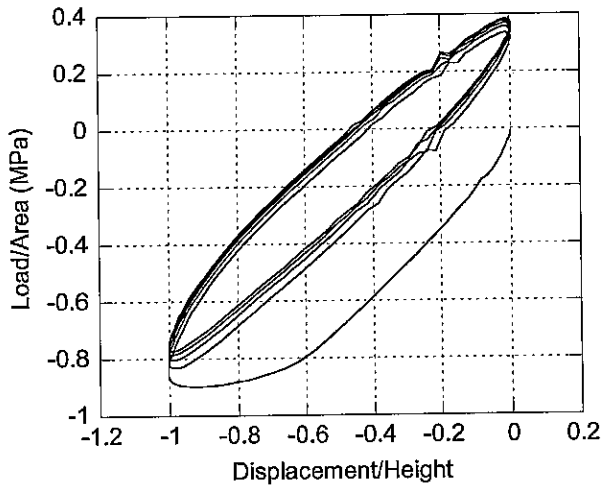
2A1-1-13



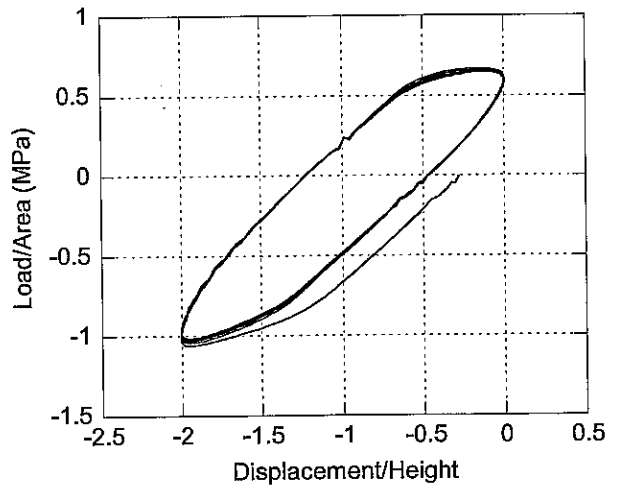
2A1-1-14



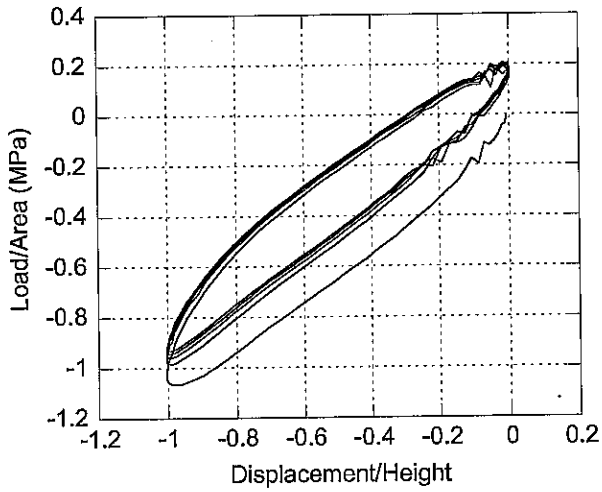
2A1-1-15



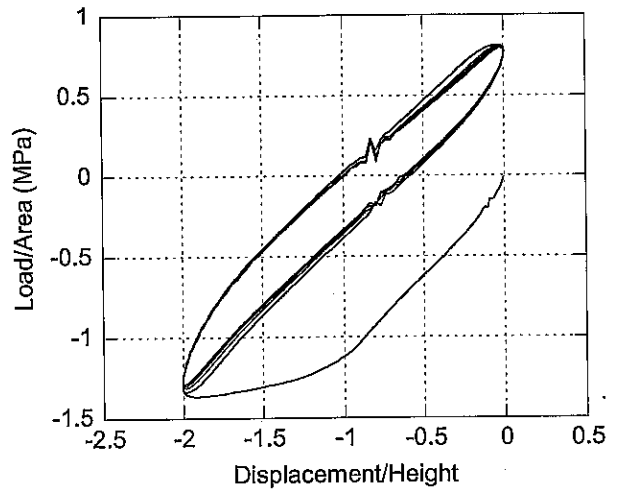
2A1-1-16



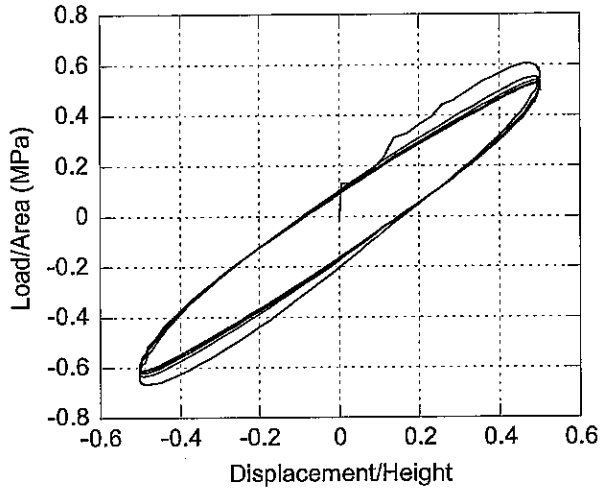
2A1-1-17



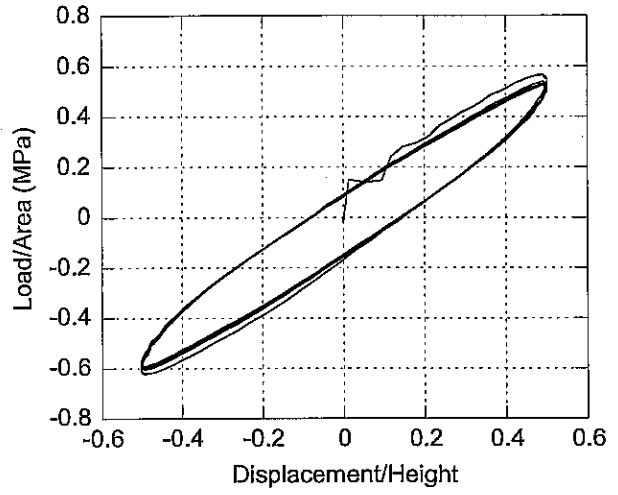
2A1-1-18



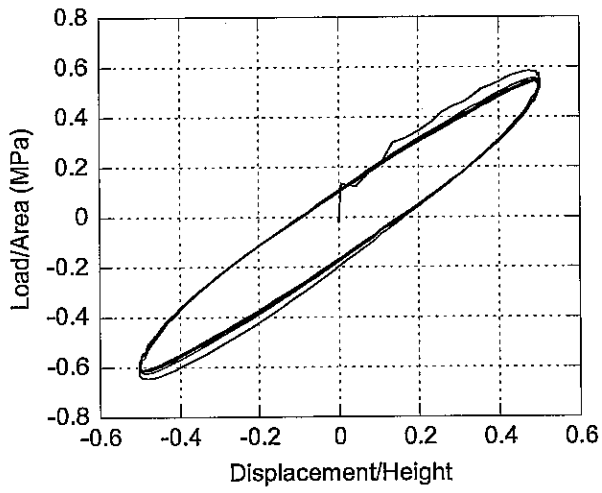
**2A2-2-01**



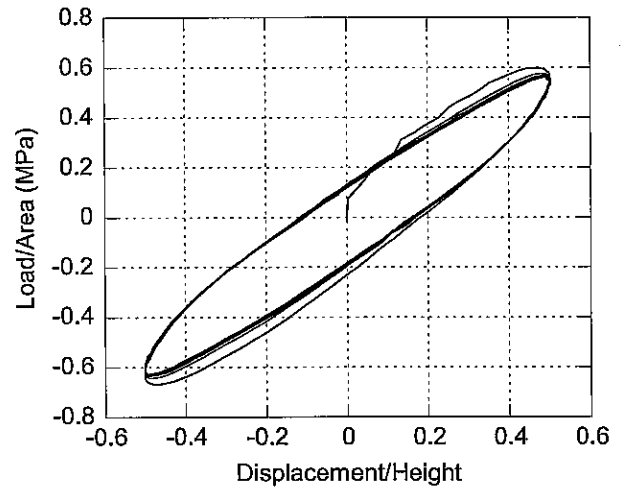
**2A2-2-02**



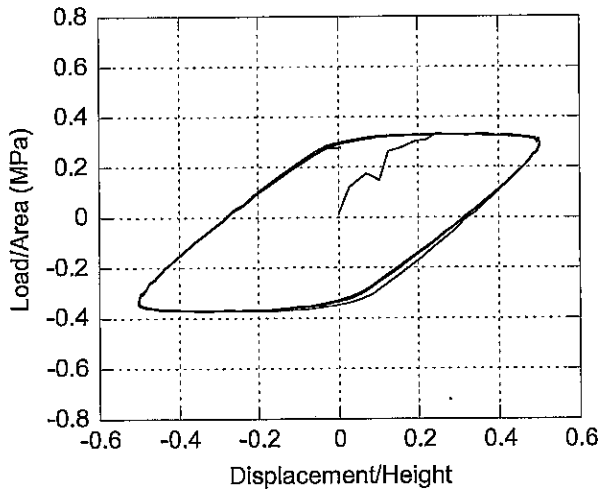
**2A2-2-03**



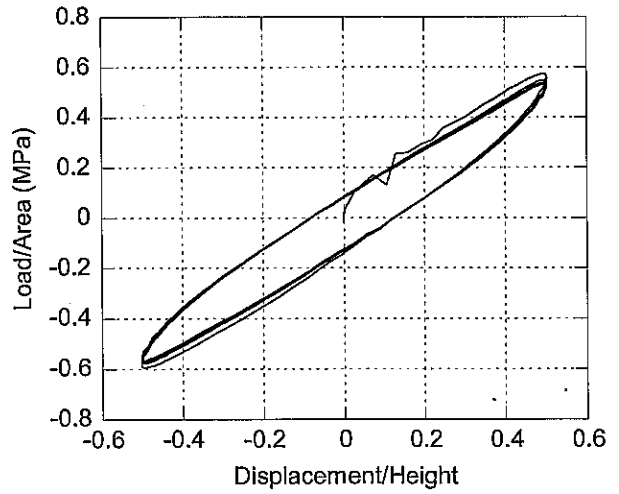
**2A2-2-04**



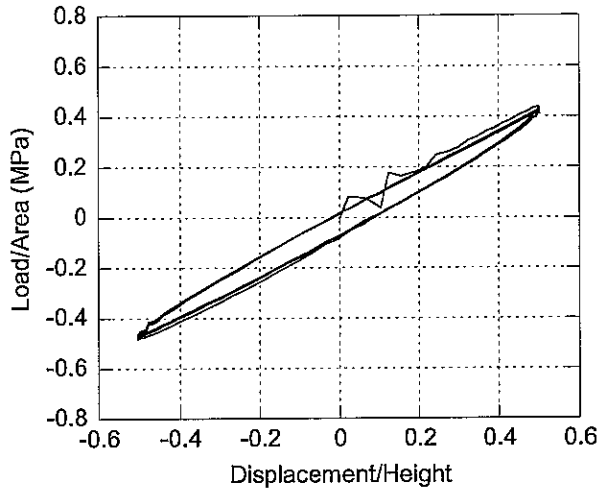
**2A2-2-05**



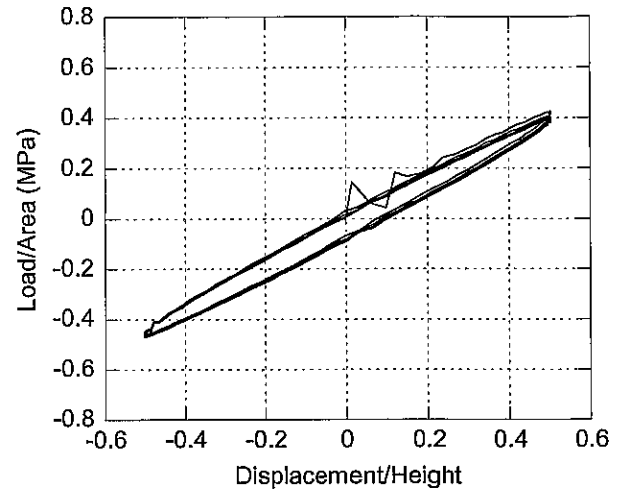
**2A2-2-06**



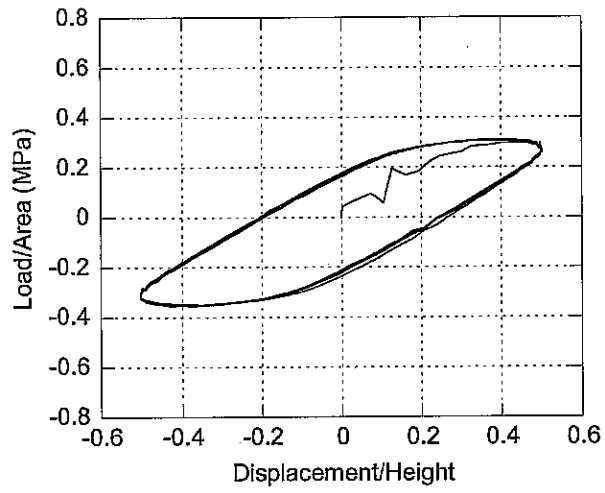
2A2-2-07



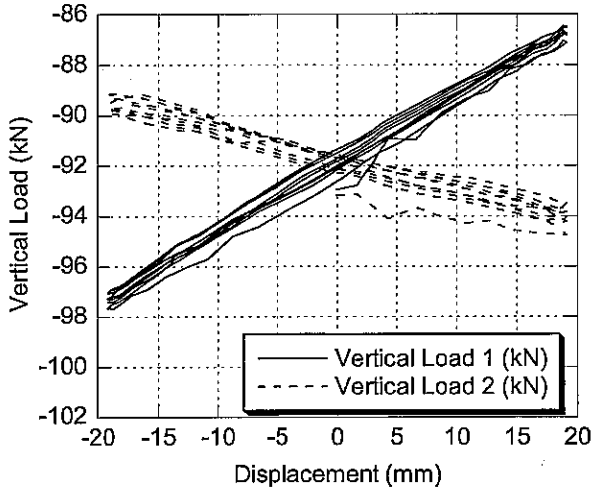
2A2-2-08



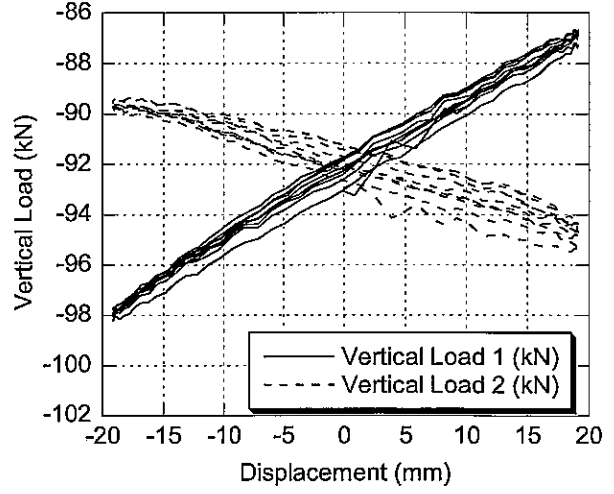
2A2-2-09



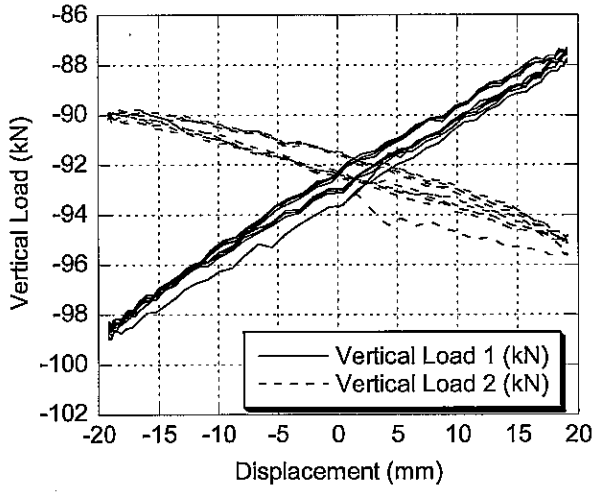
2A1-1-01



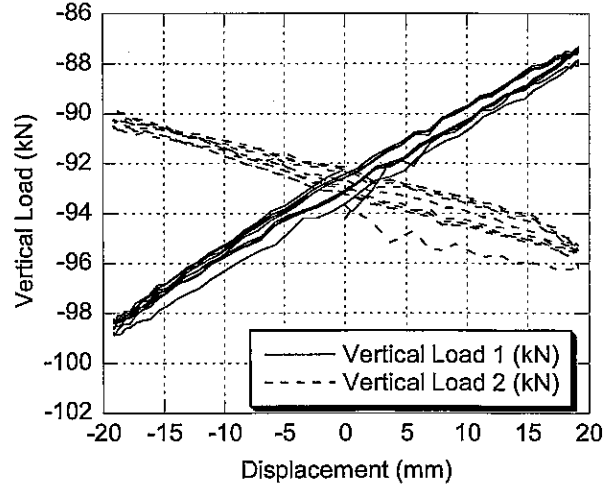
2A1-1-02



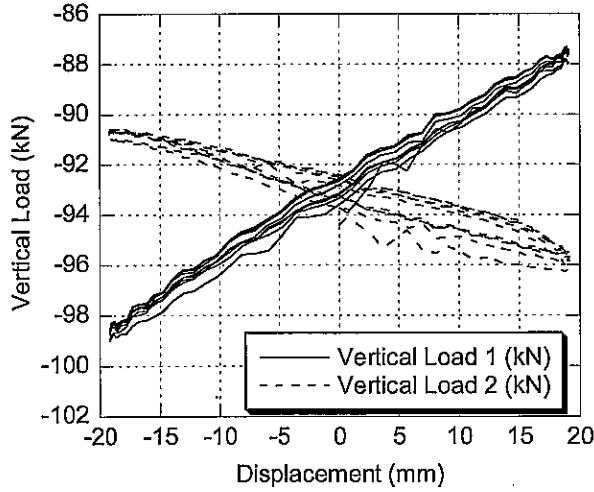
2A1-1-03



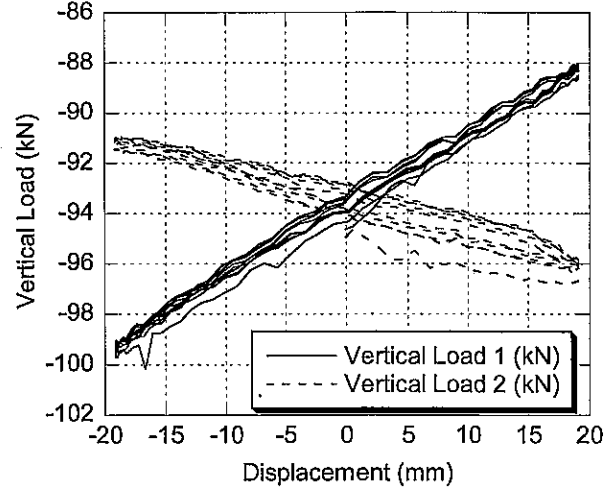
2A1-1-04



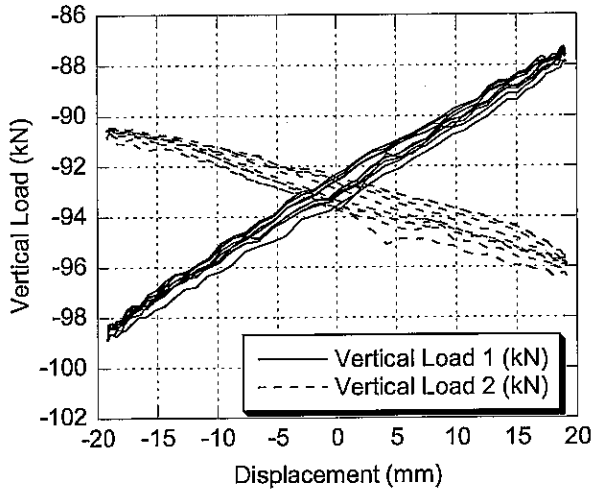
2A1-1-05



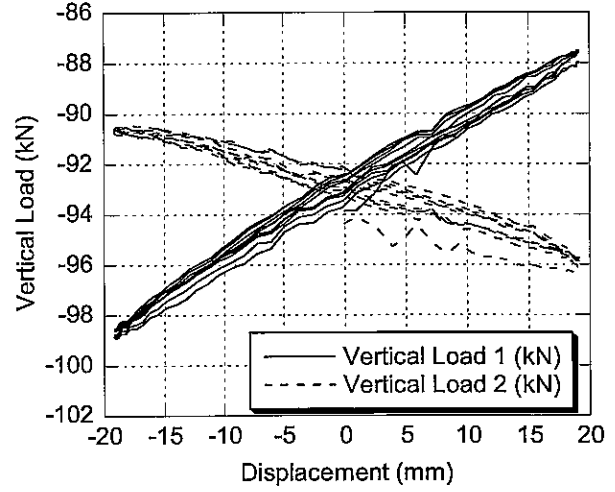
2A1-1-06



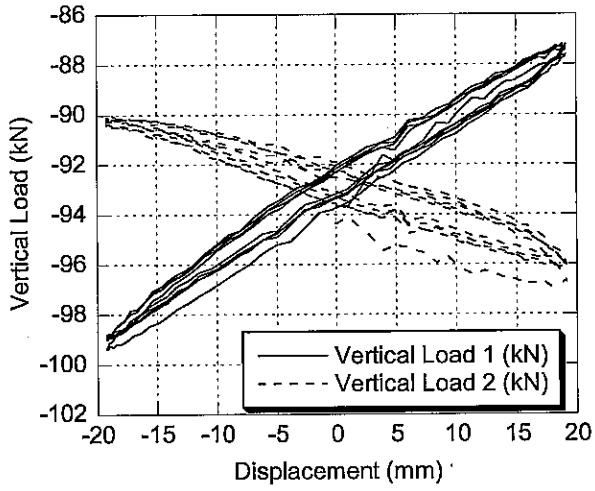
2A1-1-07



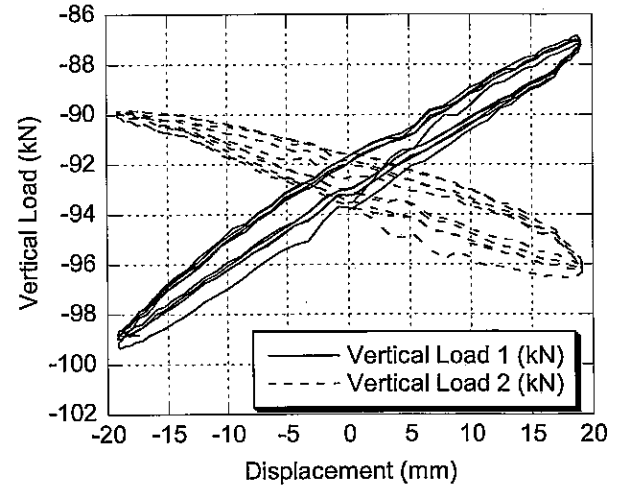
2A1-1-08



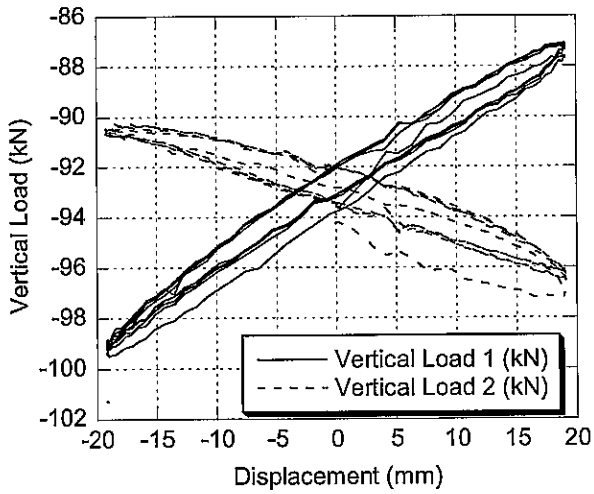
2A1-1-09



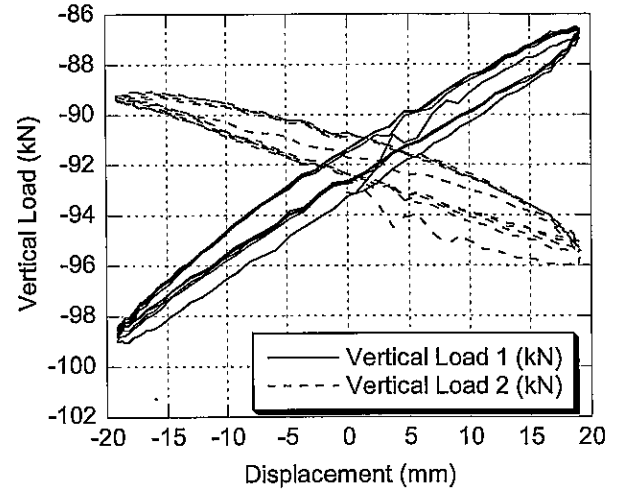
2A1-1-10



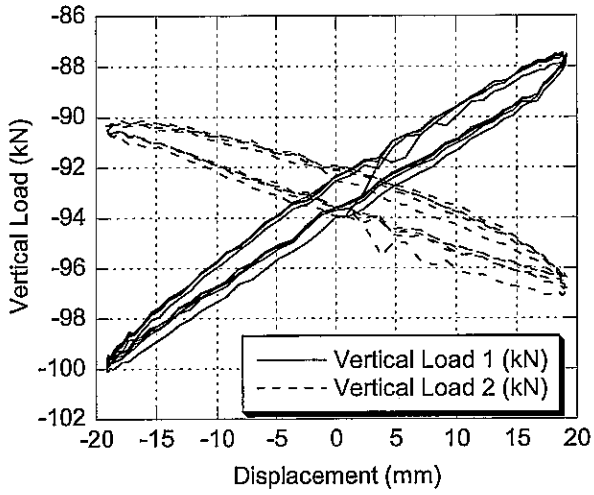
2A1-1-11



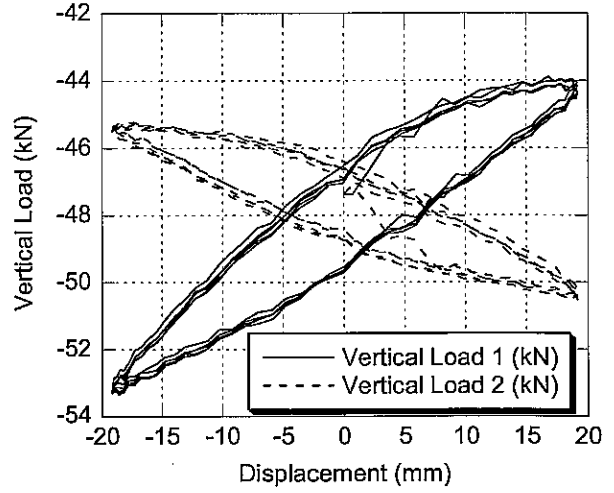
2A1-1-12



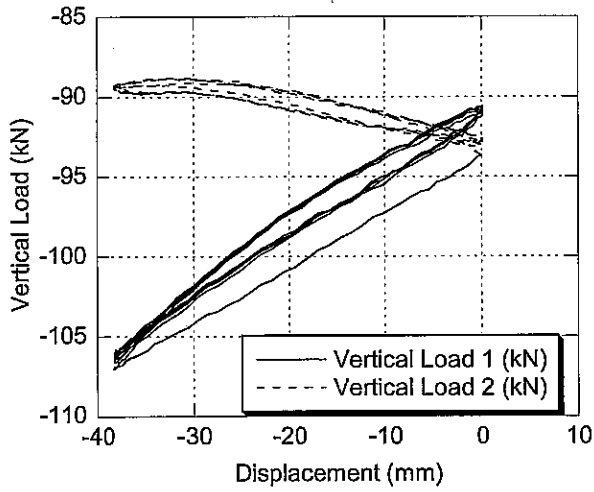
2A1-1-13



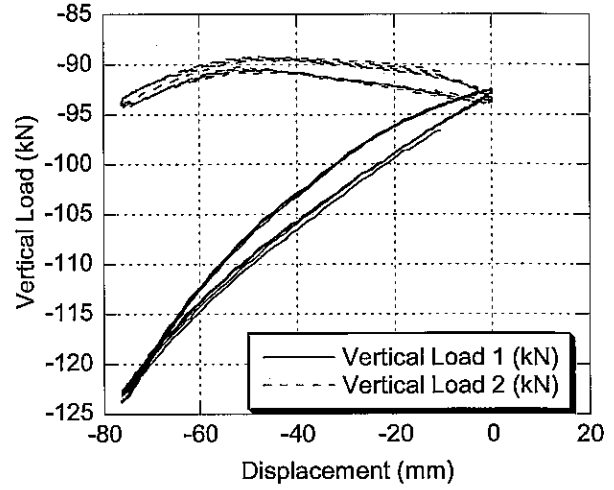
2A1-1-14



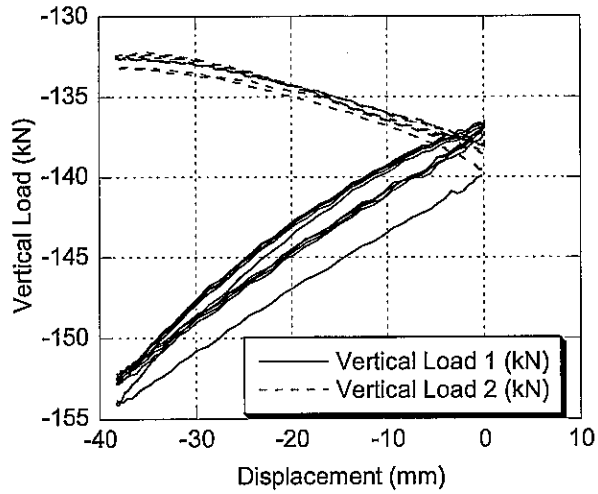
2A1-1-15



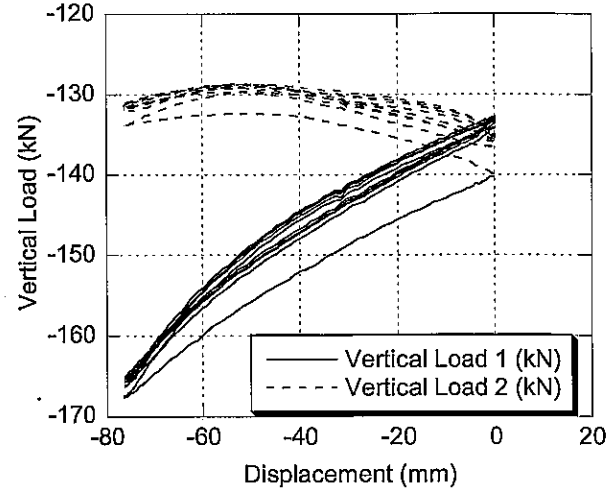
2A1-1-16



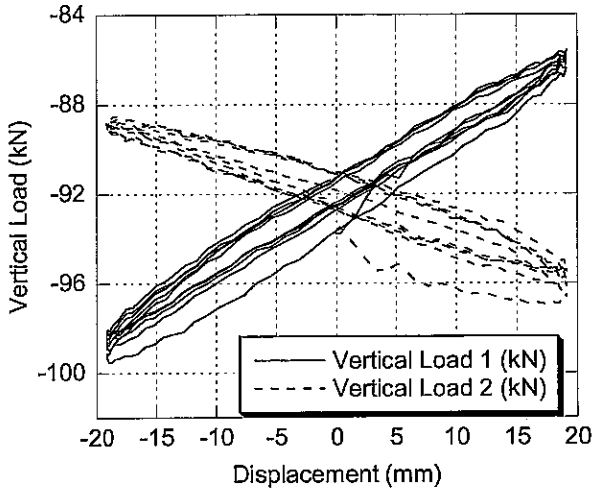
2A1-1-17



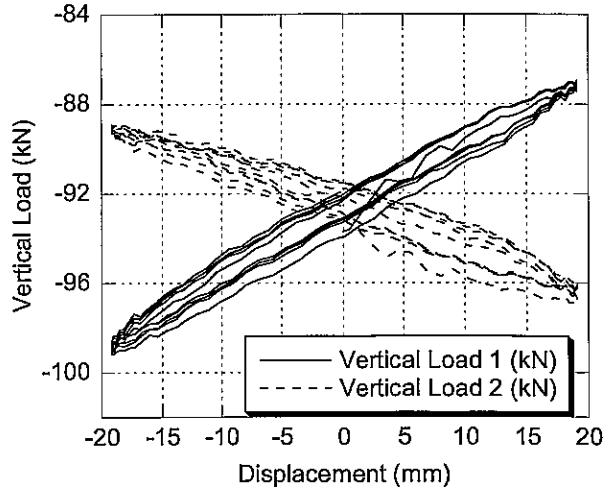
2A1-1-18



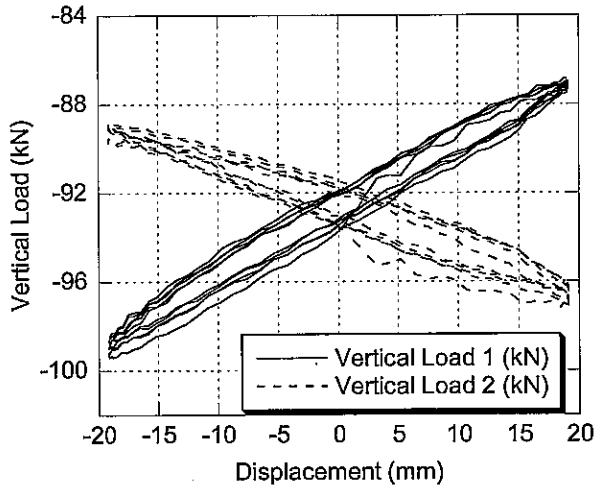
2A2-2-01



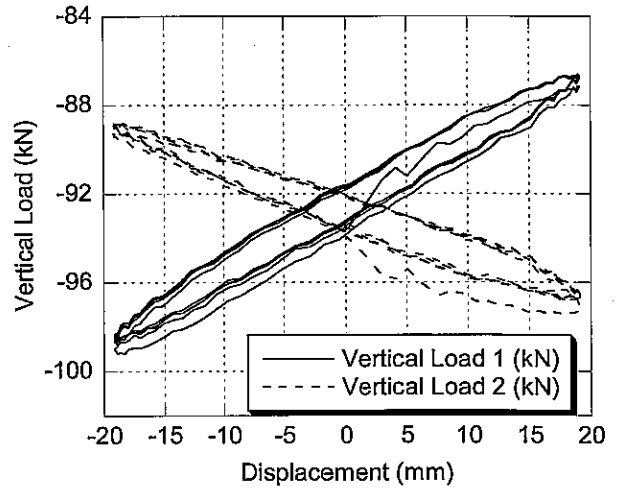
2A2-2-02



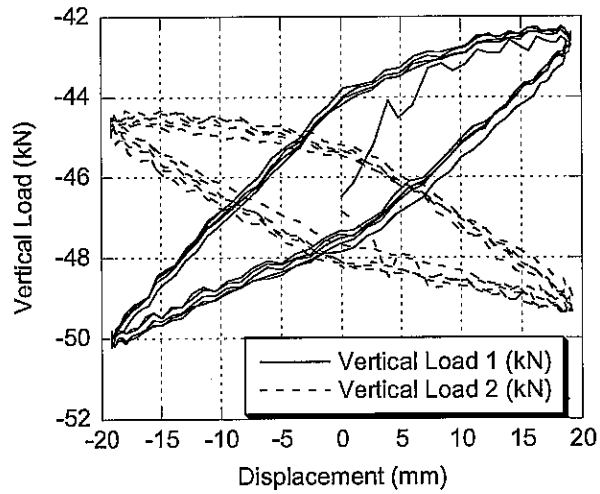
2A2-2-03



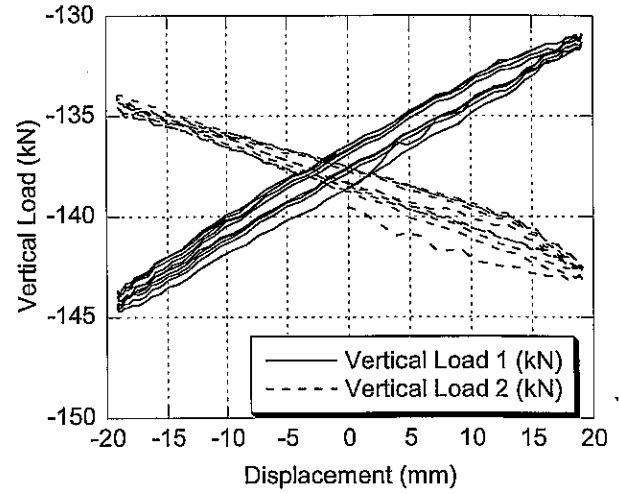
2A2-2-04



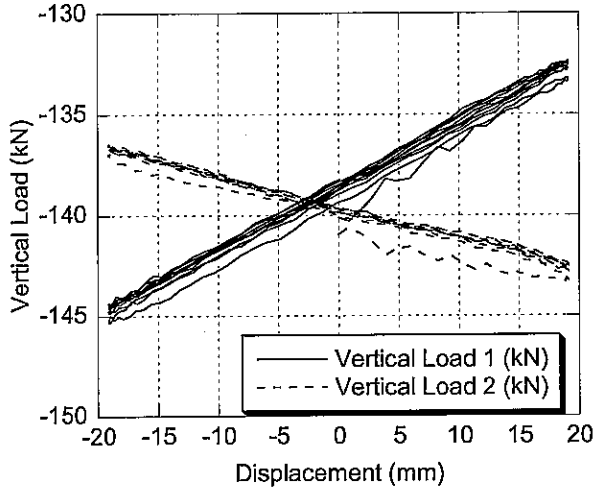
2A2-2-05



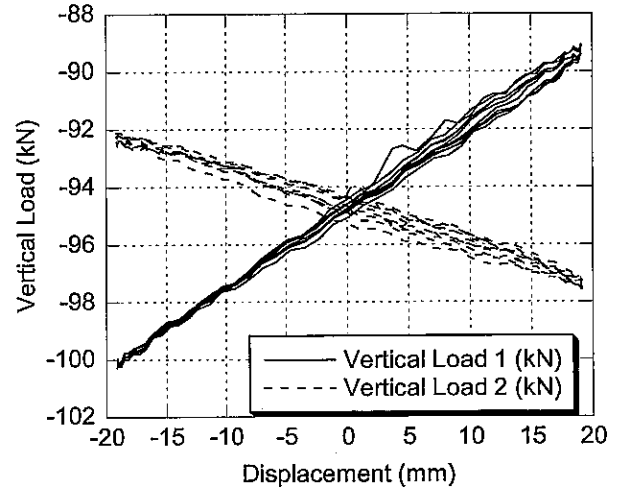
2A2-2-06



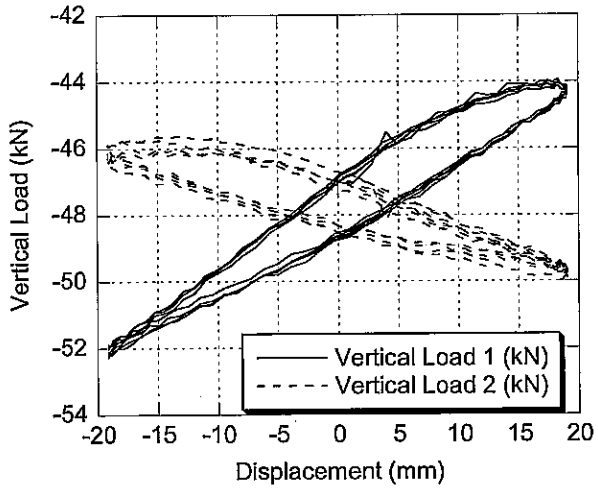
2A2-2-07



2A2-2-08



2A2-2-09







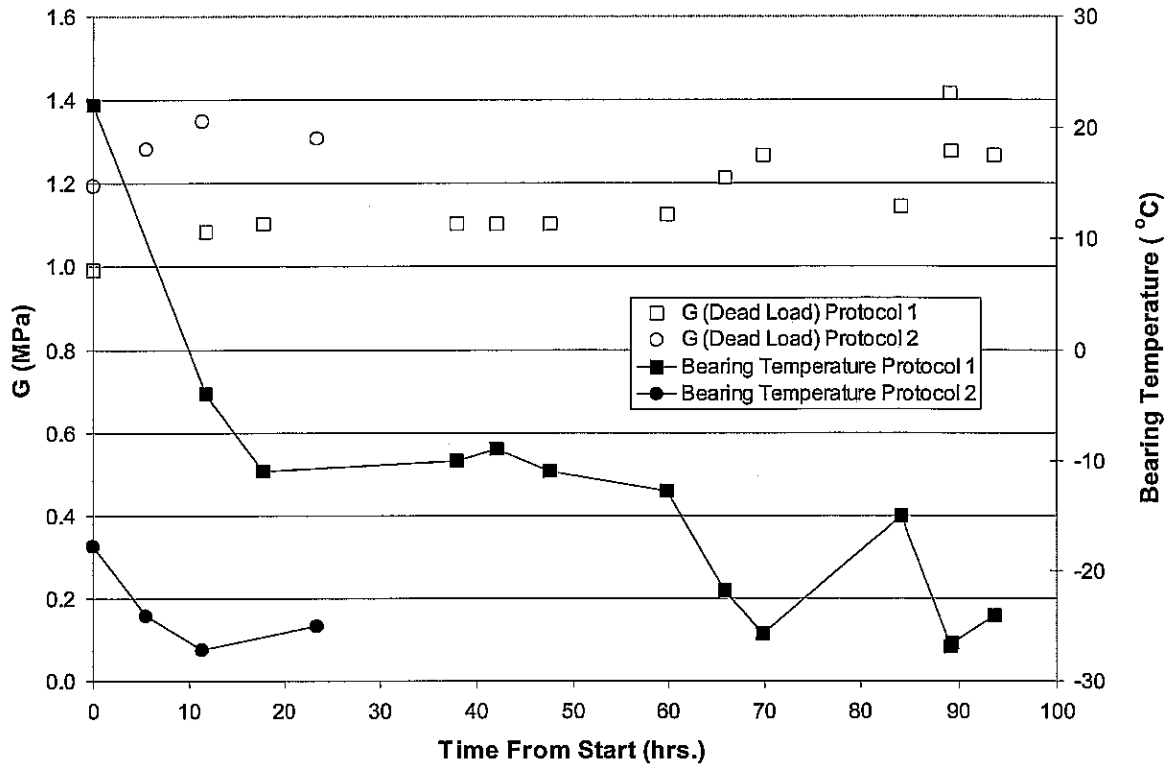
### Appendix B – Test Results for 2B1 & 2B2

Report Reference	Date & Time	Time From Start, hrs.	Brg. Temp. °C	Vert. Load		Amp.		Freq. hz	Notes
				psi	MPa	in	mm		
2B1-1-01	7/1/01 20:20	0.00	22	250	1.724	0.75	19.05	1	
2B1-1-02	7/1/01 20:23	0.05	22	500	3.447	0.75	19.05	1	
2B1-1-03	7/1/01 20:27	0.12	22	750	5.171	0.75	19.05	1	
2B1-1-04	7/2/01 8:10	11.83	-4	500	3.447	0.75	19.05	1	
2B1-1-05	7/2/01 14:10	17.83	-11	500	3.447	0.75	19.05	1	
2B1-1-06	7/3/01 10:16	37.93	-10	500	3.447	0.75	19.05	1	
2B1-1-07	7/3/01 14:23	42.05	-9	500	3.447	0.75	19.05	1	
2B1-1-08	7/3/01 19:53	47.55	-11	500	3.447	0.75	19.05	1	
2B1-1-09	7/4/01 8:11	59.85	-12.8	500	3.447	0.75	19.05	1	
2B1-1-10	7/4/01 14:10	65.83	-21.8	500	3.447	0.75	19.05	1	
2B1-1-11	7/4/01 18:09	69.82	-25.7	500	3.447	0.75	19.05	1	
2B1-1-12	7/5/01 8:31	84.18	-15	500	3.447	0.75	19.05	1	
2B1-1-13	7/5/01 13:28	89.13	-26.9	500	3.447	0.75	19.05	1	
2B1-1-14	7/5/01 13:34	89.23	-26.5	500	3.447	0.75	19.05	1	
2B1-1-15	7/5/01 18:03	93.72	-24.1	500	3.447	0.75	19.05	1	
2B1-1-16	7/5/01 18:16	93.93	-24.2	250	1.724	0.75	19.05	1	
2B1-1-17	7/5/01 18:28	94.13	-23.9	500	3.447	1.5	38.1	1	A
2B1-1-18	7/5/01 19:07	94.78	-23.5	500	3.447	3	76.2	0.5	B
2B1-1-19	7/5/01 19:16	94.93	-23	750	5.171	0.75	19.05	1	
2B1-1-20	7/5/01 19:20	95.00	-22.6	750	5.171	1.5	38.1	0.5	
2B2-2-01	7/6/01 8:44	0.00	-17.8	500	3.447	0.75	19.05	1	
2B2-2-02	7/6/01 14:09	5.42	-24.1	500	3.447	0.75	19.05	1	
2B2-2-03	7/6/01 20:05	11.35	-27.3	500	3.447	0.75	19.05	1	
2B2-2-04	7/7/01 8:05	23.35	-25	250	1.724	0.75	19.05	1	
2B2-2-05	7/7/01 8:10	23.43	-25	500	3.447	0.75	19.05	1	
2B2-2-06	7/7/01 8:22	23.63	-25	750	5.171	0.75	19.05	1	

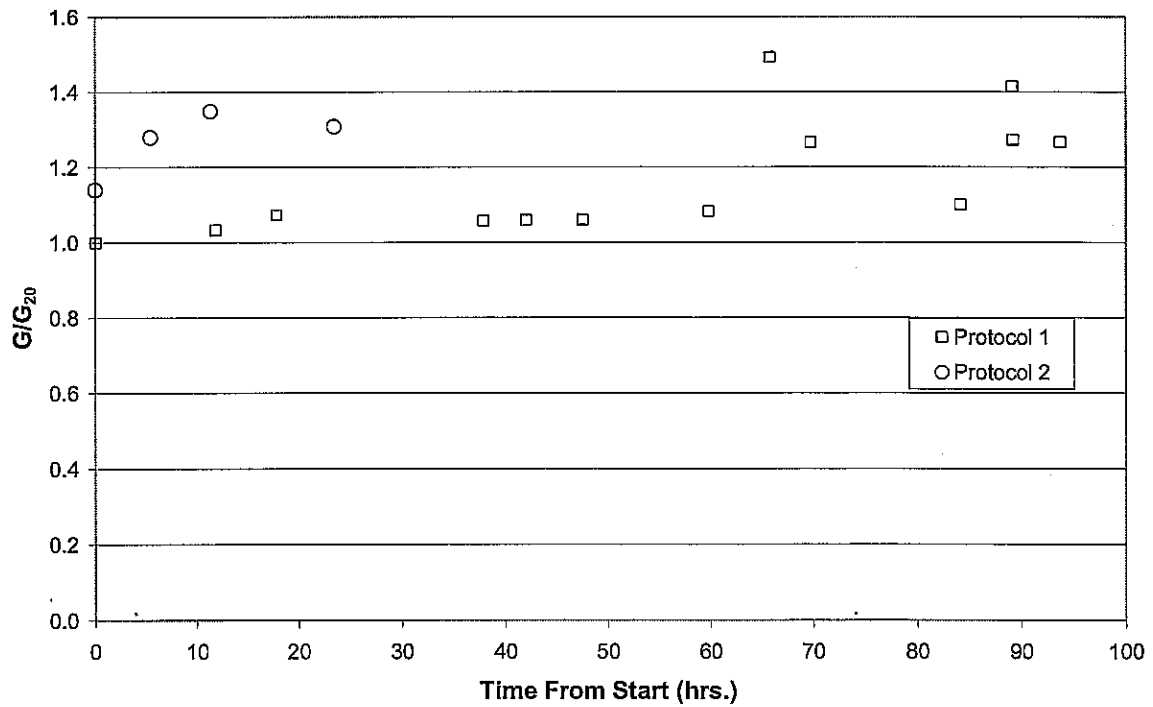
Comments:

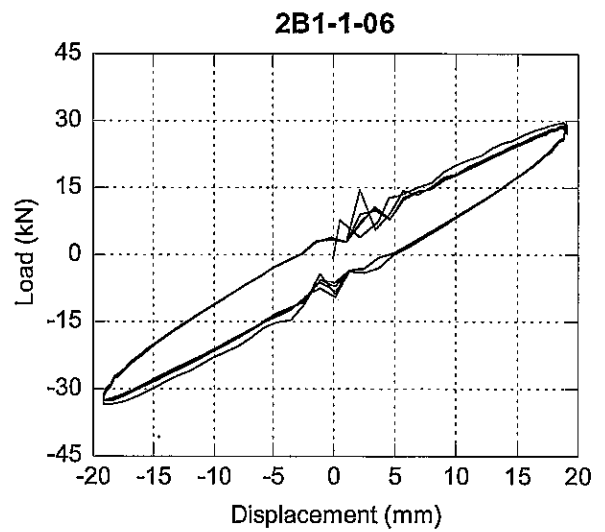
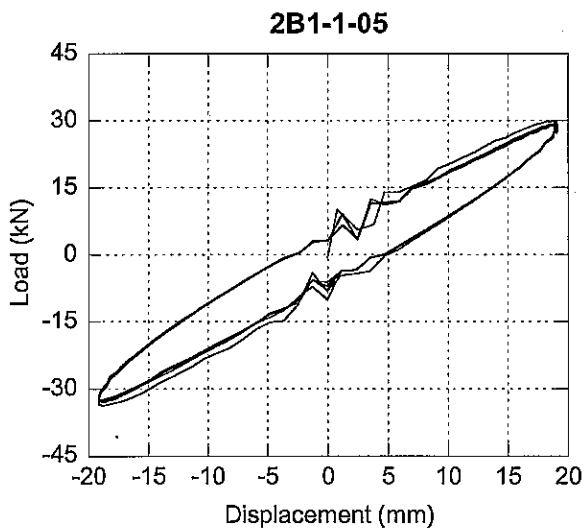
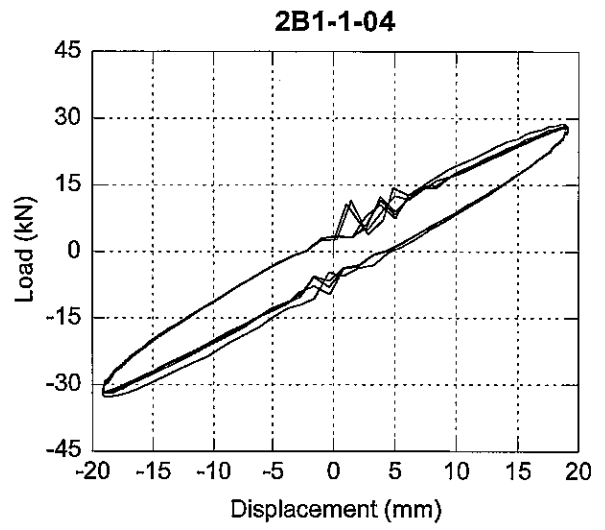
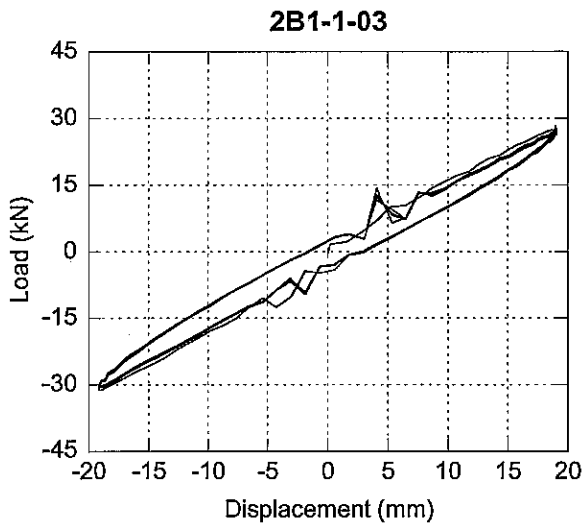
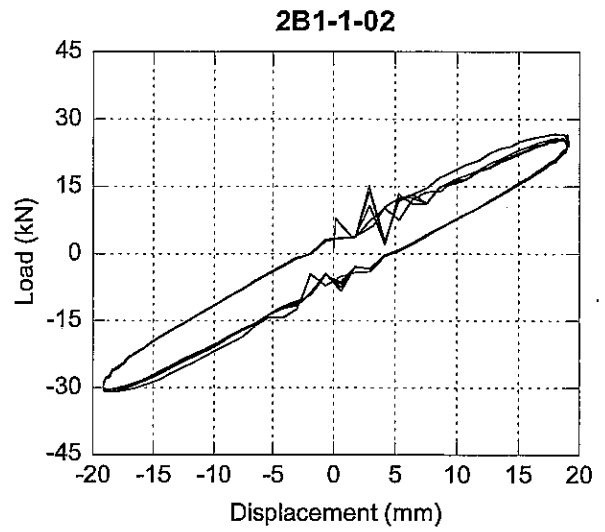
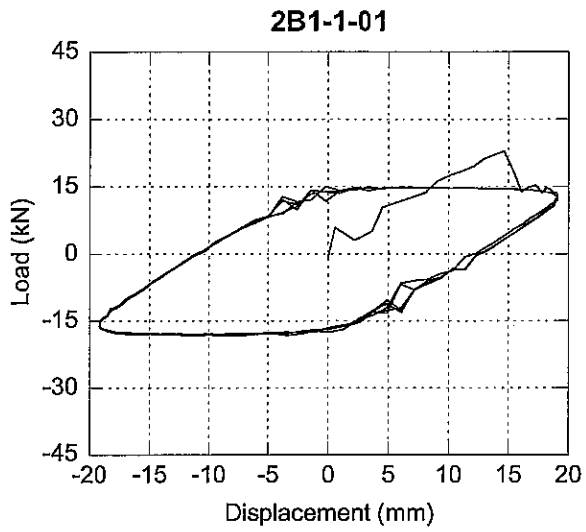
- A 0-100% (0-1.5") cyclic loading
- B 0-200% (0-3") cyclic loading

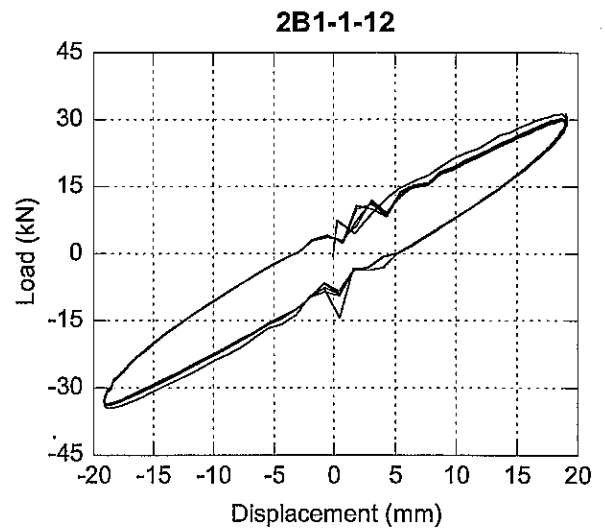
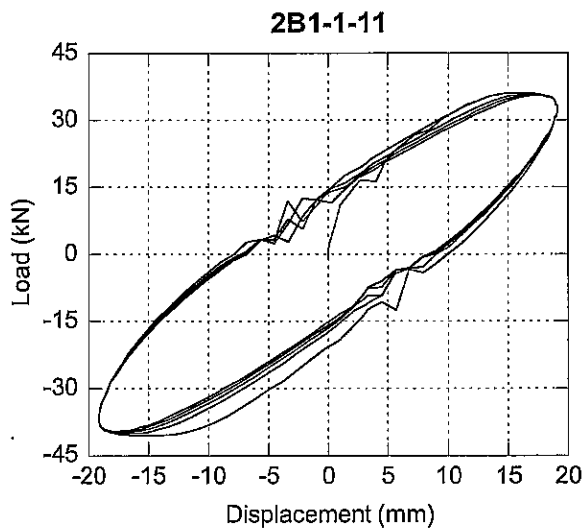
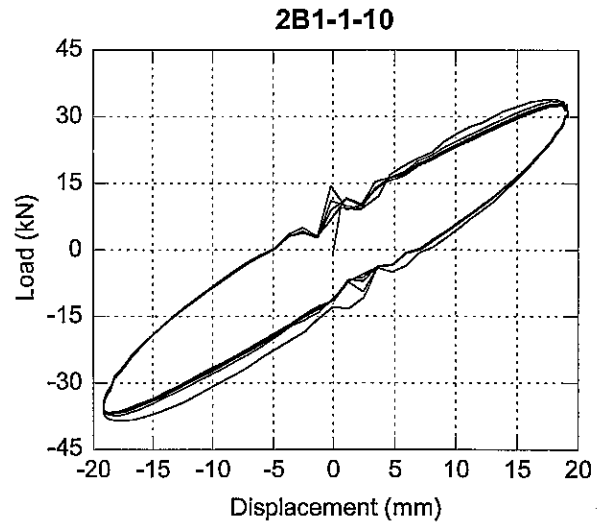
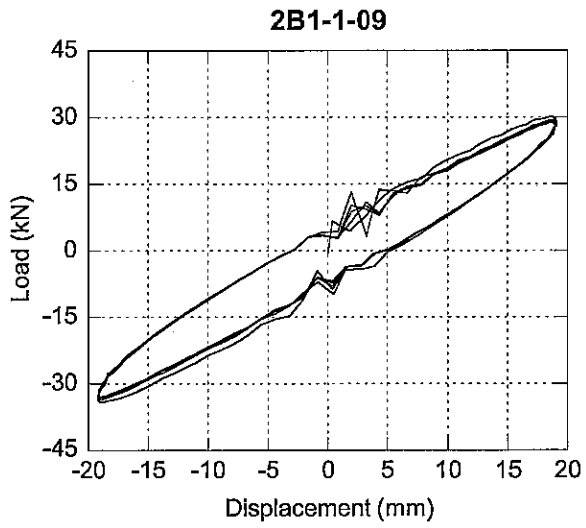
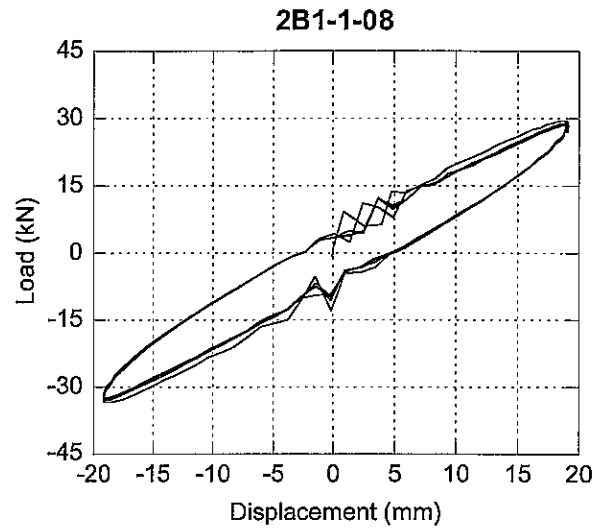
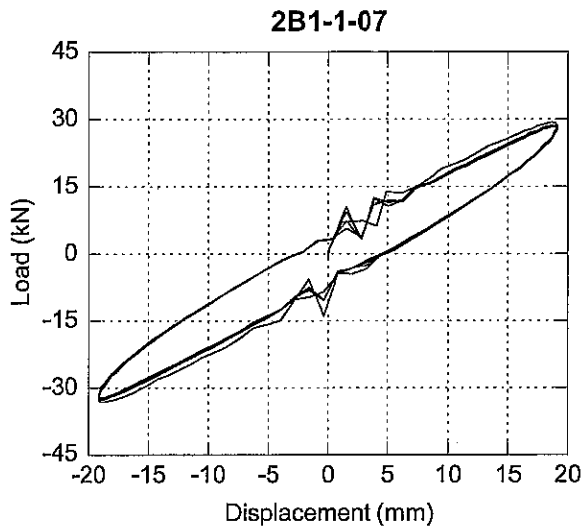
### Shear Modulus Summary - 2B1-1 & 2B2-2



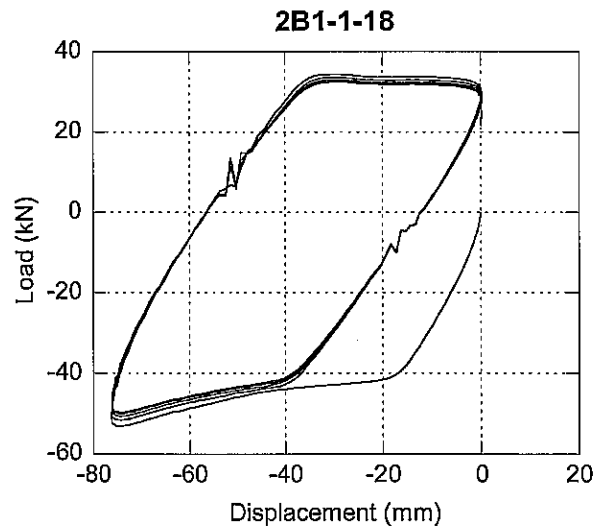
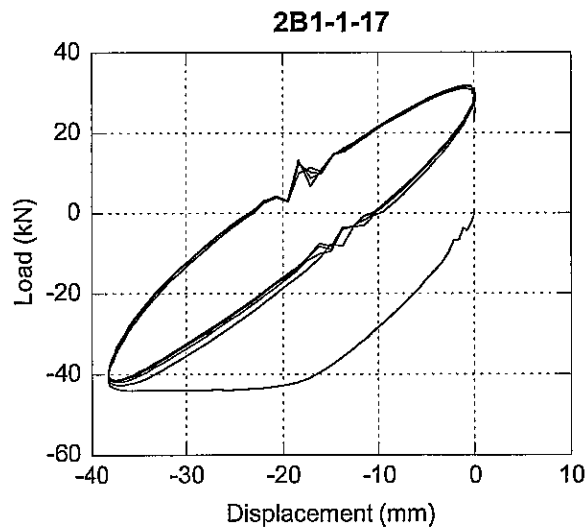
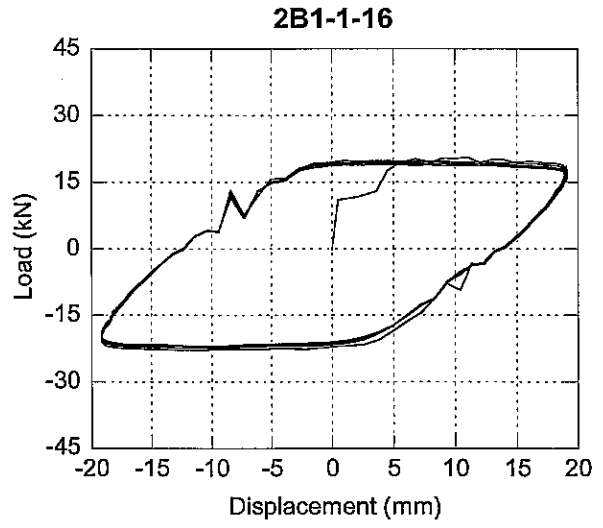
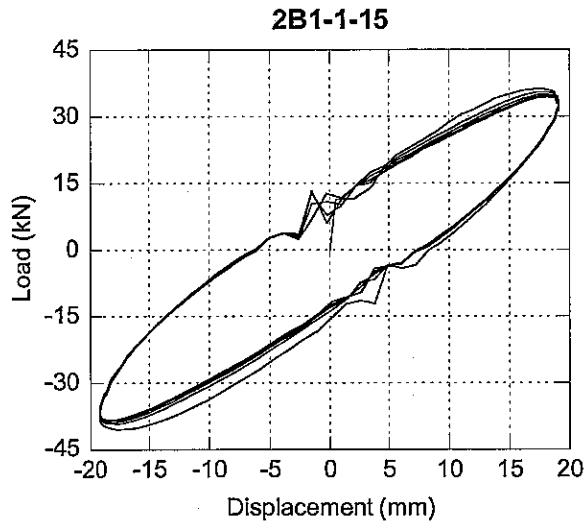
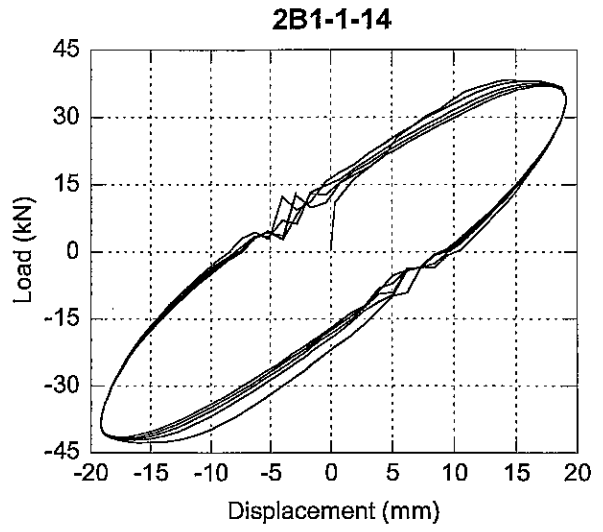
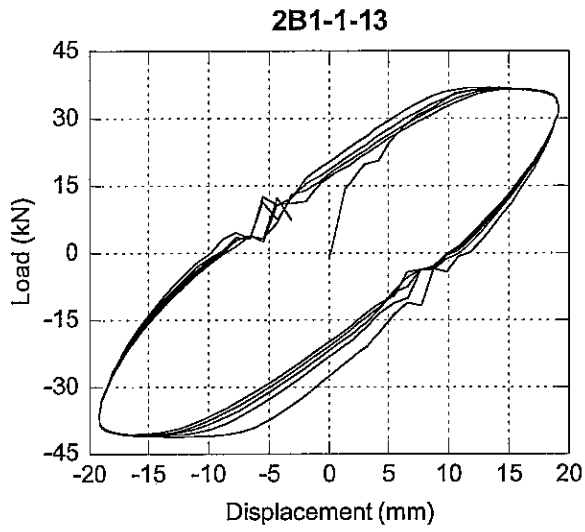
### Normalized Shear Modulus - 2B1-1 & 2B2-2



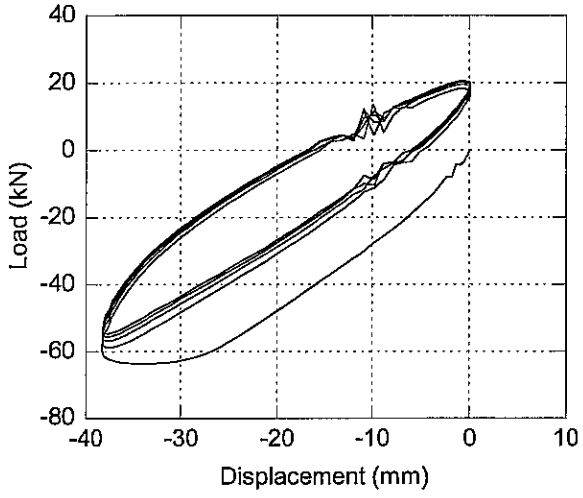




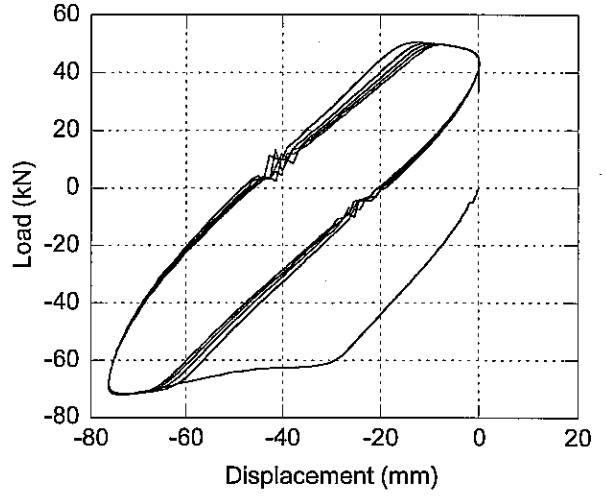
6

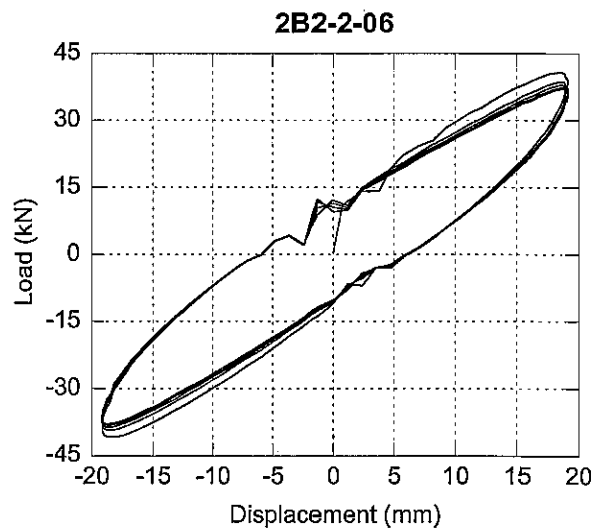
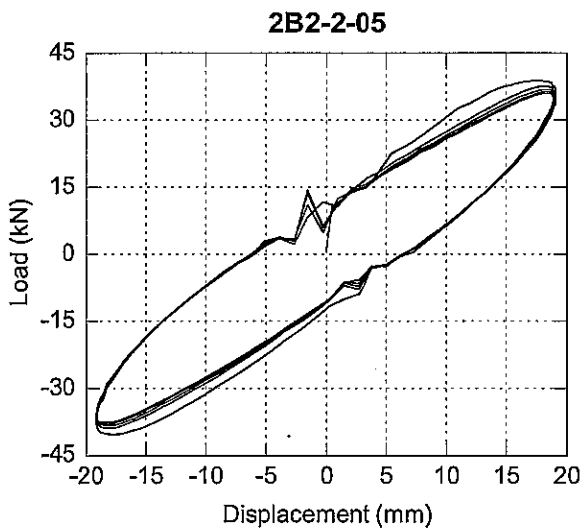
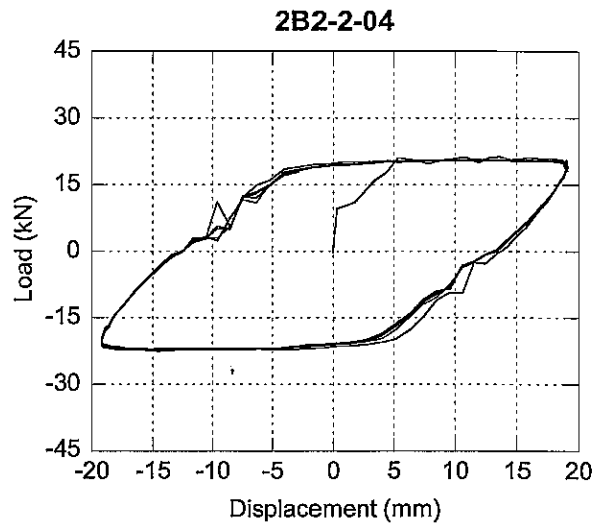
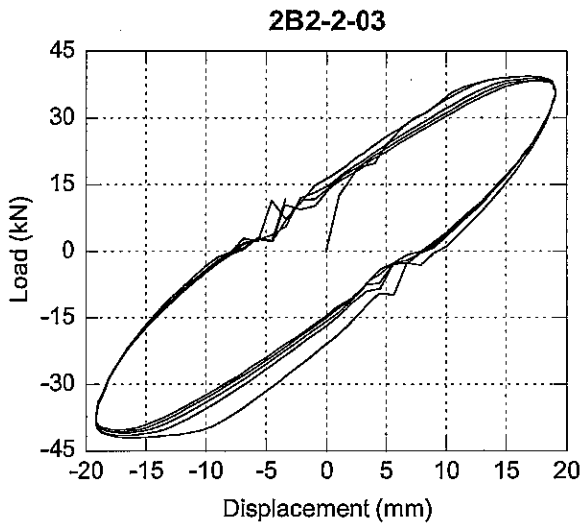
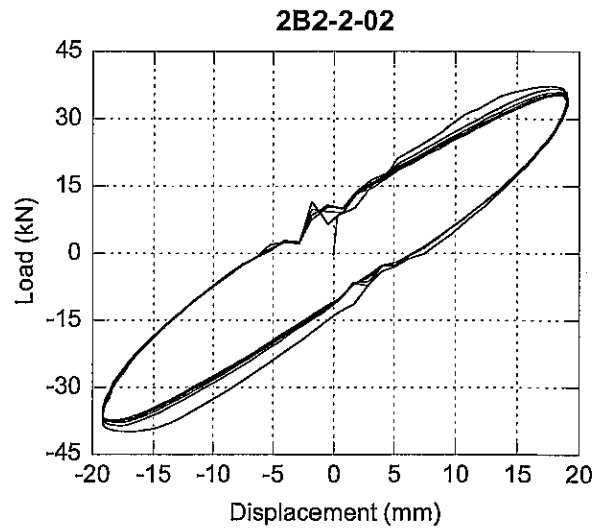
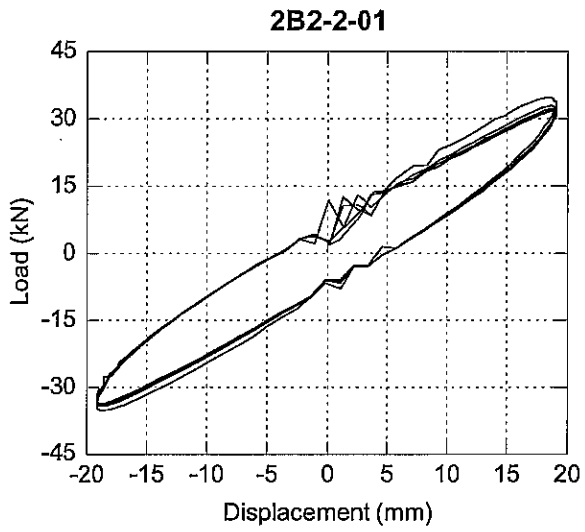


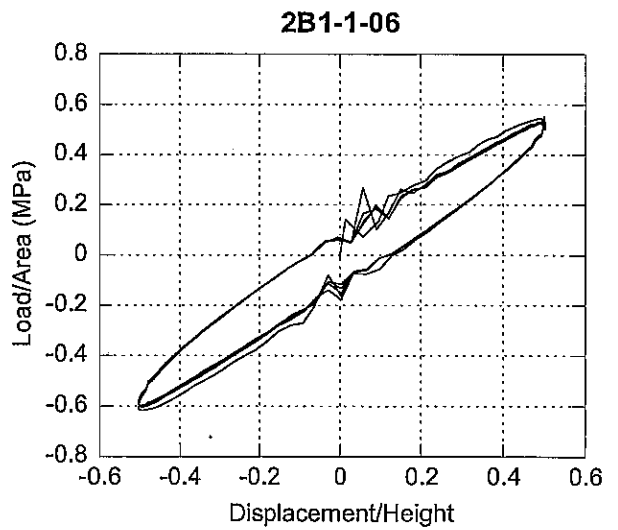
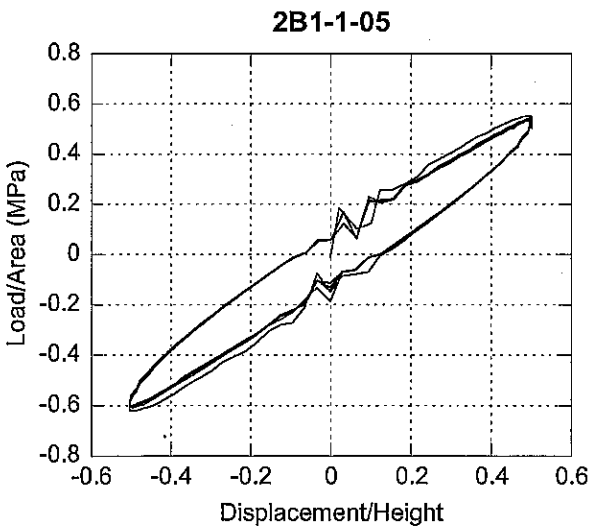
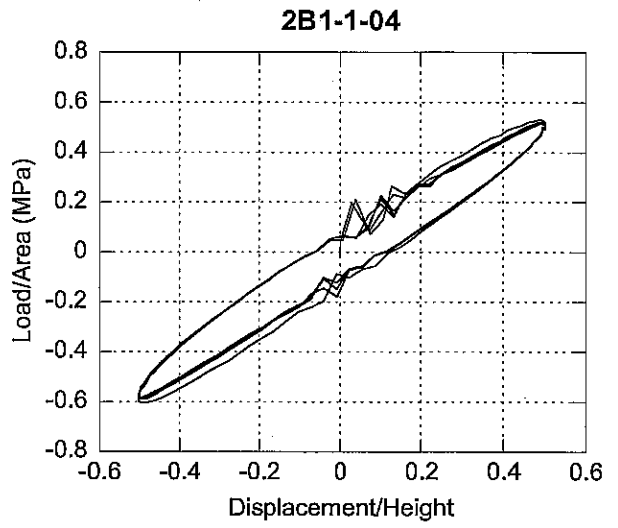
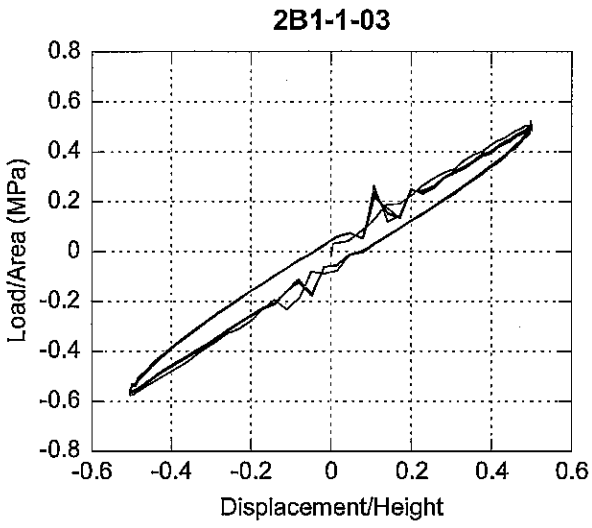
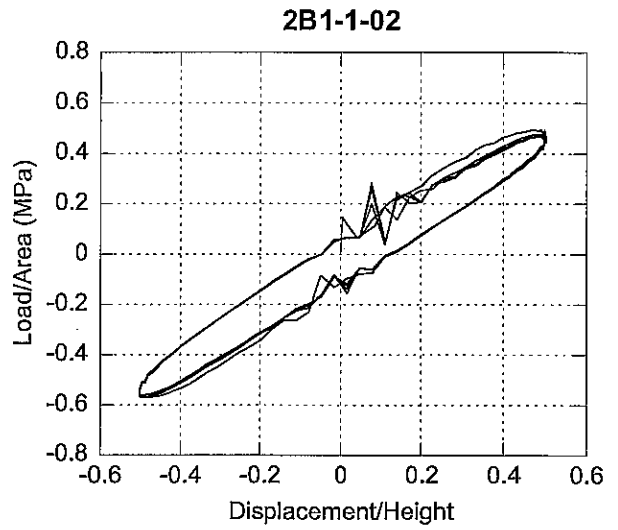
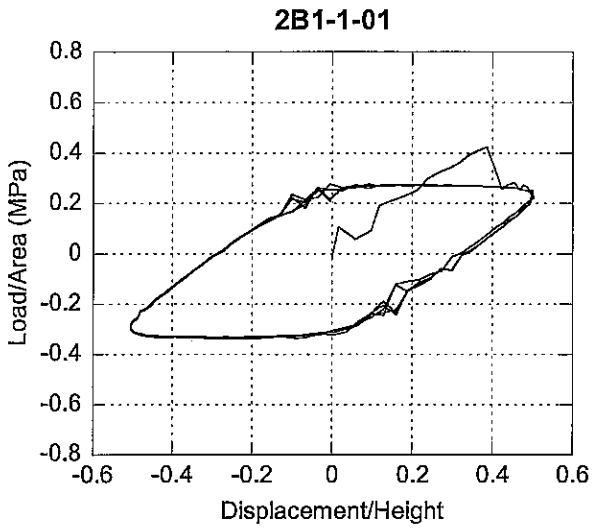
2B1-1-19

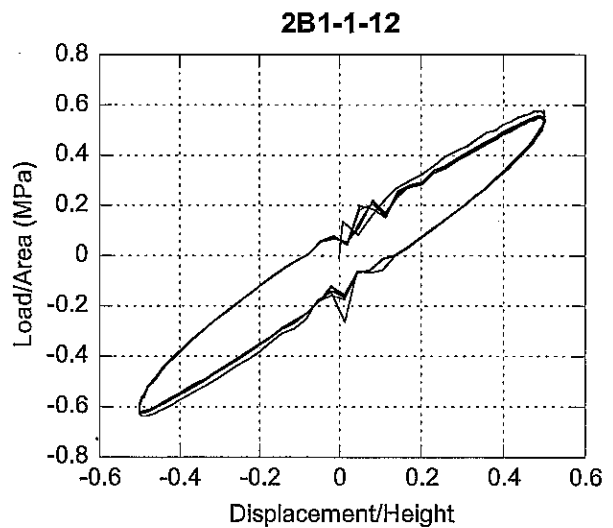
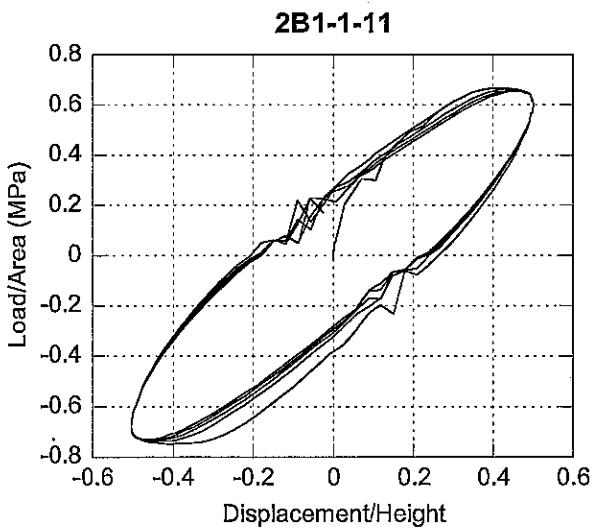
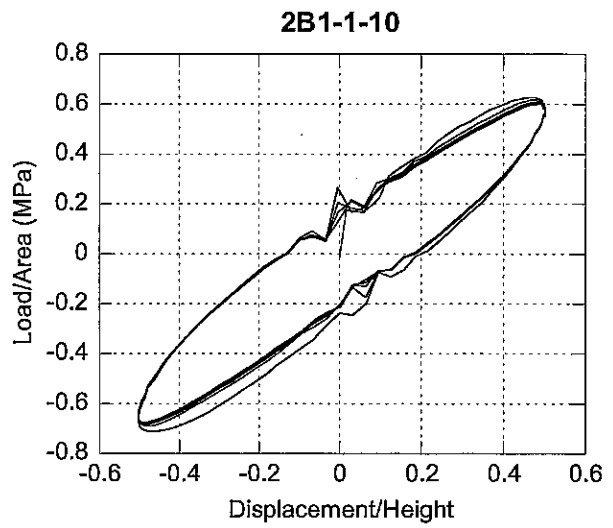
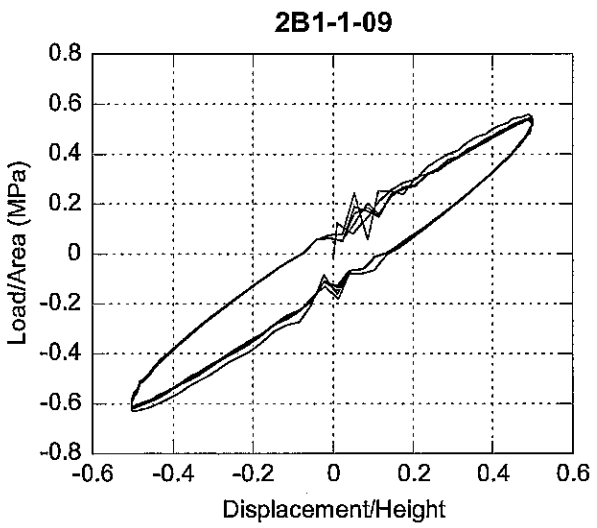
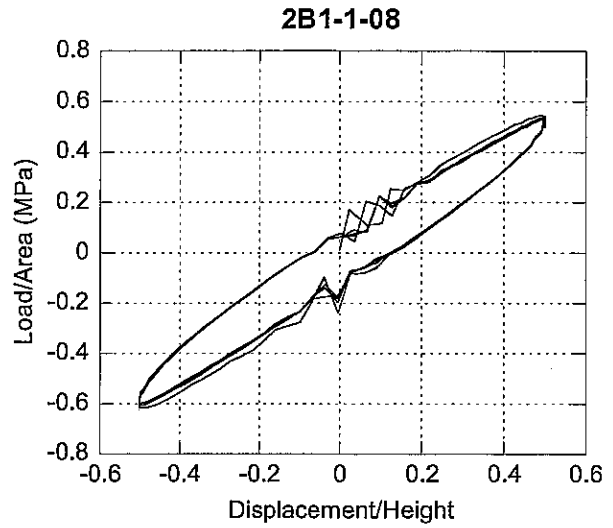
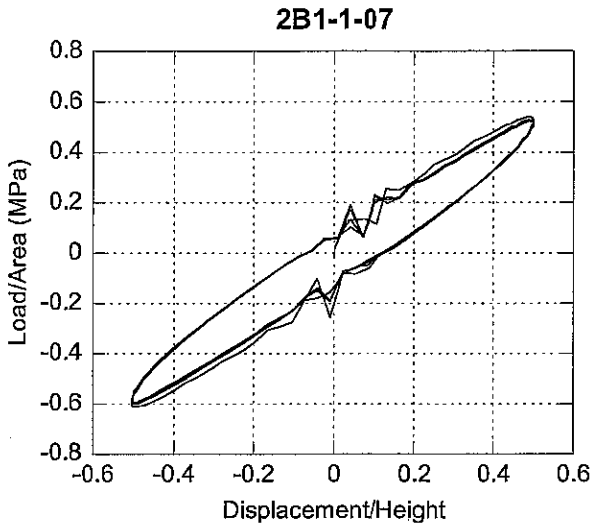


2B1-1-20

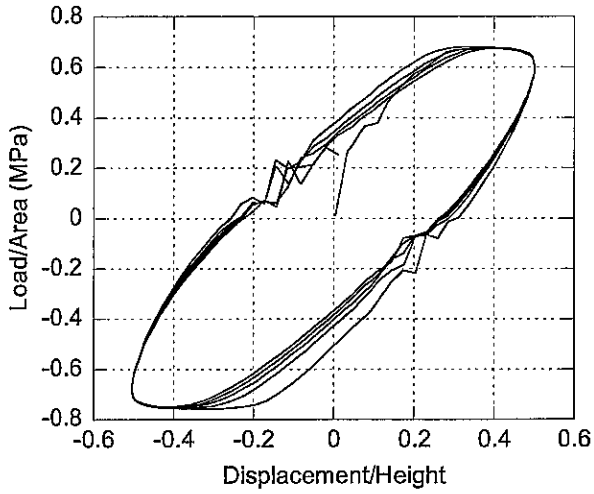




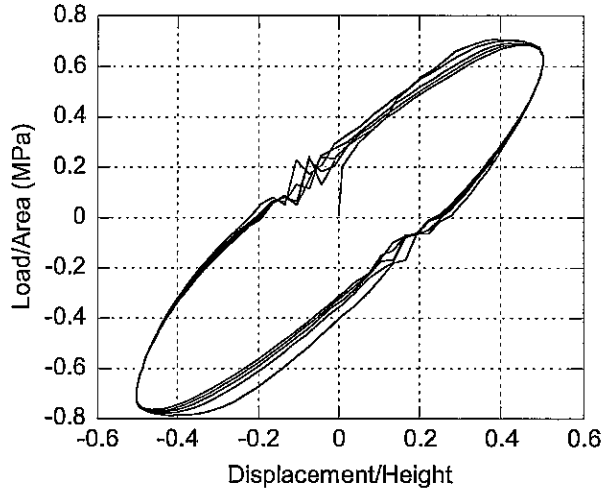




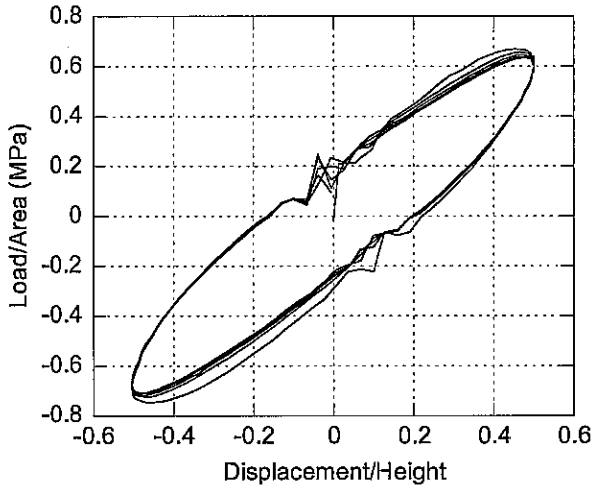
**2B1-1-13**



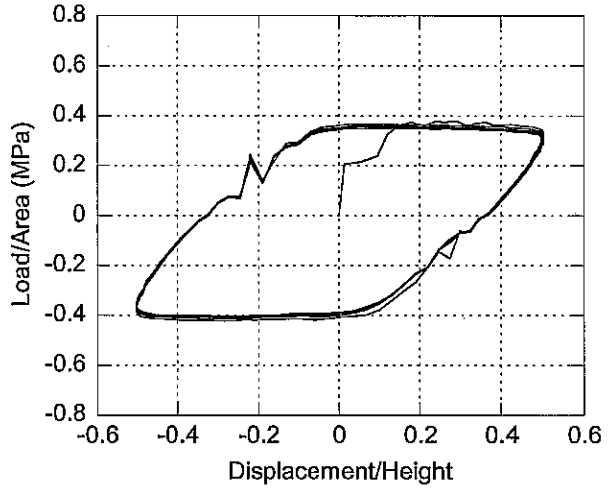
**2B1-1-14**



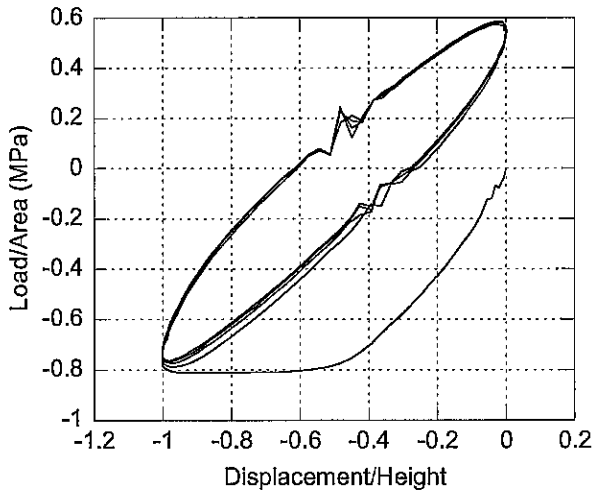
**2B1-1-15**



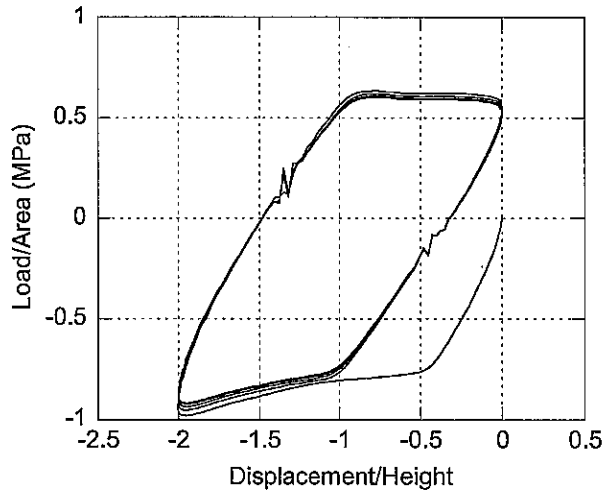
**2B1-1-16**



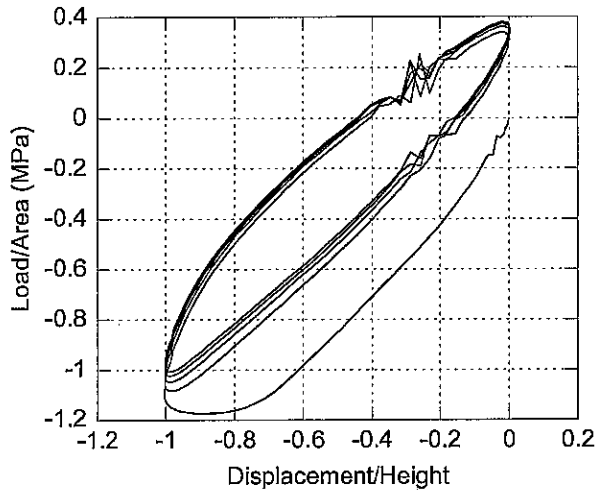
**2B1-1-17**



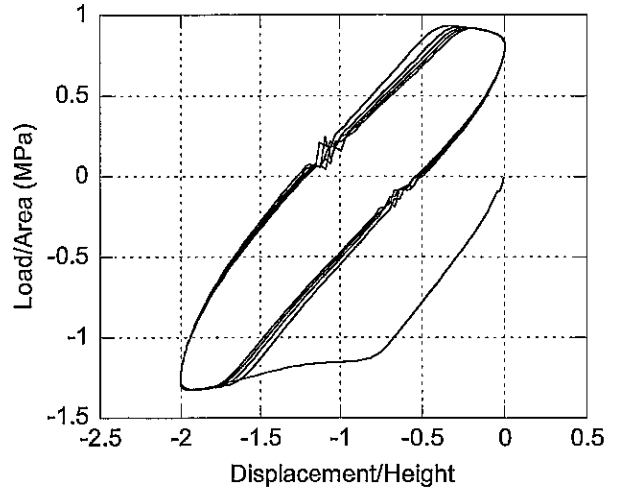
**2B1-1-18**



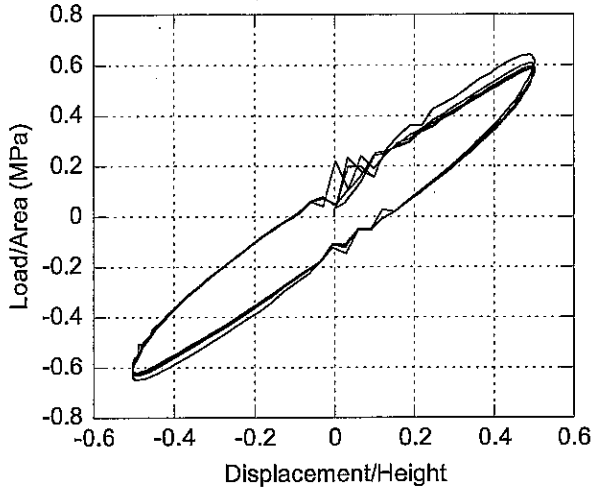
2B1-1-19



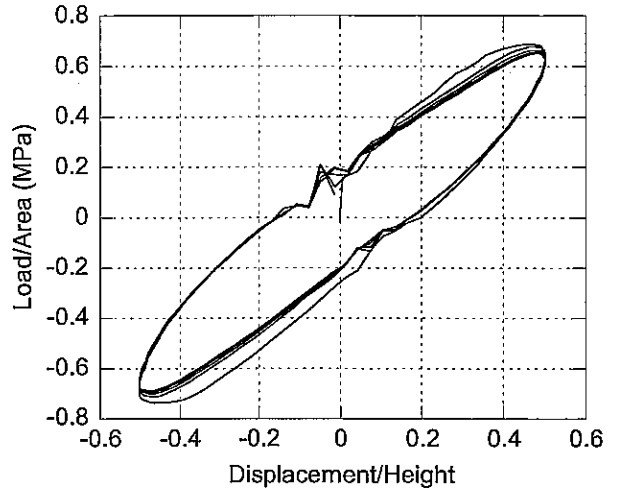
2B1-1-20



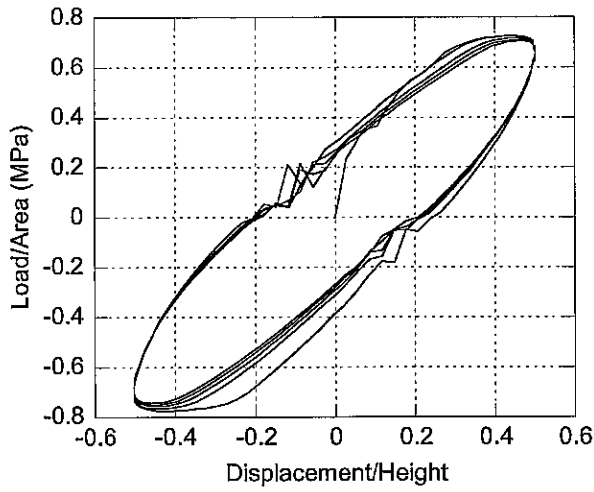
**2B2-2-01**



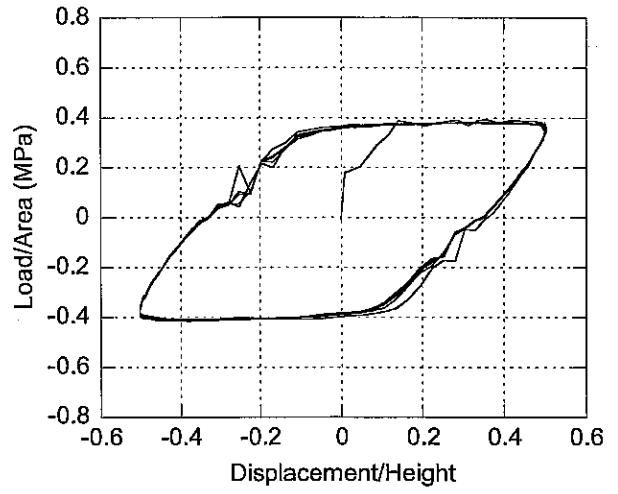
**2B2-2-02**



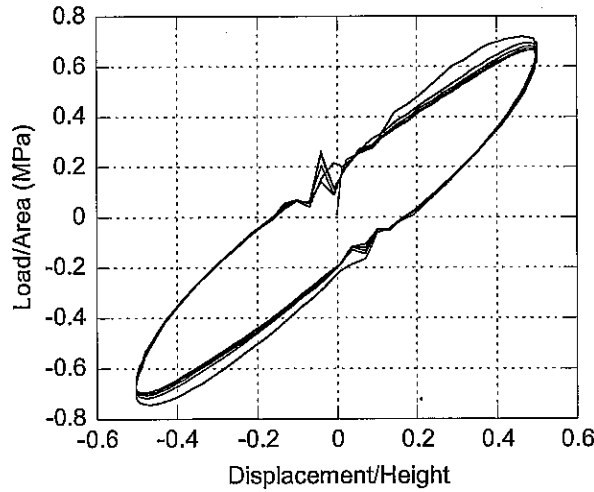
**2B2-2-03**



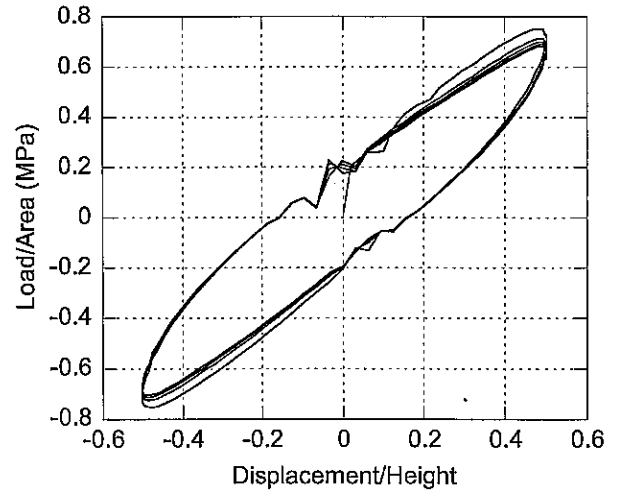
**2B2-2-04**

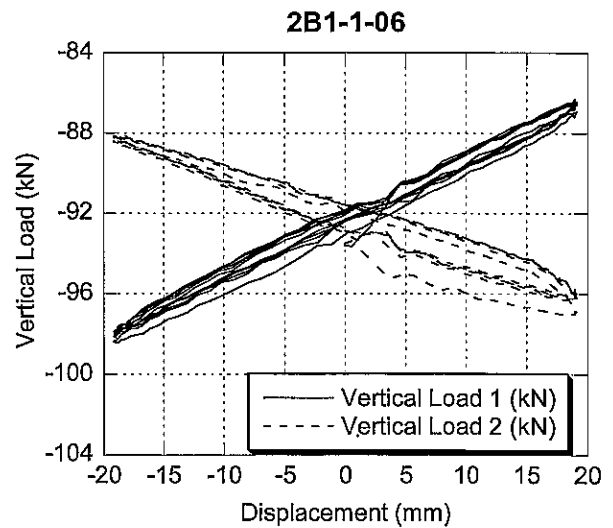
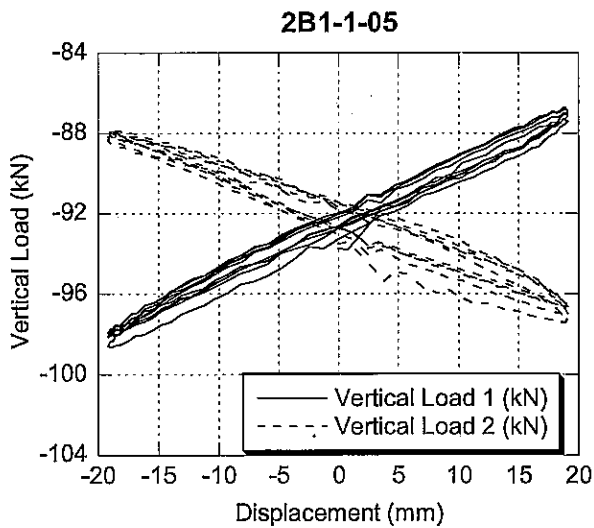
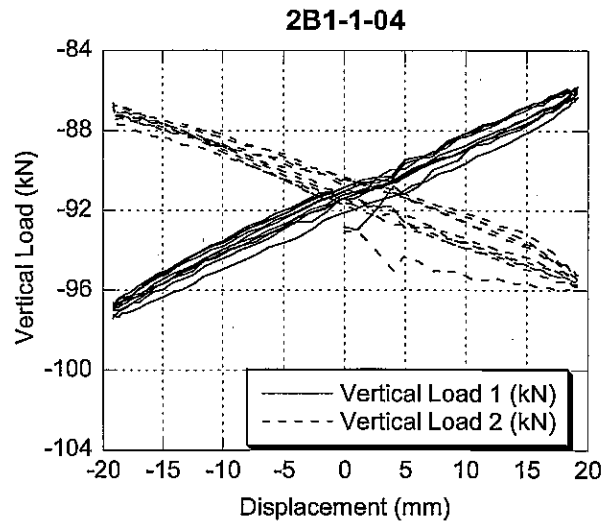
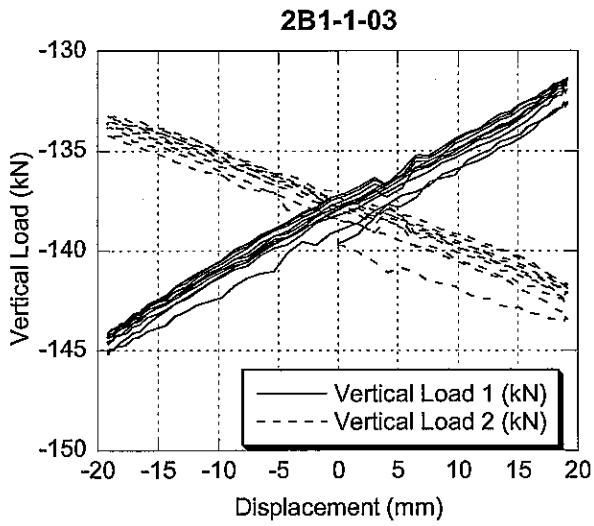
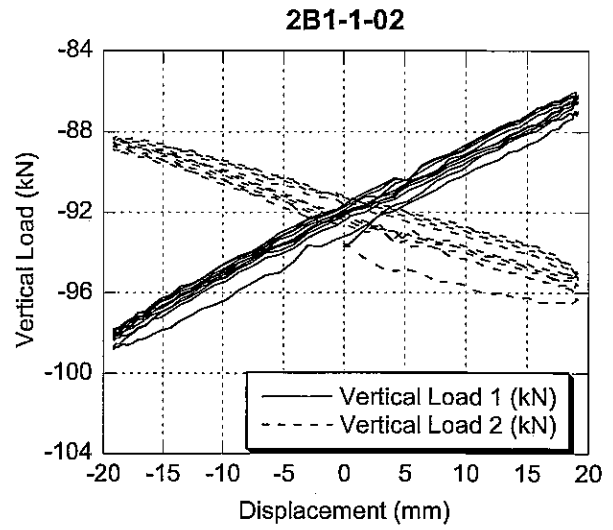
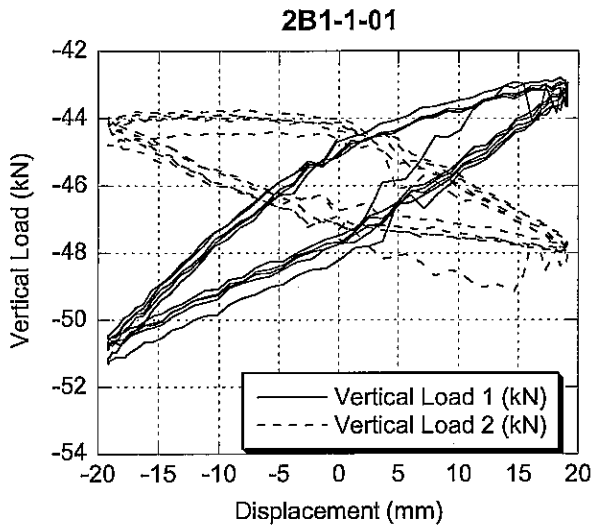


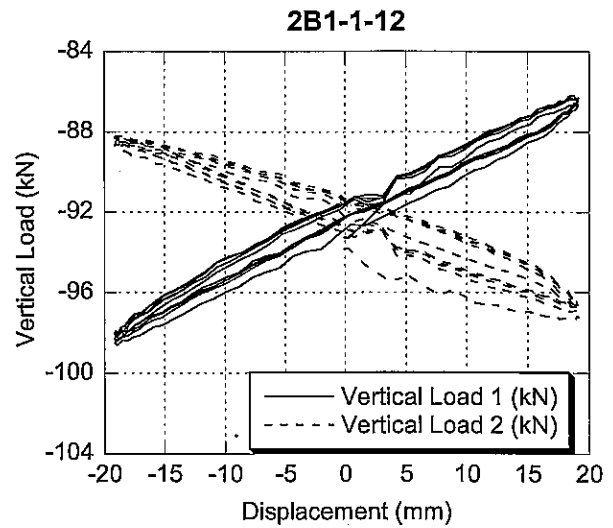
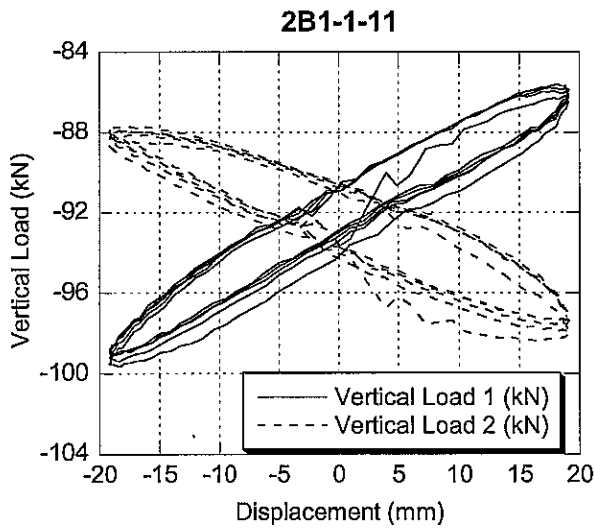
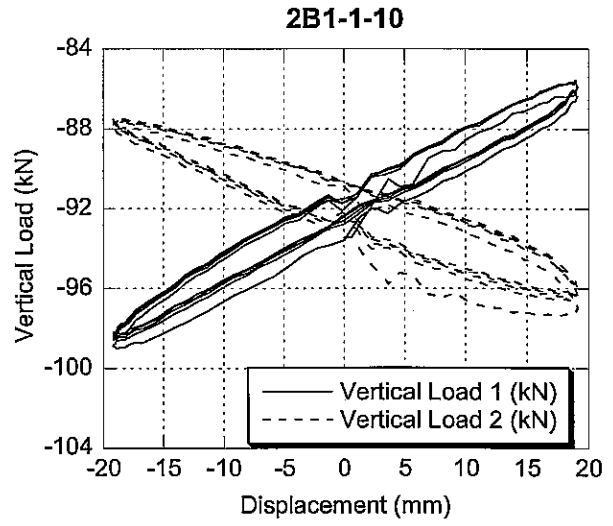
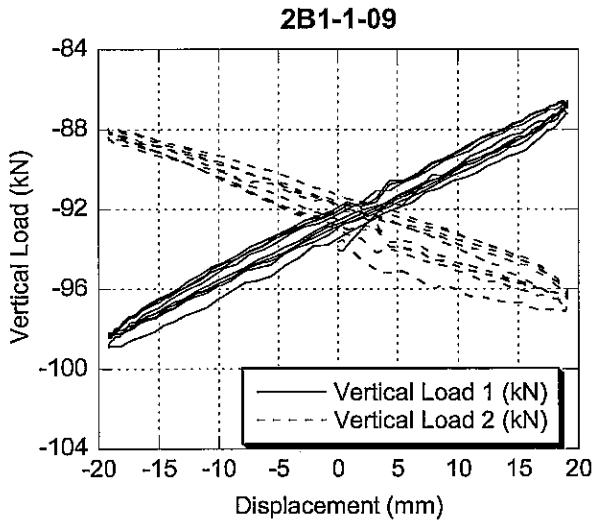
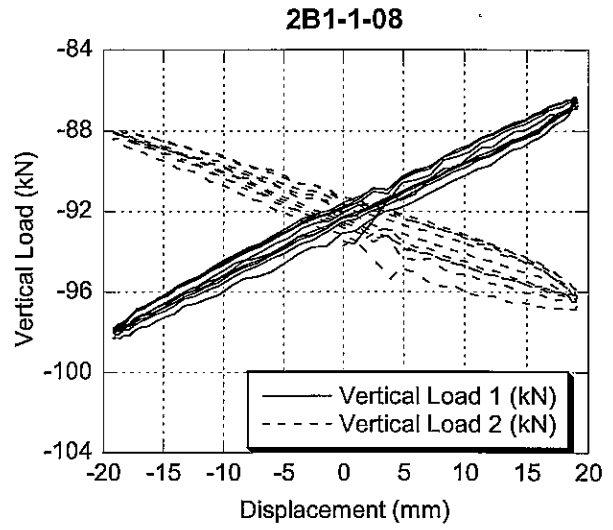
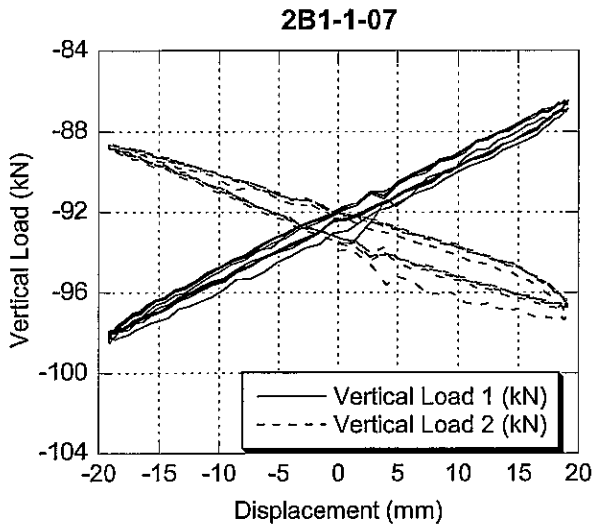
**2B2-2-05**

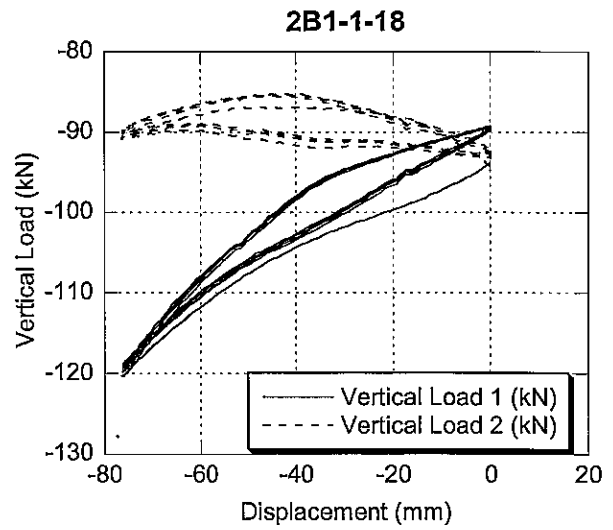
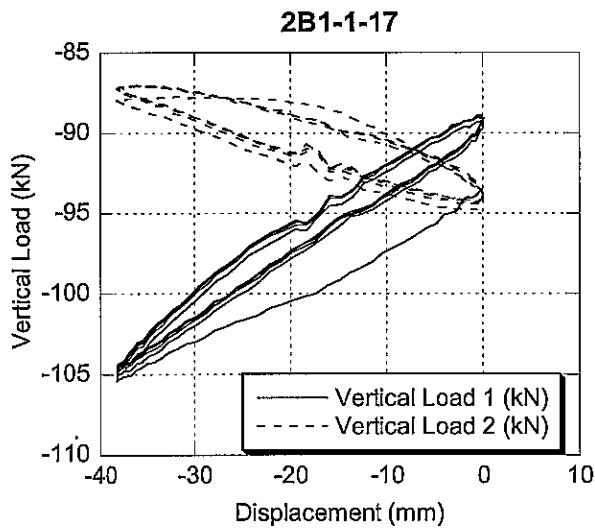
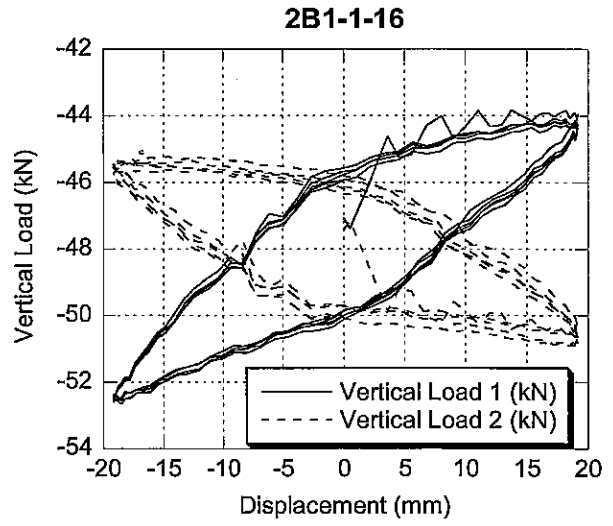
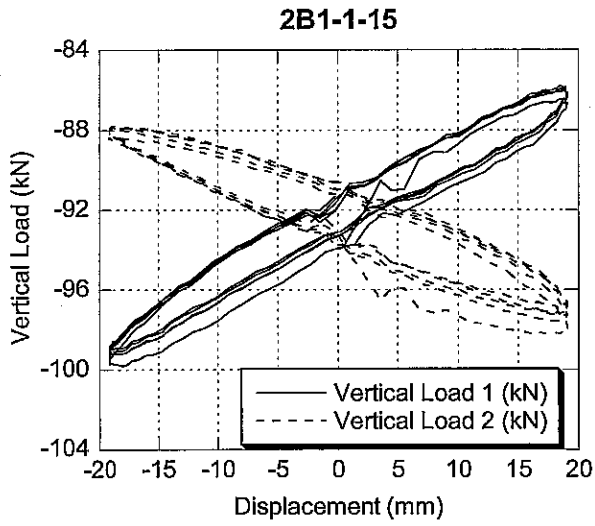
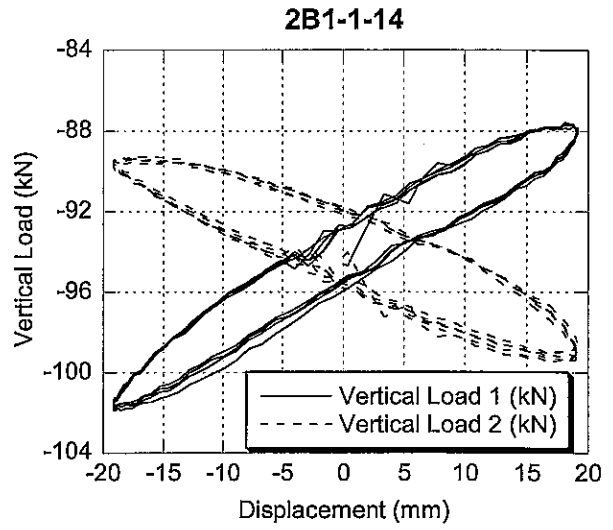
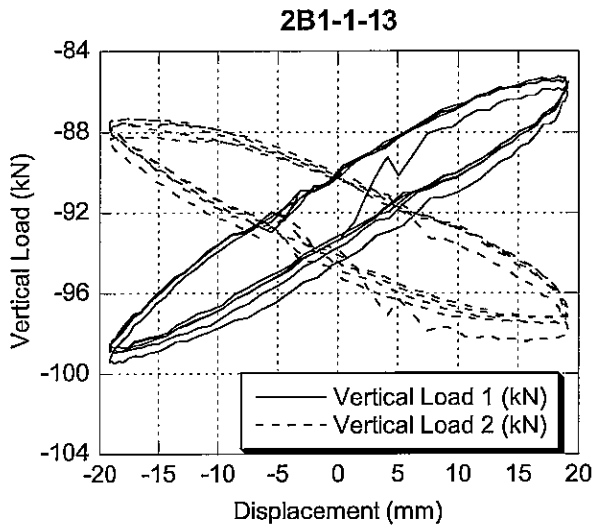


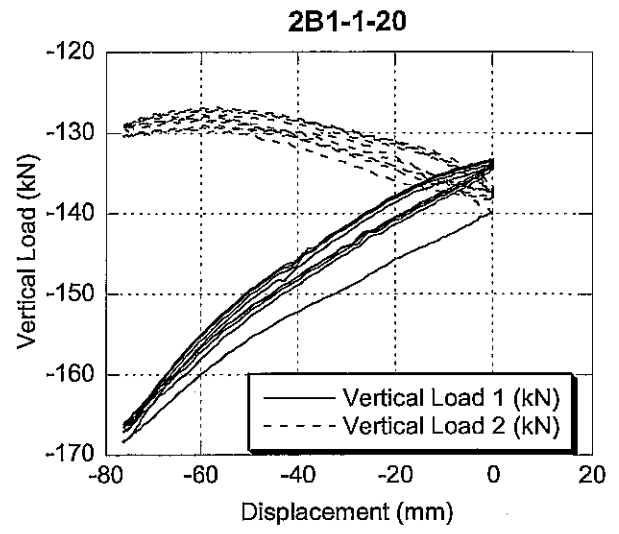
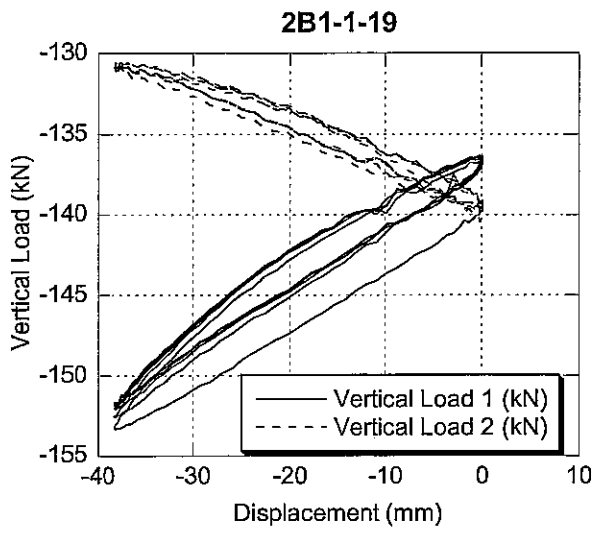
**2B2-2-06**



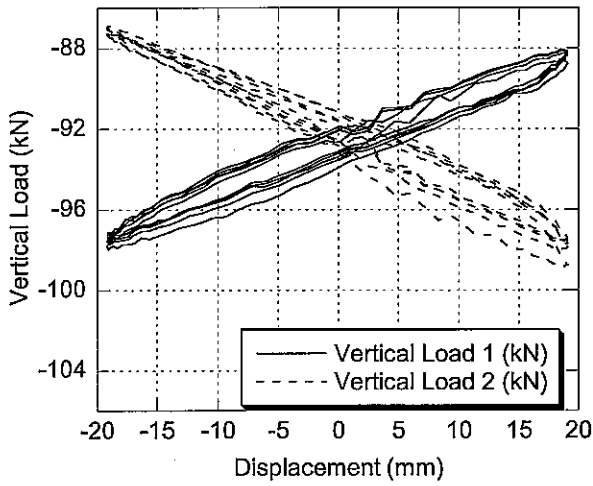




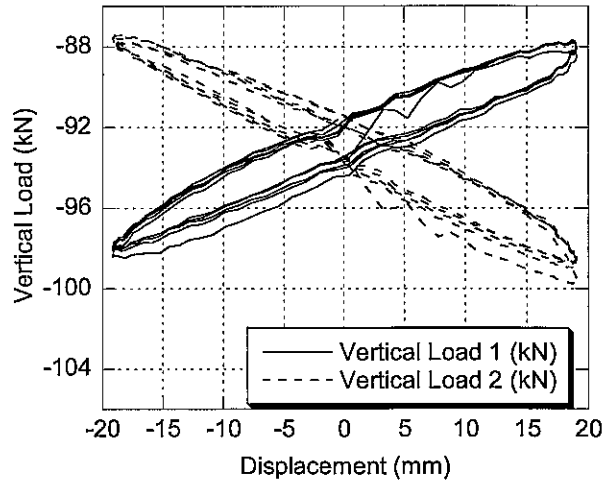




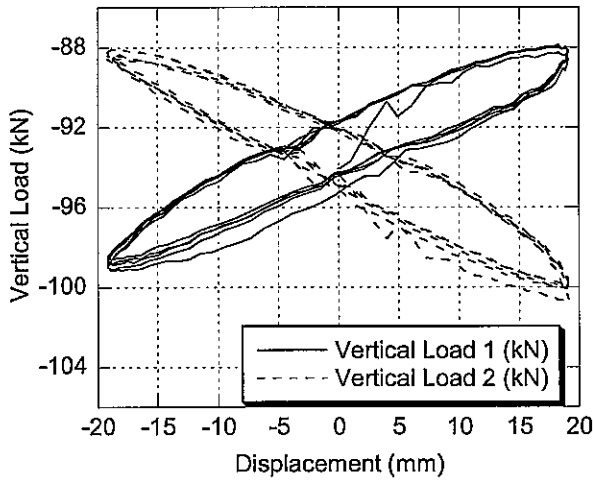
2B2-2-01



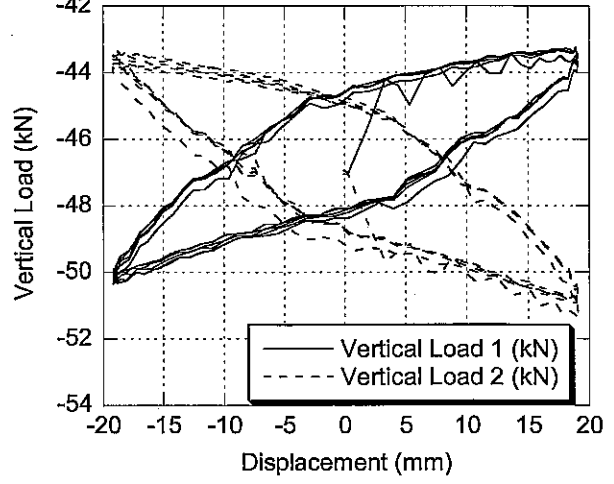
2B2-2-02



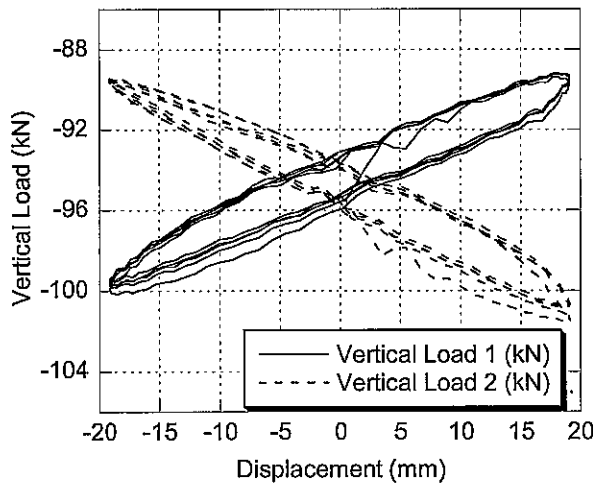
2B2-2-03



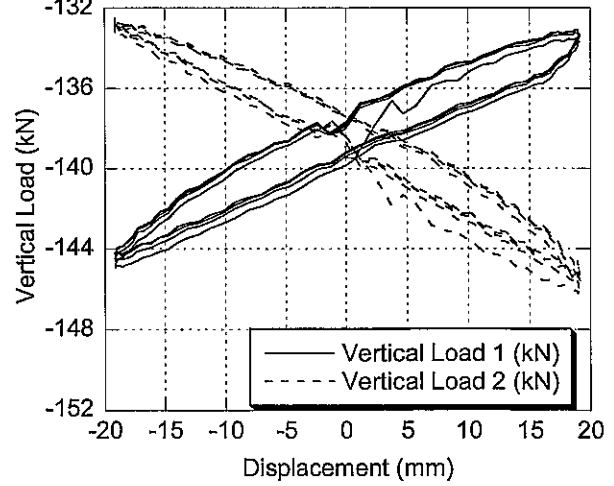
2B2-2-04



2B2-2-05



2B2-2-06





**APPENDIX C**

**Test Results for 2C1 & 2C2**



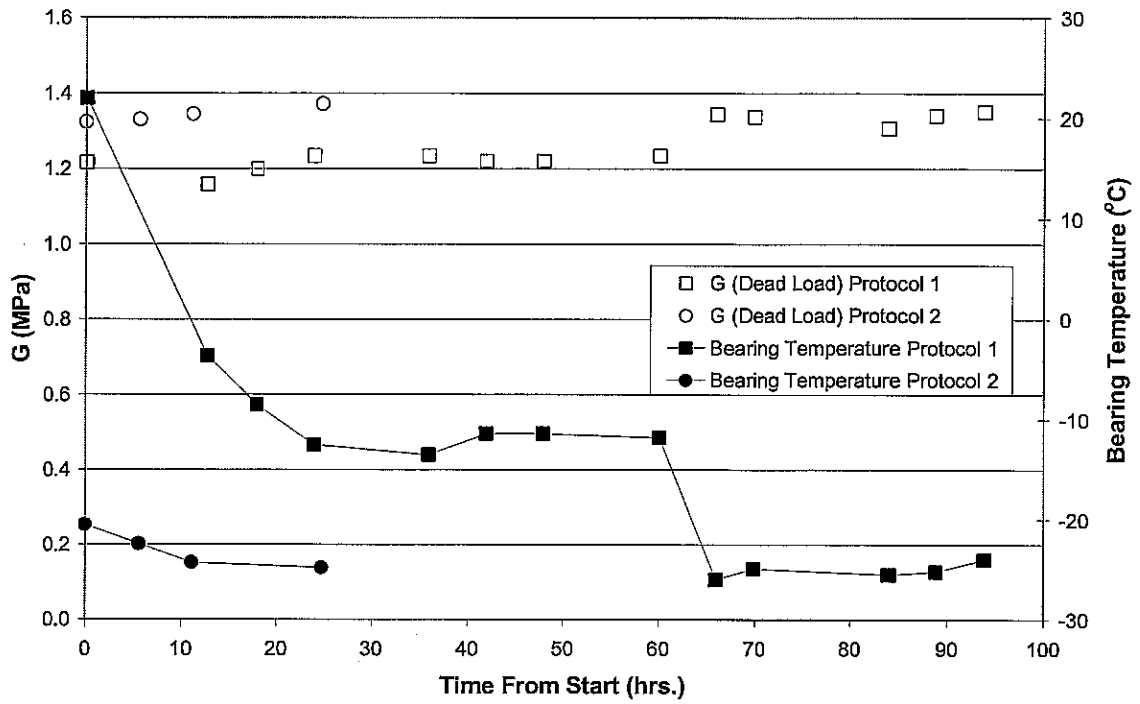
### Appendix C – Test Results for 2C1 & 2C2

Report Reference	Date & Time	Time From Start, hrs.	Brg. Temp. °C	Vert. Load		Amp.		Freq. hz	Notes
				psi	MPa	in	mm		
2C1-1-01	7/8/01 20:16	0.00	22	250	1.724	0.75	19.05	1	
2C1-1-02	7/8/01 20:22	0.10	22	500	3.447	0.75	19.05	1	
2C1-1-03	7/8/01 20:26	0.17	22	750	5.171	0.75	19.05	1	
2C1-1-04	7/9/01 8:59	12.72	-3.6	500	3.447	0.75	19.05	1	
2C1-1-05	7/9/01 14:12	17.93	-8.5	500	3.447	0.75	19.05	1	
2C1-1-06	7/9/01 20:13	23.95	-12.5	500	3.447	0.75	19.05	1	
2C1-1-07	7/10/01 8:13	35.95	-13.5	500	3.447	0.75	19.05	1	
2C1-1-08	7/10/01 14:11	41.92	-11.4	500	3.447	0.75	19.05	1	
2C1-1-09	7/10/01 20:12	47.93	-11.4	500	3.447	0.75	19.05	1	
2C1-1-10	7/11/01 8:20	60.07	-11.8	500	3.447	0.75	19.05	1	
2C1-1-11	7/11/01 14:16	66.00	-26	500	3.447	0.75	19.05	1	
2C1-1-12	7/11/01 18:09	69.88	-24.9	500	3.447	0.75	19.05	1	
2C1-1-13	7/12/01 8:18	84.03	-25.5	500	3.447	0.75	19.05	1	
2C1-1-14	7/12/01 13:08	88.87	-25.2	500	3.447	0.75	19.05	1	
2C1-1-15	7/12/01 18:05	93.82	-24.5	250	1.724	0.75	19.05	1	
2C1-1-16	7/12/01 18:10	93.90	-24	500	3.447	0.75	19.05	1	
2C1-1-17	7/12/01 18:18	94.03	-23.6	500	3.447	1.5	38.1	1	A
2C1-1-18	7/12/01 18:26	94.17	-23	500	3.447	3	76.2	0.5	B
2C1-1-19	7/12/01 18:33	94.28	-22.6	750	5.171	1.5	38.1	1	C
2C1-1-20	7/12/01 18:37	94.35	-23.3	750	5.171	3	76.2	0.5	D
2C2-2-01	7/13/01 8:34	0.00	-20.5	500	3.447	0.75	19.05	1	
2C2-2-02	7/13/01 14:13	5.65	-22.4	500	3.447	0.75	19.05	1	
2C2-2-03	7/13/01 19:43	11.15	-24.3	500	3.447	0.75	19.05	1	
2C2-2-04	7/14/01 9:22	24.80	-24.8	500	3.447	0.75	19.05	1	
2C2-2-05	7/14/01 9:37	25.05	-24.4	750	5.171	0.75	19.05	1	
2C2-2-06	7/14/01 9:42	25.13	-24.1	250	1.724	0.75	19.05	1	

Notes:

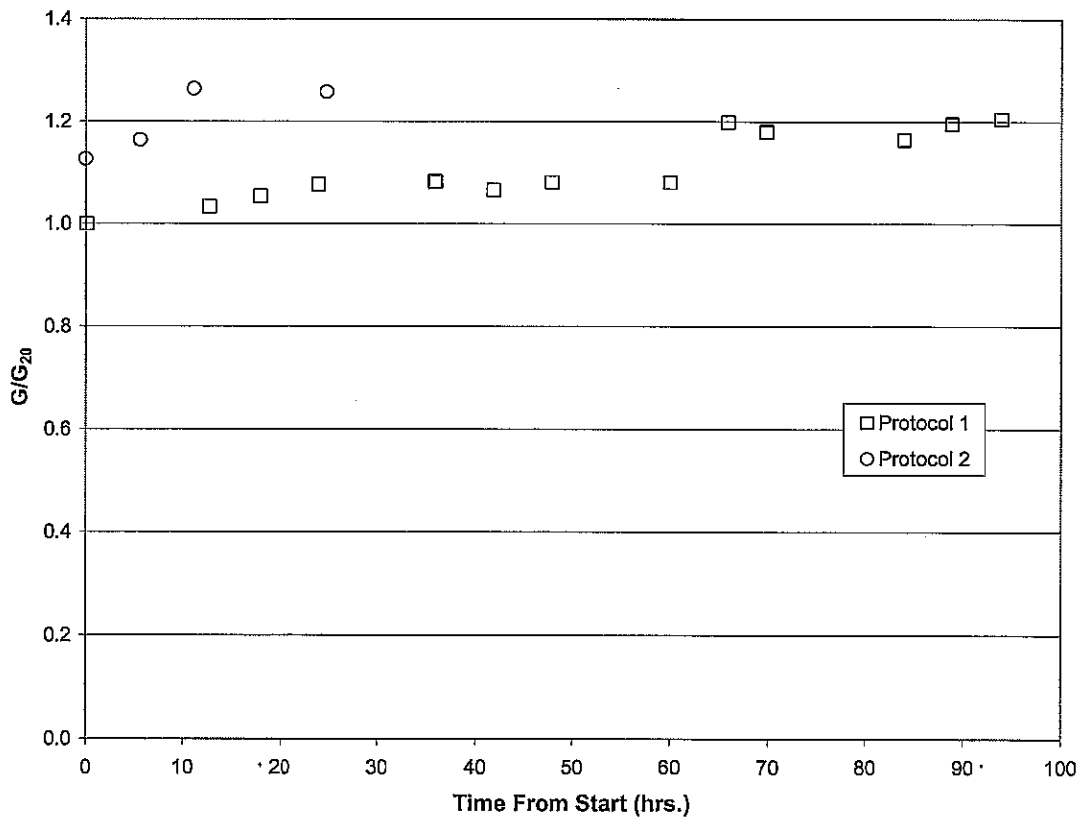
- A 0-100% (0-1.5") cyclic amplitude
- B 0-200% (0-3") cyclic amplitude
- C 0-100% (0-1.5") cyclic amplitude
- D 0-200% (0-3") cyclic amplitude

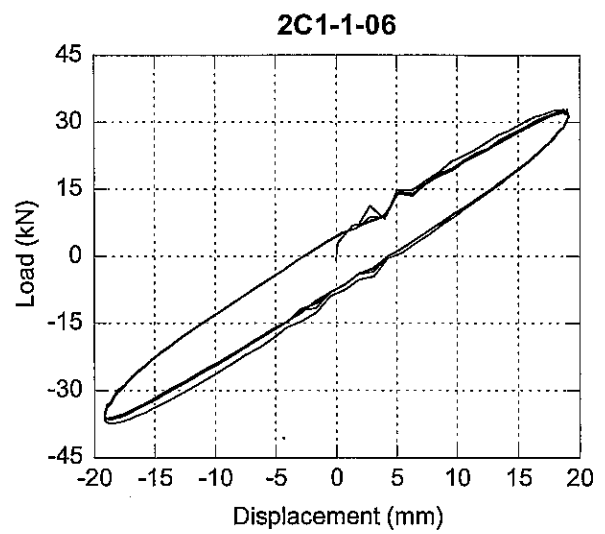
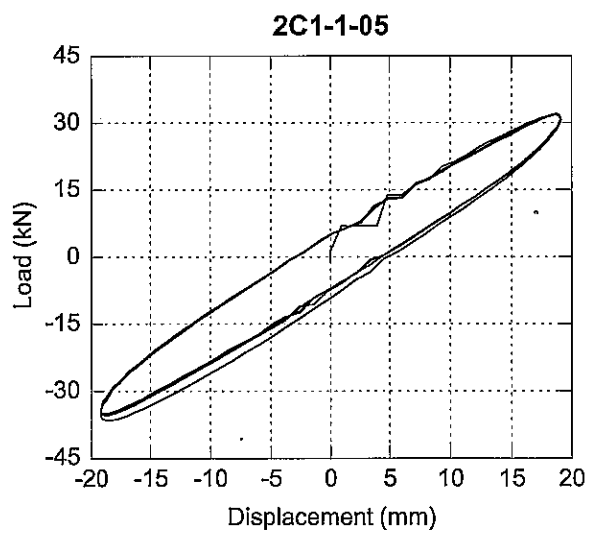
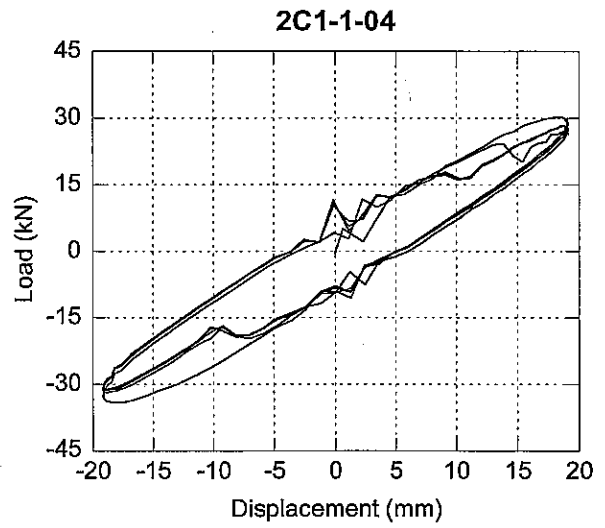
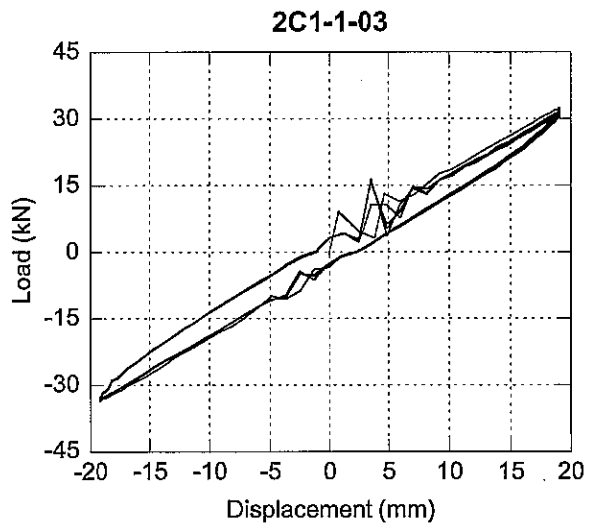
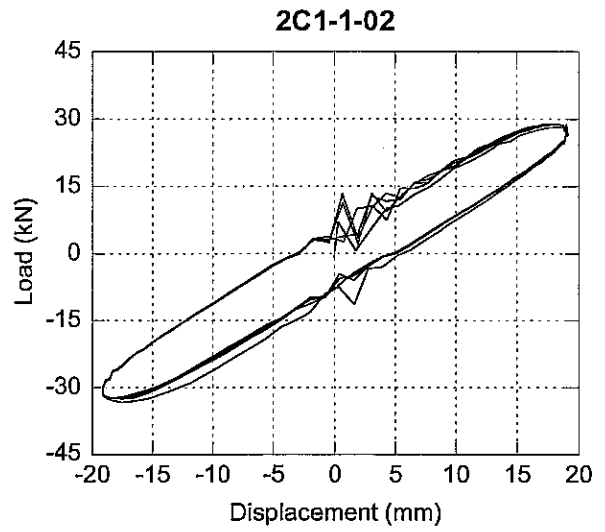
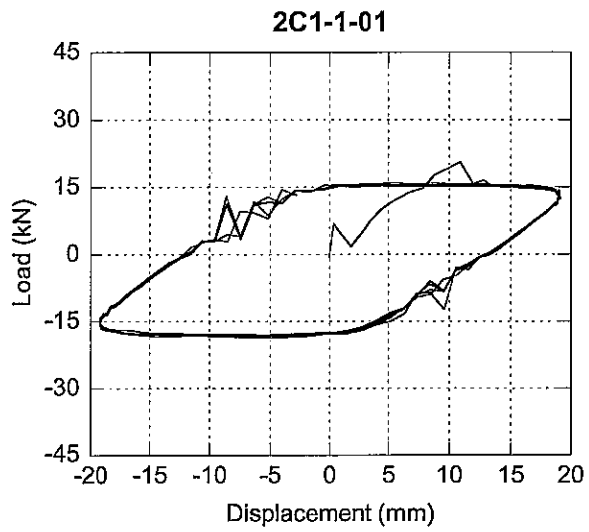
### Shear Modulus Summary - 2C1-1 & 2C2-2

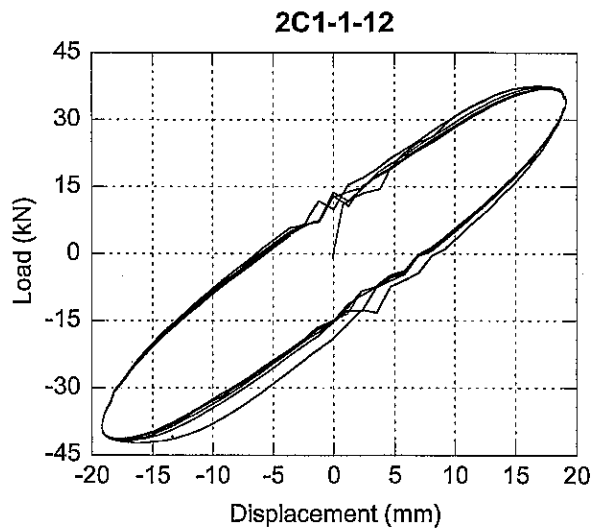
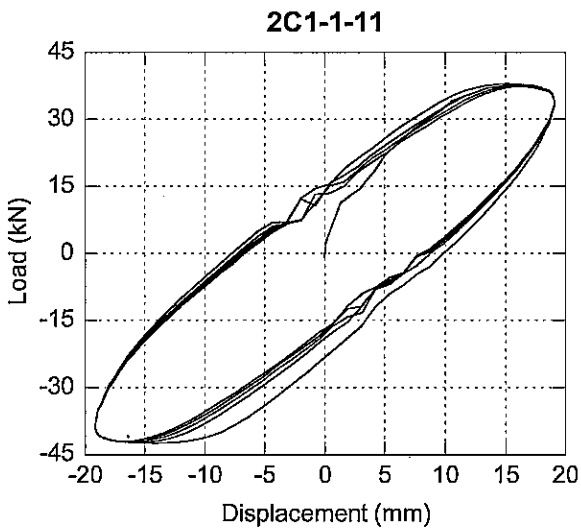
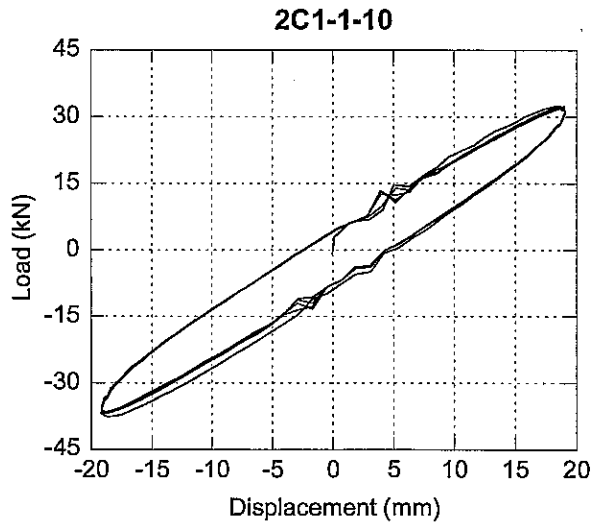
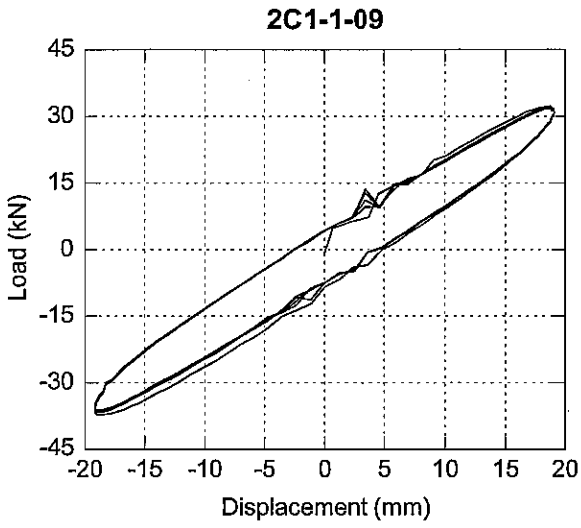
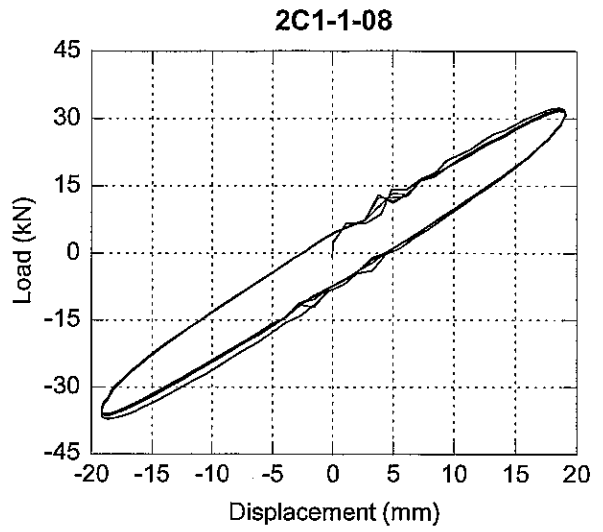
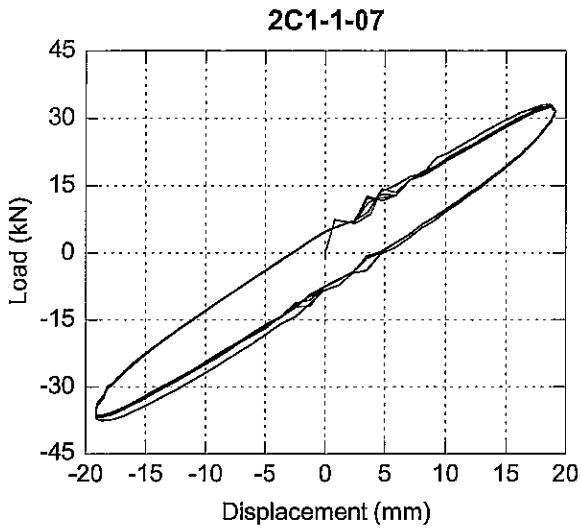


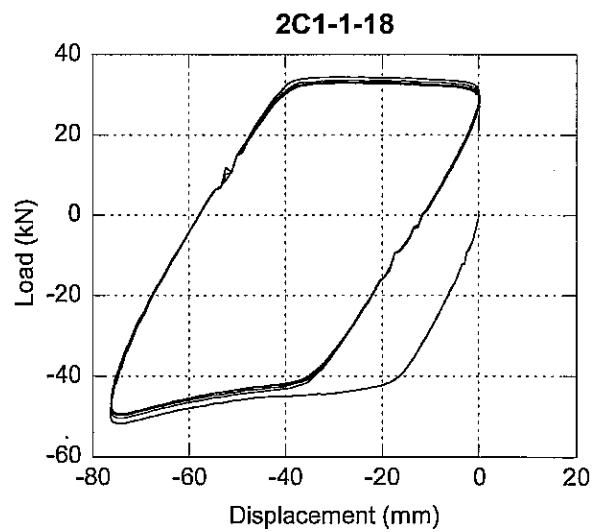
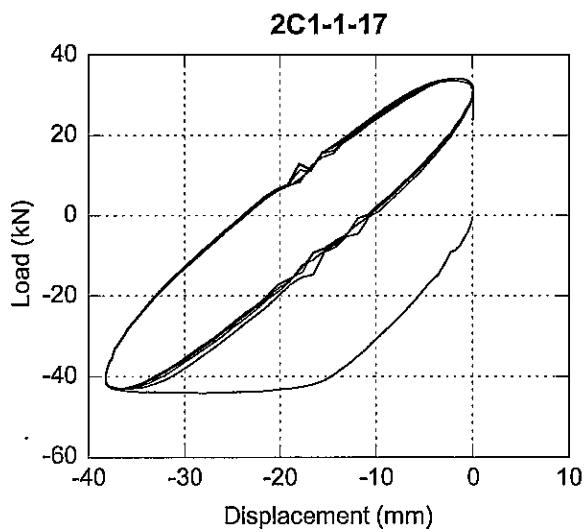
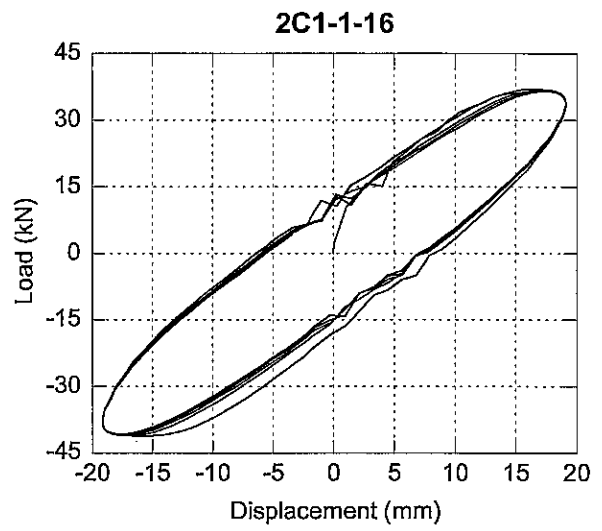
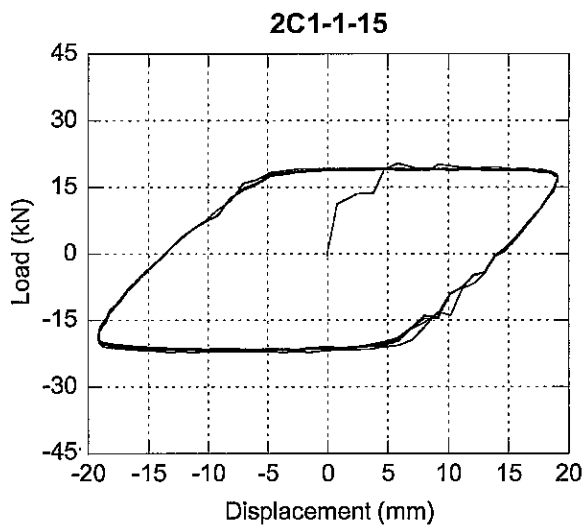
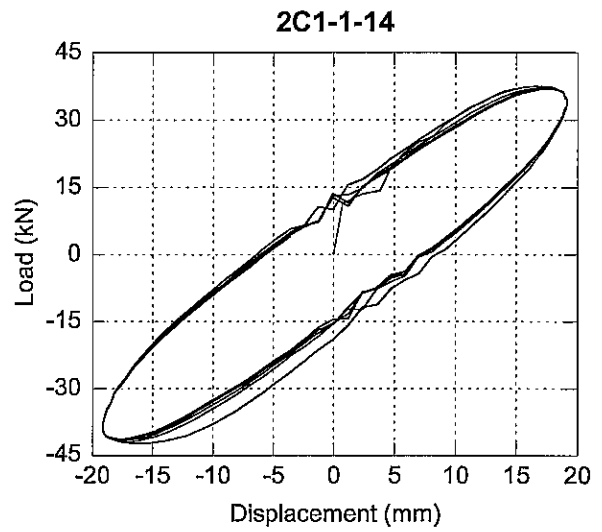
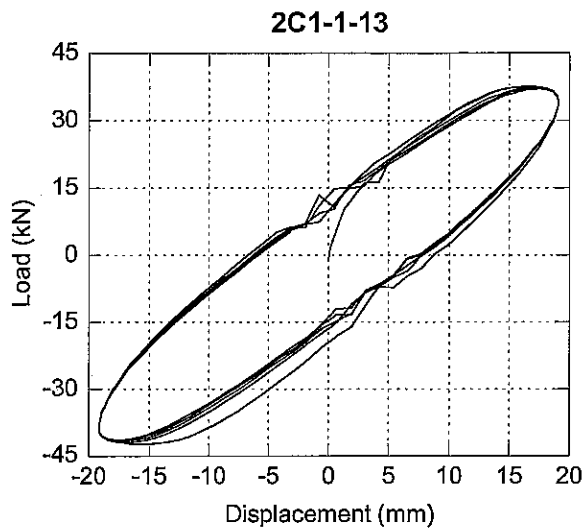
1.

### Normalized Shear Modulus - 2C1-1 & 2C2-2

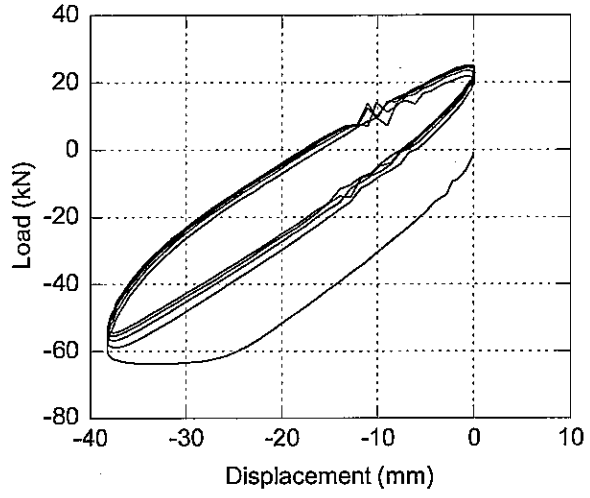




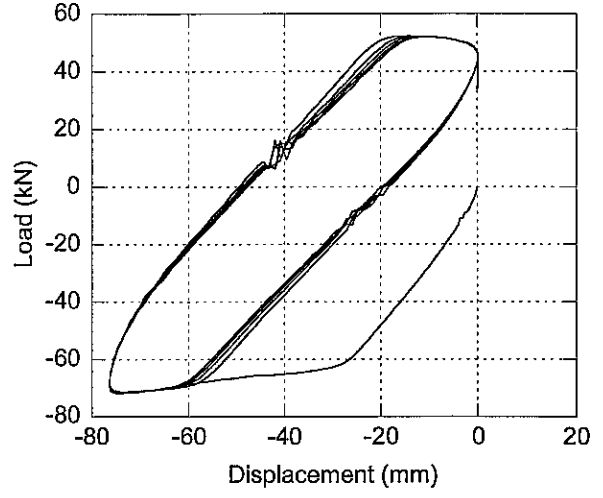


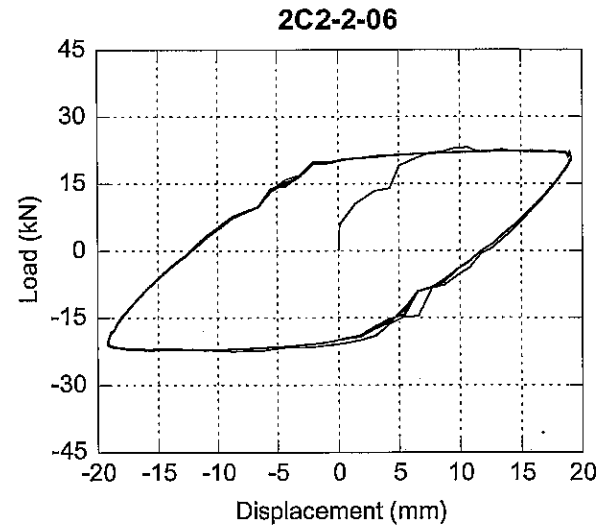
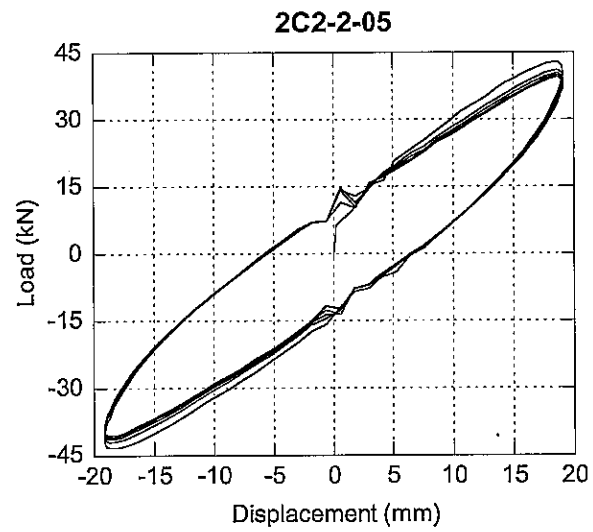
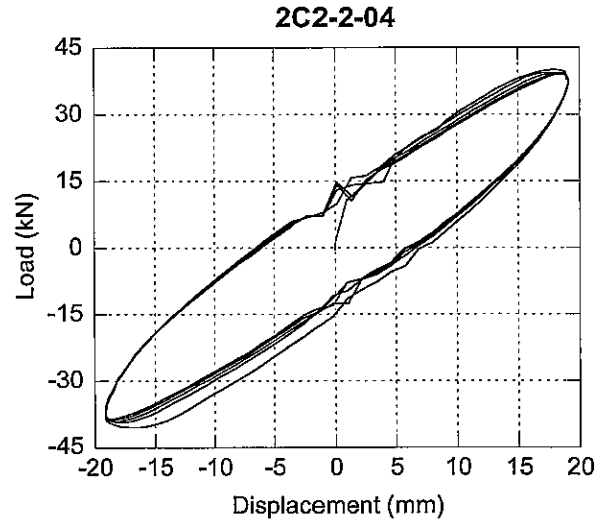
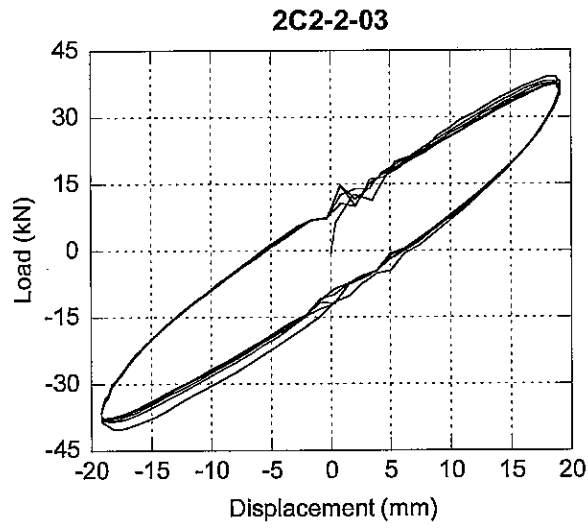
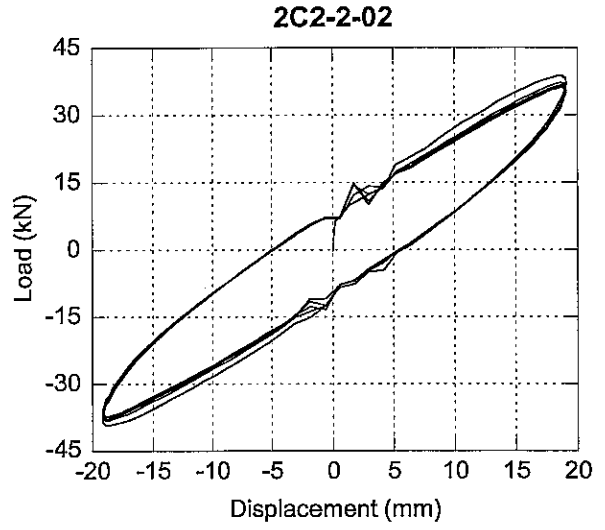
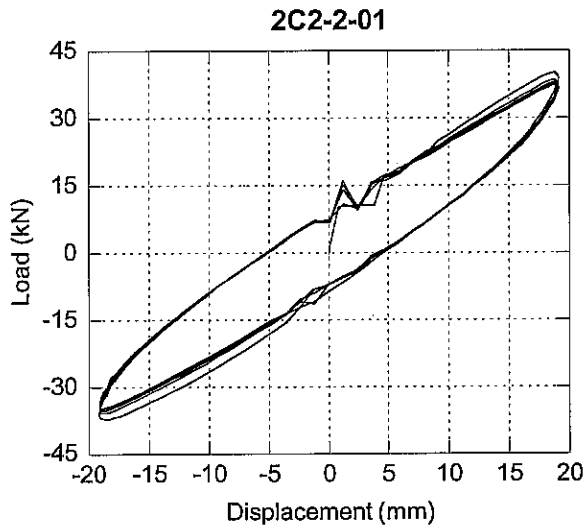


2C1-1-19

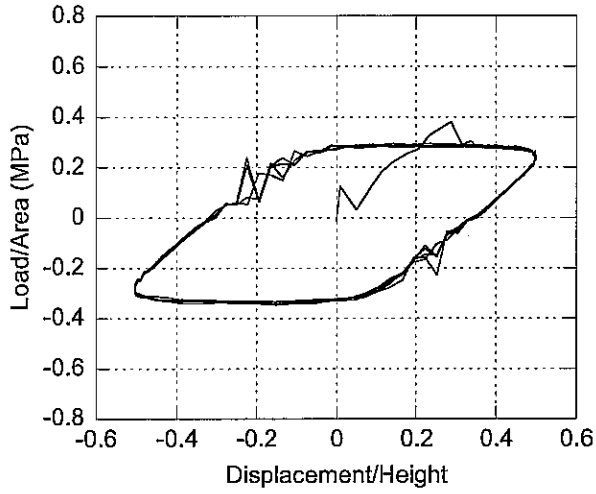


2C1-1-20

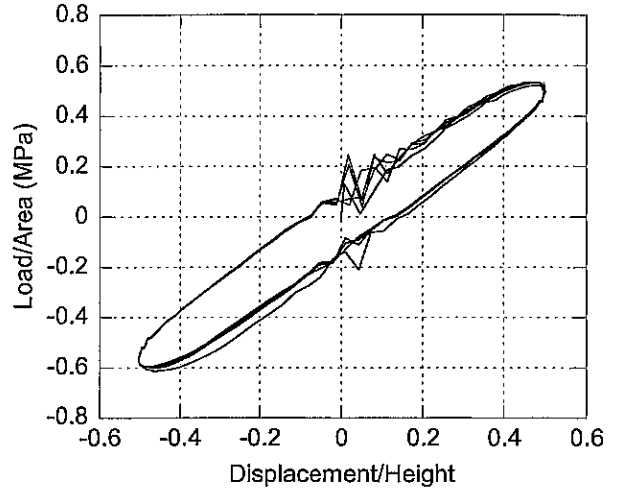




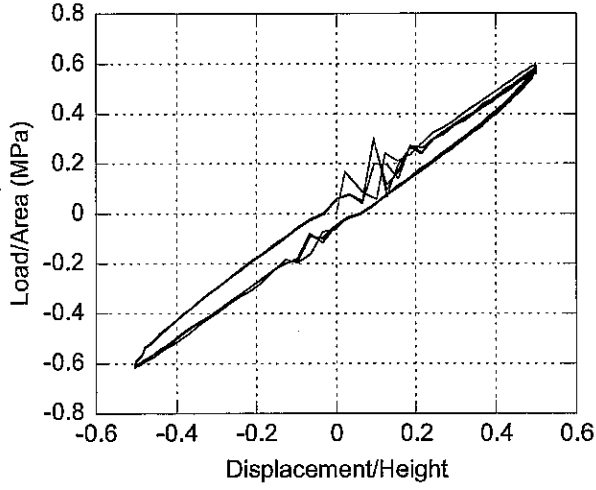
**2C1-1-01**



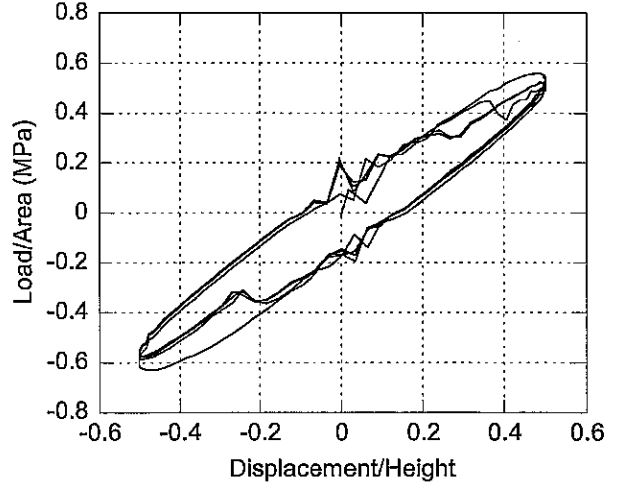
**2C1-1-02**



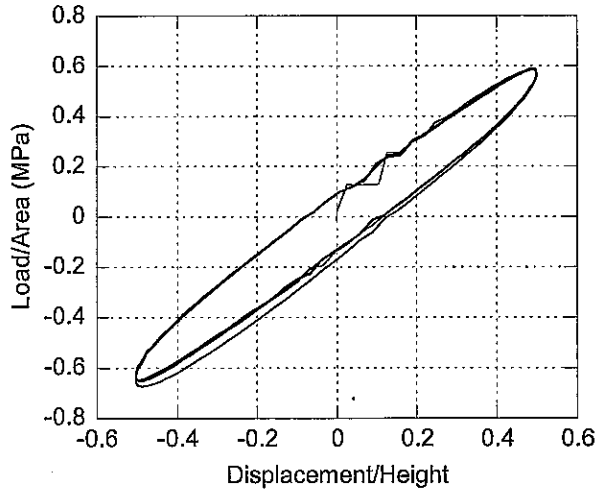
**2C1-1-03**



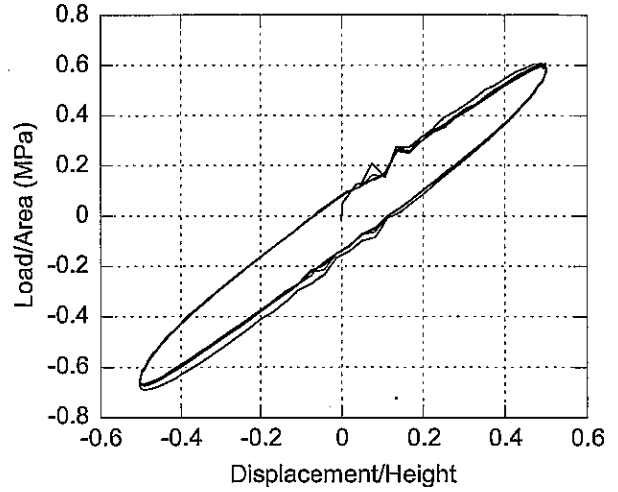
**2C1-1-04**



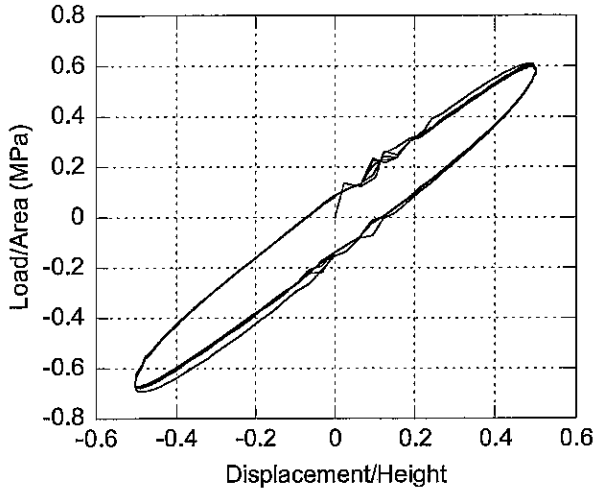
**2C1-1-05**



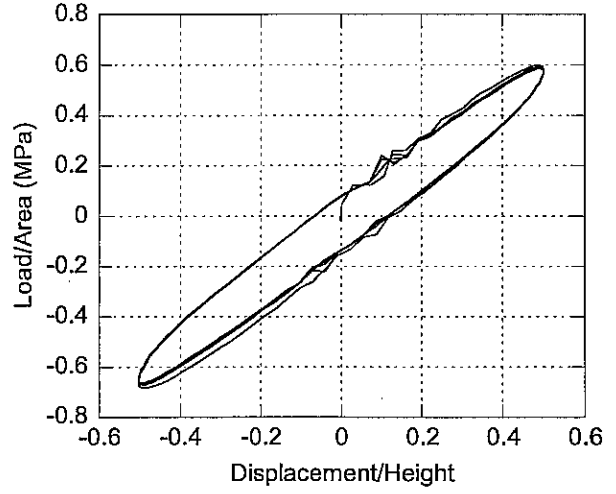
**2C1-1-06**



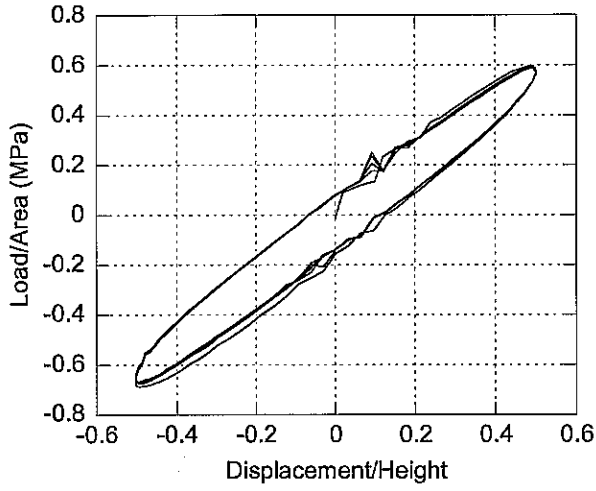
**2C1-1-07**



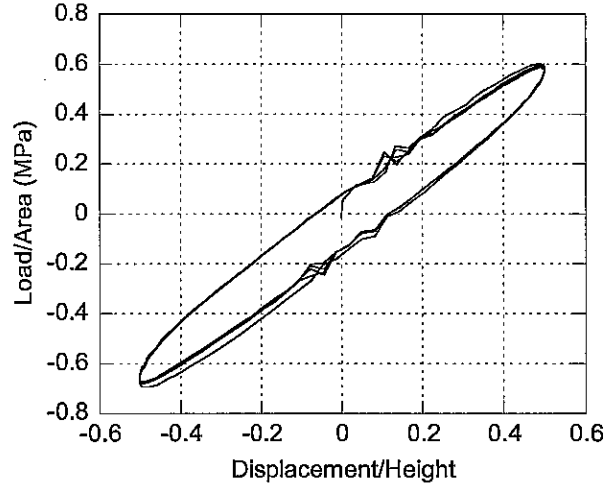
**2C1-1-08**



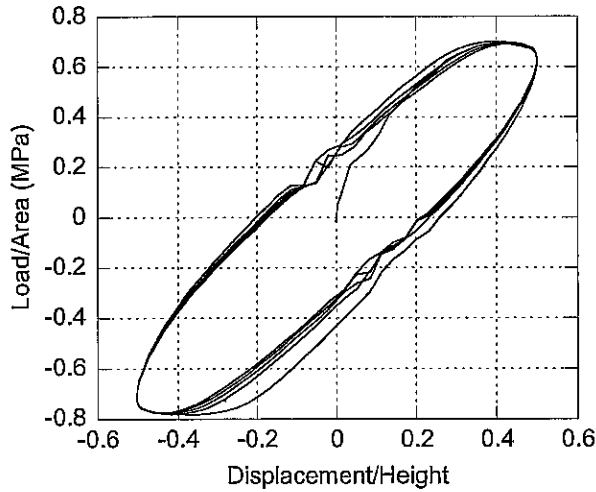
**2C1-1-09**



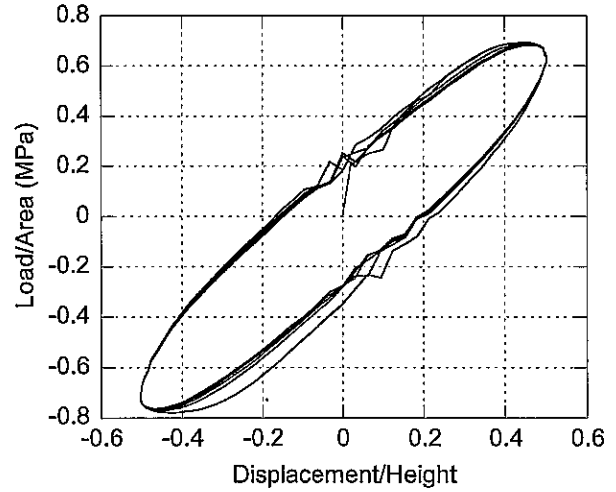
**2C1-1-10**



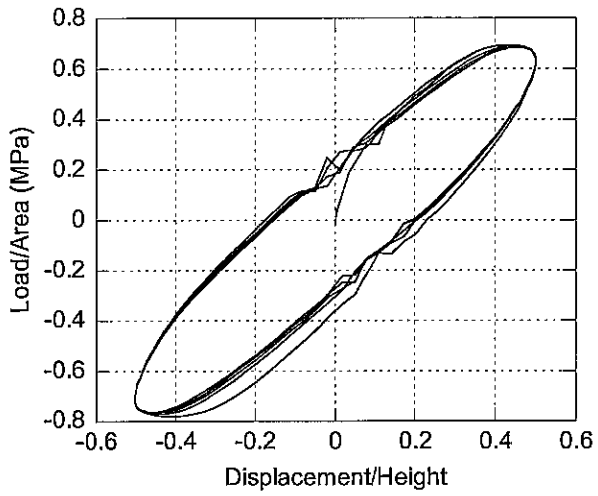
**2C1-1-11**



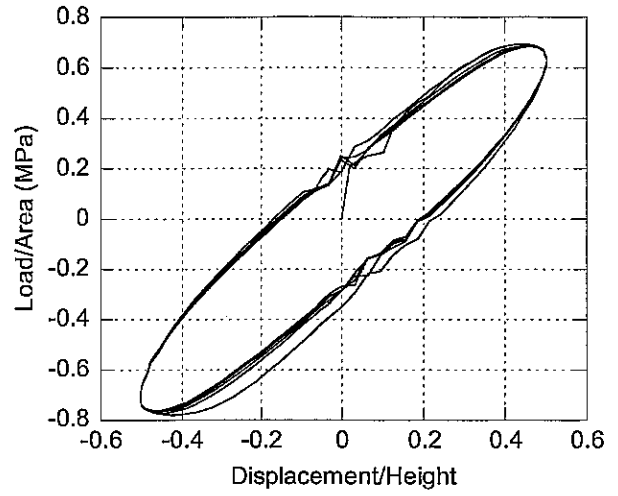
**2C1-1-12**



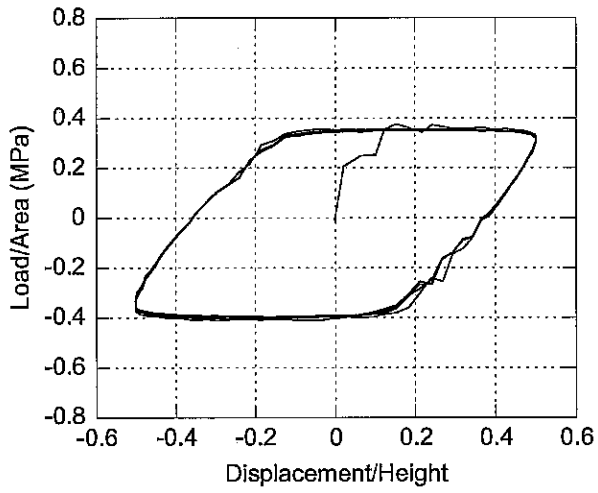
**2C1-1-13**



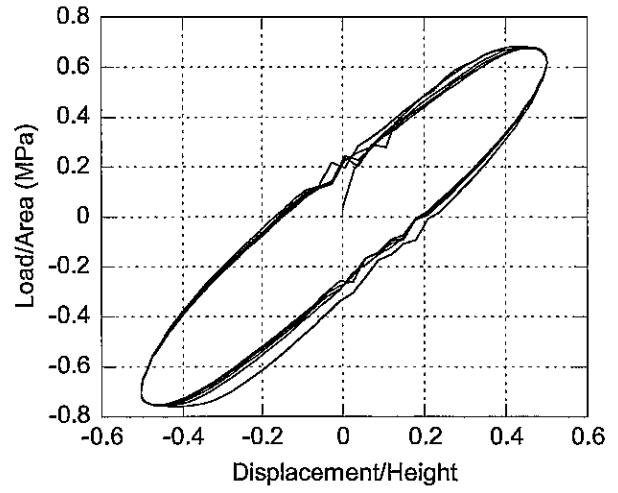
**2C1-1-14**



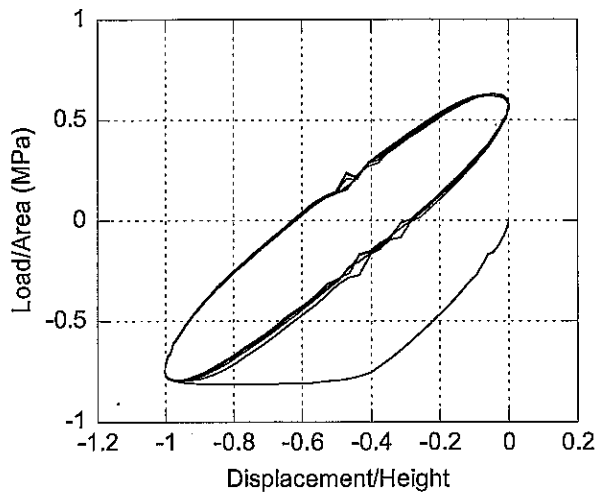
**2C1-1-15**



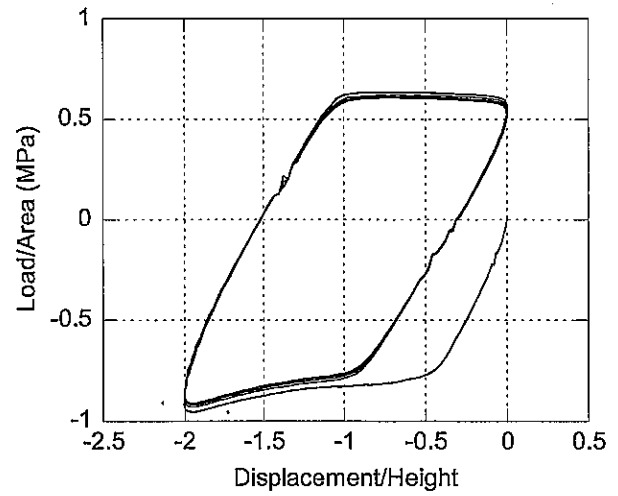
**2C1-1-16**



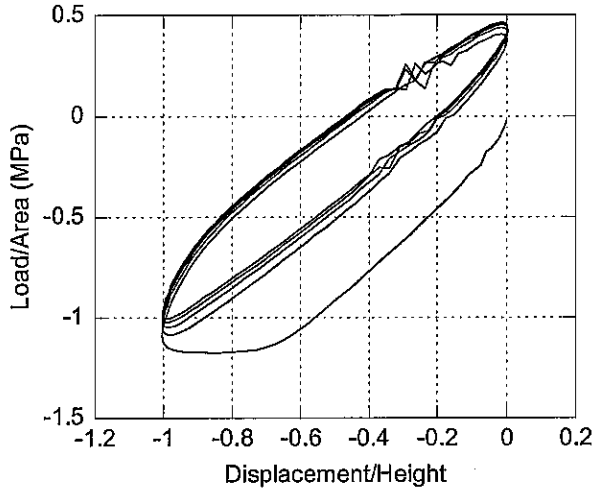
**2C1-1-17**



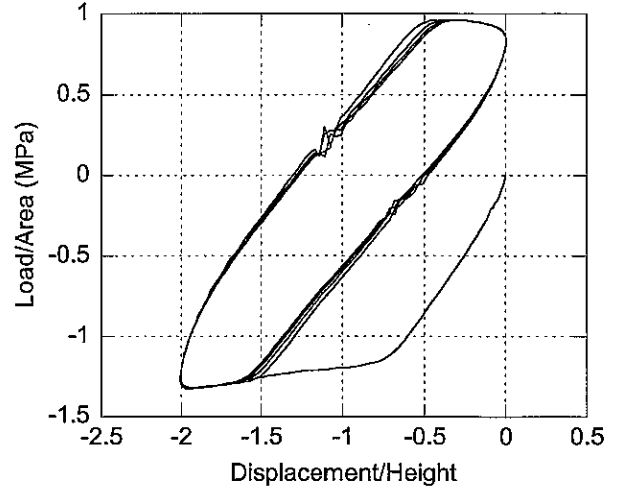
**2C1-1-18**



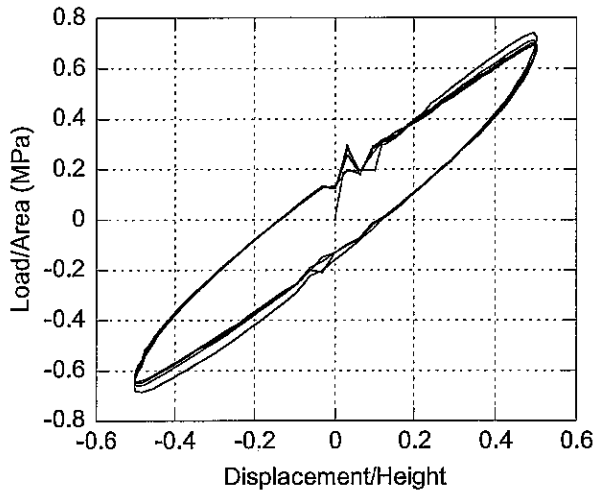
2C1-1-19



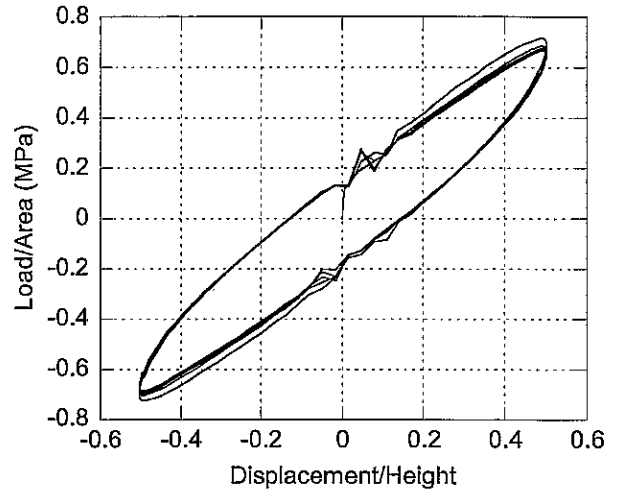
2C1-1-20



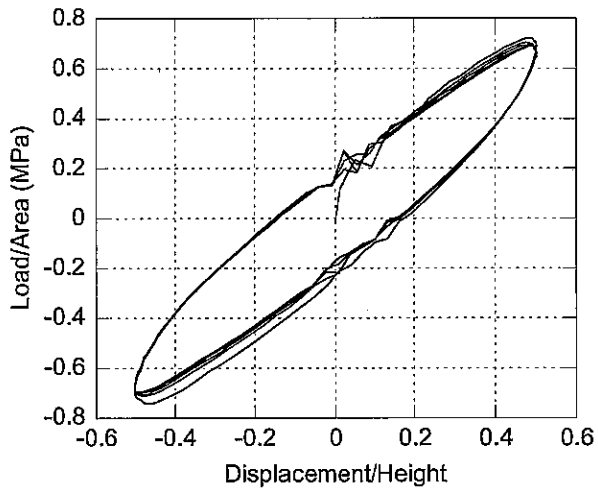
**2C2-2-01**



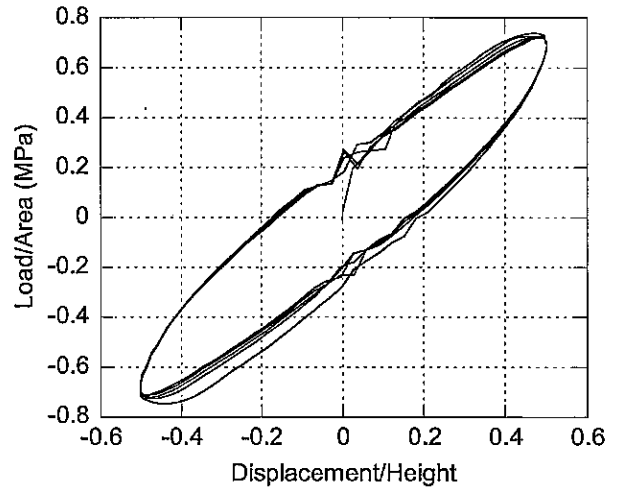
**2C2-2-02**



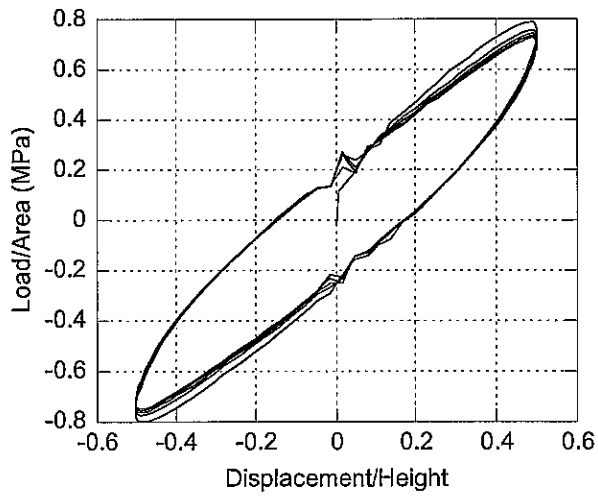
**2C2-2-03**



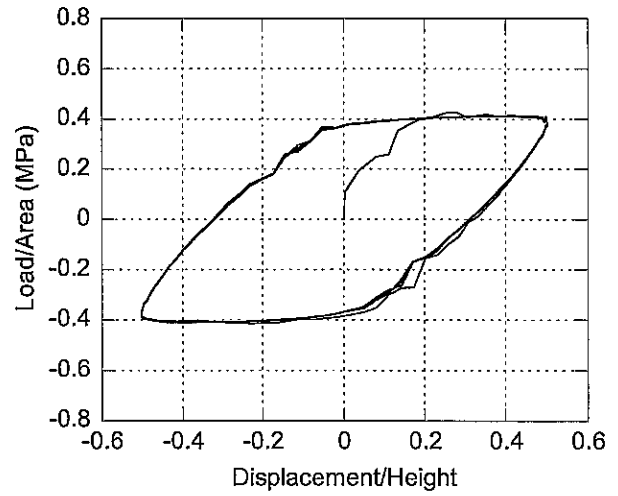
**2C2-2-04**



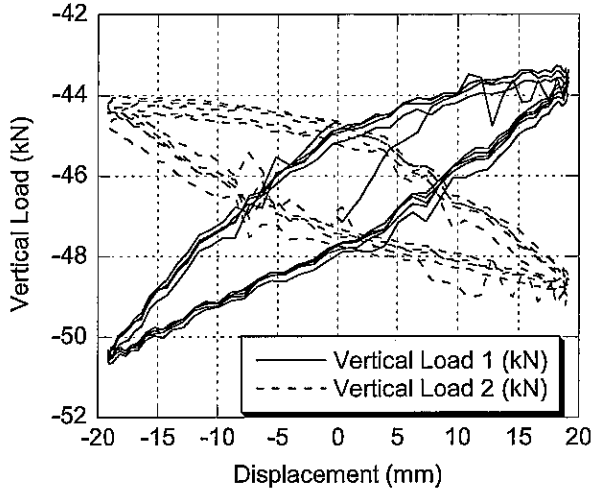
**2C2-2-05**



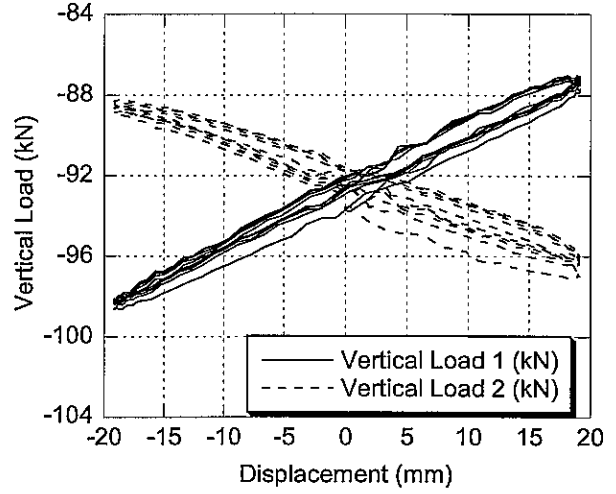
**2C2-2-06**



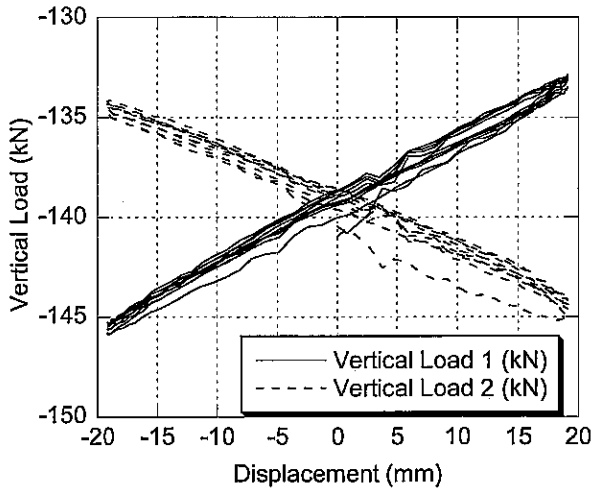
2C1-1-01



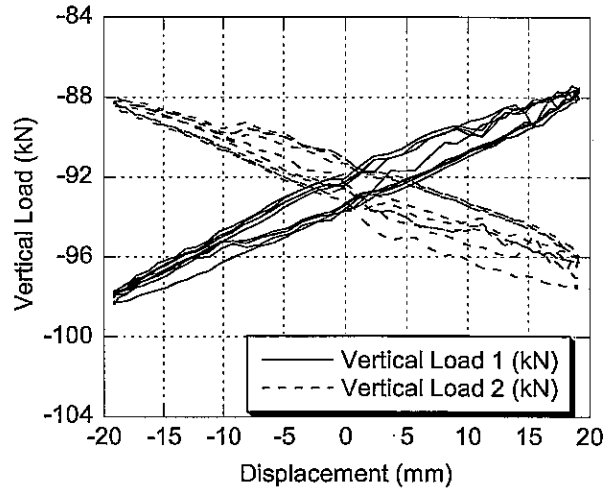
2C1-1-02



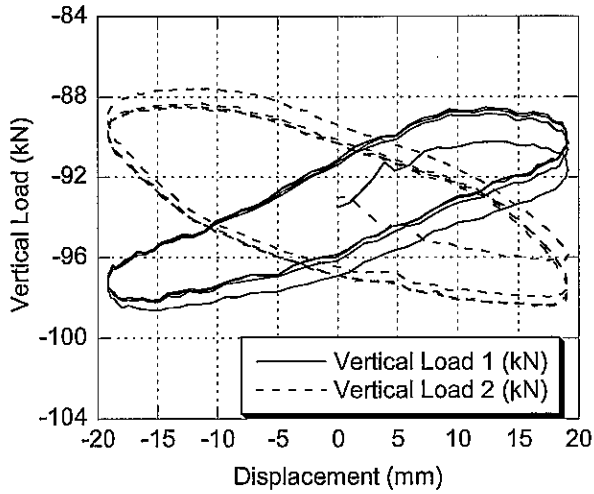
2C1-1-03



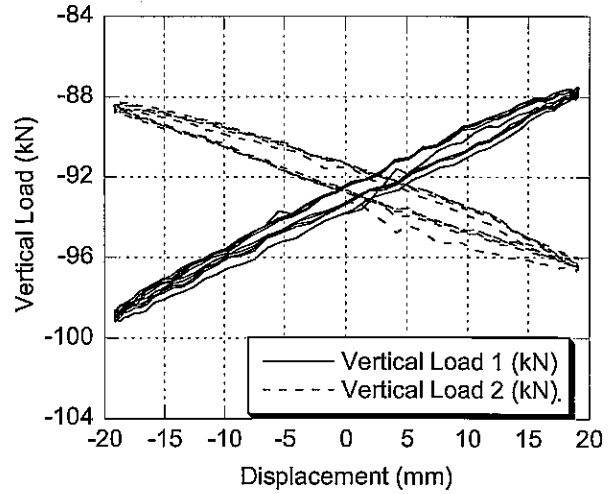
2C1-1-04



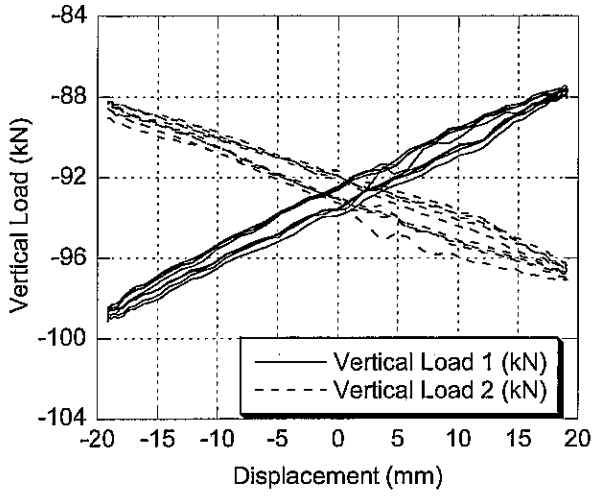
2C1-1-05



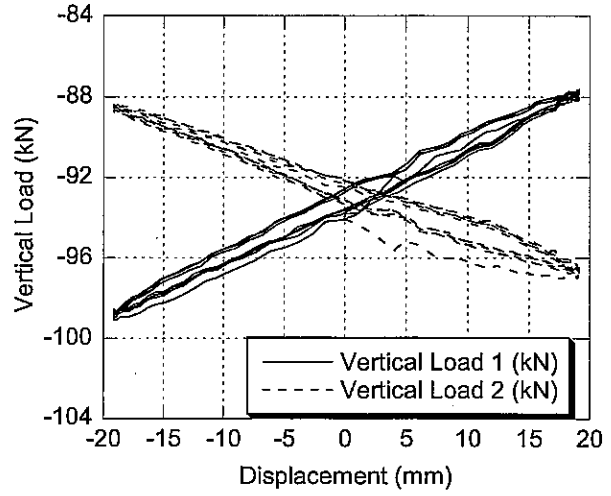
2C1-1-06



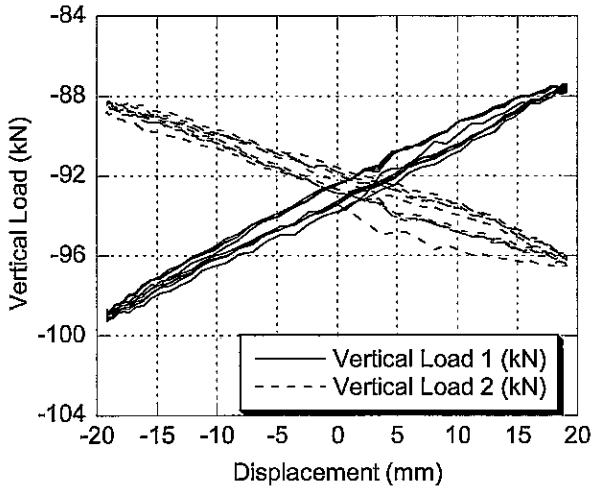
2C1-1-07



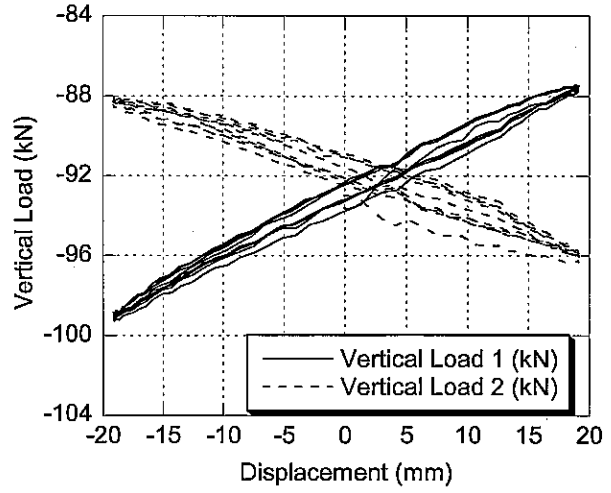
2C1-1-08



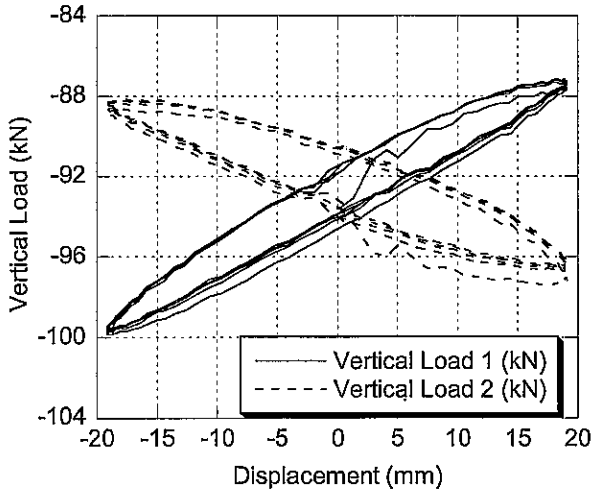
2C1-1-09



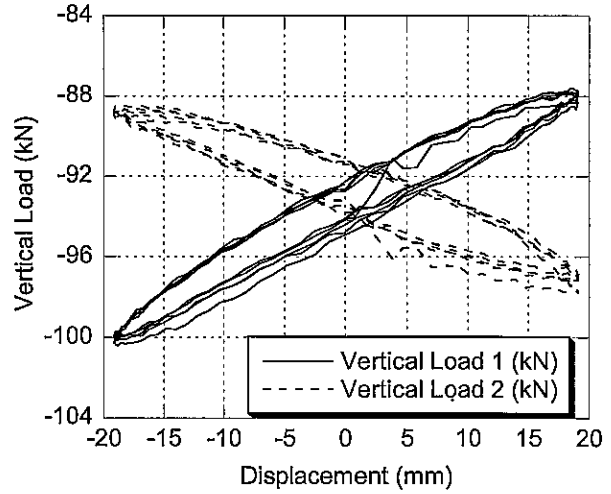
2C1-1-10

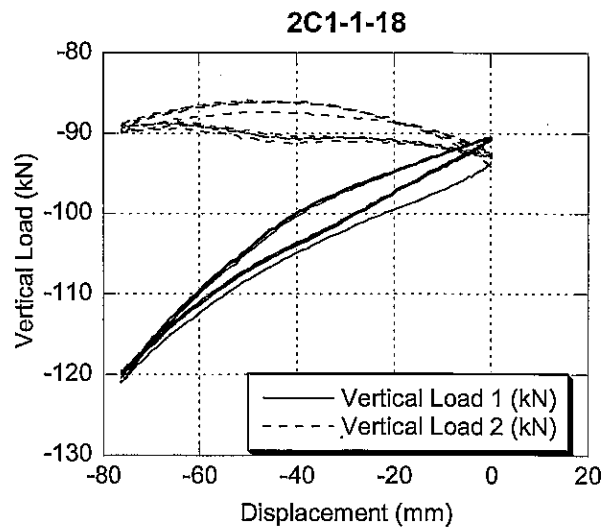
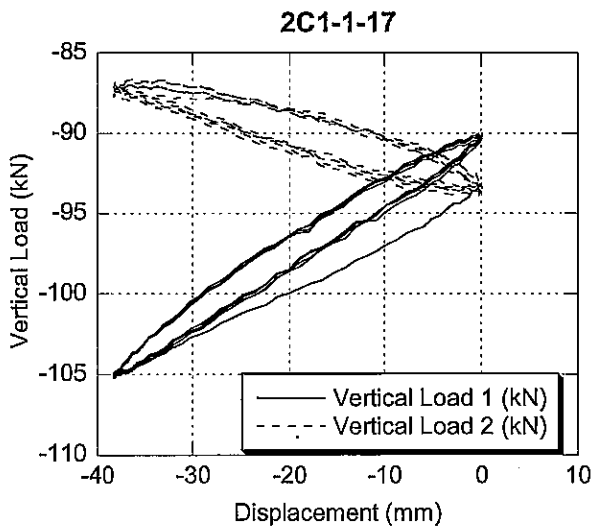
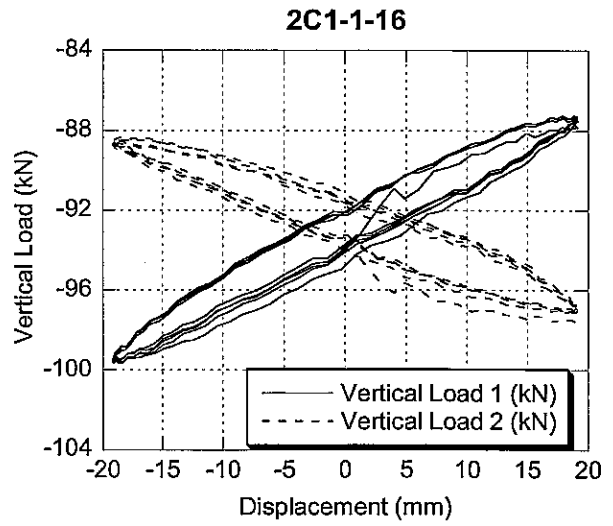
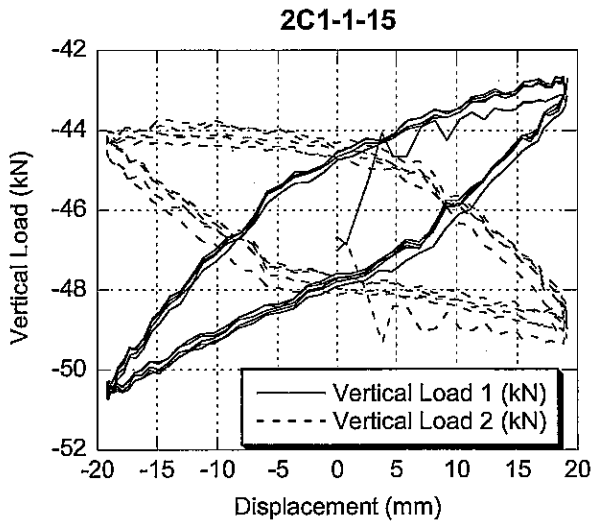
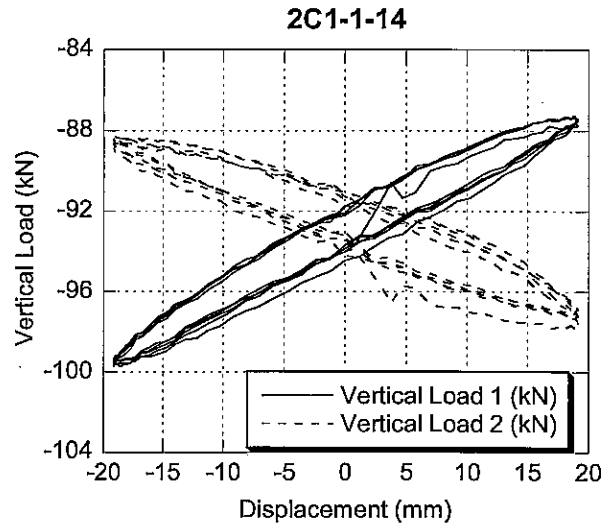
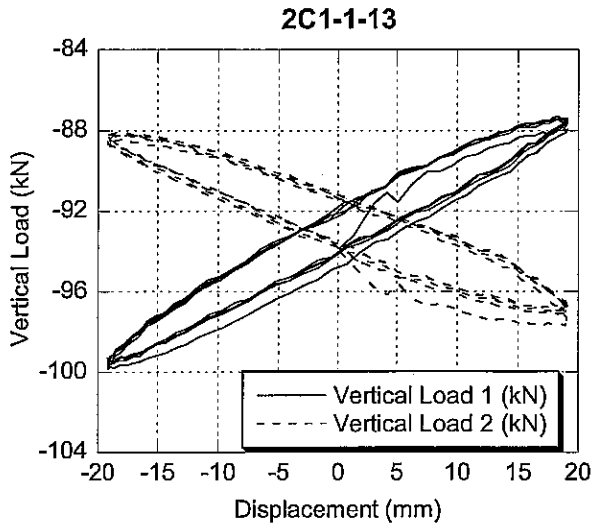


2C1-1-11

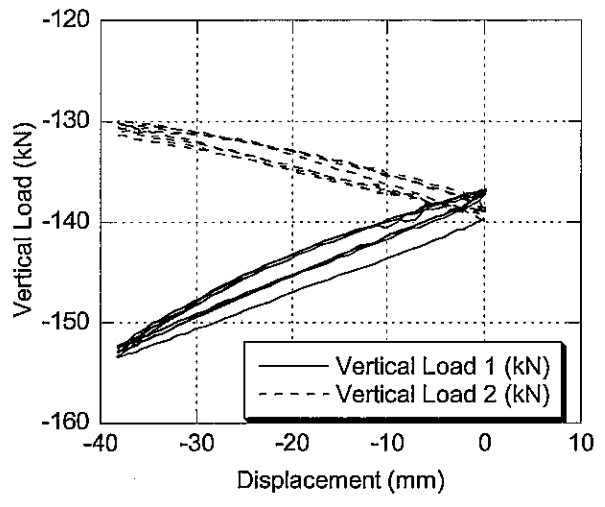


2C1-1-12

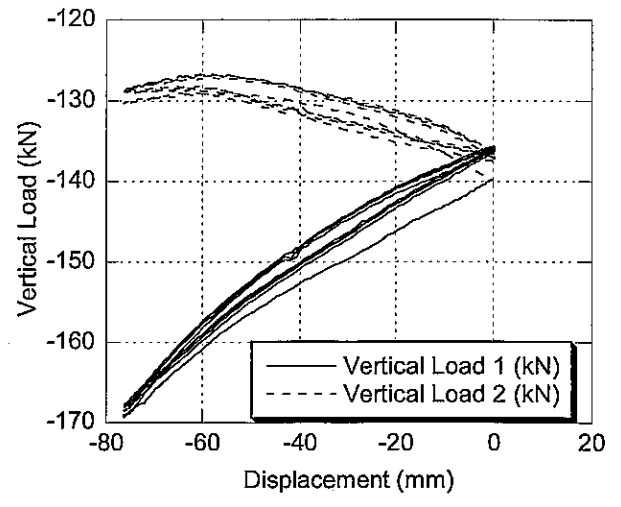


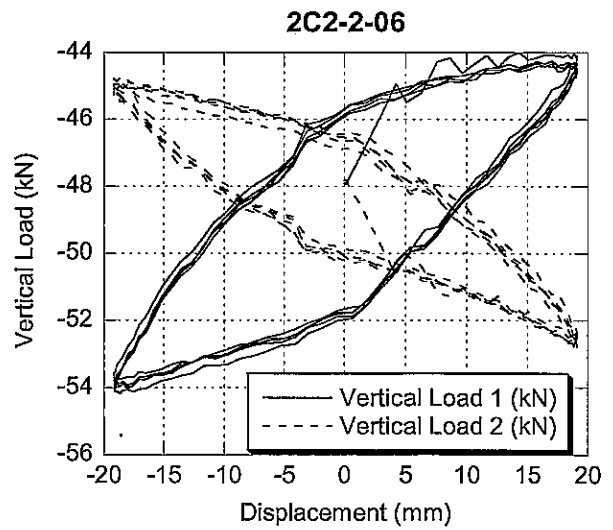
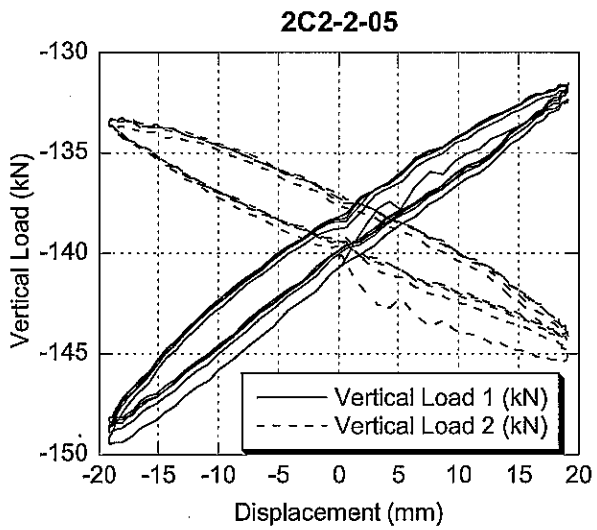
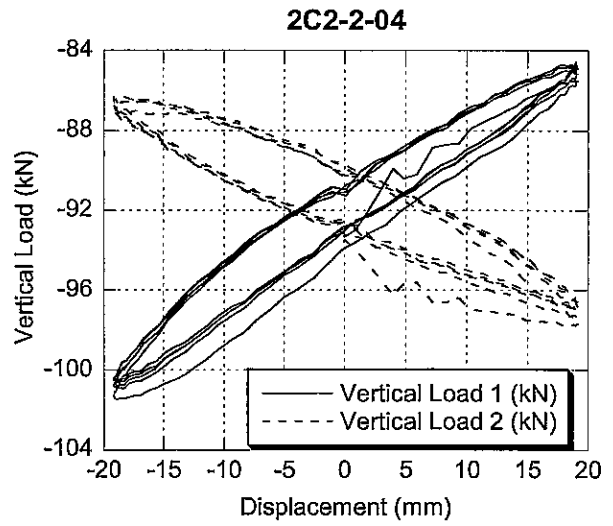
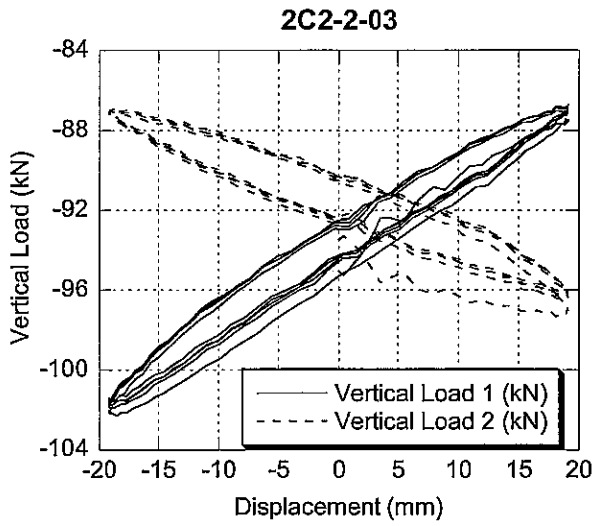
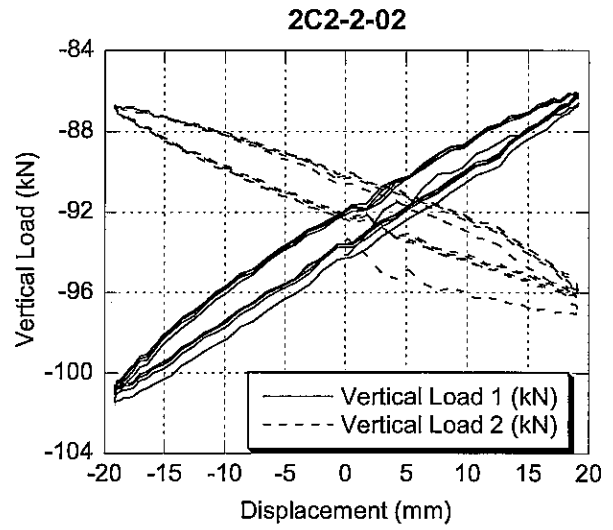
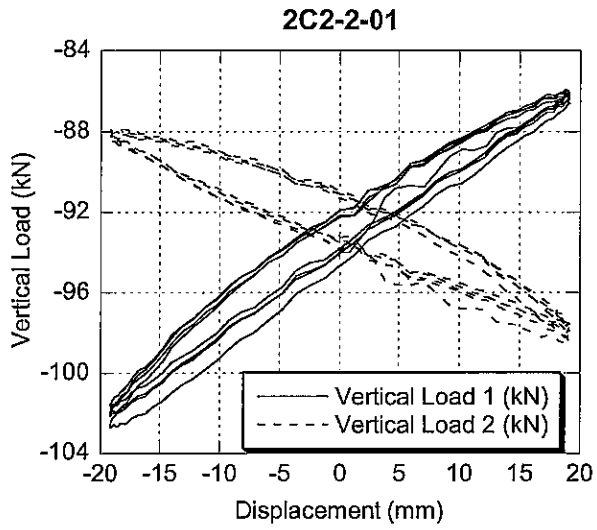


2C1-1-19



2C1-1-20







**APPENDIX D**

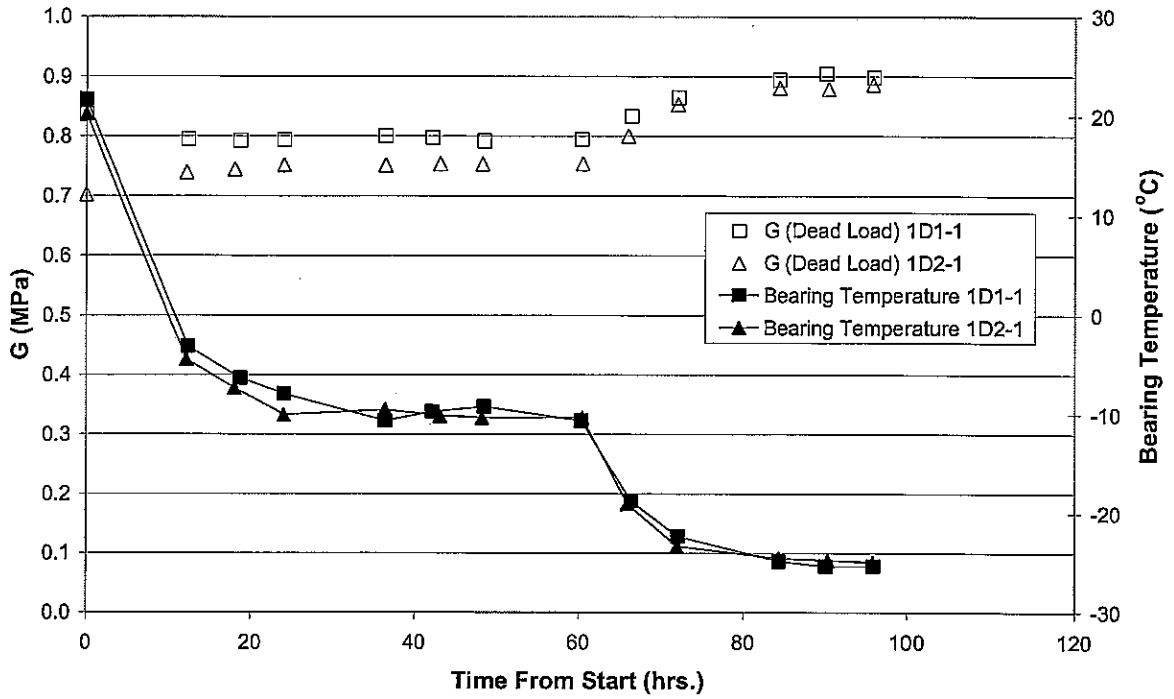
**Test Results for 1D1 & 1D2**



**Appendix D – Test Results for 1D1 & 1D2**

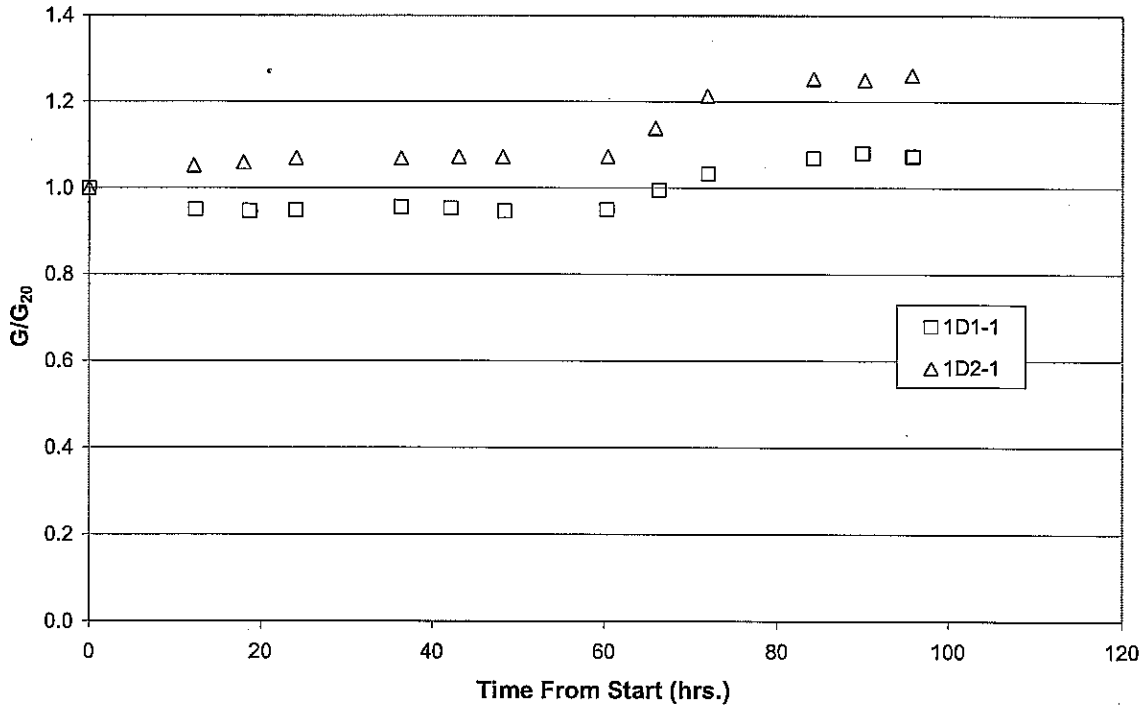
Report Reference	Date & Time	Time From Start, hrs.	Brg. Temp. °C	Vert. Load		Amp.		Freq. hz
				psi	MPa	in	mm	
1D1-1-01	10/15/01 20:00	0.00	21.7	500	3.447	1.5	38.1	0.5
1D1-1-02	10/16/01 8:30	12.50	-3.1	500	3.447	1.5	38.1	0.5
1D1-1-03	10/16/01 14:45	18.75	-6.3	500	3.447	1.5	38.1	0.5
1D1-1-04	10/16/01 20:10	24.17	-7.9	500	3.447	1.5	38.1	0.5
1D1-1-05	10/17/01 8:25	36.42	-10.6	500	3.447	1.5	38.1	0.5
1D1-1-06	10/17/01 14:10	42.17	-9.7	500	3.447	1.5	38.1	0.5
1D1-1-07	10/17/01 20:24	48.40	-9.2	500	3.447	1.5	38.1	0.5
1D1-1-08	10/18/01 8:21	60.35	-10.6	500	3.447	1.5	38.1	0.5
1D1-1-09	10/18/01 14:27	66.45	-18.7	500	3.447	1.5	38.1	0.5
1D1-1-10	10/18/01 20:10	72.17	-22.3	500	3.447	1.5	38.1	0.5
1D1-1-11	10/19/01 8:21	84.35	-24.8	500	3.447	1.5	38.1	0.5
1D1-1-12	10/19/01 14:11	90.18	-25.3	500	3.447	1.5	38.1	0.5
1D1-1-13	10/19/01 20:02	96.03	-25.3	500	3.447	1.5	38.1	0.5
1D2-1-01	10/21/01 20:00	0.00	20.3	500	3.447	1.5	38.1	0.5
1D2-1-02	10/22/01 8:18	12.30	-4.4	500	3.447	1.5	38.1	0.5
1D2-1-03	10/22/01 14:04	18.07	-7.3	500	3.447	1.5	38.1	0.5
1D2-1-04	10/22/01 20:09	24.15	-10	500	3.447	1.5	38.1	0.5
1D2-1-05	10/23/01 8:25	36.42	-9.5	500	3.447	1.5	38.1	0.5
1D2-1-06	37187.62917	43.10	-10.1	500	3.447	1.5	38.1	0.5
1D2-1-07	37187.84028	48.17	-10.3	500	3.447	1.5	38.1	0.5
1D2-1-08	10/24/01 8:28	60.47	-10.3	500	3.447	1.5	38.1	0.5
1D2-1-09	10/24/01 14:03	66.05	-19	500	3.447	1.5	38.1	0.5
1D2-1-10	10/24/01 20:04	72.07	-23.3	500	3.447	1.5	38.1	0.5
1D2-1-11	10/25/01 8:23	84.38	-24.5	500	3.447	1.5	38.1	0.5
1D2-1-12	10/25/01 14:27	90.45	-24.7	500	3.447	1.5	38.1	0.5
1D2-1-13	10/25/01 19:55	95.92	-24.9	500	3.447	1.5	38.1	0.5

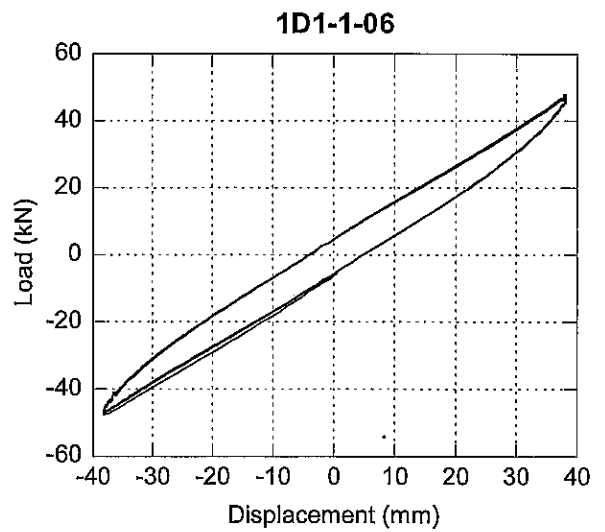
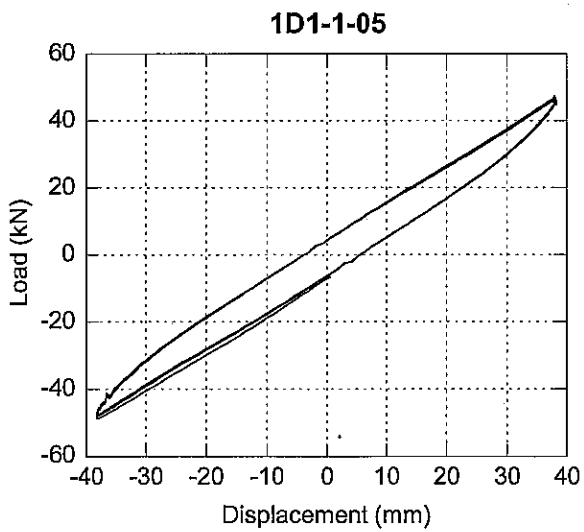
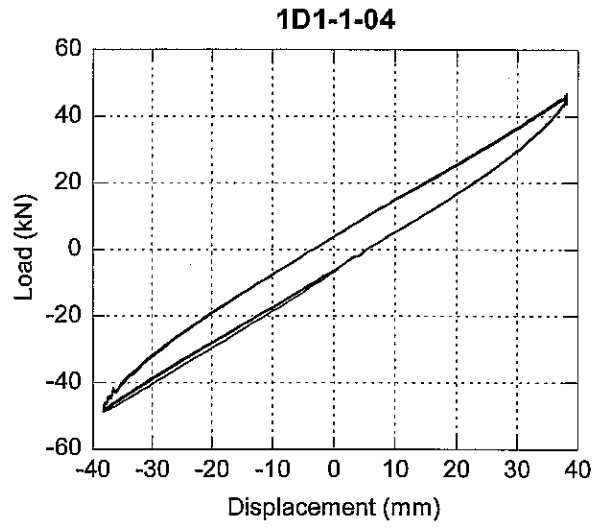
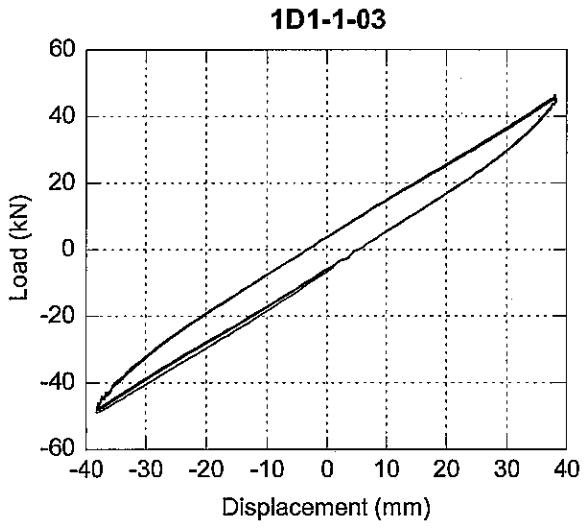
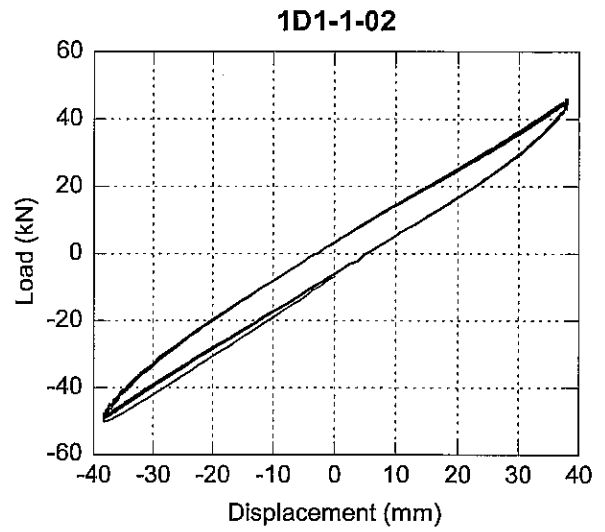
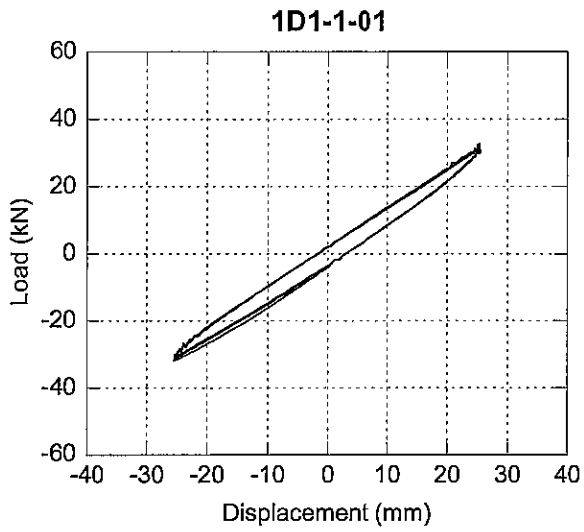
### Shear Modulus Summary - 1D1-1 & 1D2-1

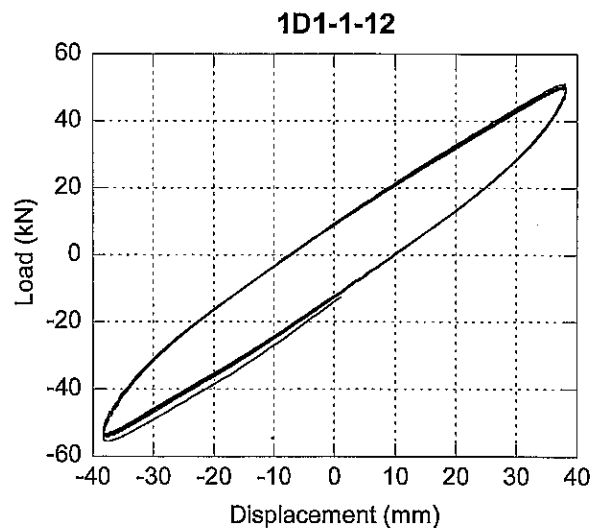
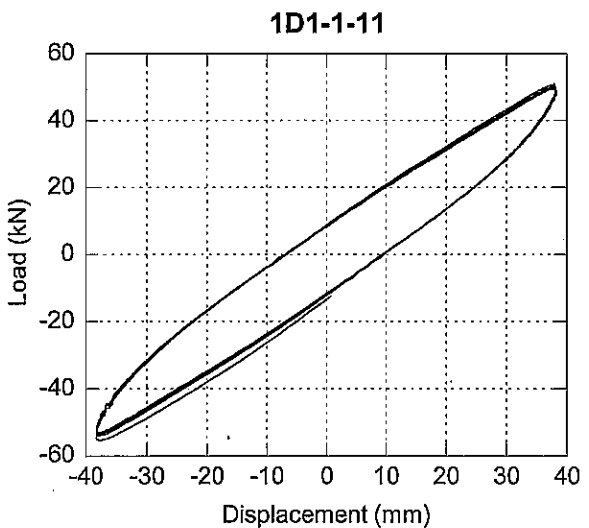
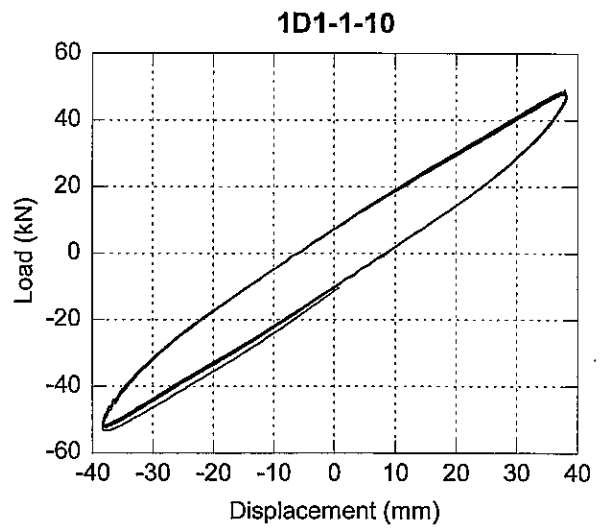
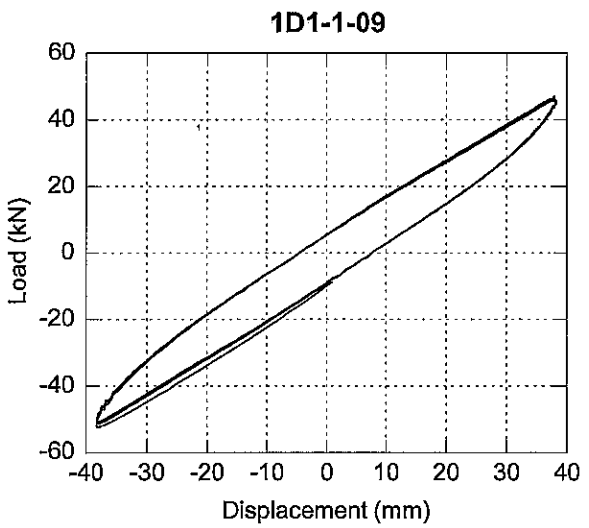
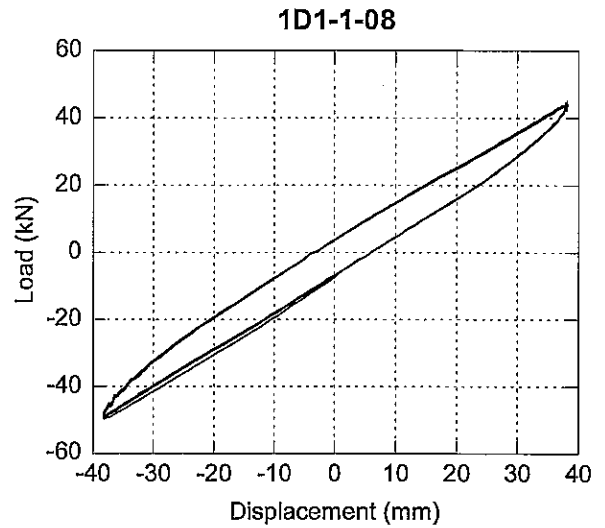
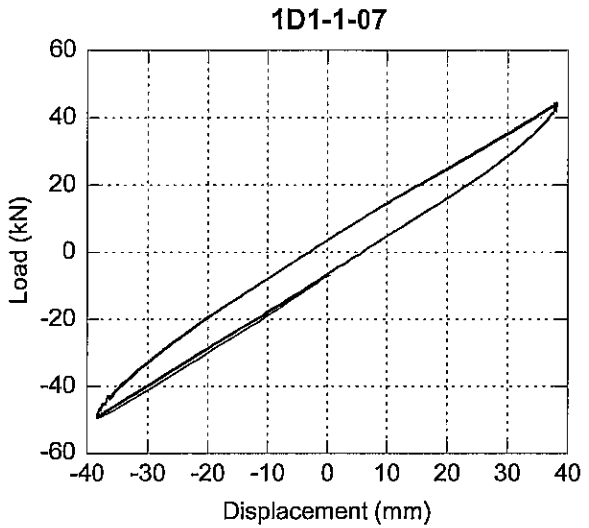


2.

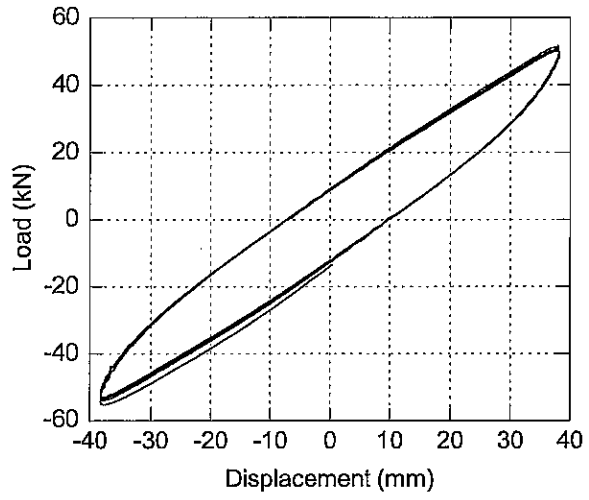
### Normalized Shear Modulus - 1D1-1 & 1D2-1

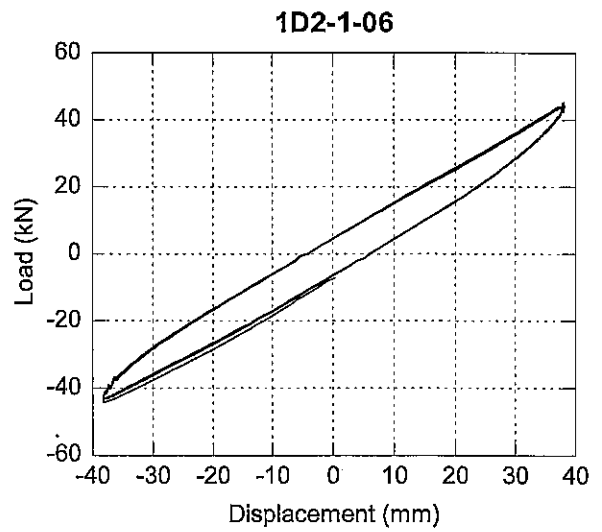
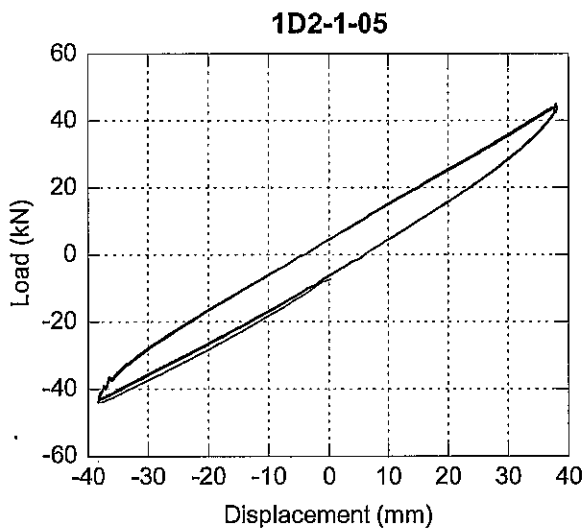
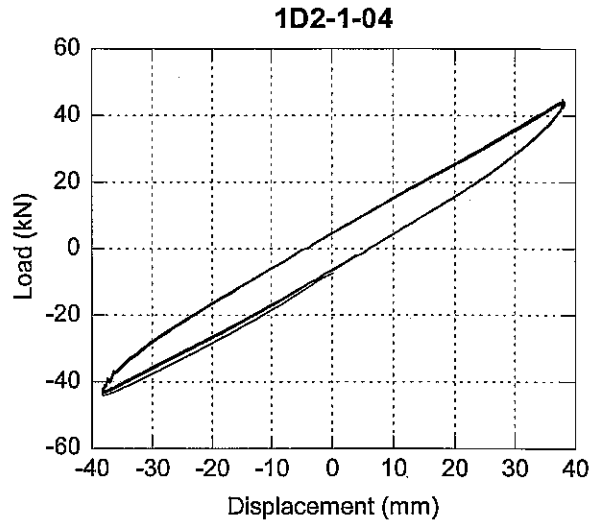
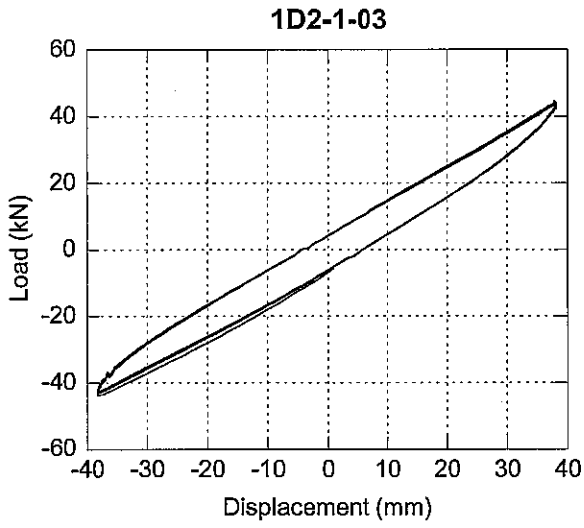
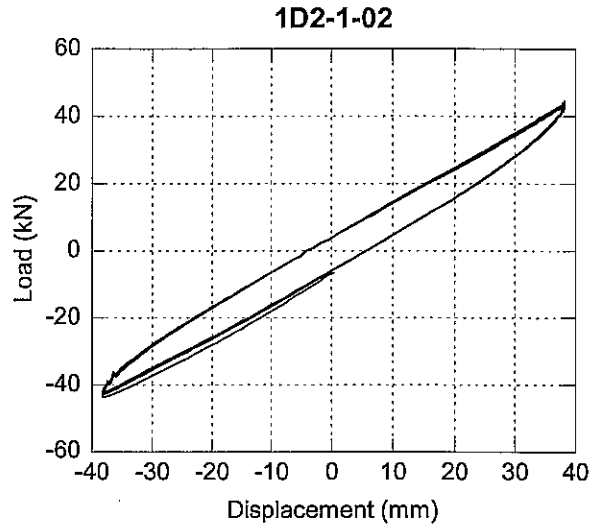
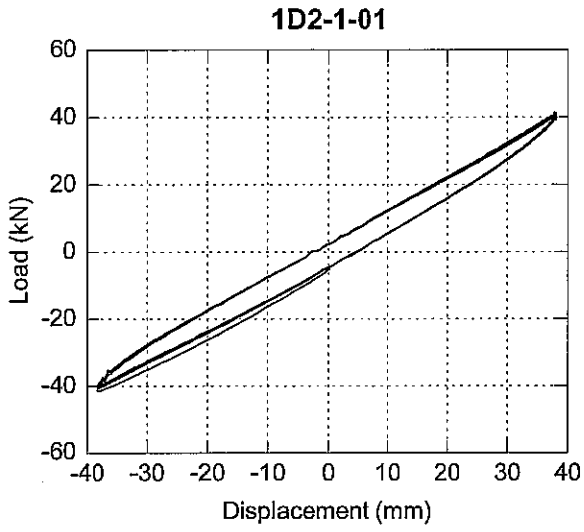


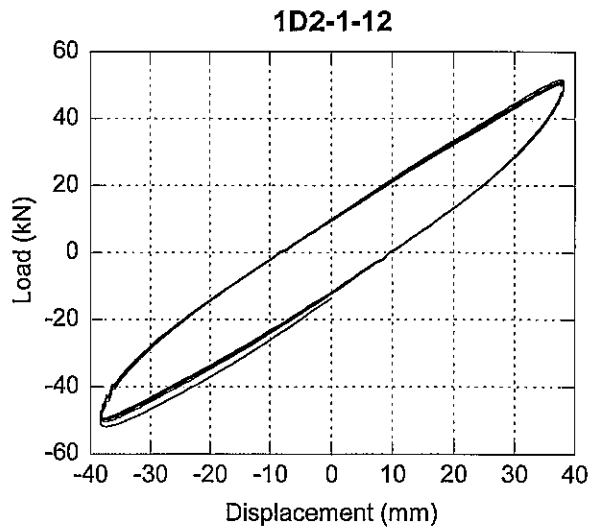
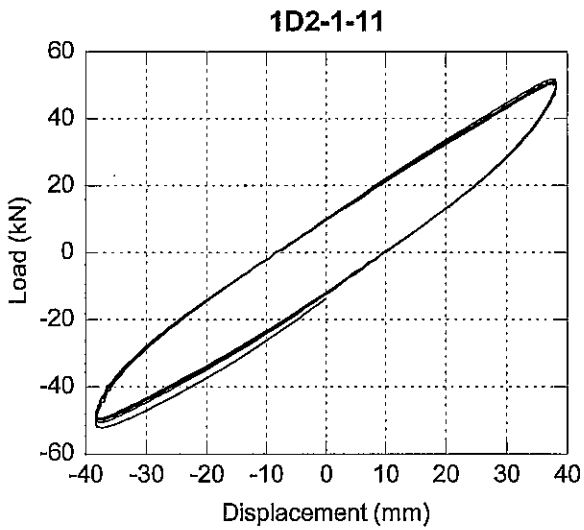
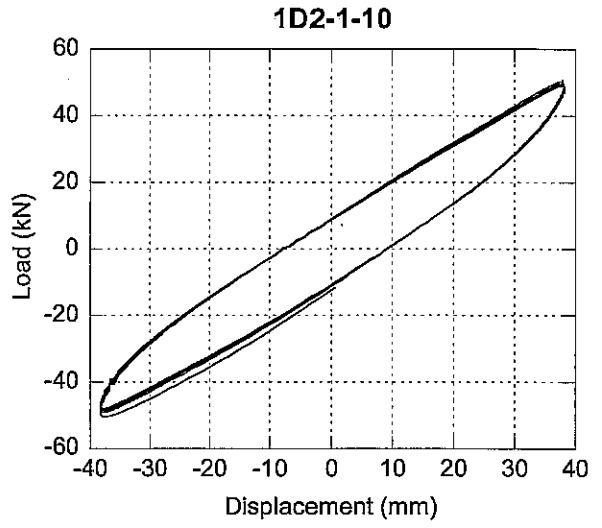
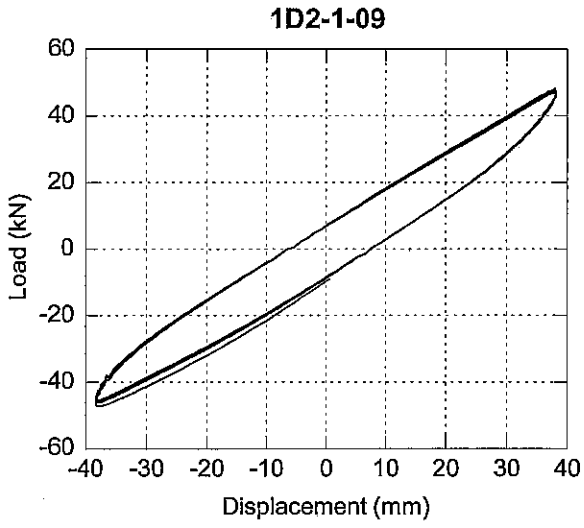
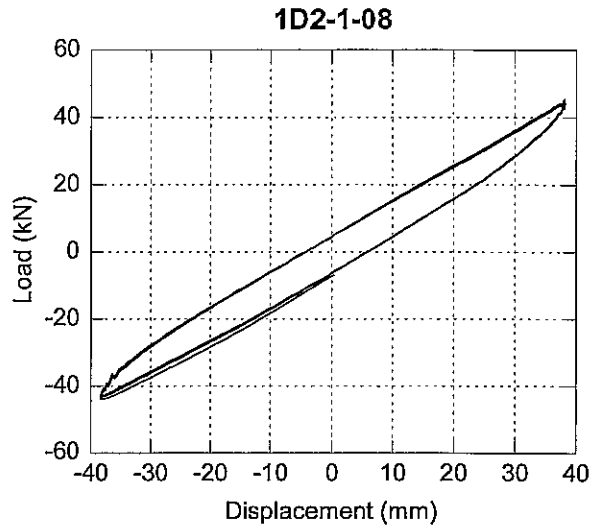
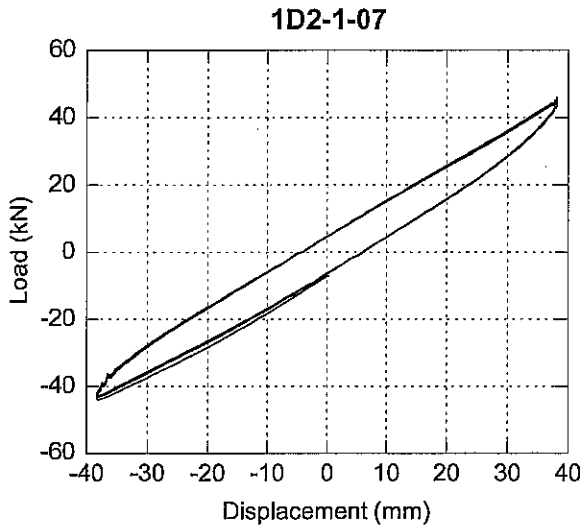




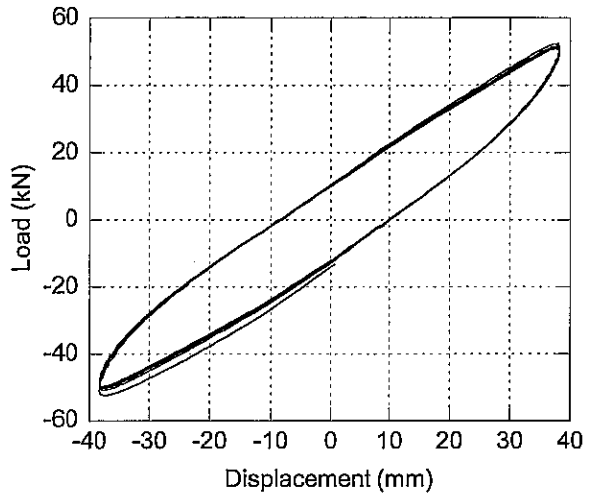
1D1-1-13



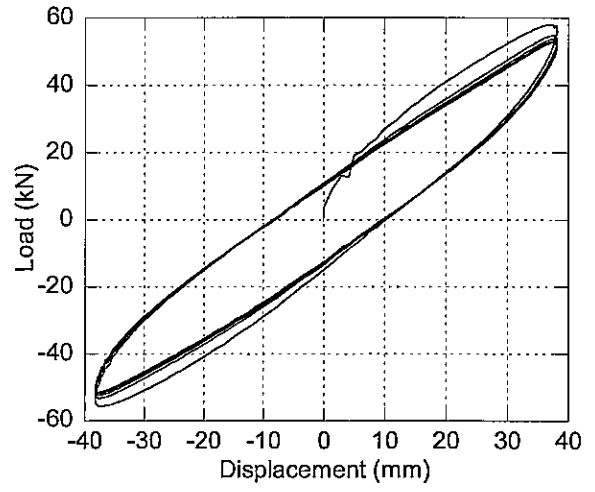


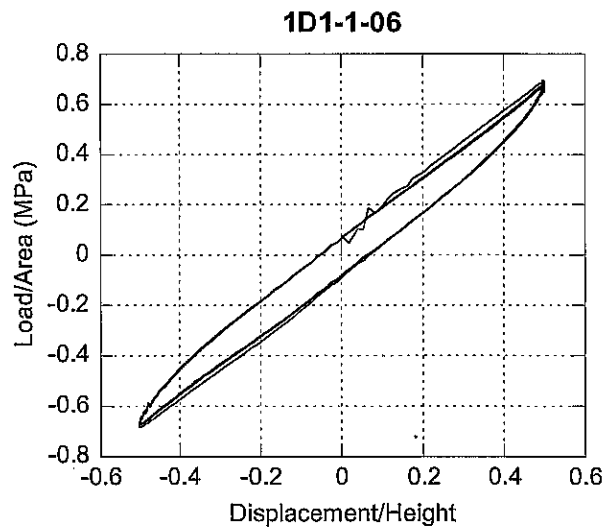
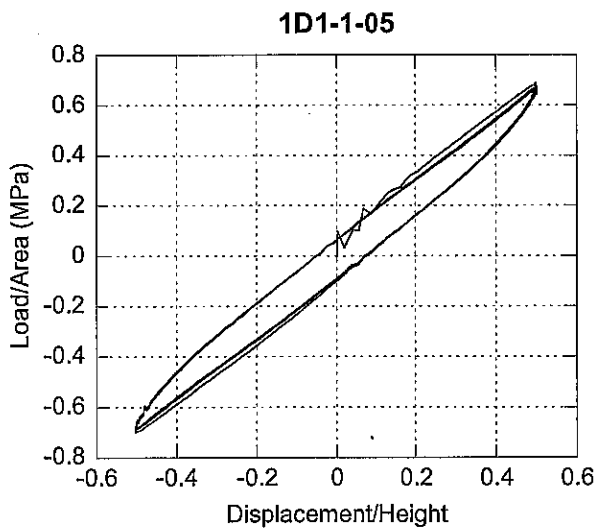
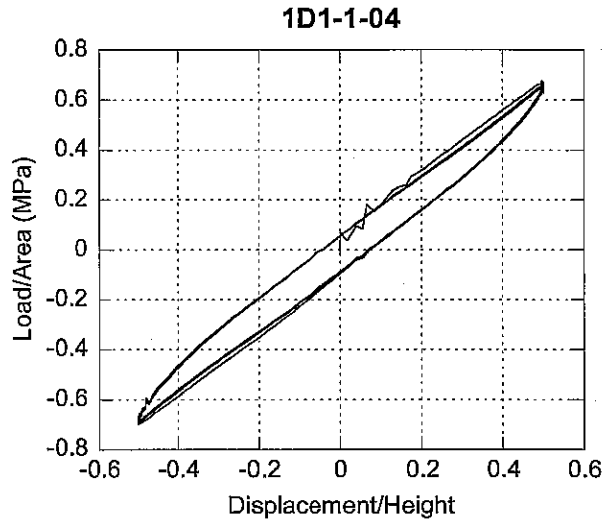
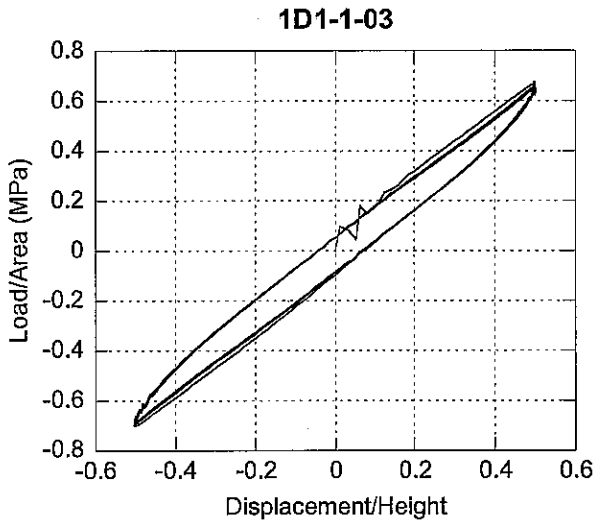
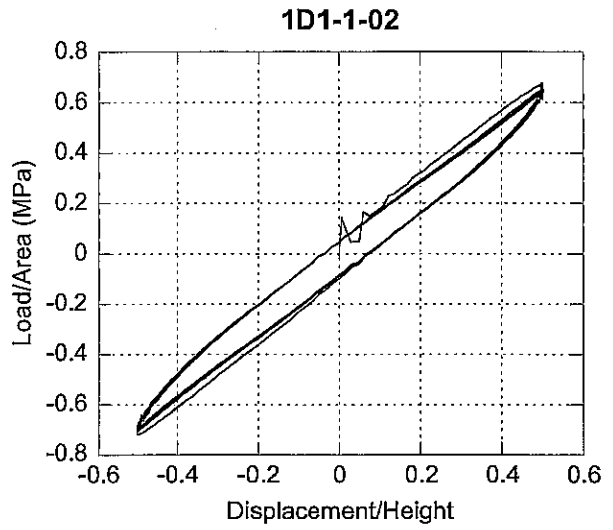
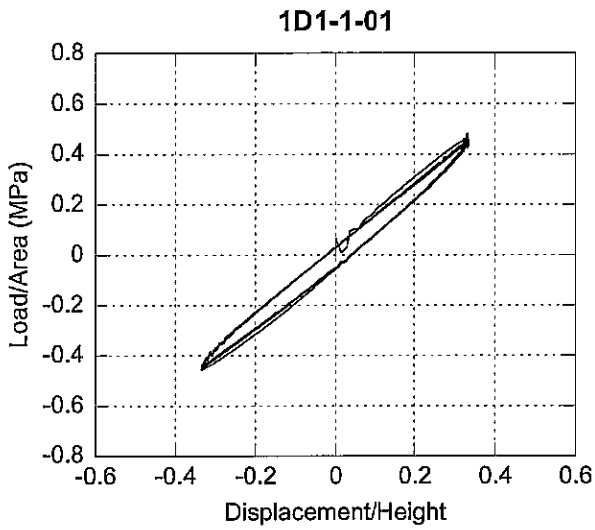


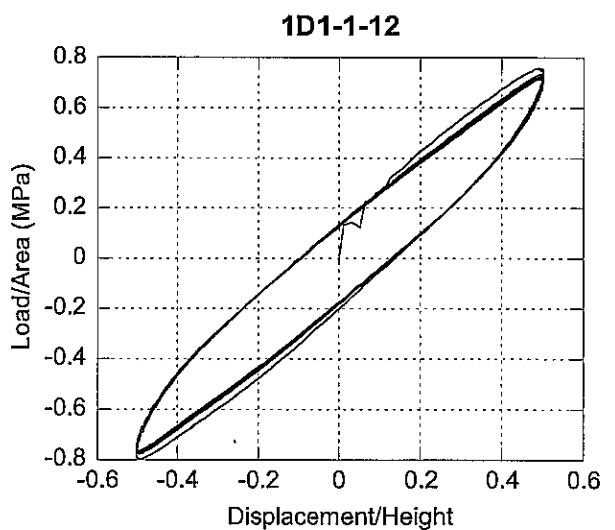
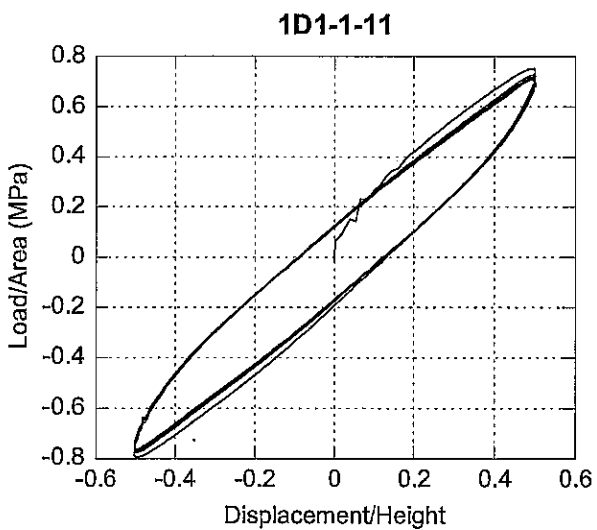
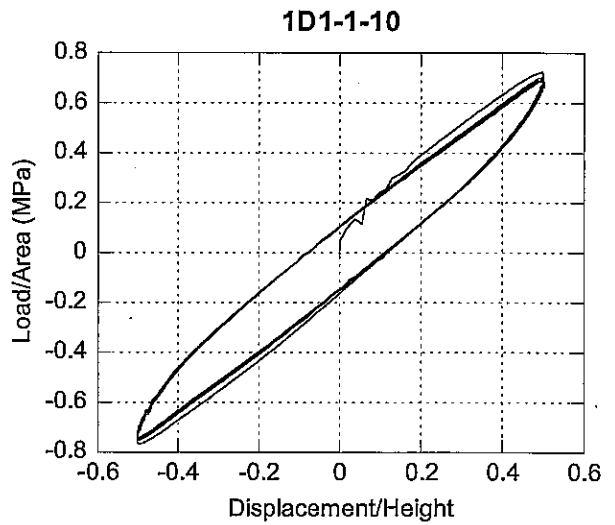
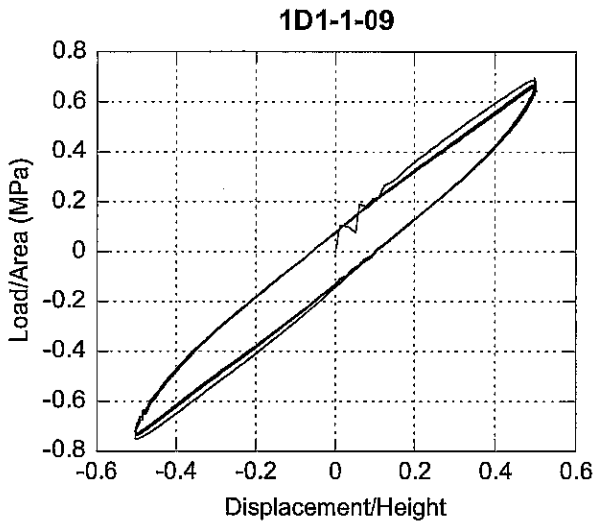
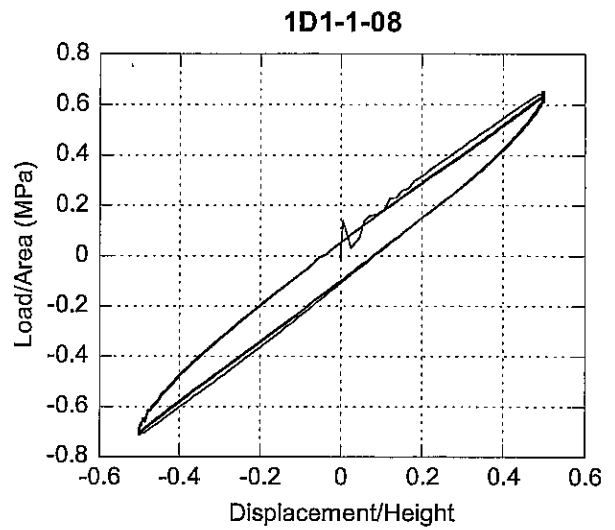
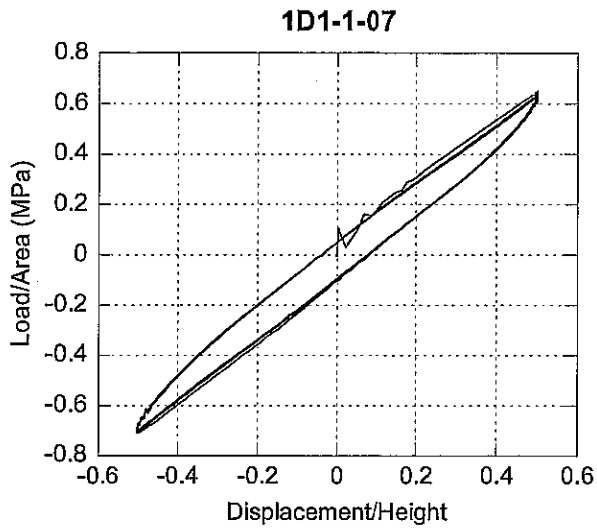
1D2-1-13



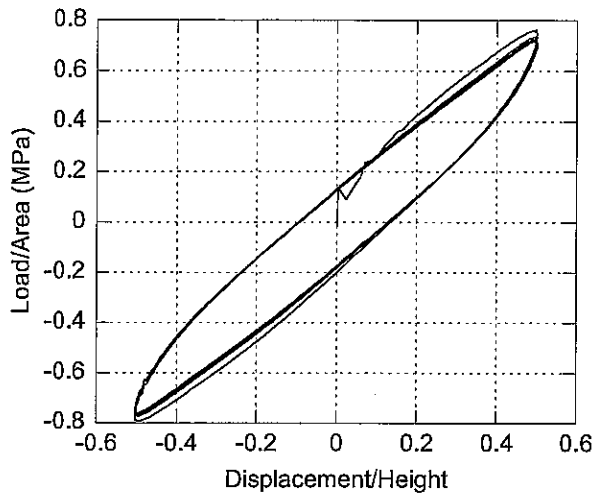
1D2-1-14

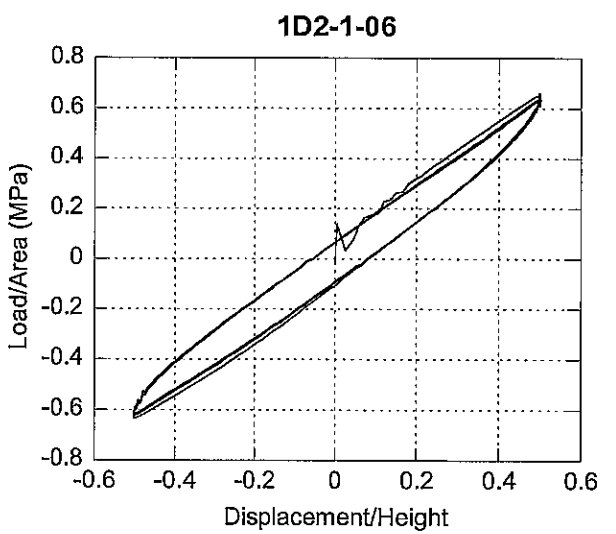
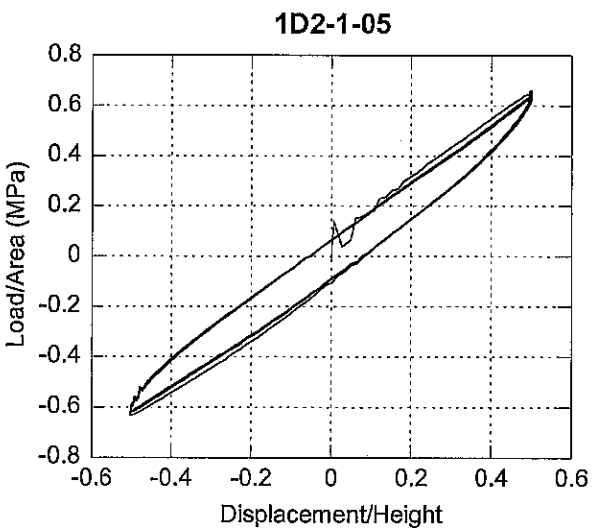
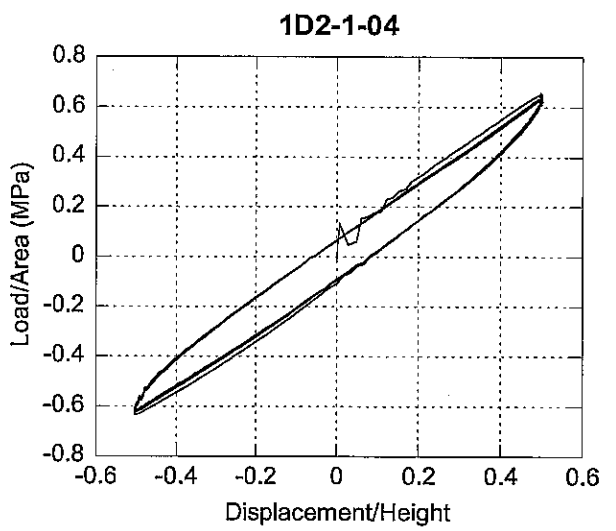
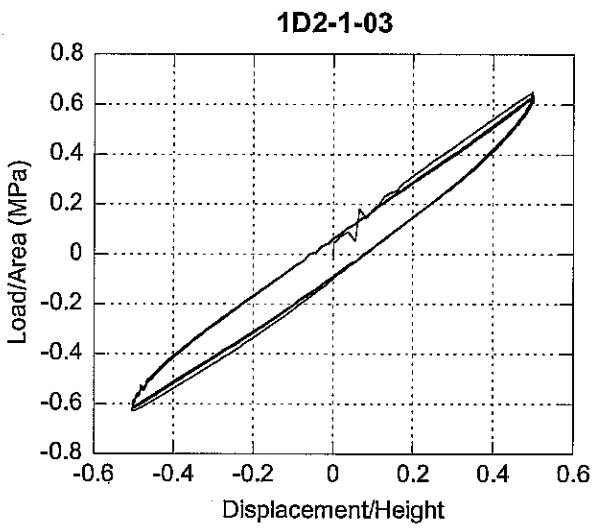
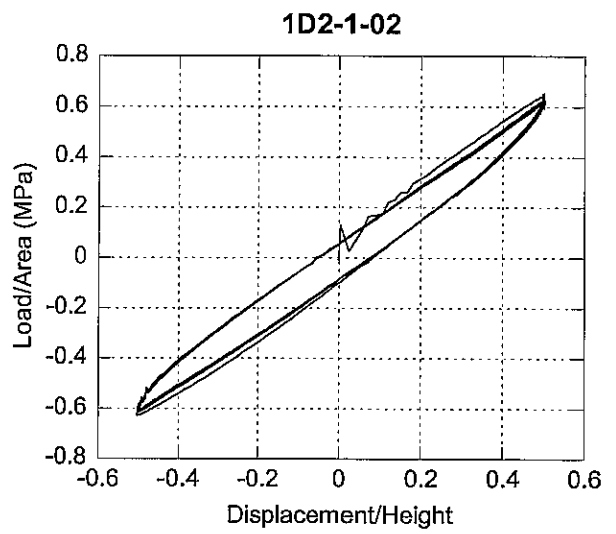
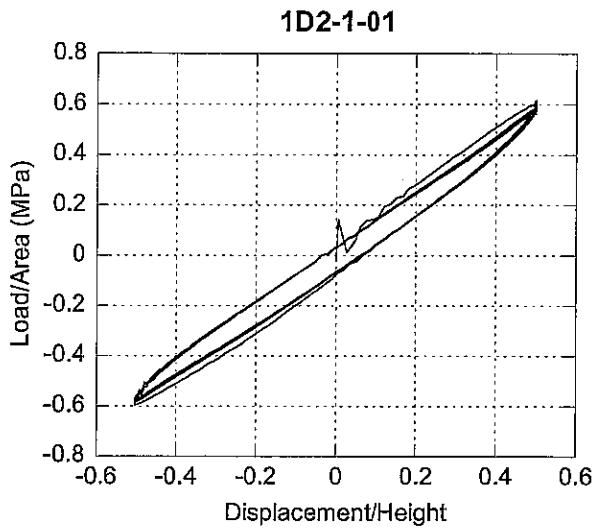


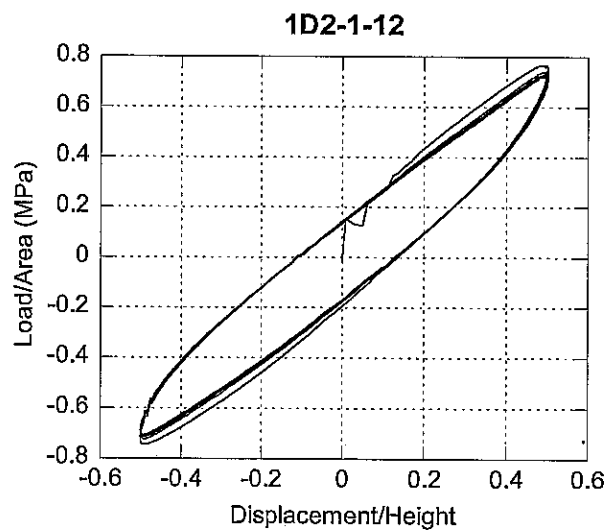
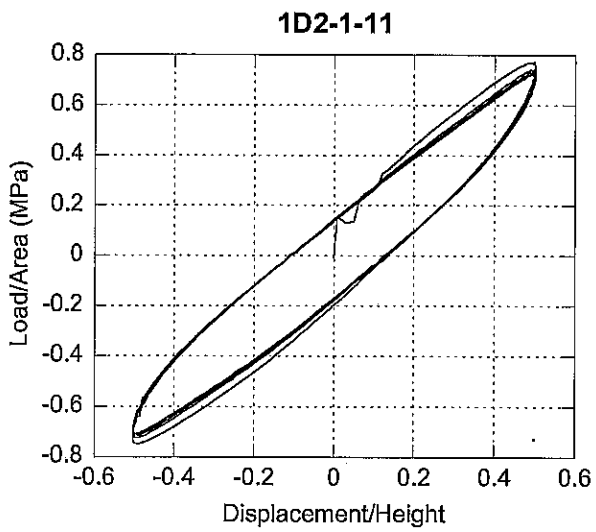
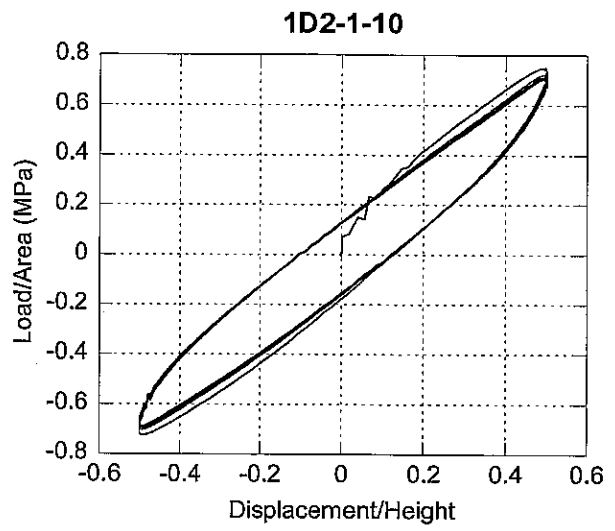
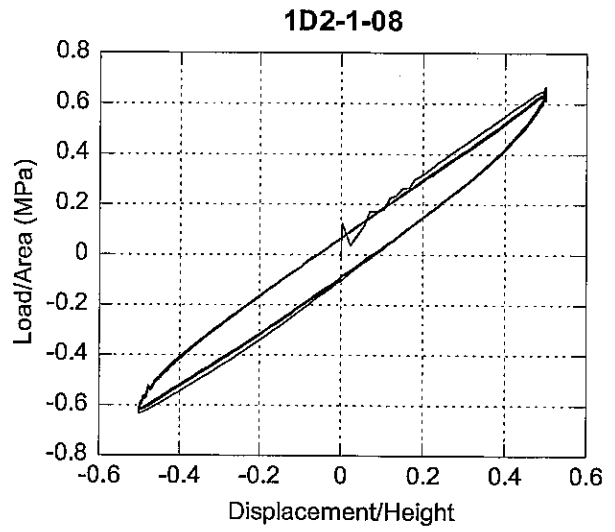
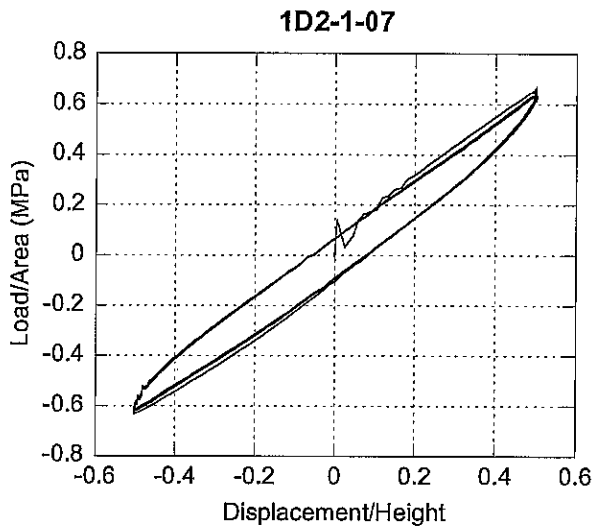




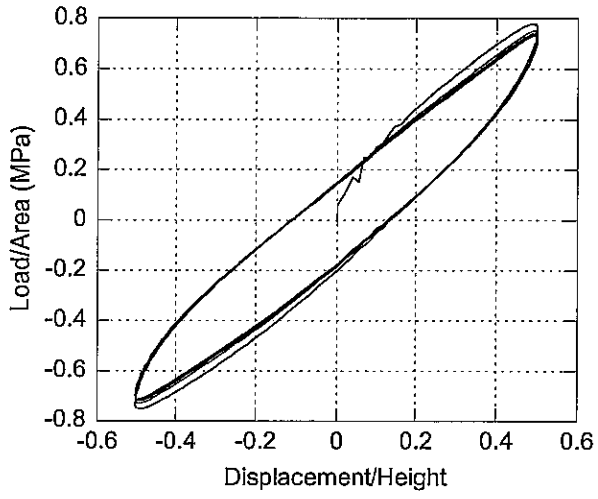
1D1-1-13

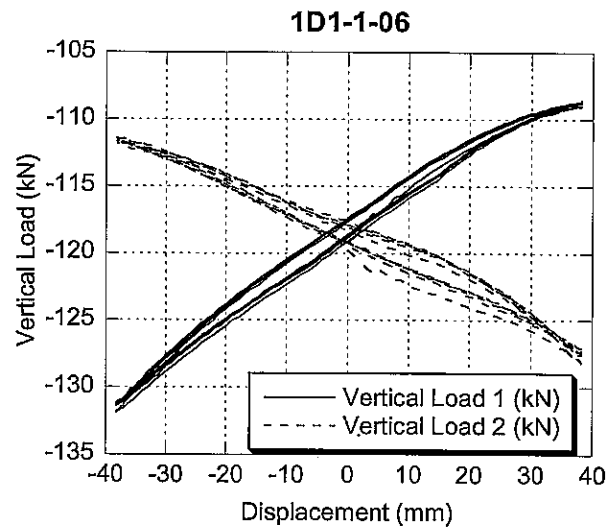
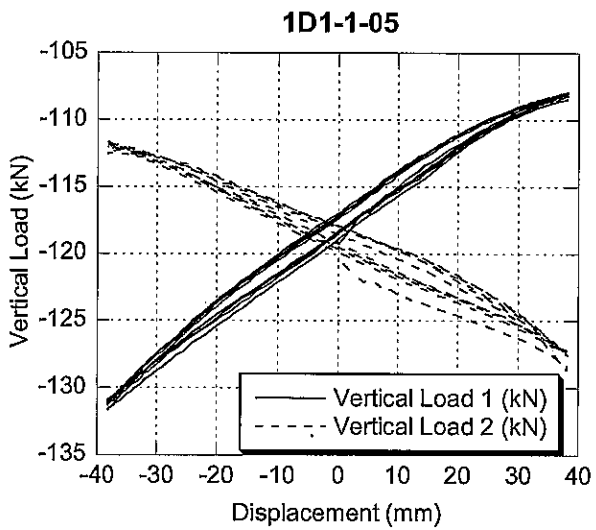
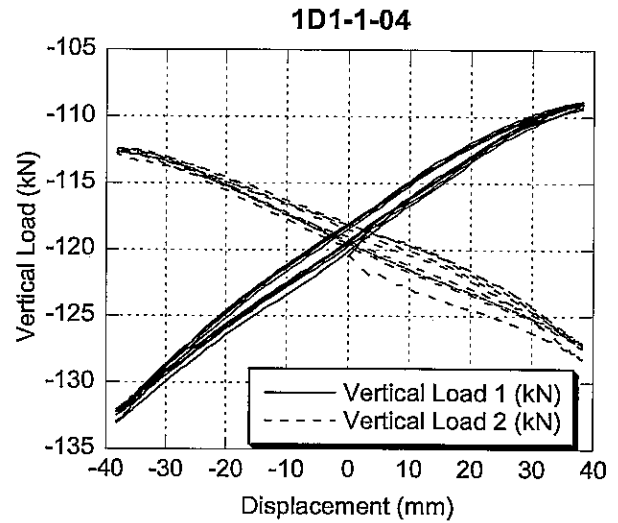
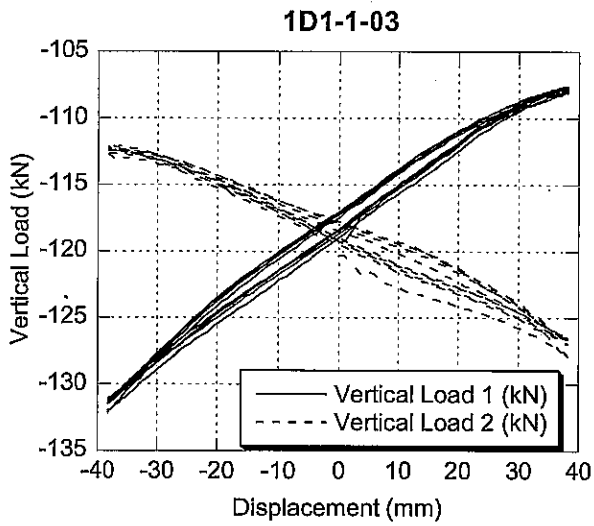
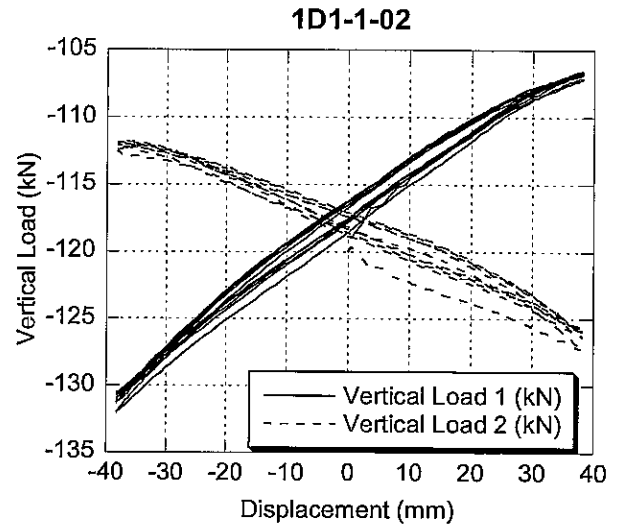
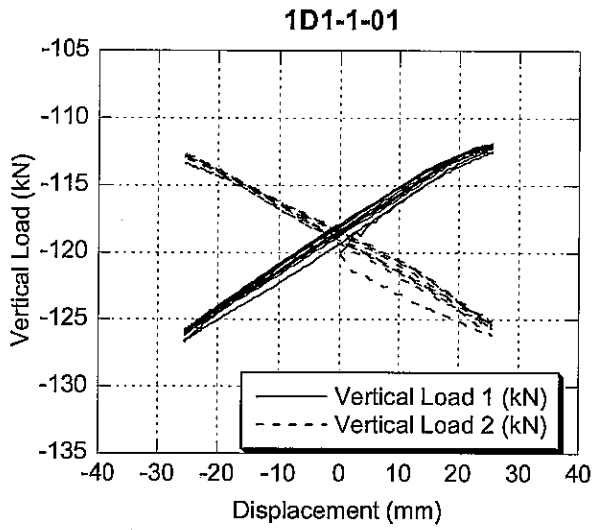


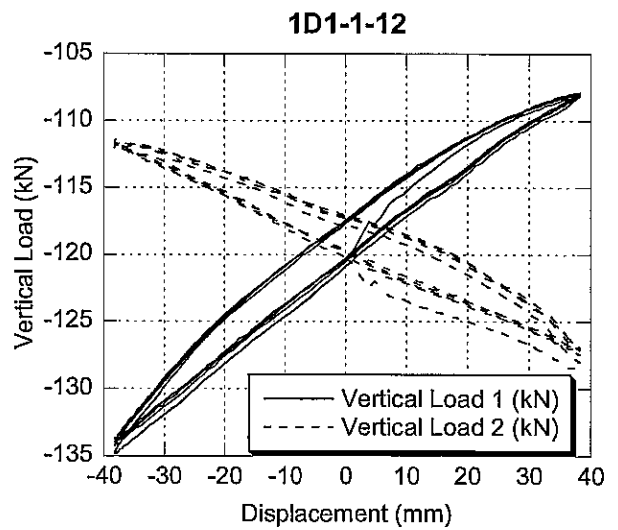
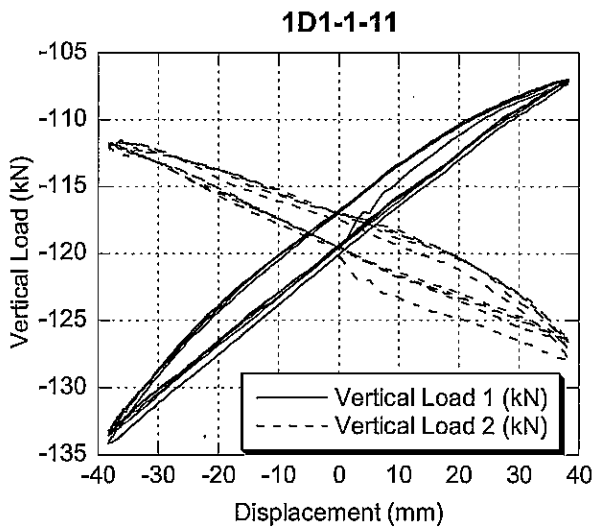
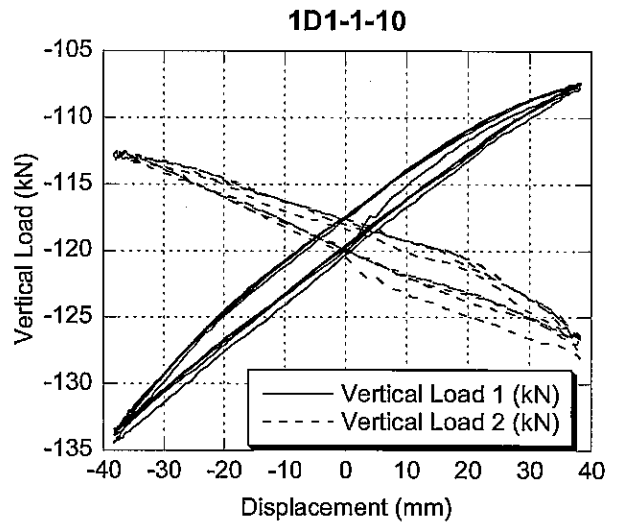
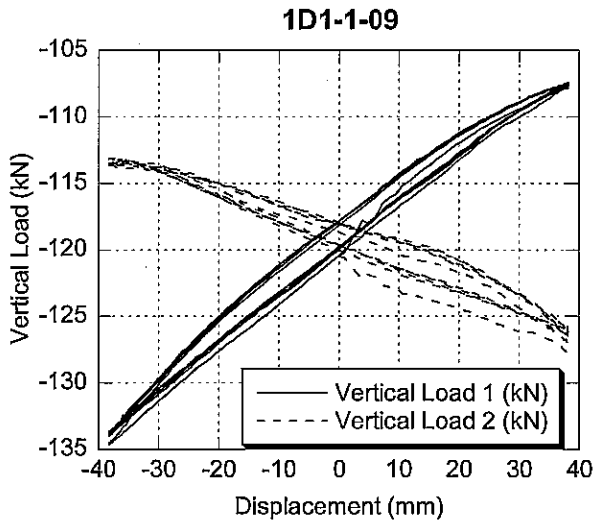
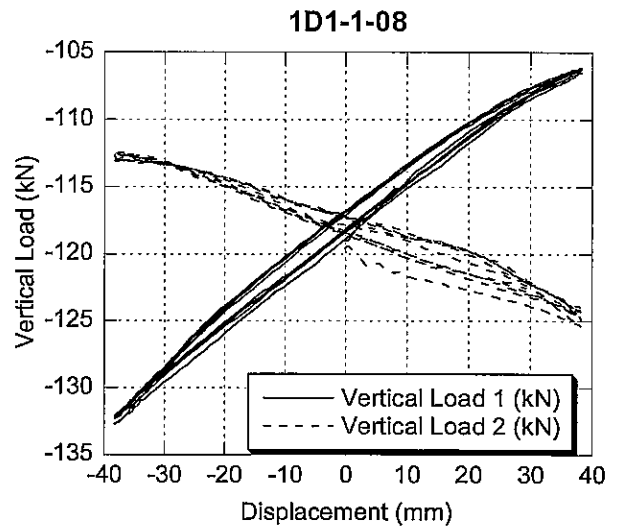
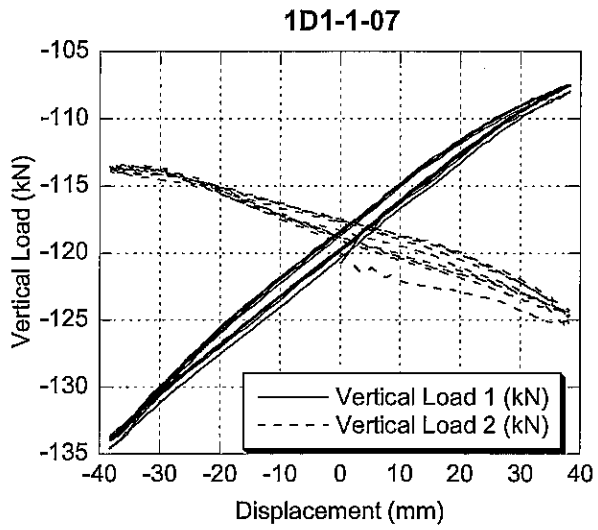




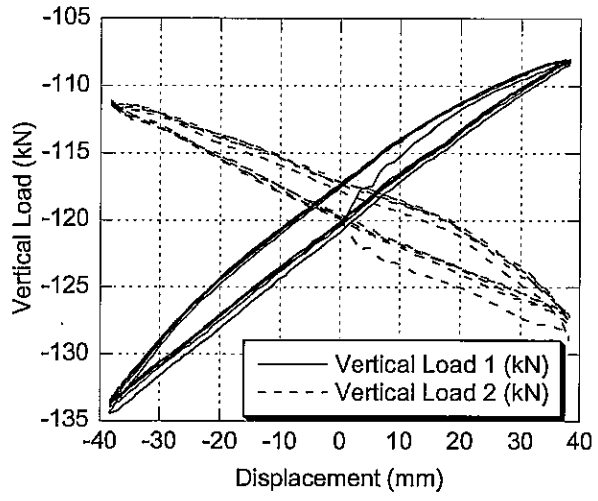
1D2-1-13

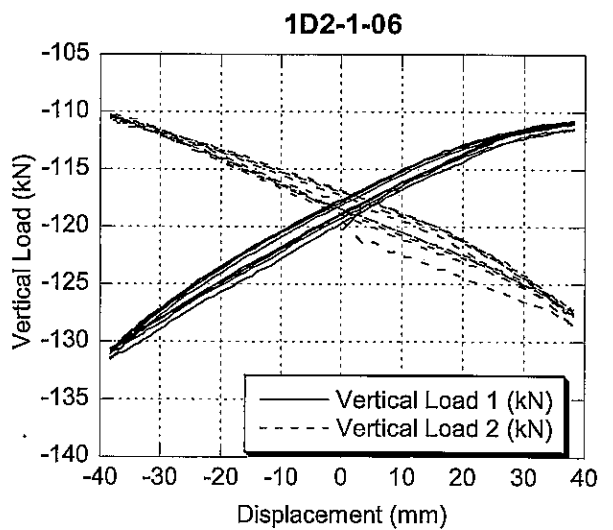
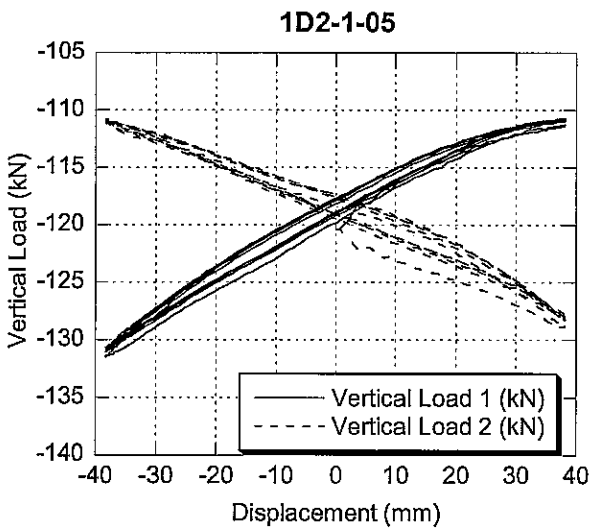
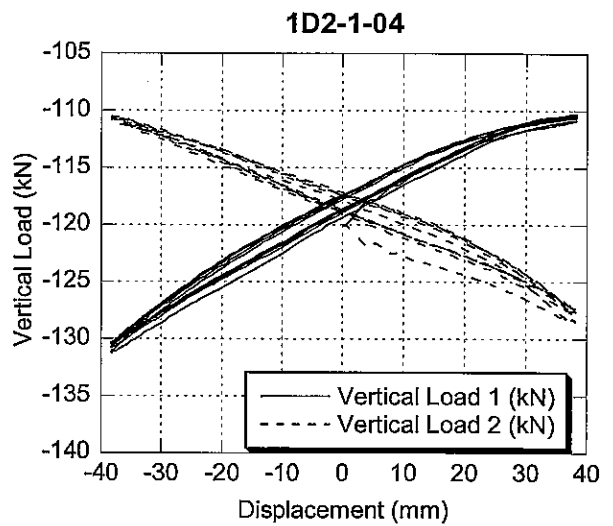
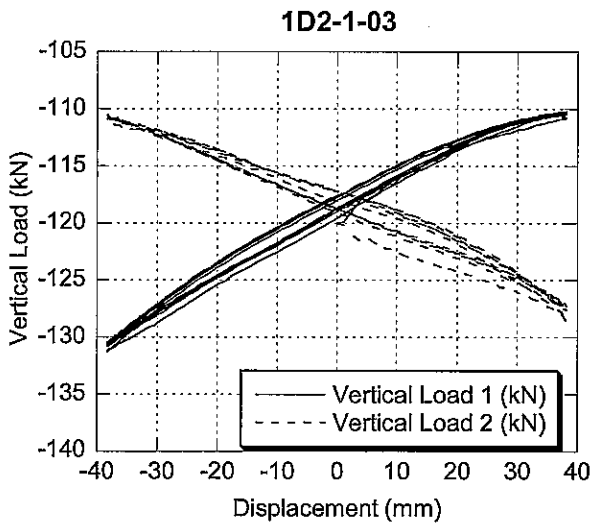
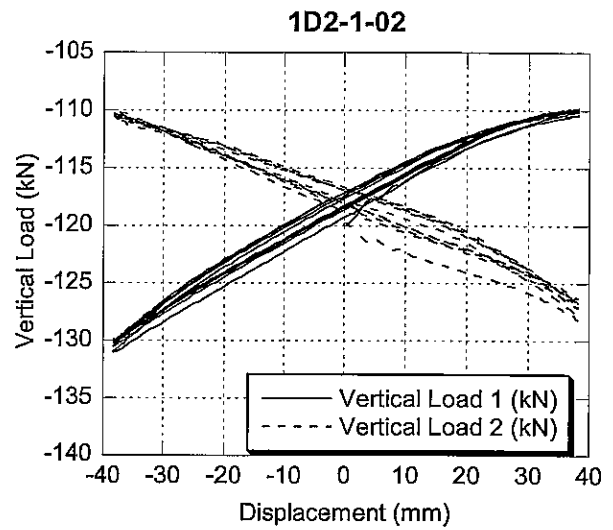
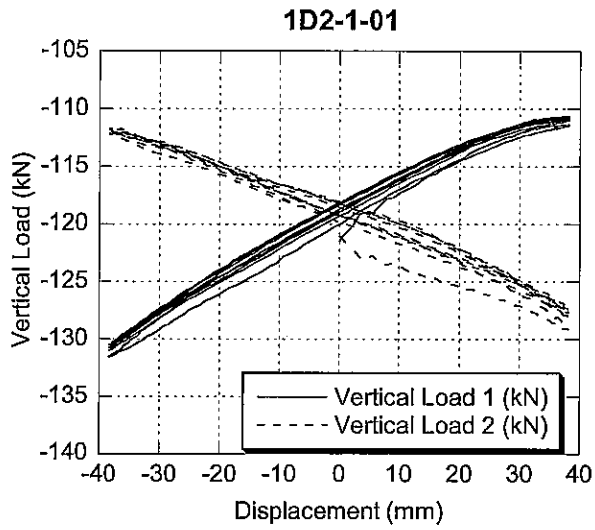




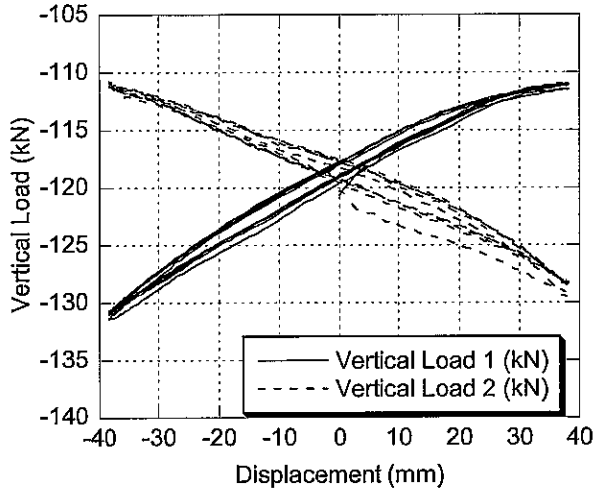


1D1-1-13

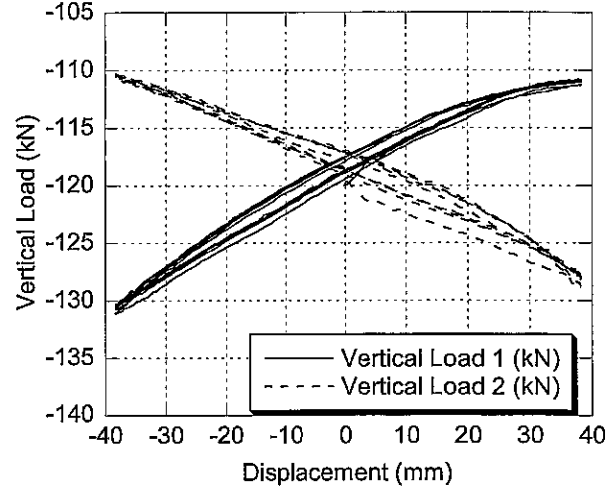




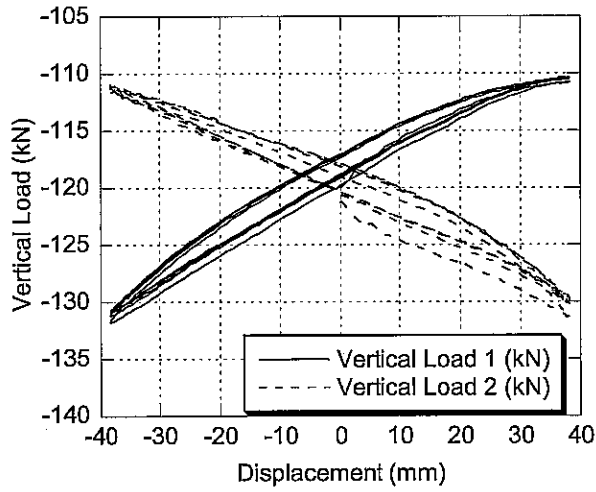
1D2-1-07



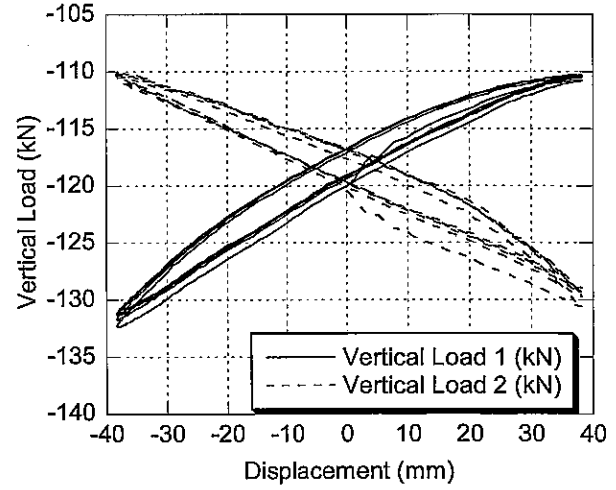
1D2-1-08



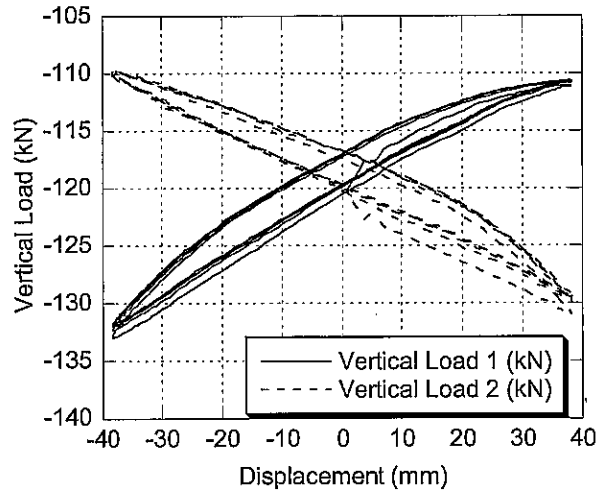
1D2-1-09



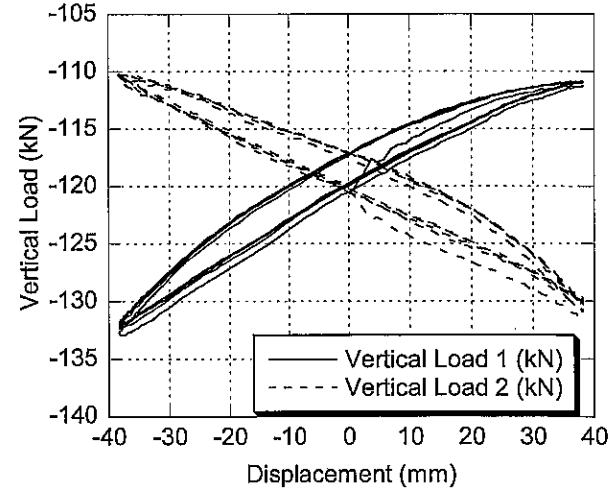
1D2-1-10



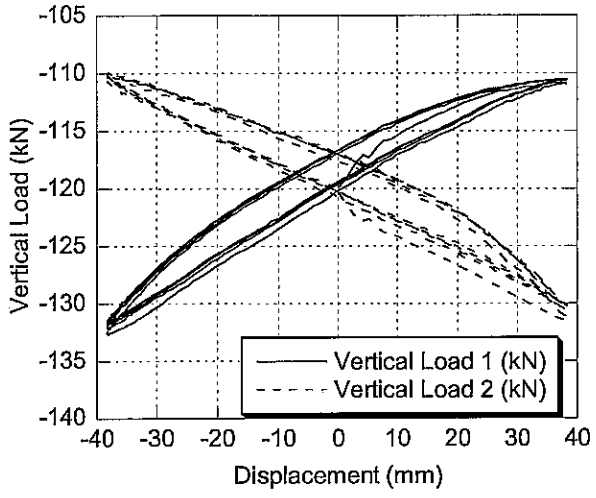
1D2-1-11



1D2-1-12



1D2-1-13



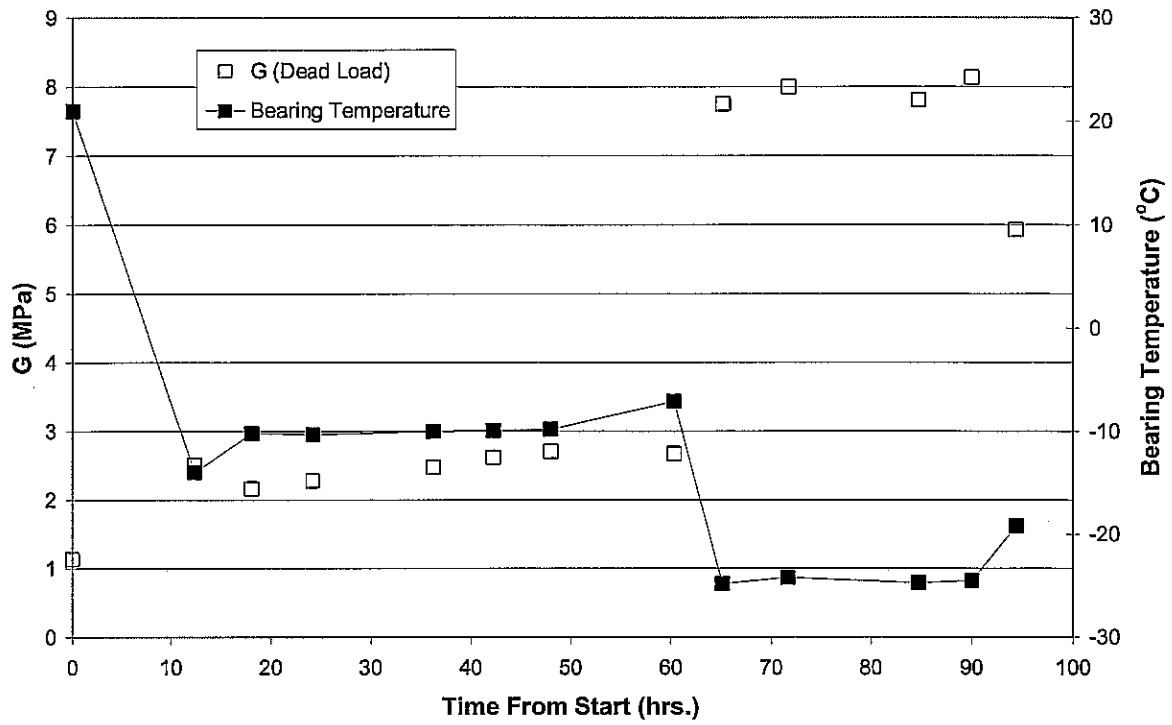
**APPENDIX E**

**Test Results for 2S1**

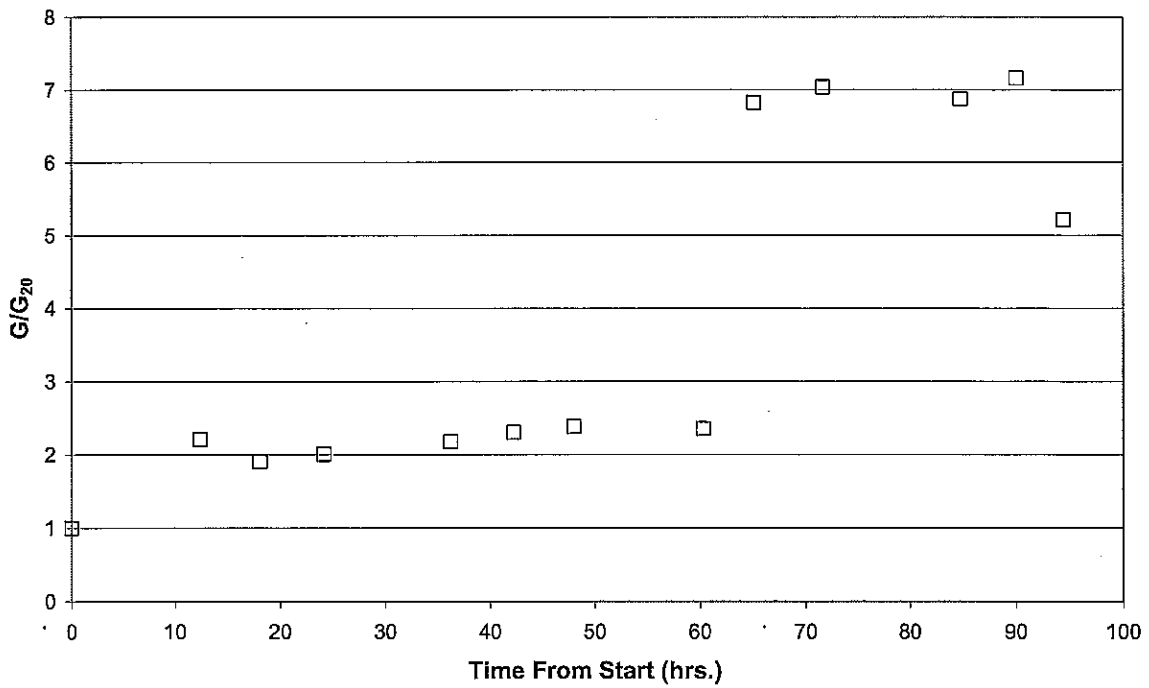
### Appendix E – Test Results for 2S1

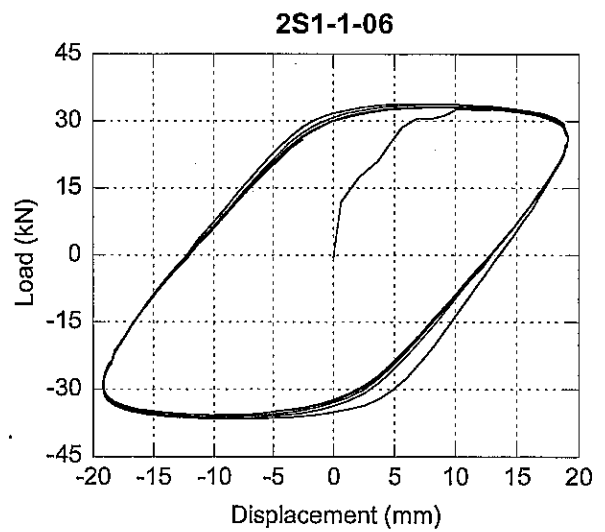
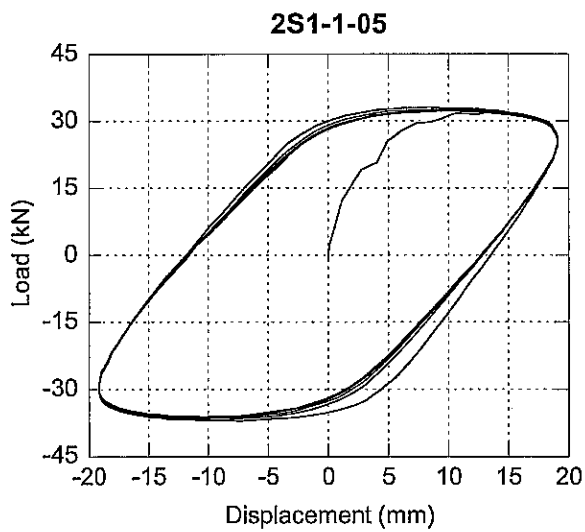
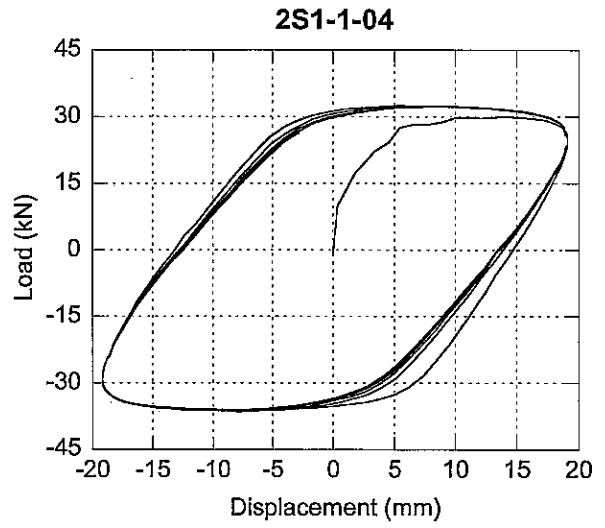
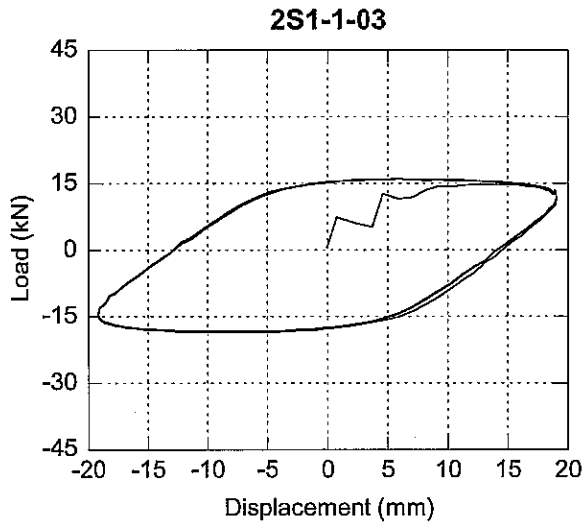
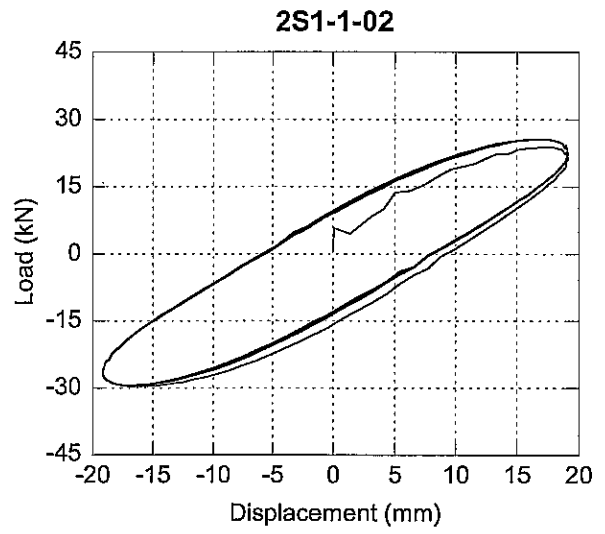
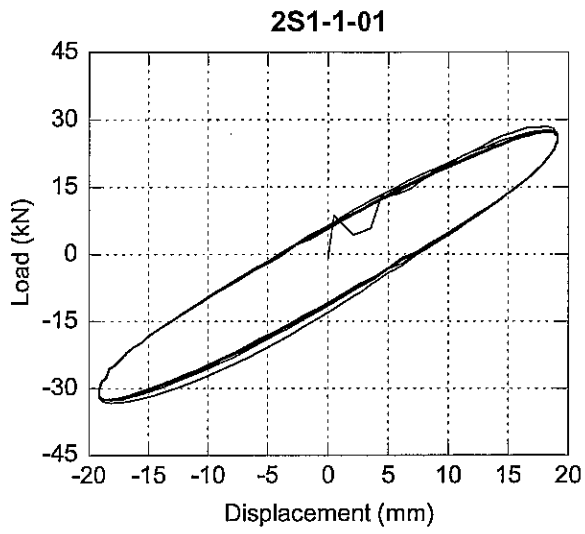
Report Reference	Date & Time	Time From Start, hrs.	Brg. Temp. °C	Vert. Load		Amp.		Freq. hz.
				psi	MPa	in	mm	
2S1-1-01	7/28/01 20:00	0.00	21	750	5.17	0.75	19.05	1
2S1-1-02	7/28/01 20:00	0.00	21	500	3.45	0.75	19.05	1
2S1-1-03	7/28/01 20:00	0.00	21	250	1.72	0.75	19.05	1
2S1-1-04	7/29/01 8:25	12.42	-14	500	3.45	0.75	19.05	1
2S1-1-05	7/29/01 14:06	18.10	-10.2	500	3.45	0.75	19.05	1
2S1-1-06	7/29/01 20:12	24.20	-10.3	500	3.45	0.75	19.05	1
2S1-1-07	7/30/01 8:16	36.27	-10	500	3.45	0.75	19.05	1
2S1-1-08	7/30/01 14:17	42.28	-9.9	500	3.45	0.75	19.05	1
2S1-1-09	7/30/01 20:00	48.00	-9.8	500	3.45	0.75	19.05	1
2S1-1-10	7/31/01 8:20	60.33	-7.1	500	3.45	0.75	19.05	1
2S1-1-11	7/31/01 13:08	65.13	-24.8	500	3.45	0.75	19.05	1
2S1-1-12	7/31/01 19:40	71.67	-24.2	500	3.45	0.75	19.05	1
2S1-1-13	8/1/01 8:48	84.80	-24.7	500	3.45	0.75	19.05	1
2S1-1-14	8/1/01 14:04	90.07	-24.5	500	3.45	0.75	19.05	1
2S1-1-15	8/1/01 18:15	94.25	-20.5	750	5.17	0.75	19.05	1
2S1-1-16	8/1/01 18:27	94.45	-19.2	500	3.45	0.75	19.05	1
2S1-1-17	8/1/01 16:40	92.67	-18.8	250	1.72	0.75	19.05	1

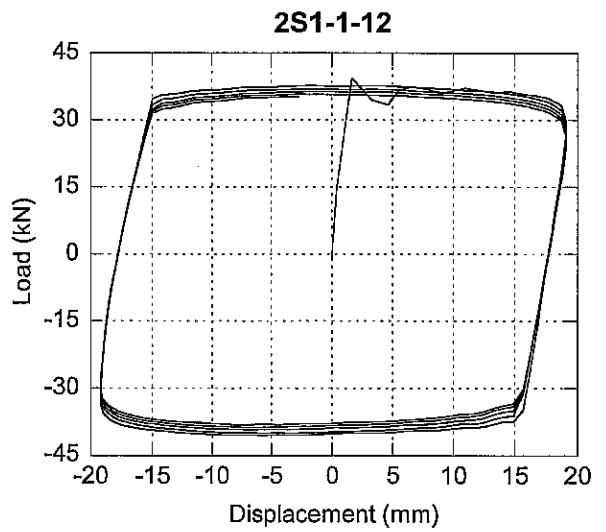
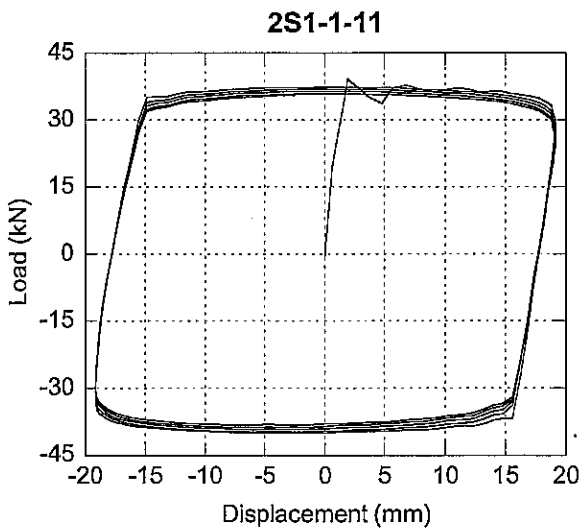
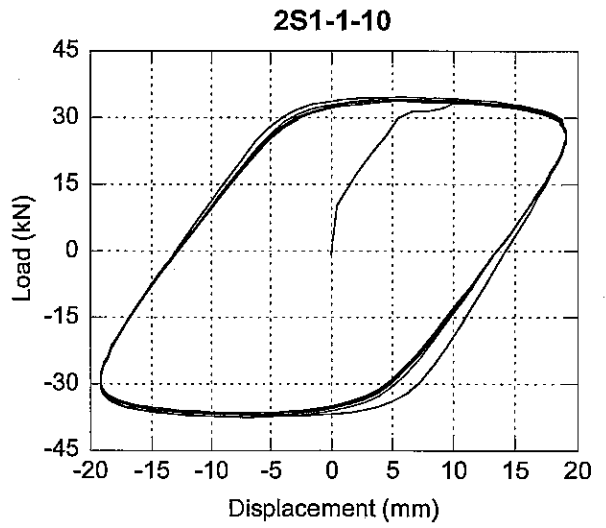
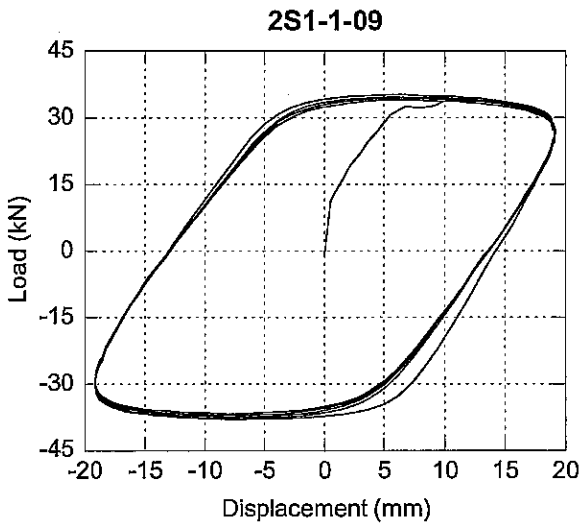
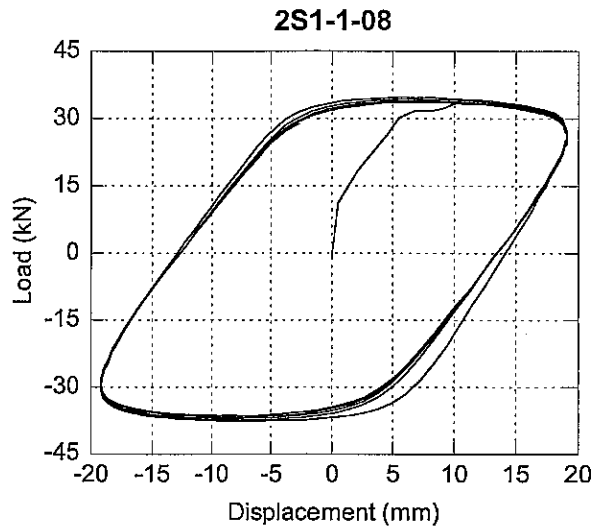
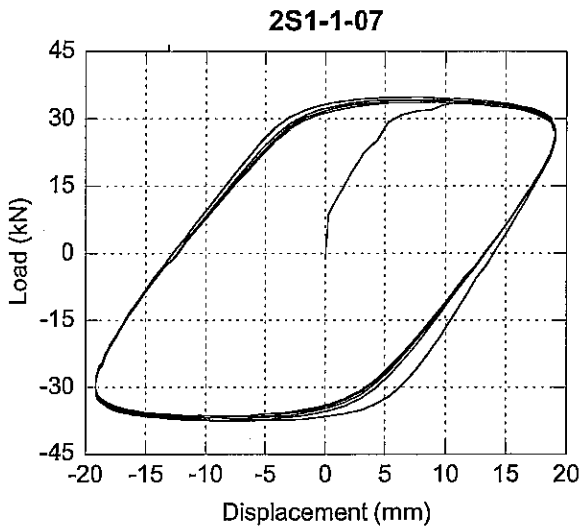
### Shear Modulus Summary - 2S1-1



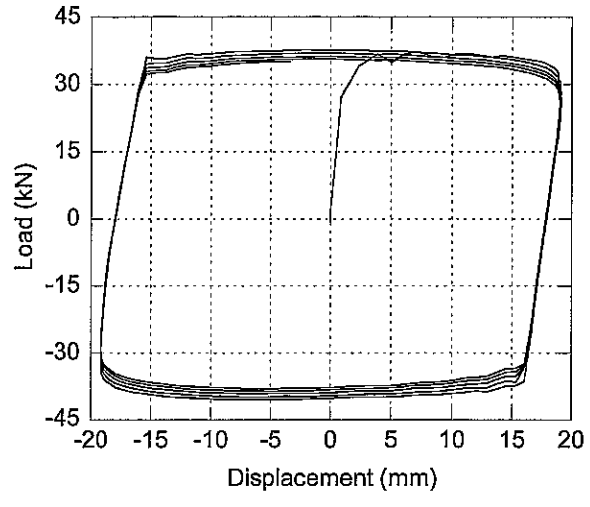
### Normalized Shear Modulus - 2S1-1



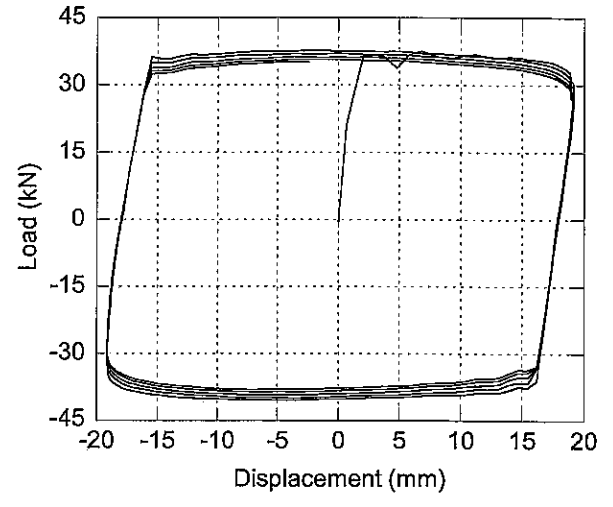




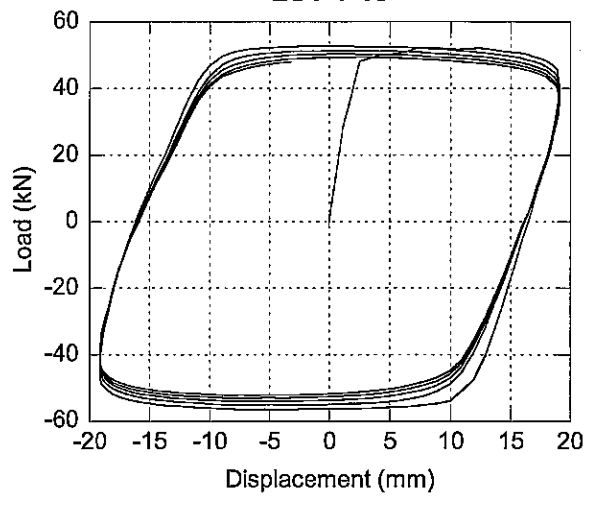
**2S1-1-13**



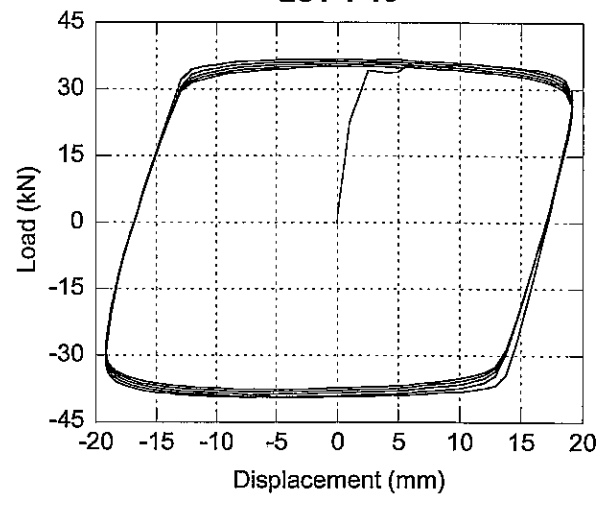
**2S1-1-14**



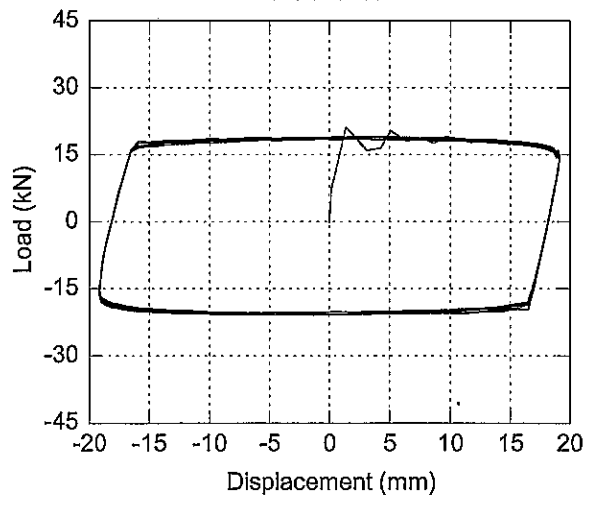
**2S1-1-15**



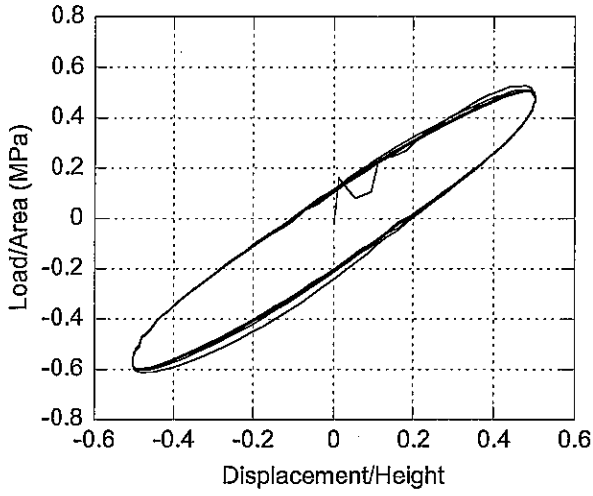
**2S1-1-16**



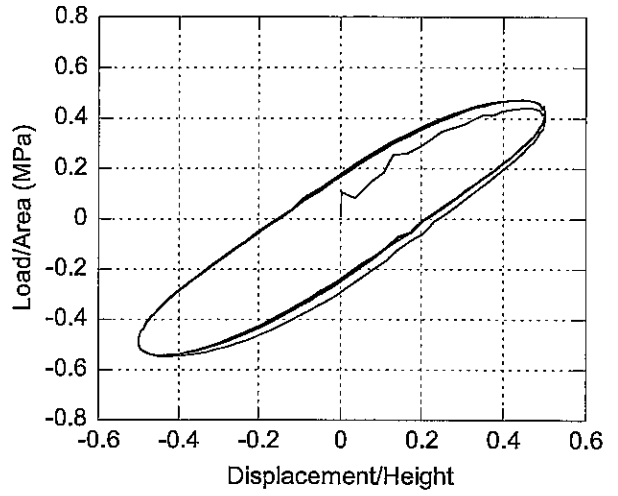
**2S1-1-17**



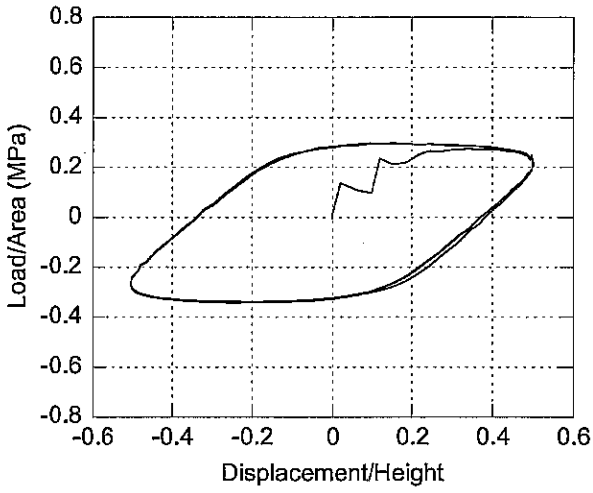
**2S1-1-01**



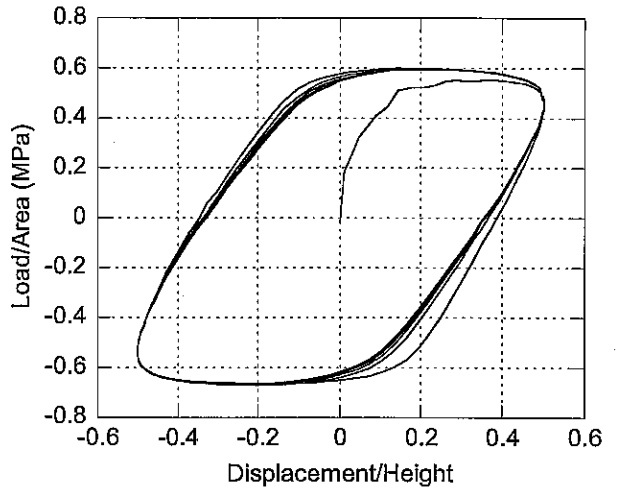
**2S1-1-02**



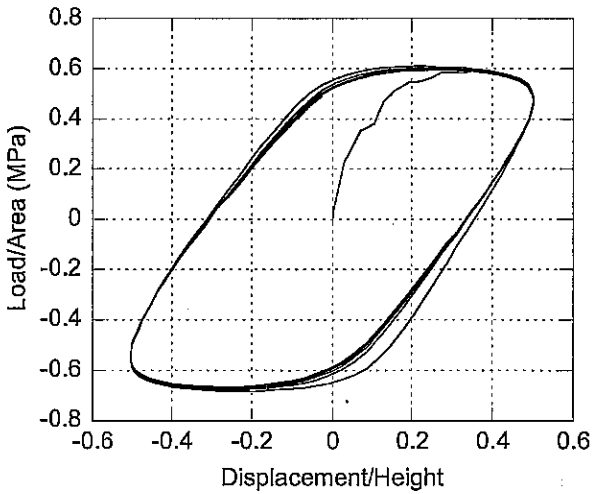
**2S1-1-03**



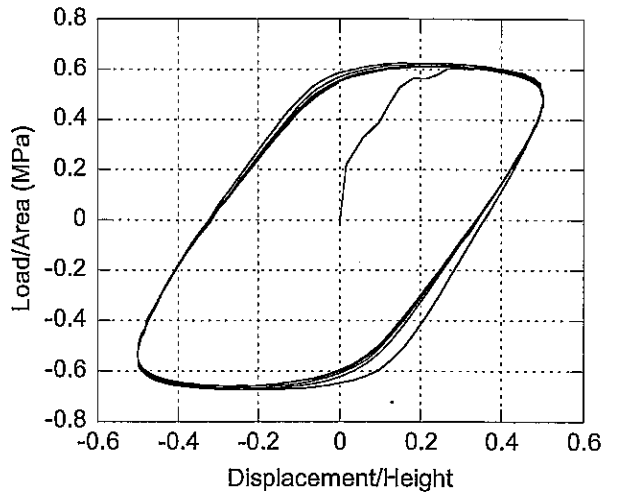
**2S1-1-04**

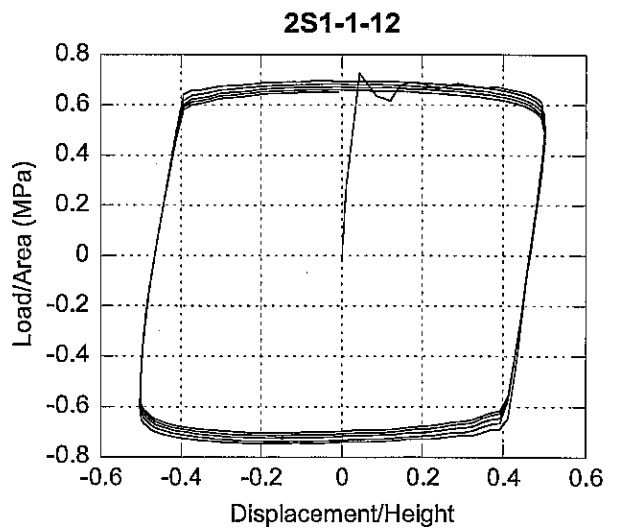
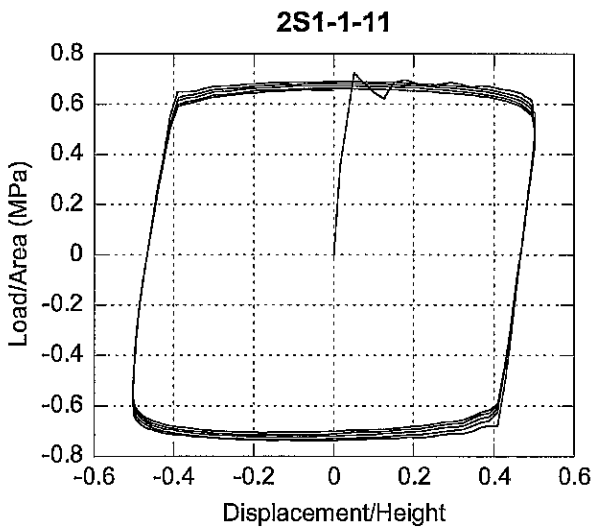
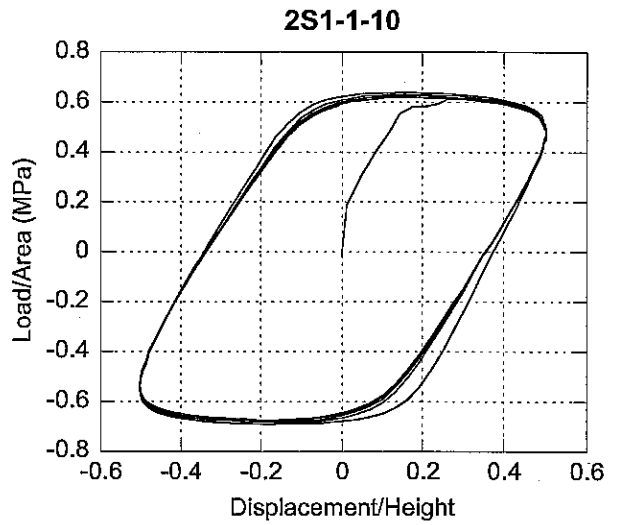
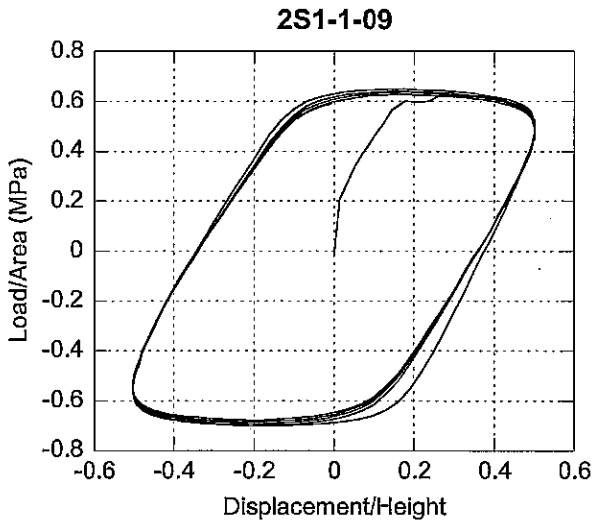
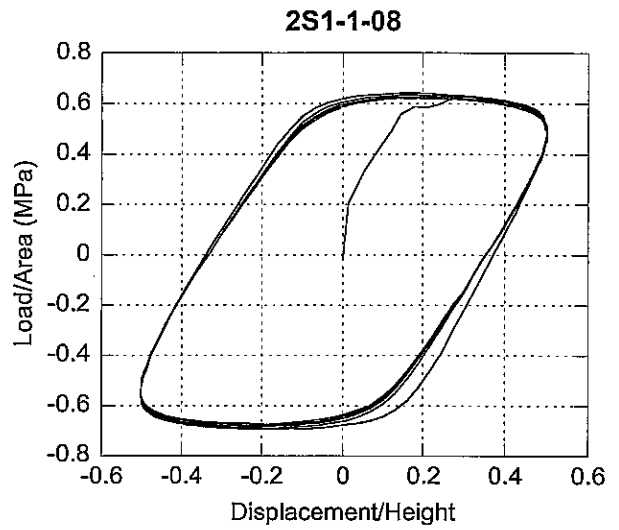
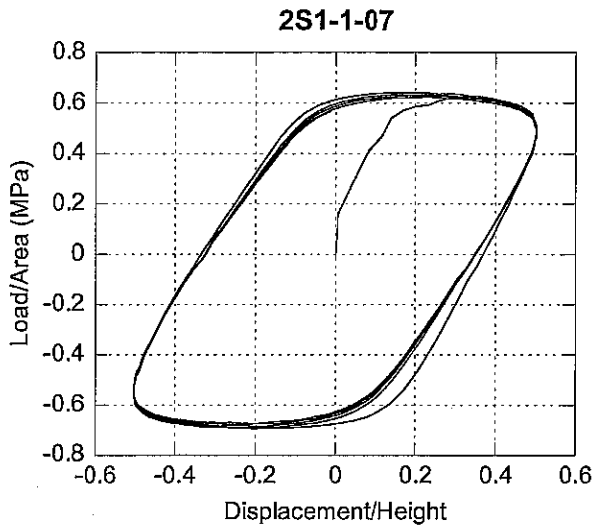


**2S1-1-05**

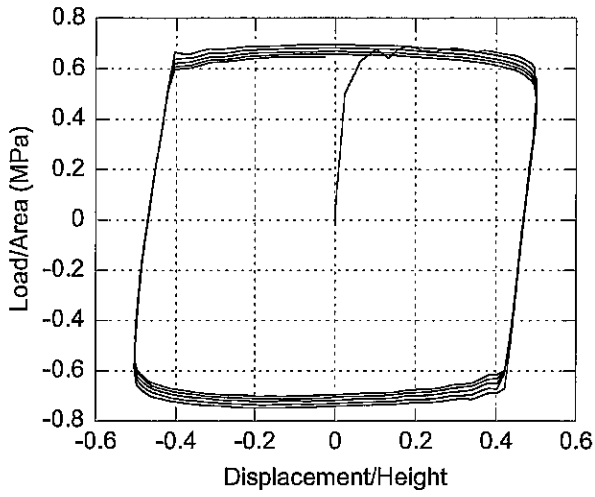


**2S1-1-06**

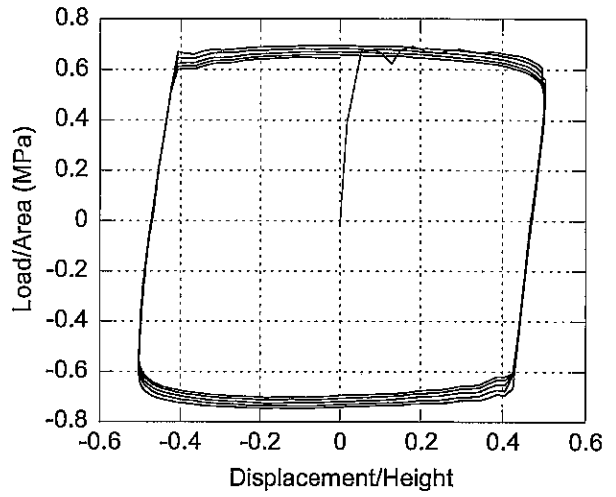




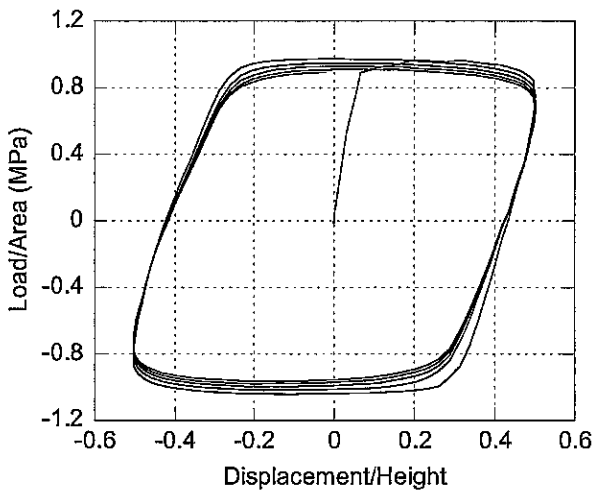
**2S1-1-13**



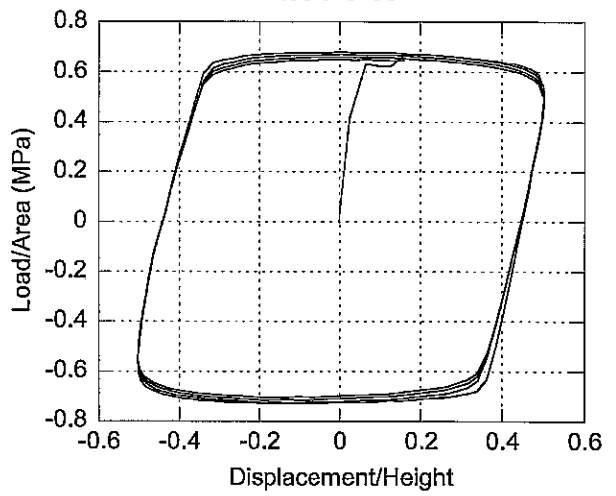
**2S1-1-14**



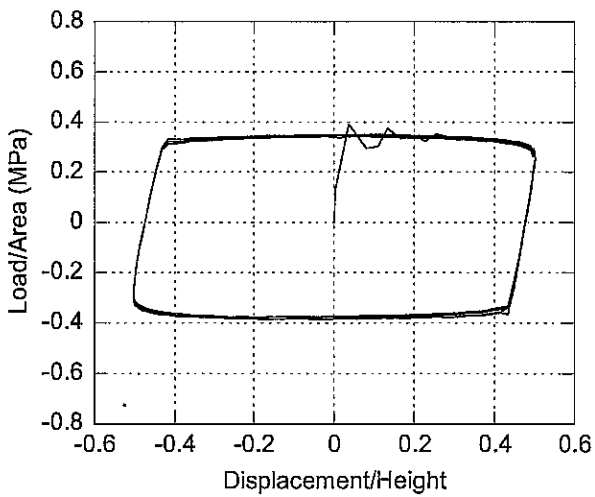
**2S1-1-15**

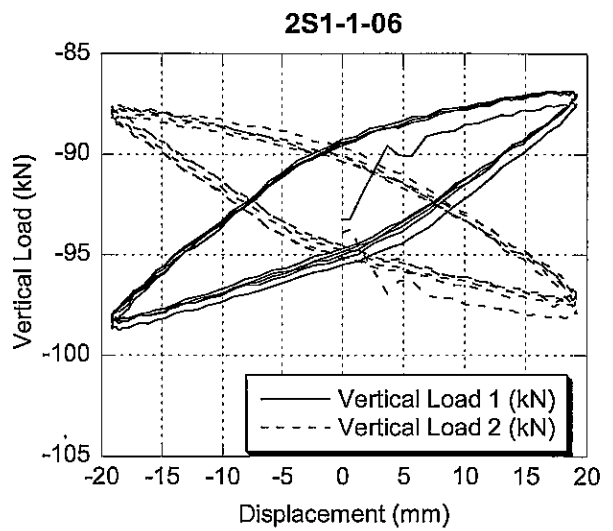
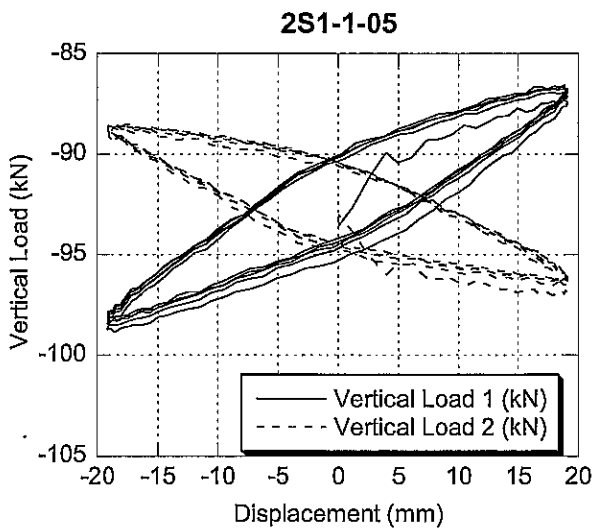
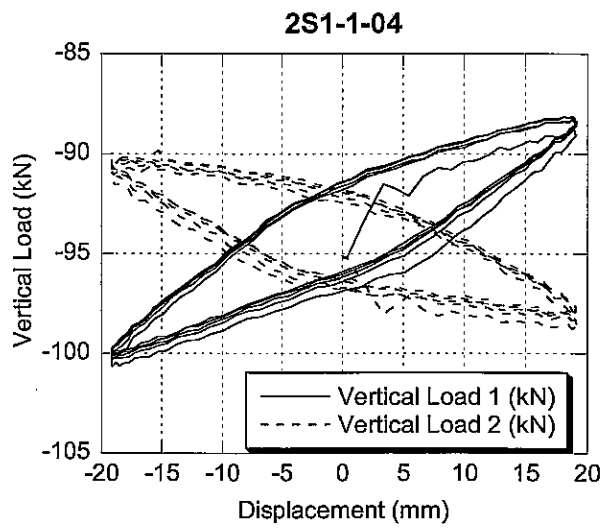
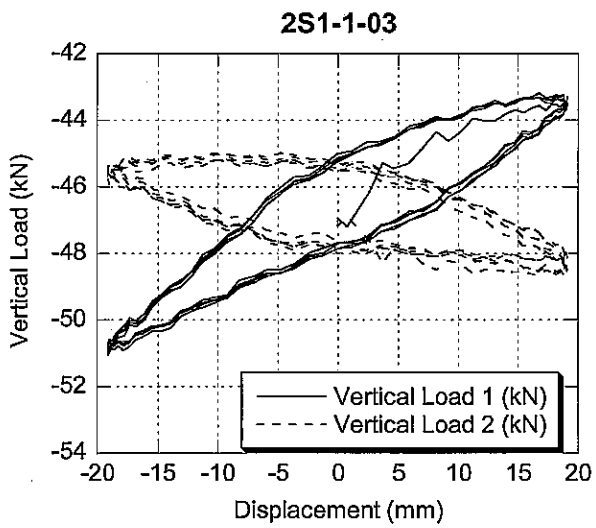
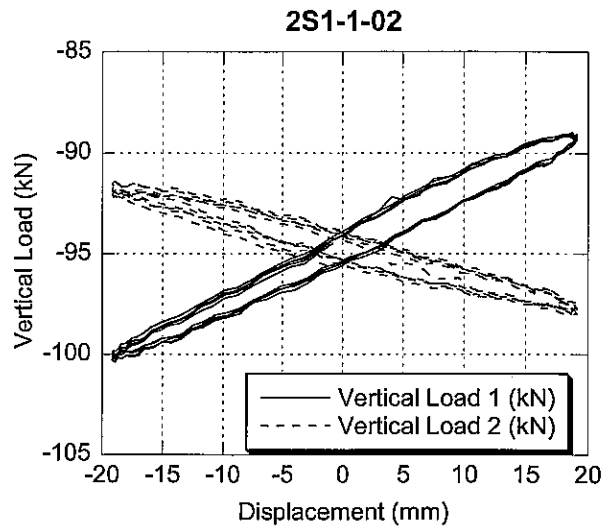
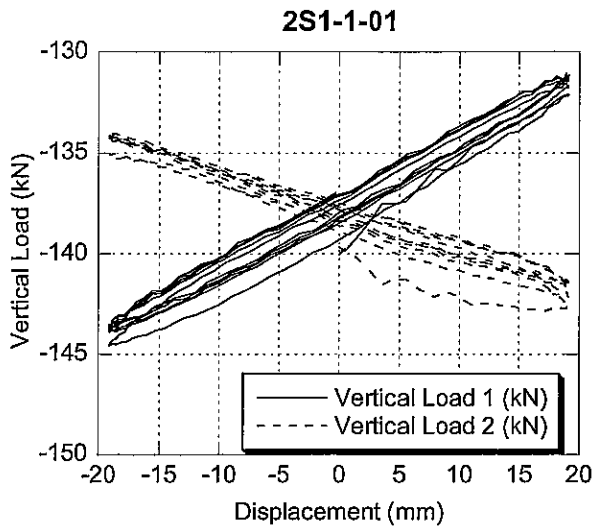


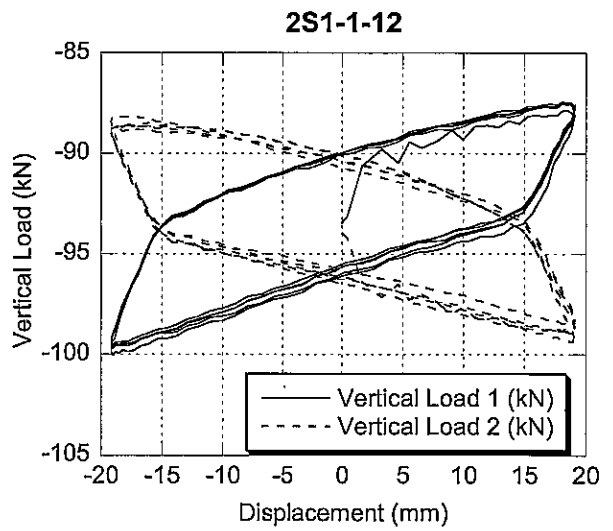
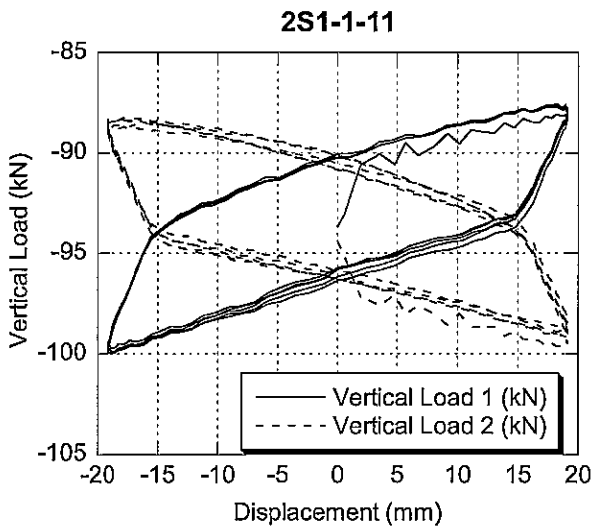
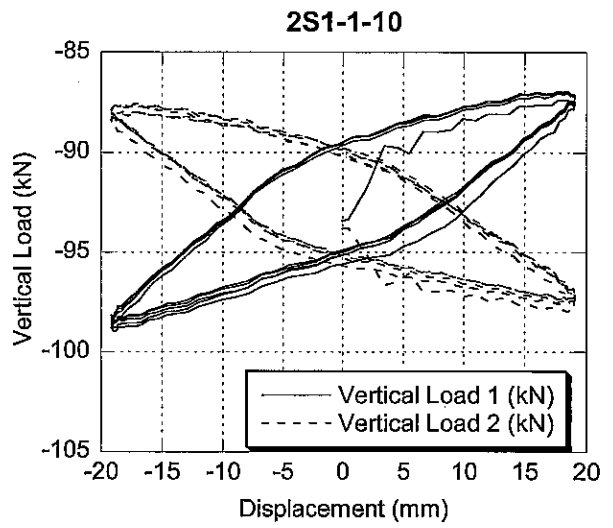
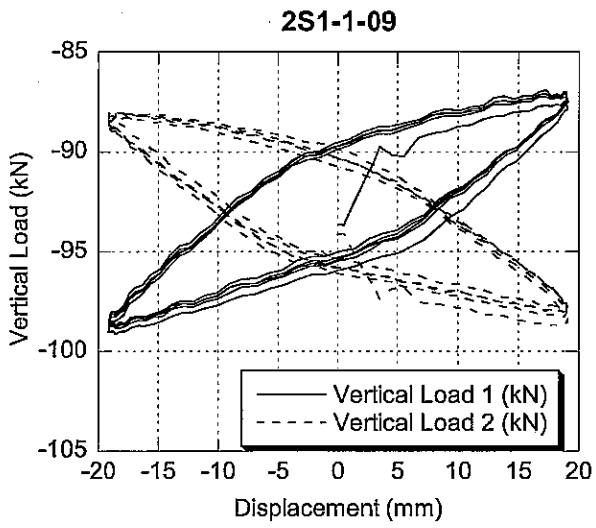
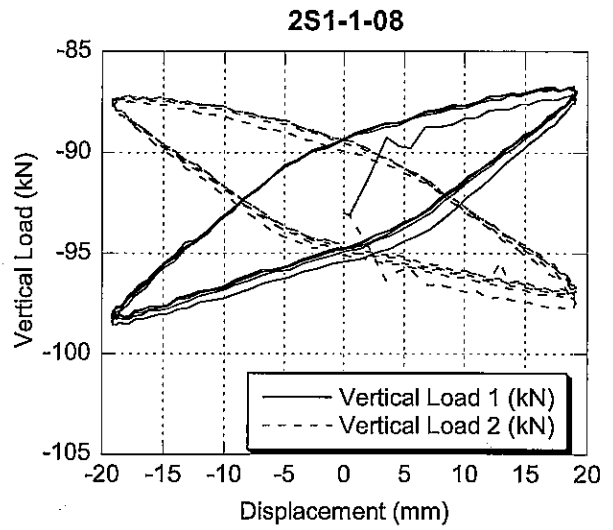
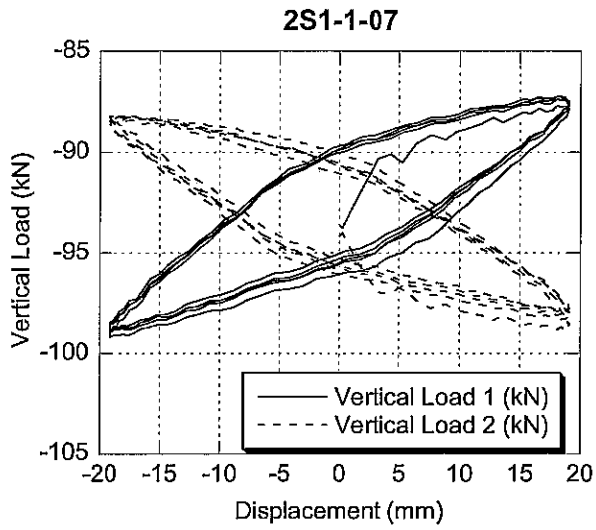
**2S1-1-16**



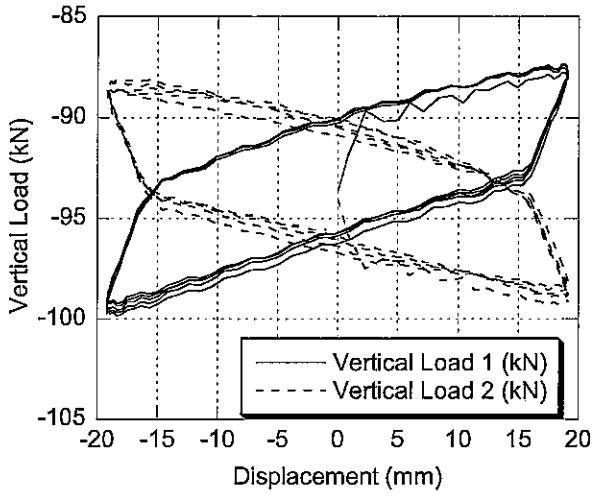
**2S1-1-17**



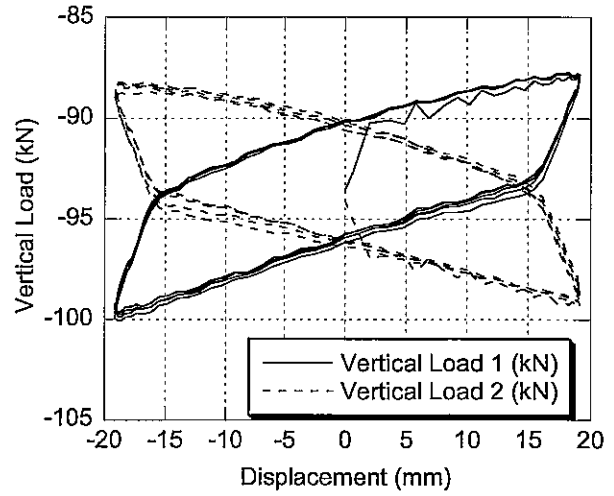




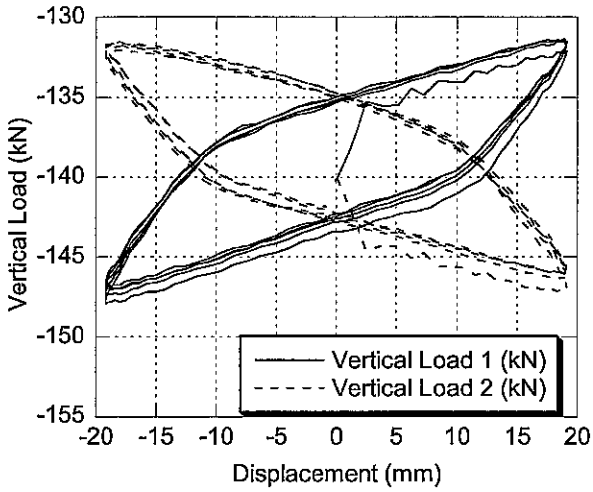
2S1-1-13



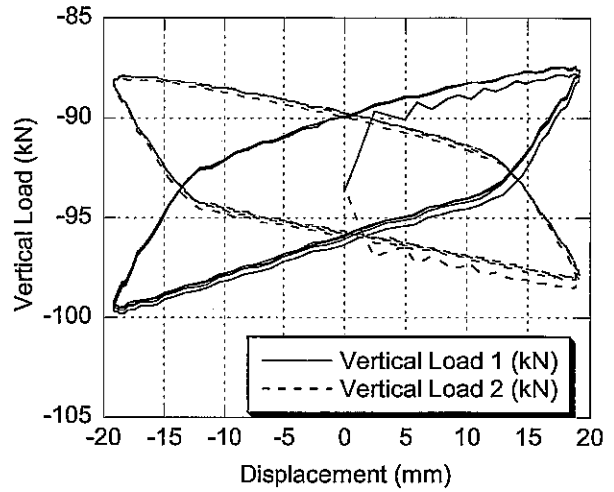
2S1-1-14



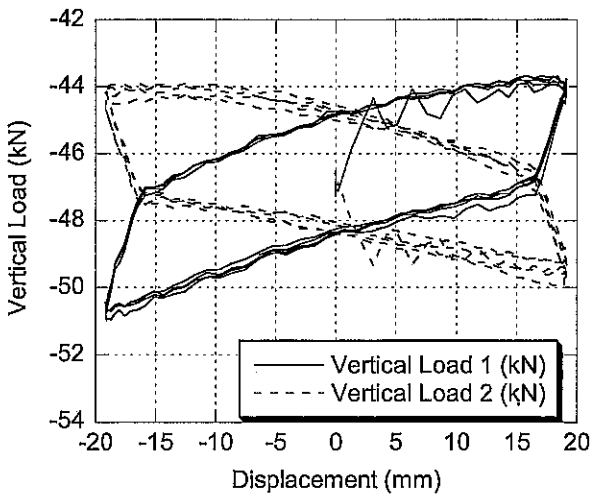
2S1-1-15



2S1-1-16



2S1-1-17





**APPENDIX F**

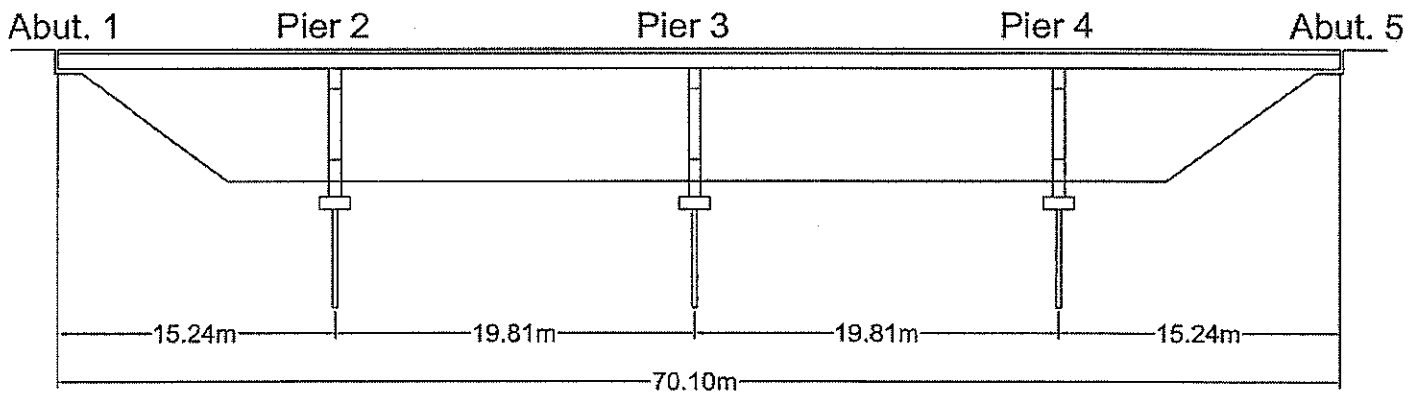
**DRAIN-2DX Input Files**



## Appendix F – DRAIN-2DX Input Files

This appendix presents input files for the nonlinear dynamic analyses, described in Chapter 8. The order of presentation is as follows with copies of both Figure 1.2 and Table 8.1 provided below as a reference:

1. Scenario 1a – pages
2. Scenario 1b – pages
3. Scenario 2a – pages
4. Scenario 2b – pages
5. Scenario 3a – pages
6. Scenario 3b – pages
7. Scenario 4 – pages



**Bridge Elevation**

Scenario	Description	Support				
		Abut. 1	Pier 2	Pier 3	Pier 4	Abut. 5
1a	Typical configuration (20°C)	Type II	Type I	Fixed	Type I	Type II
1b	Typical configuration (-25°C)	Type II	Type I	Fixed	Type I	Type II
2a	Retrofit bearing (20°C)	Type II	Type I	Retrofit	Type I	Type II
2b	Retrofit bearing (-25°C)	Type II	Type I	Retrofit	Type I	Type II
3a	All elastomeric bearings (20°C)	Type II	Type I	Type I	Type I	Type II
3b	All elastomeric bearings (-25°C)	Type II	Type I	Type I	Type I	Type II
4	All fixed	Fixed	Fixed	Fixed	Fixed	Fixed

**Appendix F.1 – Scenario 1a**  
**DRAIN input file for “Typical Configuration (20°C)”**

```

!UNITS KN, M, SEC
!
!   5   10   15   20   25   30   35   40   45   50   55   60   65   70   75   80
*STARTXX           ! IGNORE P-DELTA EFFECTS
  scela           0 1 0 1           scenario 1
*NODECOORDS
C   1000           0.0           0.0
C   2000          15.24          0.0
L   1000          2000          100    9    0.0
C   3000          35.05          0.0
L   2000          3000          100    9    0.0
C   4000          54.86          0.0
L   3000          4000          100    9    0.0
C   5000          70.10          0.0
L   4000          5000          100    9    0.0
C   1001           0.0           0.0
C   1002           0.0           0.0
C   1003           0.0           0.1
C   1004           0.0           0.1
C   1005           0.0           0.1
C   1006           0.0           0.1
C   2001          15.24          0.0
C   2002          15.24          0.0
C   2003          15.24          0.0
C   2004          15.24          0.0
C   3001          35.05          0.0
C   3002          35.05          0.0
C   3003          35.05          0.0
C   4001          54.86          0.0
C   4002          54.86          0.0
C   4003          54.86          0.0
C   4004          54.86          0.0
C   5001          70.10          0.0
C   5002          70.10          0.0
C   5003          70.10          0.1
C   5004          70.10          0.1
C   5005          70.10          0.1
C   5006          70.10          0.1
*RESTRAINTS
S 111           1002
S 111           2003
S 111           3002
S 111           4003
S 111           5002
*SLAVING
S 111           2001           2000
S 111           3001           3000
S 111           4001           4000
!   5   10   15   20   25   30   35   40   45   50   55   60   65   70   75   80
*MASSES           ! alpha = 1.0
! SLAB MASS
S 010           74.55           1000           9.81  1.0
S 010           149.10          1100           1900           100           9.81  1.0

```

```

S 010    171.45    2000                9.81  1.0
S 010    193.80    2100    2900    100    9.81  1.0
S 010    193.80    3000                9.81  1.0
S 010    193.80    3100    3900    100    9.81  1.0
S 010    171.45    4000                9.81  1.0
S 010    149.10    4100    4900    100    9.81  1.0
S 010     74.55    5000                9.81  1.0
!BENT MASS AND PIER (ABOVE)
S 010    160.0    2002                9.81  1.0
S 010    160.0    3001                9.81  1.0
S 010    160.0    4002                9.81  1.0
!
*ELEMENTGROUP
!SLIDER
!IGNORE P-DELTA    BETA = 0.0
  4    1    0    0.0    TEFLON
!INPUT SPECIFIC TO ELEMENT TYPE 4 (# OF PROPERTY TYPES)
  3
!PROPERTY TYPE
  1    5E06    1E-06    164.0    164.0    0.01    2    0
  2    5E06    1E-06    377.0    377.0    0.01    2    0
  3    5E06    1E-06    721.0    721.0    0.01    2    0
!  5    10    15    20    25    30    35    40    45    50    55    60    65    70    75    80
!ELEMENT GENERATION COMMANDS
  1    1000    1001    1
  2    5000    5001    1
!
*ELEMENTGROUP
!ELASTOMER
!IGNORE P-DELTA    BETA = ---
  4    1    0    0.001486    RUBBER
!INPUT SPECIFIC TO ELEMENT TYPE 4 (# OF PROPERTY TYPES)
  2
!PROPERTY TYPE
  1    6773    0.50    82.0    82.0    0.01    2    0
  2    10105    0.50    188.5    188.5    0.01    2    0
!  5    10    15    20    25    30    35    40    45    50    55    60    65    70    75    80
!ELEMENT GENERATION COMMANDS
  1    1001    1002    1
  2    2001    2002    2
  3    4001    4002    2
  4    5001    5002    1
!
!
*ELEMENTGROUP
!PIER
!IGNORE P-DELTA    BETA = ---
  4    1    0    0.001486    PIER
!INPUT SPECIFIC TO ELEMENT TYPE 4 (# OF PROPERTY TYPES)
  1
!PROPERTY TYPE, INELASTIC UNLOADING
  1    32400    1E-6    961    961    0.01    2    0
!  5    10    15    20    25    30    35    40    45    50    55    60    65    70    75    80
!ELEMENT GENERATION COMMANDS
  1    2002    2003    1
  2    3001    3002    1
  3    4002    4003    1

```

```

!
*ELEMENTGROUP
!DEFINE SLAB
!IGNORE P-DELTA      BETA = ---

      2      1      0      0.001486      SLAB ELEMENT
! INPUT SPECIFIC TO ELEMENT TYPE 2
      1      0      1
! STIFFNESS TYPES
      1      2.0E8      0.03      0.452      4.32  4.0  4.0  2.0      0.01
! RIGID END ZONE TYPES
! YIELD SURFACE TYPES

      1      1      177000      177000
! ELEMENT GENERATION COMMANDS
      1      1000      1100      100      1      1      1
      40      4900      5000      100      1      1      1
!
!
*RESULTS
! GET DISPLACEMENT PROFILE
NSD  001      1000
NSD  001      1001
NSD  001      1002
NSD  001      2000
NSD  001      2001
NSD  001      2002
NSD  001      2003
NSD  001      3000
NSD  001      3001
NSD  001      3002
!  5  10  15  20  25  30  35  40  45  50  55  60  65  70  75  80
! GET ELEMENT DATA
!E      001
!S      001
*ACCNREC
  chil      chile.acc  (f6.3,f10.2)      '3.10*chile'
!CONTROL INFORMATION
12000  1  1  2      3.10
!  5  10  15  20  25  30  35  40  45  50  55  60  65  70  75  80
*MODE
! PRINT MODE SHAPES, PRINT TO .OUT FILE, PRINT MODAL DAMPING RATIOS.
      14      1      1      1
*PARAMETERS
! DEFINE ALPHA AND BETA TO ACHIEVE 5% DAMPING FOR CERTAIN MODES

VS      0.696339      1.0
! PRINT TO .OUT
OD      0      0.      0      0.      1      0      0.99999      0.
!  5  10  15  20  25  30  35  40  45  50  55  60  65  70  75  80
! TURN OFF OPTIONS TO CORRECT VELOCITY AND ACCELERATION
DC 1  0  0  0
! TIME STEP PARAMETERS
DT      0.005      0.005      0.005
!  5  10  15  20  25  30  35  40  45  50  55  60  65  70  75  80
DA      0.01      0.5      2      2.0
*ACCN      GROUND ACC ANAL

```

```
!          99999 = MAX.# OF STEPS
60.0      99999   2
!GROUND ACCELERATION RECORD
2      chil      0.01      1.0
!   5   10   15   20   25   30   35   40   45   50   55   60   65   70   75   80
*STOP
```

**Appendix F.2 – Scenario 1b**  
**DRAIN input file for “Typical Configuration (-25°C)”**

```

!UNITS KN, M, SEC
!
!   5   10   15   20   25   30   35   40   45   50   55   60   65   70   75   80
*STARTXX           ! IGNORE P-DELTA EFFECTS
  sce1b           0 1 0 1           scenario 1b
*NODECOORDS
C   1000           0.0           0.0
C   2000          15.24          0.0
L   1000          2000          100   9   0.0
C   3000          35.05          0.0
L   2000          3000          100   9   0.0
C   4000          54.86          0.0
L   3000          4000          100   9   0.0
C   5000          70.10          0.0
L   4000          5000          100   9   0.0
C   1001           0.0           0.0
C   1002           0.0           0.0
C   1003           0.0           0.1
C   1004           0.0           0.1
C   1005           0.0           0.1
C   1006           0.0           0.1
C   2001          15.24          0.0
C   2002          15.24          0.0
C   2003          15.24          0.0
C   2004          15.24          0.0
C   3001          35.05          0.0
C   3002          35.05          0.0
C   3003          35.05          0.0
C   4001          54.86          0.0
C   4002          54.86          0.0
C   4003          54.86          0.0
C   4004          54.86          0.0
C   5001          70.10          0.0
C   5002          70.10          0.0
C   5003          70.10          0.1
C   5004          70.10          0.1
C   5005          70.10          0.1
C   5006          70.10          0.1
*RESTRAINTS
S 111   1002
S 111   2003
S 111   3002
S 111   4003
S 111   5002
*SLAVING
S 111   2001   2000
S 111   3001   3000
S 111   4001   4000
!   5   10   15   20   25   30   35   40   45   50   55   60   65   70   75   80
*MASSES           ! alpha = 1.0
! SLAB MASS
S 010   74.55   1000           9.81   1.0

```

```

S 010 149.10 1100 1900 100 9.81 1.0
S 010 171.45 2000 9.81 1.0
S 010 193.80 2100 2900 100 9.81 1.0
S 010 193.80 3000 9.81 1.0
S 010 193.80 3100 3900 100 9.81 1.0
S 010 171.45 4000 9.81 1.0
S 010 149.10 4100 4900 100 9.81 1.0
S 010 74.55 5000 9.81 1.0
!BENT MASS AND PIER (ABOVE)
S 010 160.0 2002 9.81 1.0
S 010 160.0 3001 9.81 1.0
S 010 160.0 4002 9.81 1.0
!
*ELEMENTGROUP
!SLIDER
!IGNORE P-DELTA BETA = 0.0
4 1 0 0.0 TEFLON
!INPUT SPECIFIC TO ELEMENT TYPE 4 (# OF PROPERTY TYPES)
3
!PROPERTY TYPE
1 5E06 1E-06 164.0 164.0 0.01 2 0
2 5E06 1E-06 377.0 377.0 0.01 2 0
3 5E06 1E-06 721.0 721.0 0.01 2 0
! 5 10 15 20 25 30 35 40 45 50 55 60 65 70 75 80
!ELEMENT GENERATION COMMANDS
1 1000 1001 1
2 5000 5001 1
!
*ELEMENTGROUP
!ELASTOMER
!IGNORE P-DELTA BETA = ---
4 1 0 0.001486 RUBBER
!INPUT SPECIFIC TO ELEMENT TYPE 4 (# OF PROPERTY TYPES)
2
!PROPERTY TYPE
1 8689 0.50 82.0 82.0 0.01 2 0
2 12963 0.50 188.5 188.5 0.01 2 0
! 5 10 15 20 25 30 35 40 45 50 55 60 65 70 75 80
!ELEMENT GENERATION COMMANDS
1 1001 1002 1
2 2001 2002 2
3 4001 4002 2
4 5001 5002 1
!
!
*ELEMENTGROUP
!PIER
!IGNORE P-DELTA BETA = ---
4 1 0 0.001486 PIER
!INPUT SPECIFIC TO ELEMENT TYPE 4 (# OF PROPERTY TYPES)
1
!PROPERTY TYPE, INELASTIC UNLOADING
1 32400 1E-6 961 961 0.01 2 0
! 5 10 15 20 25 30 35 40 45 50 55 60 65 70 75 80
!ELEMENT GENERATION COMMANDS
1 2002 2003 1
2 3001 3002 1

```

```

      3      4002      4003      1
!
*ELEMENTGROUP
!DEFINE SLAB
!IGNORE P-DELTA      BETA = ---
      2      1      0      0.001486      SLAB ELEMENT
! INPUT SPECIFIC TO ELEMENT TYPE 2
      1      0      1
! STIFFNESS TYPES
      1      2.0E8      0.03      0.452      4.32      4.0      4.0      2.0      0.01
! RIGID END ZONE TYPES
! YIELD SURFACE TYPES
      1      1      177000      177000
! ELEMENT GENERATION COMMANDS
      1      1000      1100      100      1      1      1
      40      4900      5000      100      1      1      1
!
!
*RESULTS
! GET DISPLACEMENT PROFILE
NSD      001      1000
NSD      001      1001
NSD      001      1002
NSD      001      2000
NSD      001      2001
NSD      001      2002
NSD      001      2003
NSD      001      3000
NSD      001      3001
NSD      001      3002
! 5 10 15 20 25 30 35 40 45 50 55 60 65 70 75 80
! GET ELEMENT DATA
!E      001
!S      001
*ACCNREC
      chil      chile.acc      (f6.3,f10.2)      '3.10*chile'
!CONTROL INFORMATION
12000      1      1      2      3.10
! 5 10 15 20 25 30 35 40 45 50 55 60 65 70 75 80
*MODE
! PRINT MODE SHAPES, PRINT TO .OUT FILE, PRINT MODAL DAMPING RATIOS.
      14      1      1      1
*PARAMETERS
! DEFINE ALPHA AND BETA TO ACHIEVE 5% DAMPING FOR CERTAIN MODES
VS      0.696339      1.0
! PRINT TO .OUT
OD      0      0.      0      0.      1      0      0.99999      0.
! 5 10 15 20 25 30 35 40 45 50 55 60 65 70 75 80
! TURN OFF OPTIONS TO CORRECT VELOCITY AND ACCELERATION
DC      1      0      0      0
! TIME STEP PARAMETERS
DT      0.005      0.005      0.005
! 5 10 15 20 25 30 35 40 45 50 55 60 65 70 75 80
DA      0.01      0.5      2      2.0
*ACCN
!      99999 = MAX.# OF STEPS
60.0      99999      2
      GROUND ACC ANAL

```

!GROUND ACCELERATION RECORD

2 chil 0.01 1.0

! 5 10 15 20 25 30 35 40 45 50 55 60 65 70 75 80

\*STOP

**Appendix F.3 – Scenario 2a**  
**DRAIN input file for “Retrofit Bearing (20°C)”**

```

!UNITS KN, M, SEC
!
!   5   10   15   20   25   30   35   40   45   50   55   60   65   70   75   80
*STARTXX           ! IGNORE P-DELTA EFFECTS
  sce2a           0 1 0 1           scenario 2a
*NODECOORDS
C   1000           0.0           0.0
C   2000          15.24          0.0
L   1000           2000          100    9    0.0
C   3000           35.05          0.0
L   2000           3000          100    9    0.0
C   4000           54.86          0.0
L   3000           4000          100    9    0.0
C   5000           70.10          0.0
L   4000           5000          100    9    0.0
C   1001            0.0           0.0
C   1002            0.0           0.0
C   1003            0.0           0.1
C   1004            0.0           0.1
C   1005            0.0           0.1
C   1006            0.0           0.1
C   2001           15.24          0.0
C   2002           15.24          0.0
C   2003           15.24          0.0
C   2004           15.24          0.0
C   3001           35.05          0.0
C   3002           35.05          0.0

C   3003           35.05          0.0
C   4001           54.86          0.0
C   4002           54.86          0.0
C   4003           54.86          0.0
C   4004           54.86          0.0
C   5001           70.10          0.0
C   5002           70.10          0.0
C   5003           70.10          0.1

C   5004           70.10          0.1
C   5005           70.10          0.1
C   5006           70.10          0.1
*RESTRAINTS
S 111           1002
S 111           2003
S 111           3002
S 111           4003
S 111           5002
*SLAVING
S 111           2001           2000
S 111           4001           4000
!   5   10   15   20   25   30   35   40   45   50   55   60   65   70   75   80
*MASSES           ! alpha = 1.0
! SLAB MASS

```

```

S 010      74.55      1000                                9.81  1.0
S 010     149.10      1100      1900      100          9.81  1.0
S 010     171.45      2000                                9.81  1.0
S 010     193.80      2100      2900      100          9.81  1.0
S 010     193.80      3000                                9.81  1.0
S 010     193.80      3100      3900      100          9.81  1.0
S 010     171.45      4000                                9.81  1.0
S 010     149.10      4100      4900      100          9.81  1.0
S 010      74.55      5000                                9.81  1.0
!BENT MASS AND PIER (ABOVE)
S 010     160.0      2002                                9.81  1.0
S 010     160.0      3001                                9.81  1.0
S 010     160.0      4002                                9.81  1.0
!
*ELEMENTGROUP
!SLIDER
!IGNORE P-DELTA      BETA = 0.0
      4      1      0      0.0      TEFLON
!INPUT SPECIFIC TO ELEMENT TYPE 4 (# OF PROPERTY TYPES)
      3
!PROPERTY TYPE
      1      5E06      1E-06      164.0      164.0      0.01      2      0
      2      5E06      1E-06      377.0      377.0      0.01      2      0
      3      5E06      1E-06      481.5      481.5      0.01      2      0
!      5      10      15      20      25      30      35      40      45      50      55      60      65      70      75      80
!ELEMENT GENERATION COMMANDS
      1      1000      1001      1
      2      3000      3001      3
      3      5000      5001      1
!
*ELEMENTGROUP
!ELASTOMER
!IGNORE P-DELTA      BETA = ---
      4      1      0      0.001486      RUBBER
!INPUT SPECIFIC TO ELEMENT TYPE 4 (# OF PROPERTY TYPES)
      2
!PROPERTY TYPE
      1      6773      0.50      82.0      82.0      0.01      2      0
      2      10105      0.50      188.5      188.5      0.01      2      0
!      5      10      15      20      25      30      35      40      45      50      55      60      65      70      75      80
!ELEMENT GENERATION COMMANDS
      1      1001      1002      1
      2      2001      2002      2
      3      4001      4002      2
      4      5001      5002      1
!
!
*ELEMENTGROUP
!PIER
!IGNORE P-DELTA      BETA = ---
      4      1      0      0.001486      PIER
!INPUT SPECIFIC TO ELEMENT TYPE 4 (# OF PROPERTY TYPES)
      1
!PROPERTY TYPE, INELASTIC UNLOADING
      1      32400      1E-6      961      961      0.01      2      0
!      5      10      15      20      25      30      35      40      45      50      55      60      65      70      75      80
!ELEMENT GENERATION COMMANDS

```

```

1      2002      2003      1
2      3001      3002      1
3      4002      4003      1
!
*ELEMENTGROUP
!DEFINE SLAB
!IGNORE P-DELTA      BETA = ---
2      1      0      0.001486      SLAB ELEMENT
! INPUT SPECIFIC TO ELEMENT TYPE 2
1      0      1
! STIFFNESS TYPES
1      2.0E8      0.03      0.452      4.32      4.0      4.0      2.0      0.01
! RIGID END ZONE TYPES
! YIELD SURFACE TYPES
1      1      177000      177000
! ELEMENT GENERATION COMMANDS
1      1000      1100      100      1      1      1
40     4900      5000      100      1      1      1
!
!
*RESULTS
! GET DISPLACEMENT PROFILE
NSD      001      1000
NSD      001      1001
NSD      001      1002
NSD      001      2000
NSD      001      2001
NSD      001      2002
NSD      001      2003
NSD      001      3000
NSD      001      3001
NSD      001      3002
! 5      10      15      20      25      30      35      40      45      50      55      60      65      70      75      80
! GET ELEMENT DATA
!E      001
!S      001
*ACCNREC
chil      chile.acc      (f6.3,f10.2)      '3.10*chile'
!CONTROL INFORMATION
12000      1      1      2      3.10
! 5      10      15      20      25      30      35      40      45      50      55      60      65      70      75      80
*MODE
! PRINT MODE SHAPES, PRINT TO .OUT FILE, PRINT MODAL DAMPING RATIOS.
14      1      1      1
*PARAMETERS
! DEFINE ALPHA AND BETA TO ACHIEVE 5% DAMPING FOR CERTAIN MODES
VS      0.696339      1.0
! PRINT TO .OUT
OD      0      0      0      0      1      0      0.99999      0.
! 5      10      15      20      25      30      35      40      45      50      55      60      65      70      75      80
! TURN OFF OPTIONS TO CORRECT VELOCITY AND ACCELERATION
DC      1      0      0      0
! TIME STEP PARAMETERS
DT      0.005      0.005      0.005
! 5      10      15      20      25      30      35      40      45      50      55      60      65      70      75      80
DA      0.01      0.5      2      2.0
*ACCN      GROUND ACC ANAL

```

```
!          99999 = MAX.# OF STEPS
60.0      99999    2
!GROUND ACCELERATION RECORD
2      chil      0.01      1.0
!  5   10   15   20   25   30   35   40   45   50   55   60   65   70   75   80
*STOP
```

**Appendix F.4 – Scenario 2a**  
**DRAIN input file for “Retrofit Bearing (-25°C)”**

```

!UNITS KN, M, SEC
!
!   5   10   15   20   25   30   35   40   45   50   55   60   65   70   75   80
*STARTXX           ! IGNORE P-DELTA EFFECTS
  sce2b           0 1 0 1           scenario 2b
*NODECOORDS
C   1000           0.0           0.0
C   2000          15.24          0.0
L   1000           2000          100   9   0.0
C   3000           35.05          0.0
L   2000           3000          100   9   0.0
C   4000           54.86          0.0
L   3000           4000          100   9   0.0
C   5000           70.10          0.0
L   4000           5000          100   9   0.0
C   1001            0.0           0.0
C   1002            0.0           0.0
C   1003            0.0           0.1
C   1004            0.0           0.1
C   1005            0.0           0.1
C   1006            0.0           0.1
C   2001           15.24          0.0
C   2002           15.24          0.0
C   2003           15.24          0.0
C   2004           15.24          0.0
C   3001           35.05          0.0
C   3002           35.05          0.0

C   3003           35.05          0.0
C   4001           54.86          0.0
C   4002           54.86          0.0
C   4003           54.86          0.0
C   4004           54.86          0.0
C   5001           70.10          0.0
C   5002           70.10          0.0
C   5003           70.10          0.1

C   5004           70.10          0.1
C   5005           70.10          0.1
C   5006           70.10          0.1
*RESTRAINTS
S 111           1002
S 111           2003
S 111           3002
S 111           4003
S 111           5002
*SLAVING
S 111           2001           2000
S 111           4001           4000
!   5   10   15   20   25   30   35   40   45   50   55   60   65   70   75   80
*MASSES           ! alpha = 1.0
! SLAB MASS

```

```

S 010      74.55      1000                                9.81  1.0
S 010     149.10      1100      1900      100          9.81  1.0
S 010     171.45      2000                                9.81  1.0
S 010     193.80      2100      2900      100          9.81  1.0
S 010     193.80      3000                                9.81  1.0
S 010     193.80      3100      3900      100          9.81  1.0
S 010     171.45      4000                                9.81  1.0
S 010     149.10      4100      4900      100          9.81  1.0
S 010      74.55      5000                                9.81  1.0
!BENT MASS AND PIER (ABOVE)
S 010     160.0      2002                                9.81  1.0
S 010     160.0      3001                                9.81  1.0
S 010     160.0      4002                                9.81  1.0
!
*ELEMENTGROUP
!SLIDER
!IGNORE P-DELTA      BETA = 0.0
  4   1   0          0.0          TEFLON
!INPUT SPECIFIC TO ELEMENT TYPE 4 (# OF PROPERTY TYPES)
  3
!PROPERTY TYPE
  1      5E06      1E-06      164.0      164.0      0.01      2      0
  2      5E06      1E-06      377.0      377.0      0.01      2      0
  3      5E06      1E-06      481.5      481.5      0.01      2      0
!   5   10   15   20   25   30   35   40   45   50   55   60   65   70   75   80
!ELEMENT GENERATION COMMANDS
  1      1000      1001          1
  2      3000      3001          3
  3      5000      5001          1
!
*ELEMENTGROUP
!ELASTOMER
!IGNORE P-DELTA      BETA = ---
  4   1   0          0.001486          RUBBER
!INPUT SPECIFIC TO ELEMENT TYPE 4 (# OF PROPERTY TYPES)
  2
!PROPERTY TYPE
  1      8689      0.50      82.0      82.0      0.01      2      0
  2     12963      0.50     188.5     188.5      0.01      2      0
!   5   10   15   20   25   30   35   40   45   50   55   60   65   70   75   80
!ELEMENT GENERATION COMMANDS
  1      1001      1002          1
  2      2001      2002          2
  3      4001      4002          2
  4      5001      5002          1
!
!
*ELEMENTGROUP
!PIER
!IGNORE P-DELTA      BETA = ---
  4   1   0          0.001486          PIER
!INPUT SPECIFIC TO ELEMENT TYPE 4 (# OF PROPERTY TYPES)
  1
!PROPERTY TYPE, INELASTIC UNLOADING
  1     32400      1E-6      961      961      0.01      2      0
!   5   10   15   20   25   30   35   40   45   50   55   60   65   70   75   80
!ELEMENT GENERATION COMMANDS

```

```

1      2002      2003      1
2      3001      3002      1
3      4002      4003      1
!
*ELEMENTGROUP
!DEFINE SLAB
!IGNORE P-DELTA      BETA = ---
2      1      0      0.001486      SLAB ELEMENT
! INPUT SPECIFIC TO ELEMENT TYPE 2
1      0      1
! STIFFNESS TYPES
1      2.0E8      0.03      0.452      4.32      4.0      4.0      2.0      0.01
! RIGID END ZONE TYPES
! YIELD SURFACE TYPES
1      1      177000      177000
! ELEMENT GENERATION COMMANDS
1      1000      1100      100      1      1      1
40     4900      5000      100      1      1      1
!
!
*RESULTS
! GET DISPLACEMENT PROFILE
NSD      001      1000
NSD      001      1001
NSD      001      1002
NSD      001      2000
NSD      001      2001
NSD      001      2002
NSD      001      2003
NSD      001      3000
NSD      001      3001
NSD      001      3002
! 5      10      15      20      25      30      35      40      45      50      55      60      65      70      75      80
! GET ELEMENT DATA
!E      001
!S      001
*ACCNREC
chil      chile.acc      (f6.3,f10.2)      '3.10*chile'
!CONTROL INFORMATION
12000      1      1      2      3.10
! 5      10      15      20      25      30      35      40      45      50      55      60      65      70      75      80
*MODE
! PRINT MODE SHAPES, PRINT TO .OUT FILE, PRINT MODAL DAMPING RATIOS.
14      1      1      1
*PARAMETERS
! DEFINE ALPHA AND BETA TO ACHIEVE 5% DAMPING FOR CERTAIN MODES
VS      0.696339      1.0
! PRINT TO .OUT
OD      0      0      0      0      1      0      0.99999      0.
! 5      10      15      20      25      30      35      40      45      50      55      60      65      70      75      80
! TURN OFF OPTIONS TO CORRECT VELOCITY AND ACCELERATION
DC 1      0      0      0
! TIME STEP PARAMETERS
DT      0.005      0.005      0.005
! 5      10      15      20      25      30      35      40      45      50      55      60      65      70      75      80
DA      0.01      0.5      2      2.0
*ACCN
GROUND ACC ANAL

```

```
!          99999 = MAX.# OF STEPS
60.0      99999   2
!GROUND ACCELERATION RECORD
2      chil      0.01      1.0
!  5   10   15   20   25   30   35   40   45   50   55   60   65   70   75   80
*STOP
```

**Appendix F.5 – Scenario 3a**  
**DRAIN input file for “All Elastomeric Bearings (20°C)”**

```

!UNITS KN, M, SEC
!
!   5   10   15   20   25   30   35   40   45   50   55   60   65   70   75   80
*STARTXX           ! IGNORE P-DELTA EFFECTS
  sce3a           0 1 0 1           scenario 3
*NODECOORDS
C   1000           0.0           0.0
C   2000          15.24           0.0
L   1000           2000           100   9   0.0
C   3000           35.05           0.0
L   2000           3000           100   9   0.0
C   4000           54.86           0.0
L   3000           4000           100   9   0.0
C   5000           70.10           0.0
L   4000           5000           100   9   0.0
C   1001           0.0           0.0
C   1002           0.0           0.0
C   1003           0.0           0.1
C   1004           0.0           0.1
C   1005           0.0           0.1
C   1006           0.0           0.1
C   2001           15.24           0.0
C   2002           15.24           0.0
C   2003           15.24           0.0
C   2004           15.24           0.0
C   3001           35.05           0.0
C   3002           35.05           0.0
C   3003           35.05           0.0
C   4001           54.86           0.0
C   4002           54.86           0.0
C   4003           54.86           0.0
C   4004           54.86           0.0
C   5001           70.10           0.0
C   5002           70.10           0.0
C   5003           70.10           0.1
C   5004           70.10           0.1
C   5005           70.10           0.1
C   5006           70.10           0.1
*RESTRAINTS
S 111           1002
S 111           2003
S 111           3002
S 111           4003
S 111           5002
*SLAVING
S 111           2001           2000
S 111           4001           4000
!   5   10   15   20   25   30   35   40   45   50   55   60   65   70   75   80
*MASSES           ! alpha = 1.0
! SLAB MASS
S 010           74.55           1000
S 010           149.10          1100           1900           100           9.81 1.0
                                           9.81 1.0

```

```

S 010    171.45    2000                                9.81  1.0
S 010    193.80    2100      2900      100          9.81  1.0
S 010    193.80    3000                                9.81  1.0
S 010    193.80    3100      3900      100          9.81  1.0
S 010    171.45    4000                                9.81  1.0
S 010    149.10    4100      4900      100          9.81  1.0
S 010     74.55    5000                                9.81  1.0
!BENT MASS AND PIER (ABOVE)
S 010    160.0     2002                                9.81  1.0
S 010    160.0     3001                                9.81  1.0
S 010    160.0     4002                                9.81  1.0
!
*ELEMENTGROUP
!SLIDER
!IGNORE P-DELTA      BETA = 0.0
  4  1  0           0.0           TEFLON
!INPUT SPECIFIC TO ELEMENT TYPE 4 (# OF PROPERTY TYPES)
  2
!PROPERTY TYPE
  1      5E06      1E-06      164.0      164.0      0.01      2      0
  2      5E06      1E-06      377.0      377.0      0.01      2      0
!   3      5E06      1E-06      481.5      721.0      0.01      2      0
!   5  10  15  20  25  30  35  40  45  50  55  60  65  70  75  80
!ELEMENT GENERATION COMMANDS
  1      1000      1001           1
  2      5000      5001           1
!
*ELEMENTGROUP
!ELASTOMER
!IGNORE P-DELTA      BETA = ---
  4  1  0           0.001486           RUBBER
!INPUT SPECIFIC TO ELEMENT TYPE 4 (# OF PROPERTY TYPES)
  3
!PROPERTY TYPE
  1      6773      0.50      82.0      82.0      0.01      2      0
  2     10105      0.50     188.5     188.5      0.01      2      0
  3     11255      0.50     240.0     240.0      0.01      2      0
!   5  10  15  20  25  30  35  40  45  50  55  60  65  70  75  80
!ELEMENT GENERATION COMMANDS
  1      1001      1002           1
  2      2001      2002           2
  3      3000      3001           3
  4      4001      4002           2
  5      5001      5002           1
!
!
*ELEMENTGROUP
!PIER
!IGNORE P-DELTA      BETA = ---
  4  1  0           0.001486           PIER
!INPUT SPECIFIC TO ELEMENT TYPE 4 (# OF PROPERTY TYPES)
  1
!PROPERTY TYPE, INELASTIC UNLOADING
  1     32400      1E-6      961      961      0.01      2      0
!   5  10  15  20  25  30  35  40  45  50  55  60  65  70  75  80
!ELEMENT GENERATION COMMANDS
  1      2002      2003           1

```

```

      2      3001      3002      1
      3      4002      4003      1
!
*ELEMENTGROUP
!DEFINE SLAB
!IGNORE P-DELTA      BETA = ---
      2      1      0      0.001486      SLAB ELEMENT
! INPUT SPECIFIC TO ELEMENT TYPE 2
      1      0      1
! STIFFNESS TYPES
      1      2.0E8      0.03      0.452      4.32      4.0      4.0      2.0      0.01
! RIGID END ZONE TYPES
! YIELD SURFACE TYPES
      1      1      177000      177000
! ELEMENT GENERATION COMMANDS
      1      1000      1100      100      1      1      1
      40      4900      5000      100      1      1      1
!
!
*RESULTS
! GET DISPLACEMENT PROFILE
NSD      001      1000
NSD      001      1001
NSD      001      1002
NSD      001      2000
NSD      001      2001
NSD      001      2002
NSD      001      2003
NSD      001      3000
NSD      001      3001
NSD      001      3002
!      5      10      15      20      25      30      35      40      45      50      55      60      65      70      75      80
! GET ELEMENT DATA
!E      001
!S      001
*ACCNREC
      chil      chile.acc      (f6.3,f10.2)      '3.10*chile'
!CONTROL INFORMATION
12000      1      1      2      3.10
!      5      10      15      20      25      30      35      40      45      50      55      60      65      70      75      80
*MODE
! PRINT MODE SHAPES, PRINT TO .OUT FILE, PRINT MODAL DAMPING RATIOS.
      14      1      1      1
*PARAMETERS
! DEFINE ALPHA AND BETA TO ACHIEVE 5% DAMPING FOR CERTAIN MODES
VS      0.696339      1.0
! PRINT TO .OUT
OD      0      0      0      0      1      0      0.99999      0.
!      5      10      15      20      25      30      35      40      45      50      55      60      65      70      75      80
! TURN OFF OPTIONS TO CORRECT VELOCITY AND ACCELERATION
DC      1      0      0      0
! TIME STEP PARAMETERS
DT      0.005      0.005      0.005
!      5      10      15      20      25      30      35      40      45      50      55      60      65      70      75      80
DA      0.01      0.5      2      2.0
*ACCN
      GROUND ACC ANAL
!      99999 = MAX.# OF STEPS

```

60.0        99999    2  
!GROUND ACCELERATION RECORD  
2        chil        0.01        1.0  
!    5    10    15    20    25    30    35    40    45    50    55    60    65    70    75    80  
\*STOP

**Appendix F.6 – Scenario 3b**  
**DRAIN input file for “All Elastomeric Bearings (-25°C)”**

```

!UNITS KN, M, SEC
!
!   5   10   15   20   25   30   35   40   45   50   55   60   65   70   75   80
*STARTXX           ! IGNORE P-DELTA EFFECTS
  sce3b           0 1 0 1           scenario 3b
*NODECOORDS
C   1000           0.0           0.0
C   2000          15.24          0.0
L   1000           2000          100    9    0.0
C   3000           35.05          0.0
L   2000           3000          100    9    0.0
C   4000           54.86          0.0
L   3000           4000          100    9    0.0
C   5000           70.10          0.0
L   4000           5000          100    9    0.0
C   1001            0.0           0.0
C   1002            0.0           0.0
C   1003            0.0           0.1
C   1004            0.0           0.1
C   1005            0.0           0.1
C   1006            0.0           0.1
C   2001           15.24          0.0
C   2002           15.24          0.0
C   2003           15.24          0.0
C   2004           15.24          0.0
C   3001           35.05          0.0
C   3002           35.05          0.0
C   3003           35.05          0.0
C   4001           54.86          0.0
C   4002           54.86          0.0
C   4003           54.86          0.0
C   4004           54.86          0.0
C   5001           70.10          0.0
C   5002           70.10          0.0
C   5003           70.10          0.1
C   5004           70.10          0.1
C   5005           70.10          0.1
C   5006           70.10          0.1
*RESTRAINTS
S 111    1002
S 111    2003
S 111    3002
S 111    4003
S 111    5002
*SLAVING
S 111    2001    2000
S 111    4001    4000
!   5   10   15   20   25   30   35   40   45   50   55   60   65   70   75   80
*MASSES           ! alpha = 1.0
! SLAB MASS
S 010    74.55    1000           9.81  1.0
S 010    149.10   1100    1900    100           9.81  1.0

```

```

S 010    171.45    2000                                9.81  1.0
S 010    193.80    2100    2900    100                9.81  1.0
S 010    193.80    3000                                9.81  1.0
S 010    193.80    3100    3900    100                9.81  1.0
S 010    171.45    4000                                9.81  1.0
S 010    149.10    4100    4900    100                9.81  1.0
S 010     74.55    5000                                9.81  1.0
!BENT MASS AND PIER (ABOVE)
S 010     160.0    2002                                9.81  1.0
S 010     160.0    3001                                9.81  1.0
S 010     160.0    4002                                9.81  1.0
!
*ELEMENTGROUP
!SLIDER
!IGNORE P-DELTA    BETA = 0.0
  4  1  0          0.0          TEFLON
!INPUT SPECIFIC TO ELEMENT TYPE 4 (# OF PROPERTY TYPES)
  2
!PROPERTY TYPE
  1      5E06      1E-06      164.0      164.0      0.01      2      0
  2      5E06      1E-06      377.0      377.0      0.01      2      0
!   3      5E06      1E-06      481.5      721.0      0.01      2      0
!   5  10  15  20  25  30  35  40  45  50  55  60  65  70  75  80
!ELEMENT GENERATION COMMANDS
  1      1000      1001          1
  2      5000      5001          1
!
*ELEMENTGROUP
!ELASTOMER
!IGNORE P-DELTA    BETA = ---
  4  1  0          0.001486      RUBBER
!INPUT SPECIFIC TO ELEMENT TYPE 4 (# OF PROPERTY TYPES)
  3
!PROPERTY TYPE
  1      8689      0.50      82.0      82.0      0.01      2      0
  2     12963      0.50     188.5     188.5      0.01      2      0
  3     14438      0.50     240.0     240.0      0.01      2      0
!   5  10  15  20  25  30  35  40  45  50  55  60  65  70  75  80
!ELEMENT GENERATION COMMANDS
  1      1001      1002          1
  2      2001      2002          2
  3      3000      3001          3
  4      4001      4002          2
  5      5001      5002          1
!
!
*ELEMENTGROUP
!PIER
!IGNORE P-DELTA    BETA = ---
  4  1  0          0.001486      PIER
!INPUT SPECIFIC TO ELEMENT TYPE 4 (# OF PROPERTY TYPES)
  1
!PROPERTY TYPE, INELASTIC UNLOADING
  1     32400      1E-6      961      961      0.01      2      0
!   5  10  15  20  25  30  35  40  45  50  55  60  65  70  75  80
!ELEMENT GENERATION COMMANDS
  1      2002      2003          1

```

```

      2      3001      3002      1
      3      4002      4003      1
!
*ELEMENTGROUP
!DEFINE SLAB
!IGNORE P-DELTA      BETA = ---
      2      1      0      0.001486      SLAB ELEMENT
! INPUT SPECIFIC TO ELEMENT TYPE 2
      1      0      1
! STIFFNESS TYPES
      1      2.0E8      0.03      0.452      4.32      4.0      4.0      2.0      0.01
! RIGID END ZONE TYPES
! YIELD SURFACE TYPES
      1      1      177000      177000
! ELEMENT GENERATION COMMANDS
      1      1000      1100      100      1      1      1
      40      4900      5000      100      1      1      1
!
!
*RESULTS
! GET DISPLACEMENT PROFILE
NSD      001      1000
NSD      001      1001
NSD      001      1002
NSD      001      2000
NSD      001      2001
NSD      001      2002
NSD      001      2003
NSD      001      3000
NSD      001      3001
NSD      001      3002
!      5      10      15      20      25      30      35      40      45      50      55      60      65      70      75      80
! GET ELEMENT DATA
!E      001
!S      001
*ACCNREC
      chil      chile.acc      (f6.3,f10.2)      '3.10*chile'
!CONTROL INFORMATION
12000      1      1      2      3.10
!      5      10      15      20      25      30      35      40      45      50      55      60      65      70      75      80
*MODE
! PRINT MODE SHAPES, PRINT TO .OUT FILE, PRINT MODAL DAMPING RATIOS.
      14      1      1      1
*PARAMETERS
! DEFINE ALPHA AND BETA TO ACHIEVE 5% DAMPING FOR CERTAIN MODES
VS      0.696339      1.0
! PRINT TO .OUT
OD      0      0      0      0      1      0      0.99999      0.
!      5      10      15      20      25      30      35      40      45      50      55      60      65      70      75      80
! TURN OFF OPTIONS TO CORRECT VELOCITY AND ACCELERATION
DC      1      0      0      0
! TIME STEP PARAMETERS
DT      0.005      0.005      0.005
!      5      10      15      20      25      30      35      40      45      50      55      60      65      70      75      80
DA      0.01      0.5      2      2.0
*ACCN
!      99999 = MAX.# OF STEPS
GROUND ACC ANAL

```

60.0 99999 2  
!GROUND ACCELERATION RECORD  
2 chil 0.01 1.0  
! 5 10 15 20 25 30 35 40 45 50 55 60 65 70 75 80  
\*STOP

**Appendix F.7 – Scenario 4**  
**DRAIN input file for “All Fixed Bearings”**

```

!UNITS KN, M, SEC
!
!   5   10   15   20   25   30   35   40   45   50   55   60   65   70   75   80
*STARTXX           ! IGNORE P-DELTA EFFECTS
  scen4           0 1 0 1           scenario4
*NODECOORDS
C   1000           0.0           0.0
C   2000           15.24          0.0
L   1000           2000           100   9   0.0
C   3000           35.05          0.0
L   2000           3000           100   9   0.0
C   4000           54.86          0.0
L   3000           4000           100   9   0.0
C   5000           70.10          0.0
L   4000           5000           100   9   0.0
C   1001           0.0            0.0
C   1002           0.0            0.0
C   2001           15.24          0.0
C   2002           15.24          0.0
C   2003           15.24          0.0
C   3001           35.05          0.0
C   3002           35.05          0.0
C   4001           54.86          0.0
C   4002           54.86          0.0
C   4003           54.86          0.0
C   5001           70.10          0.0
C   5002           70.10          0.0
*RESTRAINTS
S 110           1002
S 111           2003
S 111           3002
S 111           4003
S 110           5002
*SLAVING
S 111           1002           1000
S 111           2002           2000
S 111           3001           3000
S 111           4002           4000
S 111           5002           5000
!   5   10   15   20   25   30   35   40   45   50   55   60   65   70   75   80
*MASSES           ! alpha = 1.0
! SLAB MASS
S 010           74.55           1000           9.81 1.0
S 010           149.10          1100           1900           100           9.81 1.0
S 010           171.45          2000           9.81 1.0
S 010           193.80          2100           2900           100           9.81 1.0
S 010           193.80          3000           9.81 1.0
S 010           193.80          3100           3900           100           9.81 1.0
S 010           171.45          4000           9.81 1.0
S 010           149.10          4100           4900           100           9.81 1.0
S 010           74.55           5000           9.81 1.0

```

```

!BENT MASS AND PIER (ABOVE)
S 010      160.0      2002                      9.81  1.0
S 010      160.0      3001
S 010      160.0      4002                      9.81  1.0
!
!
*ELEMENTGROUP
! PIER
!IGNORE P-DELTA      BETA = ---
  4      1      0      0.001486      PIER
!INPUT SPECIFIC TO ELEMENT TYPE 4 (# OF PROPERTY TYPES)
  1
!PROPERTY TYPE, INELASTIC UNLOADING
  1      32400      1E-6      961      961      0.01      2      0
!  5  10  15  20  25  30  35  40  45  50  55  60  65  70  75  80
!ELEMENT GENERATION COMMANDS
  1      2002      2003      1
  2      3001      3002      1
  3      4002      4003      1
*ELEMENTGROUP
!DEFINE SLAB
!IGNORE P-DELTA      BETA = ---
  2      1      0      0.001486      SLAB ELEMENT
! INPUT SPECIFIC TO ELEMENT TYPE 2
  1      0      1
! STIFFNESS TYPES
  1      2.0E8      0.03      0.452      4.32  4.0  4.0  2.0      0.01
!  5  10  15  20  25  30  35  40  45  50  55  60  65  70  75  80
! RIGID END ZONE TYPES
! YIELD SURFACE TYPES
  1      1      177000      177000
! ELEMENT GENERATION COMMANDS
  1      1000      1100      100      1      1      1
  40     4900      5000      100      1      1      1
!
!
*RESULTS
! GET DISPLACEMENT PROFILE
NSD  001      1000
NSD  001      1001
NSD  001      1002
NSD  001      2000
NSD  001      2001
NSD  001      2002
NSD  001      2003
NSD  001      3000
NSD  001      3001
NSD  001      3002
!  5  10  15  20  25  30  35  40  45  50  55  60  65  70  75  80
! GET ELEMENT DATA
!E  001
!S  001
*ACCNREC
  chil      chile.acc (f6.3,f10.2)      '3.10*chile'
!CONTROL INFORMATION
12000  1      1      2      3.10
!  5  10  15  20  25  30  35  40  45  50  55  60  65  70  75  80

```

```

*MODE
! PRINT MODE SHAPES, PRINT TO .OUT FILE, PRINT MODAL DAMPING RATIOS.
  14          1    1    1
*PARAMETERS
! DEFINE ALPHA AND BETA TO ACHIEVE 5% DAMPING FOR CERTAIN MODES
VS          0.696339      1.0
! PRINT TO .OUT
OD          0          0.    0          0.    1          0          0.999999    0.
!   5   10   15   20   25   30   35   40   45   50   55   60   65   70   75   80
! TURN OFF OPTIONS TO CORRECT VELOCITY AND ACCELERATION
DC 1    0    0    0
! TIME STEP PARAMETERS
DT          0.005      0.005      0.005
!   5   10   15   20   25   30   35   40   45   50   55   60   65   70   75   80
DA          0.01          0.5          2          2.0
*ACCN
!          99999 = MAX.# OF STEPS
60.0      99999    2
!GROUND ACCELERATION RECORD
2      chil      0.01      1.0
!   5   10   15   20   25   30   35   40   45   50   55   60   65   70   75   80
*STOP

```

## APPENDIX G

### Units Conversions



## Appendix G – Units Conversions

$$1 \text{ kN} = 0.225 \text{ kip}$$

$$1 \text{ mm} = 0.0394 \text{ in}$$

$$1 \text{ m} = 39.4 \text{ in}$$

$$1 \text{ m} = 3.28 \text{ ft}$$

$$1 \text{ MPa} = 145.1 \text{ psi}$$

$$1.73 \text{ MPa} = 250 \text{ psi}$$

$$3.45 \text{ MPa} = 500 \text{ psi}$$

$$5.18 \text{ MPa} = 750 \text{ psi}$$

$$^{\circ}\text{F} = 9/5(^{\circ}\text{C}) + 32$$

$$20^{\circ}\text{C} = 68^{\circ}\text{F} \text{ (room temp.)}$$

$$-10^{\circ}\text{C} = 14^{\circ}\text{F}$$

$$-25^{\circ}\text{C} = -13^{\circ}\text{F}$$



## REFERENCES



## References

- Bruzzone, E. and E. Sorta (1978) "Elastomer Structures and Cold Crystallization", *Polymer*, Vol. 19.
- Campbell, T.I. and W.L. Kong (1989) "Laboratory Study of Friction in TFE Sliding Surfaces for Bridge Bearings."
- Constantinou, M.C., P. Tsopelas, A. Kasalanati, E.D. Wolff (1999) "Property Modification Factors for Seismic Isolation Bearings," *MCEER Technical Report*.
- Eyre, R. and A. Stevenson (1991) "Characterisation of rubber vulcanizates for bridge bearings," *Research Report 299*.
- Jacobsen, F.K. (1977) "TFE Expansion Bearings for Highway Bridges," Physical Research Report No. 71, Illinois Department of Transportation.
- Leitner, M. (1955) "Young's Modulus of Crystalline, Unstretched Rubber", *Transactions of the Faraday Society*, Vol. 51.
- Long, J.E. (1974) *Bearings in Structural Engineering*, London.
- Murray, R.M. and J.D. Detenber (1961) "First and Second Order Transitions in Neoprene," *Rubber Chemistry and Technology*, Vol. 34.
- National Earthquake Hazards Reduction Program "NEHRP Recommended Provisions of Seismic Regulations for New Buildings and Other Structures – 2000 Edition," Building Seismic Safety Council, Washington, D.C., 2001.
- Prakash, V. and G.H. Powell (1993) "DRAIN-2DX: Base Program Description and User Guide," University of California, Berkeley.
- Roeder, C.W., J.F. Stanton, and T. Feller (1989) "Low Temperature Behavior and Acceptance Criteria for Elastomeric Bridge Bearings," *NCHRP Report 325*.
- Roeder, C.W., J.F. Stanton, and A.W. Taylor (1987) "Performance of Elastomeric Bearings", *NCHRP Report 298*.
- United States Geological Survey "Earthquake Hazards Program – National Seismic Hazard Mapping Project" <http://eqint.cr.usgs.gov/eq/html/zipcode.shtml>
- Wissawapaisal, C. (2000) "Modeling the Seismic Response of Short Bridge Overcrossings," Ph.D. Dissertation, University of Illinois, Urbana.
- Wood, L.A., and N. Bekkedahl (1946) "Crystallization of Unvulcanized Rubber at Different Temperatures", *National Bureau of Standards Journal of Research*, Vol. 36.

Yakut, A. (2000) "Performance of Elastomeric Bridge Bearings at Cold Temperatures: Development of Performance Based Specifications and Related Test Procedures," Ph.D. Dissertation, University of Texas, Austin.

Yura, J., A. Kumar, A. Yakut, C. Topkaya, E. Becker, and J. Collingwood (2001) "Elastomeric Bridge Bearings: Recommended Test Methods," *NCHRP Report 449*.

Zhong, Q. (2001) "Assessing the Effectiveness of Reducing Seismic Vulnerability by a Program of Bridge Pier Wrapping," Ph.D. Dissertation, University of Illinois, Urbana.